CATALYSIS BY NANO SULFATED TITANIA

MODIFIED BY TRANSITION METALS

Thesis submitted to the
Cochin University of Science and Technology
in partial fulfillment of the requirements for the Degree of

Doctor of Philosophy
in
Chemistry

In the Faculty of Science

By

SUNAJA DEVI K.R.

Department of Applied Chemistry
Cochin University of Science and Technology
Kochi – 682022

September 2004

ओं भूर्भुवः स्वः।

तत्सवितुर्वरेण्यम्

भर्गो देवस्य धीमहि।

धियो यो नः प्रचोदयात्।।

Oh God! Thou art the Giver of Life, Remover of pain and sorrow, The Bestower of happiness, Oh! Creator of the Universe, May we receive thy supreme sin-destroying light, May Thou guide our intellect in the right direction

In the loving memory of my father ....

CERTIFICATE

Certified that the present work titled **"Catalysis by nano sulfated titania modified by transition metals"** submitted by Ms. Sunaja Devi. K.R. is an authentic record of research work carried out by her under my supervision at the Department of Applied Chemistry in partial fulfillment of the requirements for the degree of Doctor in Philosophy of the Cochin University of Science and Technology. No part thereof has been previously submitted for the award of any other degree.

Dr. S. Sugunan
Professor
(Supervising Guide)
Department of Applied Chemistry
Cochin University of Science & Technology
Kochi – 682022
India

Kochi-22
22-09-2004

DECLARATION

I hereby declare that the work presented in the thesis titled **"Catalysis by nano sulfated titania modified by transition metals"** is based on the original work done by me independently under the guidance and supervision of Dr. S. Sugunan (Professor, Physical Chemistry) at the Department of Applied Chemistry in partial fulfillment of the requirements for the degree of Doctor of Philosophy of the Cochin University of Science and Technology. I further declare that this thesis has not formed the basis of any degree, diploma, fellowship, associateship or similar title of any other University or Institution.

Sunaja Devi. K.R.

Kochi-22

22-08-2004

FORWARD

Catalysis has been playing a dominant role in the growth of the chemical industry year after year. More than 80% of industrially important chemical reactions are catalytic in nature. Today a large number of catalysts are used in all areas of chemical industry ranging from petroleum, petrochemicals, fertilizers, commodity, fine and speciality chemicals, drugs and drug intermediates to foodstuffs. Catalysis play a key role in modern chemical technology, in fact, it is the backbone of chemical industry. The replacement of liquid acids by solids is now considered as highly desirable in order to design clean processes for better protection of the environment.

Titania is a versatile metal oxide with multiple applications. It has gained much attention in catalyst industry due to its application as a catalyst by itself and as a support for metal or metal oxide catalysts. Photo degradation of organic compounds in water by means of economically advantageous and environmental friendly process is a topic of growing interest and much attention has been devoted in recent years to TiO_2 based photocatalysts for the oxidative degradation of various kinds of organic pollutants. By virtue of their acidic properties, they can be promising catalysts in acid catalyzed reactions. In recent years, considerable interest has been focused on heterogeneous catalysis of organic retains by sulfated metal oxides.

In the present study, we have prepared and evaluated the physical and chemical properties and catalytic activities of transition metal loaded sulfated titania *via* the sol-gel route. Sol-gel method is widely used for preparing porous materials having controlled properties and leads to the formation of oxide particles in nano range, which are spherical or interconnected to each other.

Characterization using various physico-chemical techniques and a detailed study of acidic properties are also carried out. Some reactions of industrial importance such as Friedel-Crafts reaction, *tert*-butylation of phenol,

Beckmann rearrangement of cyclohexanone oxime, nitration of phenol and photochemical degradation of methylene blue have been selected for catalytic activity study in the present venture.

The work is organized into eight chapters. The first chapter giving the brief introduction and literature survey on titania and their catalysis. The materials and the experimental methods employed in the work are discussed in the second chapter. Results and discussion regarding the characterization and catalytic activity studies are discussed in subsequent chapters. There is plenty of scope for further research in this field, current and future chemists are being trained to design products and processes with an increased awareness for environmental impact.

Acknowledgements

"Let noble thoughts come to us from every side"

-RigVeda, 1-89-i

At this moment of great satisfaction, I have to acknowledge a number of people who helped and encouraged me for the successful completion of this Thesis. I have indeed immense pleasure to express my deepest sense of gratitude and obligation to Prof. (Dr.) S. Sugunan, Department of Applied Chemistry, for constant encouragement, invaluable advice and excellent guidance given to me from time to time. I shall ever remain grateful to him.

I would like to express my deep gratitude and heartfelt thanks to Dr. M.R. Prathapachandra Kurup, Head, Department of Applied Chemistry, for providing the necessary advice and facilities for carrying out my research. I would like to thank all teachers and non-teaching staff of the Department for their help and warm wishes. I acknowledge with thanks the help rendered by RSIC, Mumbai, SIF, IISc, Bangalore, Dept. of Physics and PS & RT, CUSAT for providing the necessary instrumental analysis datas. I remember with heart-felt thanks the help rendered by Mr. Gopi Menon, Mr. Murali, Mr. Kashmiri, Mr. Jose and other technical staff of USIC, CUSAT, and Mr. Suresh, Service Engineer, Chemito for their technical assistance during various occasions.

The endless support, judicious advice and sisterly affection shown by my seniors Dr. Rahna, Dr. Suja, Dr. Nisha, Dr. Sreejarani, Dr. Deepa and Manju during the initial stages of my research are remembered with great appreciation and deep sense of gratitude. I am extremely thankful to my colleagues Bejoy, Sanjay, Smitha and

Fincy for their lively company, sincere cooperation, well timed suggestions and encouragement throughout my research period. I extent my earnest thanks to my dear juniors Binitha, Shali, Maya, Radhika, Kochurani, Ajitha teacher, Ramanathan and Salini for their support and cooperation on various occasions. Their cheerful readiness to help was an important ingredient in the successful completion of this work. My sincere thanks to Dr. C. G. Ramankutty and Dr. Rahna for their valuable advice and critical scrutiny of the manuscript. I thank all my friends Sreeja, Vidhya, Suni, Chandhini, Ambily, Rema and all other research scholars and students for their readiness to help in hard-hitting occasions and making my research work enjoyable and memorable.

I would like to record my deep love for my mother Saradha Bai, my brother Girish and all other family members for their constant and affectionate encouragement and care which proved to be useful in fulfilling this venture. I don't have the words to compensate the unconditional support and cooperation given by my in laws, Ramanatha Pai and Suryakala R. Pai for the completion of my research work.

I am greatly thankful to my husband Naresh Kumar Pai for his perpetual and unreserved support and was always ready to assist at any moment for the completion of my research work. I am indebted to him for the companionship over the days and for the days to come.

Sunaja Devi. K. R.

CONTENTS

Chapter 1

Introduction

And

Literature Survey

Over the course of the past decades, green chemistry has demonstrated how fundamental scientific methodologies can protect human health and the environment in an economically beneficial manner. Significant progress is being made in several key research areas, such as catalysis, the design of safer chemicals and environmentally benign solvents and the development of renewable feedstocks. Catalysis is an area of research, which still continues to be a premier frontier area of chemistry. The drive to develop increasingly active and selective heterogeneous catalysts continues with considerable vigour. There is much renowned interest in the field of metal oxides since they are microporous materials with interesting physical as well as catalytic properties depending on the kind of active components and the preparation method. The present innovative research is on sulfated titania systems, their acidity generation by the sulfate anion modification and their use in several reactions having industrial importance. This chapter deals with the general introduction and literature review of the different components of the newly developed systems and the various reactions undertaken for the present investigation.

1.1 GENERAL INTRODUCTION

Even before Berzelius coined the term 'catalysis' in 1836, human beings have used catalysts in the fermentation of drinks (wine) and preparation of food

materials like cheese. Today, catalysis plays a vital role or occupies the center stage in almost 95% of all the processes in chemical manufacturing, petroleum and other petrochemical industries. According to Berzelius, catalyst is a compound, which increases the rate of a chemical reaction, but which is not consumed by the reaction. This definition allows for the possibility that small amounts of the catalyst are lost in the reaction or that the catalytic activity is slowly lost. However, the catalyst affects only the rate of the reaction, it changes neither the thermodynamics of the reaction nor the equilibrium composition. The basic requirements of a catalyst are activity, selectivity, stability, and it should be regenerable, reproducible, economical, mechanically and thermally stable, and should have suitable morphological characteristics.

Catalysis in some form or other is involved in more than 90% of the processes in the petroleum, petrochemical and fertilizer industries. The principal theme in catalysis is the desire to control the rate of chemical reactions and the secondary theme is to understand the mechanism of the control. The application of catalysis has been a necessity for the chemical industry for at least 150 years. Catalysis forms a link between the three main branches of chemistry namely inorganic, physical and organic chemistry. Most of the catalysts, being of inorganic nature, are prepared employing the basic principles of inorganic chemistry whereas their complete characterization requires the application of techniques that form part of physical chemistry. The application of catalysis, being mainly in organic reactions and syntheses, requires a fundamental knowledge of the nature of reactions and their mechanisms. Catalysis is of crucial importance for the chemical industry, the number of catalysts applied in industry is very large and catalysts come in many different forms, from heterogeneous catalysts in the form of porous solids over homogeneous catalysts dissolved in the liquid reaction mixture to biological catalysts in the form of enzymes. Heterogeneous catalysis is an interdisciplinary area, which has become the basis of industrial and

environmental chemistry during this century. The important types of heterogeneous catalysts are metals, metal oxides, clays, zeolites and solid supported heteropoly acids.

Among all the catalysts in use, acid catalysts account a majority of applications both in terms of volume and economy. It is possible to modify the acid properties of the solid acids by adopting various syntheses and post synthesis routes, and confirms these modifications by the available techniques. Conventional industrial acid catalysts such as sulfuric acid, $AlCl_3$ and BF_3 possess unavoidable drawbacks because of their severe corrosive nature and high susceptibility to moisture. The search for environmentally benign heterogeneous catalysts has driven worldwide research towards the development of new materials, which can act as substitutes for current liquid acids and halogen based solid acids[1]. The generation of new acid sites on mixed oxides was first proposed by Thomas[2] and further developed by Tanabe and co-workers[3]. Recently, Connell and Dumesic[4,5] have studied the generation of new acid sites on a silica surface by the addition of several kinds of dopant cations.

The present day chemists are faced with the challenge of developing catalysts, which are highly active, selective and stable and that can be easily recycled. The stress is on a technology that will reduce the dispersion of harmful chemicals in the environment and impart regenerability and durability to the catalysts in such a way as to increase the industrial competitiveness.

1.2 TITANIA

Titanium is the 9th most abundant element in the earth crust and is the 4th most abundant structural element[6]. It was given its name after 'the titans' who in Greek mythology were 'the sons of earth'. Titanium is known for its rare combination of properties such as 'lighter than iron', 'stronger than aluminium'

and 'corrosion resistant as platinum' and has been called the 'wonder metal' because of its unique and useful properties. It is very hard, having high melting point (1667°C) and low density. Being highly reactive, it is never found in the metallic form in nature. It is always found combined with oxygen and other metal oxides. Titanium minerals occurring in nature are ilmenite ($FeTiO_3$), rutile, anatase, brookite, perovskite ($CaTiO_3$), sphene ($CaTiSiO_5$) and geikielite ($MgTiO_3$). Among them ilmenite is the most common and its reserves are wide spread throughout the world including India. Titania, the stable dioxide, exists in three crystalline forms, anatase, rutile and brookite[7]. Anatase and rutile form a tetragonal lattice, whereas brookite is orthorhombic. The structural unit in all three forms is TiO_6 octahedron and different stacking of these octahedra causes the different crystal structures. Out of these, rutile is the thermodynamically most stable form, anatase and brookite are meta stable, which readily get converted to rutile on calcination at higher temperature. Anatase transforms irreversibly and exothermically to rutile in the range of 500-800°C depending on the method of preparation, pressure, presence of impurities, etc.

1.3 INDUSTRIAL APPLICATIONS OF TITANIA

Titania is a versatile material used widely in industry, research and environmental cleaning. The chemical and industrial interest of titania are due to its high opacity, relative chemical inertness and the comparative abundance of titanium ores. It is one of the top twenty inorganic chemicals of industrial importance. It has been used as a pigment from the very beginning of 20th century. In the manufacture of quality papers, anatase is used as filler. Since it is a wide band gap semiconductor, it can absorb UV light and emit radiations of higher wavelength, which is the main requirement for optical brightners[8]. The possibility of using hydrated titania as an ion-exchange agent for treatment of liquid radioactive wastes from nuclear reactor installations and for the separations of uranium from sea water has also been reported[9]. Titania

coatings have been studied for a wide variety of uses, such as antifouling, antibacterial, de-odorising agent and in wet type solar cells[10]. In view of its chemical stability, high refractive index and high dielectric constant, it has also got applications in opto-electronic devices[11]. The high refractive index and chemical inertness make titania an ideal pigment for plastics. Addition of TiO_2 into ceramic materials improves their acid resistance and lowers the sintering temperature[12]. The industrial use of titania has increased many folds recently in the field of its expanded applications as photochromic and photovoltaic sensors[13]. Barium titanate has wide application in thermistor, piezo electric actuator, multi player capacitor, non-linear resistor, thermal switch, passive memory storage device[14] and chemical sensor[15] (due to its surface sensitivity to gas adsorption). Synthetic gems have been produced from rutile, since its refractive index is significantly higher than that of diamond, which makes it a very spectacular gem[16]. Most applications of titania depend on its structural and textural characteristics. Recently use of titania thin films has been extended to medical applications, for example, as an active surface of orthopedic/dental implants[17,18] and as an artificial heart valve[19,20]. Rutile is known to possess unique optical and electronic properties[21] and biological compatibility[19,20]. Titania is mainly used in pigments as an opacifier[22], as a catalyst support[23] and as a semiconductor.

1.4 TITANIA AS CATALYST AND CATALYST SUPPORT

Metal oxides due to their ability to exchange electrons, protons or oxide ions are used as catalysts in both redox and acid-base catalysis[24]. The acidic and basic properties of oxide catalysts are very important for the development of scientific criteria in catalyst application. The surface acidic and basic sites of oxides are involved in the catalytic activity for various reactions such as cracking, isomerization and polymerization. In metal oxides, co-ordinatively unsaturated surface sites are believed to be responsible for their ability towards

adsorption and catalysis towards various reactions. The exposed cations and anions of the metal oxide surface form acidic and basic sites, which accounts for the acid-base catalysis of the oxide systems. Besides this, the variable valency of the cation results in the ability of the oxides to undergo oxidation and reduction. Incorporation of superacidity in solids has been a subject matter of great interest to the scientists working in the field of heterogeneous catalysts ever since the first report of superacidity.

Titania has gained much attention in catalyst industry due to its applications as a catalyst or catalyst support for metal or metal oxide catalysts used in heterogeneous catalysis including photocatalysis of industrially and environmentally important reactions. The major function of a support are to provide higher surface area, better dispersion of active component over it, give thermal and mechanical stability, reduce the quantity of required active component for a particular reaction and thereby to increase the overall efficiency of the catalyst, etc. The use of titania as a catalyst or catalyst support has been gaining importance day by day due to its unique properties, such as presence of acidic, basic, redox sites, thermal shock resistance capacity, ionic conductivity, chemical inertness, and metal support interaction. Recently, much attention has been paid to prepare super-acid titania for many industrially important acid demanding reactions. From the catalytic point of view, TiO_2 possesses a unique type of surface involving both redox and acid-base sites. In addition to high thermal stability, its amphoteric character makes titania a promising catalytic material.

Wei and co workers[25] reported the characterization of mesoporous titania and silica titania materials prepared by urea templated sol-gel method. Acidic properties of TiO_2/SiO_2 mixed oxide modified with H_2SO_4 are also reported[26]. MoO_3-TiO_2 catalysts are used for the catalytic oxidation of 1-butene and butadiene[27]. Acid base properties of mixed oxides of TiO_2 with chromia[28],

silica[29], vanadia[30] and iron[31] have also been reported. It is becoming more and more notable due to its photocatalytic properties. Titania has created strong foundations in today's industrial and manufacturing world. Its uses revolve around its properties to detect the amount of oxygen in the air and its photocatalytic properties. Photocatalysis (catalysis under light irradiation) is attracting a great deal of attention from viewpoints of fundamental science and applications for practical use[32]. Among the semiconductors, TiO_2 is the most frequently investigated one, due to its ability to degrade a variety of harmful organic pollutants including halogenated and nonhalogenated ones, adaptability to work in a specially designed reactor systems even in the presence of solar UV light[33]. These properties can help cleanup the environment by utilizing photocatalytic oxidation of organic compounds by titania powder. Metals or metal oxides supported on TiO_2 are used as a catalyst in phtodegradation of chloroflurocarbons[34] and dichloro acetic acid[35], reduction of NO_x[36], hydro desulfurization[37], ammonia synthesis and selective oxidation of o-xylene[38].

1.5 DIFFERENT METHODS OF PREPARATION OF METAL OXIDES.

Several methods have been used to prepare supported metal catalysts, the most important ones being

i. Precipitation or coprecipitation – In this method, one or more soluble salts which contain the metal of interest are neutralized through the addition of a base (usually ammonia) to form a precipitate or coprecipitate of the corresponding metal oxide[39].

ii. Impregnation – In this method, the support is contacted with a solution, which contains the metal to be deposited on the support. A suspension is initially formed, which is heated under continuous mixing in order to evaporate the solvent and to disperse the metal on the support[40,41].

7

iii. Ion-exchange – This method consists in exchanging either hydroxyl groups or protons from the support with cationic or anionic species in solution. It is important to adjust the pH in order to maximize the electronic interaction between the support and the metal precursor[42].

iv. Deposition method – In this method, the hydroxide of the active components and support are coprecipitated together onto the support, after drying and calcination the active components are surrounded by a thin layer of freshly formed support depositing on the original support surface. This method allows the preparation of catalyst with smaller particle sizes in better dispersion and with larger surface area and allows incorporation of higher loading of the active components[43].

v. Sol-gel method – Here, metal organic precursors are mixed with metal precursors to form a homogeneous solution. The metal organic precursor is hydrolyzed through the addition of water while carefully controlling the pH and the reaction temperature. As hydrolysis and polymerization occur, colloidal particles or micelles with an approximate diameter of 10 nm are formed. These particles continue to increase in size until a metal oxide gel is formed. The solvent can be eliminated by heat treatment in air to form a xerogel or in an autoclave under supercritical conditions to form an aerogel[44-47].

Han *et al.*[48] reported the synthesis of nanocrystalline titania films by micro-arc oxidation. Zhang and coworkers[49] prepared nanosized titania powders by $TiCl_4$ hydrolysis. Synthesis of phosphorous-free mesoporous titania *via.* templating with amine surfactants was reported by Antonelli[50]. Synthesis of mesoporous titania and silica titania materials by urea templated sol-gel reactions was also investigated[51]. Huang *et al.*[52] reported the preparation of sulfated titania catalyst by the decomposition of titanyl sulfate at high temperatures.

1.6 THE SOL-GEL PROCESS

Sol-gel method has its origin in the early work on colloidal chemistry by Thomas Graham in 1861. Since then, the study of colloidal sols were slowly progressing and the chronology of events lead to the evolution of sol-gel science as a viable process for technological applications[53]. Sols and gels are having extremely high surface area. This made them increasingly interesting in the field of catalysis. The Sol-gel process is used for making many different ceramic and glass-like materials. It involves the transition of a mixture from a liquid 'sol' phase into a solid 'gel' phase[53]. Using the sol-gel process it is possible to make ceramic materials from a wide variety of elements. Sol-gel method have attracted much interest in the preparation of titania powders and colloids because of the many uses of these material, as a pigment, filler and, more recently, as a membrane, anti reflection coating, catalyst and photocatalyst. Titania sol-gel synthesis has been developed from inorganic precursors and from metal organic precursors like titanium isopropoxide $(Ti(OPr)_4)$[54]. It is mixed with water containing nitric acid. Reaction occurs between them to give titanium hydroxide. Upon heating the sol, $Ti(OH)_4$ links together to form a three dimensional lattice of linked TiO_2 forming the gel in a process called condensation[55].

1.7 MECHANISM OF SOL-GEL PROCESS

During the initial stage usually referred to as 'pregelation', the reactants (alkoxides and metal precursors) hydrolyze and condense to form a gel. The hydrolysis occurs when water is added to alkoxide, which is usually dissolved in alcohol or some other appropriate solvent. Intermediate obtained as a result of this reaction inclulde: oligomers of the acid, which corresponds to the alkoxide used, which are finally transformed into gels and contain large amounts of water in their structure. In the condensation or polymerization reactions, alkoxide groups (M-OR) react with hydroxyl groups (M-OH) formed

9

during the hydrolysis to form metaloxanes (M-O-M). During this step primary structure and properties of the gel are determined. It is important to note that the conditions under which the condensation reactions occur are important in determining the nature of the final product.

Condensation/hydrolysis can take place by two different mechanisms, which depend on the coordination of the central metal atom. When the preferred coordination is satisfied hydrolysis occurs by nucleophilic substitution and when it is not satisfied it occurs by nucleophilic addition. These mechanisms require that the coordination of oxygen be increased from 2 to 3. The creation of the additional bond involves a lone pair of electrons on the oxygen, and the bond, which is formed, may be equivalent to the other two bonds[56,57]. During the condensation stage a large number of hydroxyl groups can be formed. These hydroxyl groups may either be bridging groups between metal centers or simple OH ligand[58]. The second stage in the sol-gel synthesis is referred to as the 'postgelation' step. Changes, which occur during the drying and calcination of the gel include, desorption of water, evaporation of the solvent, desorption of organic residues, dehydroxylation reactions and structural changes. The evaporation of solvent during drying leads to the formation of strong capillary forces. These capillary forces arise from the difference between solid-vapour and solid-liquid interfacial energies.

1.8 ADVANTAGES OF SOL-GEL METHOD

Sol-gel processing provides a new approach to the preparation of supported metal catalysts. A well-defined pore size distribution can be obtained. A greater degree of control over the catalyst preparation can be achieved in comparison to traditional methods of preparation. One can 'tailor make' catalysts to fit particular applications by using this method. The potential advantages of sol gel processing include: high purity, superior homogeneity, improved thermal stability of the supported metals, the ease with which

additional elements can be added and controlled porosity combined with the ability to form large surface area materials at low temperatures. Particle sizes are in the nano range and they have additional physical and chemical properties, which make them useful as either catalysts or catalyst supports[59-61]. The important variables in the synthesis of supported metals by sol-gel method include: pH, reactant stoichiometries, gelation temperature, metal loading, solvent removal and pretreatment condition. Gonzalez *et al.*[62] had reviewed the effect of important variables in the synthesis of supported metal catalysts using sol-gel method.

1.9 ANATASE AND RUTILE

Titanium dioxide is known to exist in three crystalline modifications, namely rutile (tetragonal), anatase (tetragonal) and brookite (orthorhombic). Anatase and rutile are the common polymorphs of synthetic titania (figure 1.1). In fact, crystallization is highly influenced by their hydrolysis conditions[63]. During the condensation process, the formation of the kinked chains of edge-sharing octahedra corresponding to anatase appears more probable than the formation of the straight chains typical of rutile. Therefore anatase is obtained in processes under kinetic control, whereas processes involving Ostwald ripening lead to the equilibrium phase; i.e. rutile[64]. On the other hand, the brookite structure, in which each octahedron shares one edge, has not been X-ray characterized to date, to our knowledge, in sol-gel process.

Usually, amorphous TiO_2 crystallizes into anatase below 400°C, which is further converted to rutile from 600°C to 1100°C[65]. The rates of transformation are markedly influenced by the particle size or the presence of impurities[66]. The anatase-rutile phase transformation process has been extensively studied over the past decades[67,68]. The temperature for the transition can vary from 400 to 1200°C, depending on (a) the type and amount of additives (b) powder preparation method, and (c) atmosphere. The mechanism by which the additives either inhibit or promote anatase-rutile transformation has been

related to the defect structure of titania, *i.e.,* the concentration of oxygen vacancies or Ti interstitials. It was suggested that the additives, which increases the concentration of oxygen vacancies would also tend to promote the transformation, while some additives would retard the transformation by increasing the lattice defect concentration of Ti interstitials in titania[69]. The inhibitory effect of the alumina, silica and a mixture of the two oxides on the transformation of anatase to rutile in the sol-gel derived titania powders was investigated by Yang and Ferreira[70]. The attention paid to the preparation of fine metal oxides powders has been increasing in the last few years. Investigations of the preparation of fine, monodispersed TiO_2 has played an important role in basic as well as in applied research.

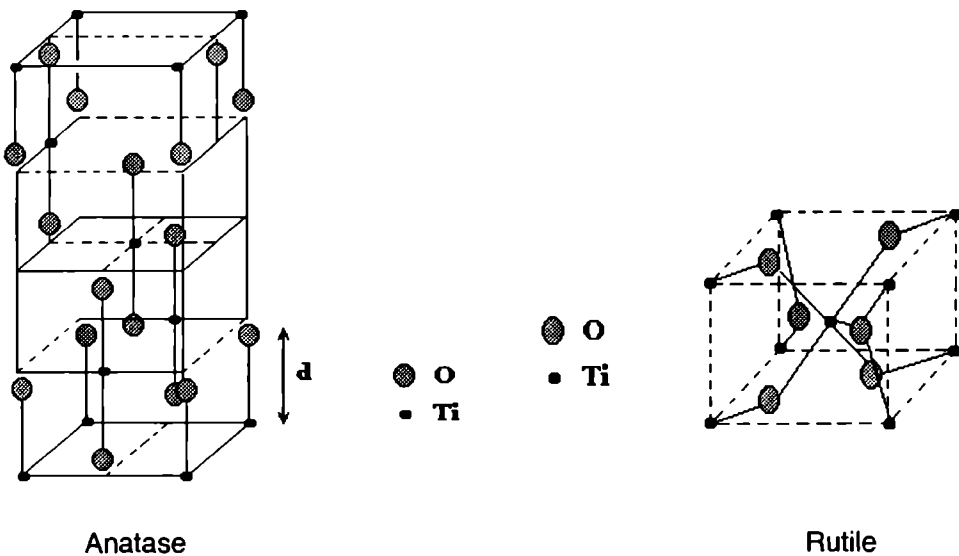Anatase   Rutile

Figure 1.1 Structure of anatase and rutile

1.10 MECHANISM OF ANATASE AND RUTILE CRYSTALLIZATION

It is known that both anatase and rutile TiO_2 can grow from TiO_6 octahedra and their phase transition proceeds by the rearrangement of the octahedra. Arrangement of octahedra and related species through face sharing

initiates the anatase phase, while the edge-sharing leads to the rutile phase[71]. Acids should disperse the aggregated TiO_6 octahedra and the related species in the amorphous phase into discrete TiO_6 octahedra by protonation of the surface Ti-OH groups giving $Ti-OH_2^+$. These protonated surfaces easily combine with -OH groups of other TiO_6 octahedra to form Ti-O-Ti oxygen bridge bonds by eliminating a water molecule. The protonation process followed by phase sharing will result in the favorable formation of anatase phase from the TiO_6 octahedra. Rutile involves both edge sharing and corner sharing-type of linkage. Two opposite edges of each octahedron are edge shared forming a linear chain and the linear chains are linked together through corner oxygen atoms. Anatase, however, has four edges shared per octahedron[72].

Any spatial effect beneficial to the edge sharing polycondensation between TiO_6 octahedra results in rutile phase formation. For example; presence of citrate results in rutile formation. The high degree of protonation of the TiO_6 octahedra enhanced their dispersion in favor of chelation of citrate to TiO_6 octahedra for the formation of the rutile phase and prevented the formation of the anatase phase caused by aggregation of the TiO_6 octahedra in the absence of chelation by citrate or lower degree of protonation. The primary rutile nanocrystallites were formed by the deposition and growth of the dissolved discrete TiO_6 octahedra on the existing nuclei[73]. Suyama and Kata[74] stated that the presence of silica would prevent the nucleation of rutile by impeding the mutual contact of titania particles.

1.11 SULFATED TITANIA

Industrial processes still use mineral liquid acids such as HF and H_2SO_4, which pose an increasing threat to the environment. New stringent environmental regulations limit the use of some of these mineral acids, eg. HF, bringing new opportunities forward to replace them by strong solid acids[75,76].

Sulfated metal oxides such as sulfated zirconia, titania, tin oxide and iron oxide are solid acids that have increasing interest in recent years because of their high thermal stability, strong acidity and unique catalytic activities in many environmentally benign reactions[76-80]. Sulfated titania has been found to be efficient for catalyzing isomerization[81-83], alkylation[84-87], Friedel-Crafts acylation[88,69], esterification[90-92], CFC decomposition[93,94], and selective catalytic reduction of NO_x [95]. Choice of an SO_4^{2-} ion as TiO_2 promoter is attractive since it has high activity in high temperature reactions between 400 and 600°C[96]. Huang et al.[52] reported the use of silica supported sulfated titania for cumene cracking reaction. Sulfated metal oxides were used for protecting carbonyl groups in the synthesis and hydrolysis of dimethyl acetals[97].

The textural properties of these sulfated metal oxides are very poor eg. low surface areas and wide pore distributions. The number of acid sites and acid strength depend on the metal oxide content, nature and method of preparation. To explain the origin of the development of acidic properties in binary metal oxides, Tanabe et al.[1] proposed a model based on the oxidation and coordination number of the involved metals; an excess of positive charge would yield Lewis type acidity while an excess of negative charge would be responsible for the Brönsted acidity. It is reported in the literature [76,98-102] that amorphous $Ti(OH)_4$ should be used as the precursor for sulfation to ensure high sulfur content and strong acidity. The concentration influenced some what the TiO_2 catalyst; the maximum activity and sulfate content were observed with 0.5-1 M sulfuric acid. The catalysts can also be obtained by the treatment with ammonium sulfate, but the catalytic activity is usually lower than that with sulfuric acid[103].

1.12 SURFACE ACIDITY MEASUREMENTS

The acidity of solids plays a significant role when these are used as supports. Interaction of the support with the active component can influence

their catalytic properties. Thus, characterization of the acidity of catalysts is an important step in the prediction of their catalytic utility. The acid-base properties of metal oxide carriers can significantly affect the final selectivity of heterogeneous catalysts[104]. In acid catalysis, the activity, selectivity and stability of solid acids are determined to a large extent by their surface acidity, *i.e.*, the number, nature, strength and density of acid sites. The acid sites (Lewis and/or Brönsted) and base sites, which co-exist in adjacent positions on the surface of acid catalysts, participate together in most of the reactions[3].

Adsorption of bases followed by calorimetry or thermodesorption of stable bases followed by gravimetry or volumetry gives the total number of acid sites (Lewis and Brönsted) and their distribution according to their strength but do not differentiate between Lewis and protonic acid sites[3,105]. Temperature programmed desorption is a useful method to estimate the acid strength of the solid surface for both coloured and colorless materials[106]. Gaseous base molecules, which are adsorbed on an acidic surface, desorb at different elevated temperatures depending upon the strength of acid sites to which they are adsorbed. Molecules that are adsorbed to weak sites will be evacuated preferentially compared to those adsorbed to the strong acid sites at low temperatures. Thus the proportion of adsorbed base evacuated at various temperatures can give a measure of the acid strength of the catalyst. Temperature programmed desorption (TPD) of ammonia is one of the most often used methods to determine the amount and strength of acid sites. In principle, both the concentration of sites having similar acid strengths and the average heat of adsorption or activation energy of ammonia desorption can be determined using TPD method. This method allows the determination of both the protonic and cationic acidities by titrating acid sties of any strength.

Infrared spectroscopic method using pyridine as an adsorbate is extensively used and considered to be the most reliable method to distinguish

between the two types of acid sites. When pyridine is co-ordinatively bonded to Lewis acid sites, characteristic bands are observed at 1450, 1490 and 1610 cm^{-1}. The adsorption of pyridine on Brönsted acid site leads to the formation of pyridinium ion, which gives a band at 1540 cm^{-1} [107]. Upon sulfation the intensity of band corresponding to pyridine coordinated to Lewis sites increases, showing a large number of Lewis acid sites[108]. Pyridine and dimethylpyridine, which specifically adsorb on Lewis and Brönsted sites, have been used as probe molecules to investigate the surface acidic properties. Pyridine is adsorbed on the Lewis acid sites by donation of lone pair of nitrogen to the acid site (sigma donation to a co-ordinatively unsaturated cation) whereas pyridinium ions are formed on Brönsted acid sites. DMP is specifically adsorbed on Brönsted sites due to steric effect and due to its higher basic strength it will detect even the weakest acid centers[101,110]. Lunsford *et al.*[111] pointed out that strong Brönsted acidity requires the interaction of the bisulfate groups with the adjacent Lewis acid sites. Presence of Lewis sites adjacent to Brönsted acid sites results in enhancement of the Brönsted acidity due to the electron withdrawing inductive effect. Huang and coworkers[52] proved that sulfated titania obtained by the decomposition of titanyl sulfate contains acid sites and they are formed as a result of the interaction product of titania with sulfate ions.

The highest acid strength apparently increases with a decrease in the particle size, indicating the generation of new and strong acid sites on small-sized TiO$_2$ particles. Consequently, even on the single- component oxides, *i.e.*, even with the absence of new *M*(1)-O-*M*(2) bonding, new and strong acid sites are generated when the oxide powders are composed of finely divided particles. This is likely to be due to the presence of many oxygen vacancies existing on the surface of small-sized TiO$_2$ particles, since TiO$_2$ is considered to be an n-type semiconductor. The oxygen vacancies generate considerable numbers of dangling bonds, whose energy levels are located in the band gap

region between the valence and the conduction bands. Electrons trapped in these levels probably cause the local charge imbalances, and hence the generation of new and strong acid sites over the surface of finely divided TiO_2 particles[112]. TiO_2 properties can be modified by the addition of other metal oxides. Saur *et al.*[113] proposed that tridentate type bonds $((MO)_3-S=O)$ are present on sulfate supported TiO_2. Tsutomu[114] also proposed that the acidity difference between the TiO_2 and SiO_2 modified with sulfate is due to the difference in coordination number of metal cations in metal oxide, and that the characteristics of the metal cations affect the acid strength and stability of sulfate.

Unsaturated coordination site is necessary to stabilize the sulfate on the surface and to generate the acidic properties. The model for generation of acid sites by sulfation has been explained by the inductive effect due to the difference in the electronegativity between the metal oxide and sulfate ion. In the sulfate ion, $S=O$ structure is essential for the generation of acidic sites on sulfate promoted oxide samples. The strong ability of $S=O$ in sulfate complexes to accommodate electrons from a basic molecule is the driving force in the generation of strong acid properties[26]. The increase of Lewis acid sites due to sulfation mainly leads to the increase of SCR activity in the case of pure TiO_2, but in the case of TiO_2-SiO_2 phase samples, the increase of Ti-O-Ti bonds due to the agglomeration of TiO_2 from the Ti-O-Ti structure through sulfation also contributes to the increase of SCR reactivity[26]. It is reported in the literature[115] that after sulfation large amount of Brönsted and Lewis acid sites are created on the surface of TiO_2. The sulfate species modified the electronic environment around the Ti^{4+} ion by anchoring SO_4^{2-} in either bridging bidentate or chelating bidentate complexes (figure 1.2)[76,96]. Ma *et al.*[116] reported that the surface properties and catalytic activity of sulfated titania prepared by sol-gel method is greater than those prepared from ordinary method. The sulfated precursor is calcined at a high temperature to produce highly covalent sulfate structure on

the surface, which is considered as the source of the strong acidity on this type of material. FT-IR characterization of the surface acidity of different titanium dioxide samples was analyzed[117]. A number of papers have been devoted to the IR characterization of titania surfaces of different origins, and have been reviewed[118,119].
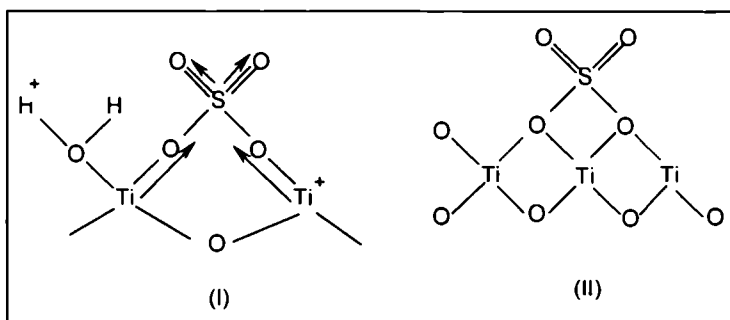
Figure 1.2   The structure (I) bridged bidentate and (II) chelating bidentate SO_4^{2-} and their influence on the neighboring Ti^{4+} ion on TiO_2 surface.

1.13 TEST REACTIONS FOR ACIDITY

Cumene is a conventional model compound for testing the catalytic acidity since it undergoes different reactions over different types of acid sites. It is well known that acidity of the mixed oxide supports has a substantial effect on the activity of cumene cracking. Cumene cracking mainly depends on Brönsted acid sites, whereas dehydrogenation occurs on Lewis acid sites[120,121]. Thus it is possible to compare both Brönsted and Lewis acid sites in a catalyst through cumene conversion reaction. Recently, Zenon[122] reported cumene decomposition over fluoride modified alumina. The cumene decomposition increases marginally and the selective products are benzene and propylene; while sodium modified alumina leads the cumene cracking into α-methyl styrene, which reveals that alumina surface is completely inactive in dealkylation.

The catalytic activity of AISBA towards cumene cracking was investigated by Gedeon[123] to ascertain the acidic property. The cracking

products were only benzene and propene, indicating that the active sites are of Brönsted type. Mishra *et al.*[124] studied the cumene conversion over chromia pillared montmorillonite. Yamagishi[125] found a linear correlation between activity and concentration of Brönsted acidic site over HZSM-5 zeolite. Boorman *et al.*[116,127] prepared a series of catalysts containing fluoride, cobalt and molybdenum as additive to γ-alumina, both individually and in combination and the surface acidity of these systems was correlated with their reactivity for cumene conversion. Sulfated titania obtained by the decomposition of titanyl sulfate at high temperatures shows good cumene conversion at 180°C[52]. Sarbak *et al.*[128] studied the effect of fluoride ions on the activity of γ-alumina for cumene cracking and observed that pure γ-alumina that gave mainly α-methyl styrene on cracking, showed drastic increase in the activity and high selectivity towards benzene after the incorporation of fluoride ions. Sohn and Jang[129] correlated the activity for cumene dealkylation with both acidity and acid strength distribution of sulfated ZrO_2-SiO_2 catalysts. Cumene conversion over sulfated titania catalysts prepared by various methods was explained by Ma *et al.*[116]. Parida and co workers[130] reported the cumene conversion over SO_4^{2-}/TiO_2-SiO_2 with varying amount of SO_4^{2-}, and they obtained α-methyl styrene as the major product. The increase in the acid strength in the case of sulfated catalysts is mainly due to the increase in the number of Lewis acid sties, which facilitate the dehydrogenation reaction.

Selectivity in an alcohol decomposition reaction is regarded as a typical test reaction for investigating the acid-base properties of the catalytic sites on the metal oxides[131-135]. Metal oxide surface can catalyze both dehydration and dehydrogenation of alcohols. Studies utilizing different alcohols showed that acid sites on the catalyst surface cause dehydration of the alcohol molecule and the basic sites cause dehydrogenation[136]. The reaction proceeds through different routes on different active sites. There are two basic modes of reaction

during alcohol decomposition, (i) dehydration to form an olefin and water and (ii) dehydrogenation to form an aldehyde (in the case of primary alcohols) or a ketone (in the case of secondary alcohol) and hydrogen. Rachel *et al.*[137] studied the selectivity for dehydrogenation reaction in the decomposition of cyclohexanol as a function of copper loading. Aramendia *et al.*[138] observed an increase in selectivity towards cyclohexanone in the decomposition of cyclohexanol by doping sodium carbonate in zinc phosphate. Investigations on alumina by Pines *et al.*[139] spot out the formation of methyl cyclopentene on stronger acidic sites, which is formed by the isomerization of cyclohexene.

1.14 REACTIONS SELECTED FOR THE PRESENT STUDY

I. Alkylation of arenes

The Friedel-Crafts reaction is probably one of the most important reactions in organic chemistry, and is of great interest due to their importance and common use in synthetic and industrial chemistry. These are important means for attaching alkyl chains to aromatic rings and are widely used in the synthesis of large number of fine chemicals such as drugs, fragrances, dyes and pesticides[140,141]. Alternative ways to replace the common Lewis acids, such as $AlCl_3$ by catalytic reagents in Friedel-Crafts reactions are of considerable industrial interest because these stoichiometric reagents, which are destroyed after usual aqueous workup required to isolate the organic products, cause severe environmental pollution. Alkyl groups normally activate the aromatic ring towards electrophilic substitution reactions and formation of polyalkylate products is always observed in Friedel-Crafts alkylation, leading to decreased yields and laborious separation procedures. Therefore, in recent years, a great deal of effort has been directed towards the promotion of this reaction and several synthetic procedures have been reported for this reaction. These methods involve montmorillonite[142], zeolite[143], sol-gel derived silica or

alulminosilicates[144] and other catalysts[145-148]. Laszlo *et al.*[147] and Cseri *et al.*[148] reported the benzylation of benzene and toluene with benzyl chloride and benzyl alcohol over cation exchanged K10.

Samantaray[87] studied the physico-chemical properties and catalytic activity of sulfated titania for the gas phase alkylation of benzene and substituted benzenes using isopropanol as alkylating agent. Catalytic activity was found to be dependent on the sulfate ion concentration in the catalyst and also benzene to alcohol molar ratio. Sulfated oxides of tin, zirconium, titanium, aluminium, hafnium and iron gave good conversions. Supported oxides like WO_3/ZrO_2, WO_3/TiO_2 WO_3/SnO_2 and MoO_3/ZrO_2 were also active whereas WO_3/Fe_2O_3 and B_2O_3/ZrO_2 were completely inactive[148]. James Clark[151] investigated the use of sulfated zirconia as catalysts for the alkylation of benzene with long chain linear alkenes to form linear alkylbenzenes. He *et al.*[152] studied the alkylation of benzene with benzyl chloride over iron supported mesoporous materials. A comparative study on H_2SO_4, HNO_3 and $HClO_4$ treated metakaolinite as Friedel-Crafts alkylation catalyst has been reported[153]. The effect of impregnating $ZnCl_2$, $FeCl_3$, $MnCl_2$, $SnCl_2$ and $AlCl_3$ on the catalytic activity of natural kaolinite and its activated form for the Friedel-Crafts alkylation of benzene with benzyl chloride is examined[154].

para-Tertiary-butylphenol is widely used in the manufacture of phenolic resins as well as antioxidants and polymerization inhibitors. In general, tertiary butylation of phenol is carried out in homogeneous medium using sulfuric acid, fluro sulphonic acid, phosphoric acid, and aluminum chloride-boric acid or boron trifluoride etherate as catalysts[155]. However owing to environmental problems, such as disposal of liquid waste and separation of product from the catalyst, considerable attention has been focused towards the development of solid acid catalysts for this reaction. It is reported that molecular sieve based catalysts like SAPO-11[156], zeolite[157], AlMCM-41[158] and FeMCM-41[159] were

proved to be potential catalysts for the *tert*-butylation of phenol among the various solid catalysts. However, the reaction of *tert*-butylation of phenol gives numerous products depending on the nature of the catalysts as well as on the reaction temperature. Sakthivel *et al.*[160] reported the vapour phase *tert*-butylation of phenol over sulfated zirconia catalyst with a high selectivity to *para* isomer.

II. Beckmann rearrangement of cyclohexanone oxime

ε-caprolactam is used as a monomer for nylon-6 fibers, engineering plastics and for the preparation of L-lysine, which is an essential ingredient in animal food. Conventional method of preparation of ε-caprolactam involves treating cyclohexanone oxime with concentrated sulfuric acid or phosphoric acid as catalyst and followed by neutralization with liquid ammonia. Although this procedure is convenient from a chemical point of view, the large amount of ammonium sulfate formed during the subsequent neutralization of the oleum, the use of large amounts of fuming sulfuric acid and the corresponding problem of corrosion make this process environment non-friendly. To overcome these problems, a vapour phase Beckmann rearrangement of cyclohexanone oxime using various solid catalysts has been extensively investigated. The solid acid catalysts tested for this reaction include alumina-supported boria[161], ZSM-5[162], silicate-1[163], TS-1[164], SAPO-11[165] and Al_2O_3-supported B_2O_3[166]. Butler *et al.*[167] used the H-Y and H Pd-Y as catalysts and found that highly proton exchanged zeolites were active and selective for this rearrangement. Yashima *et al.*[168] studied the vapour phase rearrangement of cyclohexanone oxime on different zeolites catalyst and reported relatively low cyclohexanone conversion and selectivity towards ε-caprolactam over ferrierite catalyst. Sumitomo Chemical Co. Ltd. began to manufacture caprolactam with a new vapour phase process by applying high silica MFI zeolites catalyst in 2003[169]. Ishida *et al.*[170] reported the theoretical study on the Beckmann rearrangement over silicalite-1.

22

Corma *et al.*[171,172] reported that ε-caprolactam is converted to 5-cyanopent-1-ene on H-Na-Y zeolites. Sato *et al.*[173] found that on high siliceous ZSM-5, a catalyst with low acidity, leads to high selectivity of ε-caprolactam due to the smooth desorption of caprolactam. B_2O_3/ZrO_2 was reported to be highly active and selective for the synthesis of ε-caprolactam at 300-320°C during 8 h process time, the ε-caprolactam yield is parallel to the number of intermediate strong acid sites[174]. The acidic and catalytic properties of boria supported on TiO_2-ZrO_2 binary oxide for vapour phase Beckmann rearrangement of cyclohexanone oxime were found to be affected by the boria loading. It is suggested that the medium acid sites are responsible for the selective formation of ε-caprolactam[175]. Solvent effect has been investigated in the vapour phase Beckmann rearrangement over B_2O_3/TiO_2-ZrO_2 It is revealed that the performance of the reaction is strongly dependent on the nature of the solvent[176]. The facility of protonation of oxime is primarily dependent upon the competitive adsorption between substrate and the solvent. Polar solvents gave higher selectivity to lactam and lower deactivation rates than non-polar solvents, since desorption of lactam from the catalyst surface was promoted by the attack of a polar solvent molecule.

Xu and co workers[174,177] reported that the catalytic performance of boria supported on zirconia, a characteristic carrier that possesses both acidic and basic properties, was much better than that of other boria catalysts supported on Al_2O_3, SiO_2, TiO_2 and MgO. Acid function is essential for the rearrangement reaction, but concomitantly the acid sites of the catalysts will also adsorb caprolactam product strongly due to the acid-base interaction. Izumi *et al.*[178] suggested that higher selectivity and less coking might be expected if a catalyst contains a basic component in addition to the acid one and if the former promote the desorption of lactam without impairing the acid function.

III. Nitration of phenol

Industrial aromatic nitrations are carried out in a mixture of nitric acid and sulfuric acid predominantly giving *ortho-* and *para-* substituted products for substituted benzene. However, this process has a major problem of the spent acid disposal. The formation of water during the reaction causes the dilution of the nitrating mixture, thus reducing the rate of nitration as the reaction proceeds. Recent advances in superacid catalysts have brought considerable research importance to this reaction. Attempts are being made to reduce the spent acid generated during this reaction and increase the selectivity by properly substituting the type of catalyst with proper solvents. A variety of combinations of solid acids have been investigated for their suitability as nitration systems for aromatics[179]. Different solid acids tested so far include zeolites[180], partially dealuminated[181] or cation exchanged zeolites[182], sulphonated ion exchange resins (polystyrenesulphonic acid)[183], clay supported metal nitrates[184], Fe^{3+} on K-10 montmorillonite[185], modified silica[180], silica-alumina and supported acids[186,187]. Various nitration procedures have been described in the last few years making use of different nitrating agents like NO_2 (N_2O_4), N_2O_5, molten nitrate salts, alkyl and acyl nitrates, etc[179,188].

Prins *et al.*[181,189] already reported several types of efficient catalysts for the vapour phase nitration by dilute nitric acid. Halvarson and Melander[190] found a high *o/p* ratio in the nitration of anisole with benzoyl nitrate in acetonitrile. Currie *et al.*[191] reported the nitration of phenols and anisols in micro emulsion media based on the cationic surfactants. Catalytic performance of various solid acid catalysts for benzene nitration with nitric oxide (NO_2) as nitration agent in the vapour phase has been studied by Sato *et al.*[188]. Very high regioselective nitration of phenol was achieved with a surfactant suspended in acetonitrile treated with nitronium tetrafluoroborate[192]. Nitration has been performed by $AcONO_2/HNO_3$ and aromatic solvents[193],

N-nitropyrazole/BF$_3$, Et$_2$O/CH$_2$Cl$_2$[194] *viz.* nitroso compounds and their subsequent oxidation to nitro compounds with HNO$_3$[195], metal nitrates[196], clay supported nitrates[197], impregnated alumina and silica with N$_2$O$_4$[198], AcONO$_2$[199] and TfONO$_2$[200]. Waller *et al.*[201,202] reported the use of lanthanide (III) triflates, water tolerant Lewis acids, as catalysts for the nitration of simple arenes with 69% nitric acid in 1,2-dichloroethane. Sato *et al.*[203] investigated nitration over different solid acid catalysts using nitric acid as the nitrating agent. Montmorillonite ion exchanged with multivalent cations and mixed metal oxides containing TiO$_2$ and ZrO$_2$ exhibited high activity.

IV. Photochemical degradation of methylene blue

The chemistry and interaction of molecules and ions at the surface /solution interface has been the subject of recent research and the absorption of organic molecules is of interest as it concerns titania particulates[204-208]. Waste water generated by the textile industries are known to contain considerable amounts of non-fixed dyes, especially of azo-dyes, and a huge amount of inorganic salts. It is well known that some azo-dyes and degradation products such as aromatic amines are highly carcinogenic[209]. Among the different process for the treatments of textile dyes, heterogeneous photocatalysis was found as an emerging destructive technology leading to the total mineralization of most of organic pollutants[210-212]. In most cases, the degradation is conducted for dissolved compounds in water with UV illuminated TiO$_2$ powder. Nanosized materials can have enhanced photochemical properties with respect to bulk specimens because it shows low band bending, facilitating the presence of both type of charge carriers (electron and holes) at or near the surface of titania (n type semiconductor) being thus readily available for both reductive and oxidizing steps of the photocatalytic process[213,214].

After the discovery of photo induced water splitting at titanium dioxide (TiO$_2$) electrodes[215], the phenomenon has been applied to TiO$_2$-mediated

heterogeneous photocatalysts[216-231]. Because electrons and holes photogenerated in the TiO_2 photocatalysts have strong reduction and oxidation power, they can drive a variety of reactions. It has been reported that pollutants in air and water can be effectively decomposed[216,218-220,232] by utilizing this property. It has also been reported that unique organic synthetic reactions occur on irradiated TiO_2[216-231]. Most of these investigations have been carried out under UV light, because TiO_2 absorbs light of wavelength 400 nm or shorter. In order to utilize sunlight or rays from artificial sources more effectively in photocatalytic reactions, photocatalysts with strong absorptions in the visible region should be developed. For this purpose, doping of TiO_2 powder with transition metals has been investigated[233,234]. Recently, Umebayashi *et al.*[235] succeeded in synthesizing TiO_2 doped with S atoms. However, the absorption spectra of these compounds in the visible region are extremely small. It is noted that the dopants are incorporated as anions and take the place of oxygen in the lattice of TiO_2. Illumination of semiconductors with energy greater than the band gap energy promotes electrons from the valence band to conduction band, leaving behind positive holes. When TiO_2 is illuminated with light of $\lambda < 390$ nm, it generates electron/hole pairs for this purpose so one employs titania as photocatalysts. The valence band potential is positive enough to generate hydroxyl radicals at the surface and the conduction band potential is negative enough to reduce molecular O_2. The hydroxyl radical is a powerful oxidizing agent and attacks organic pollutants present at or near the surface of titania resulting usually in their complete oxidation to CO_2[49,236].

It is reported [237] that the overall rate of photocatalytic reactions in liquid systems is governed by the capture of electrons and positive holes by surface adsorbed substrates and also by the electron-hole recombination (e^- - h^+). This implies that a highly active TiO_2 photocatalyst should simultaneously possess two properties: a large surface area to adsorb a substrate and a high degree of

crystallinity to reduce e^- - h^+ recombination. The photodegradation of a cationic dye, Malachite Green, is examined both in an anionic surfactant and in a cationic surfactant under visible irradiation using titania[238]. Ohno and coworkers[239] studied photocatalytic activity of S-doped TiO_2 photocatalyst under visible light for the degradation of methylene blue. Photocatalytic kinetics of phenol and its derivatives over UV irradiated TiO_2 was studied[240]. Photodegradation of 4-nitrophenol using titania[241], TiO_2/SiO_2[242], and SO_4^{2-} /TiO_2[243] were also studied.

1.15 OBJECTIVES OF THE PRESENT WORK

Catalysis is probably one of the most ancient chemical phenomena to find an application in that, many of the early molecules were formed by catalytic processes involving metal or photocatalysis. An exceptional heterogeneous catalyst must possess both high activity and long-term stability. But the most important quality is selectivity, which reflects its ability for direct conversion of reactants in a specific way. Titania has attracted considerable attention as catalysts for a variety of acid-mediated reactions. Now a days titania photocatalysts has attracted a great deal of attention in environmental waste-water treatment, because it generates highly oxidative hydroxyl free radicals, which can degrade refractory organics under UV irradiation, and because it has chemical stability, non-toxicity, and is of low cost. Sulfated metal oxides have attracted considerable attention in the last decade and among the sulfated oxides the most studied systems are based on zirconia and titania. A systematic investigation of the influence of sulfate ions and transition metals on the properties of titania has been carried by various physico-chemical characterization techniques. Catalytic activity of the systems was screened for various industrially important reactions. The main objectives of the present work are the following.

➢ To prepare titania, sulfated titania and transition metal loaded sulfated titania by sol-gel method.

✑ Physico-chemical characterization of the prepared samples using XRD, EDX, SEM, TGA, FTIR, UV-Vis DRS, ^{1}H NMR, and surface area pore volume measurements.

✑ To explore the acidic character of all the catalysts through various independent techniques. Total acidity as well as acid site distribution obtained by ammonia TPD method. Adsorption studies using perylene as electron acceptor provided information regarding the Lewis sites in presence of Brönsted acid sites. The TG analysis of the samples after adsorption of sterically hindered 2,6-dimethylpyridine served to obtain a comparative evaluation of the Brönsted acidity of different systems.

✑ To compare the surface acidic properties using cyclohexanol decomposition and cumene conversion as test reaction.

✑ To investigate the catalytic efficiency of the prepared systems towards industrially important Friedel-Crafts benzylation of aromatics and to examine the impact of the various reaction parameters like substrate to benzyl chloride molar ratio, reaction temperature, reaction time etc on the activity and selectivity. To study the metal leaching and deactivation of the systems during the reaction.

✑ To test the applicability of the catalytic systems for the vapour phase *tert*-butylation of phenol at different reaction temperatures, molar ratios and flow rates.

✑ To evaluate the catalytic performance of these systems in Beckmann rearrangement of cyclohexanone oxime and in the nitration of phenol under different experimental conditions.

✑ To test the photocatalytic activity of the prepared systems for the degradation of methylene blue under solar irradiation.

ଓ ଔଶୋଔଶୋଔଶୋ ଓ
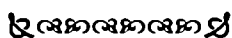
REFERENCES

1. K. Tanabe, M. Misono, Y. Ono, H. Hattori, *"Solid acids and bases and their catalytic properties"*, Tokyo, Kodansha, Academic Press (1990).

2. C.L. Thomas, *Ind. Eng. Chem.*, 41 (1949) 2564.

3. K. Tanabe, *"Solid Acids and Bases"*, Academic Press, New York (1970) 103.

4. G. Connell, J.A. Dumesic, *J. Catal.*, 102 (1986) 216.

5. G. Connell, J.A. Dumesic, *J. Catal.*, 105 (1987) 285.

6. Jelks Barksdale, *"Titanium-its occurrence, chemistry and technology"*, The Ronald Press Co. USA (1966).

7. Kirk-Othmer, *"Encyclopedia of Chemical Technology"*, Wiley Inter Science Publication, John Wiley & sons, 3^{ed} Eds. (1983).

8. *"Technology in Indian titanium industry"*, DSIR, Ministry of Sci. & Tech., New Delhi (1993).

9. G.R. Dhoshi, V.N. Sastry, *Ind. J. Chem.*, (1977) 904.

10. B.O. Regan, M. Gretzel, *Nature*, 353 (1991) 737.

11. P.V. Kamat, *"Semiconductor Nanoparticles – Physical, Chemical and Catalytic aspects"*, Eds. P.V. Kamat, D. Maisel, Elsevier, Amsterdam (1997).

12. E.A. Barringer, H.K. Boowen, *J. Am. Ceram. Soc.*, 65 (1982) 199.

13. C.J. Barbe, M. Gretzel, *Mat. Res. Soc. Symp. Proc.*, (1996) 43.

14. M.Z.C. Hu, G.A. Miller, E.A. Payzant, C.J. Rown, *J. Mat. Sci.*, 35 (2000) 2927.

15. H. Nishizava, M. katsube, *J. Solid State Chem.*,131 (1997) 43.

16. R.T. Lidd, Coat jr in *"Hand book of gem identification"*, Gemological Institute of America, Los Angeles (1966).

17. P.J. Li, C. Ohtsuki, T. Kokubo, K. de Groot, J. Biomed, *Mater. Sci.*, 28 (1994) 7.

18. T. Kitsugi, T. Nakamura, M. Oka, *J. Biomed. Mater. Res.*, 32 (1996) 149.

19. X.H. Wang, F. Zhang, C.R. Li, *Surf. Coat. Technol.*, 128-129 (2000) 36.

20. Y.X. Leng, J.Y. Chen, Z.M. Zeng, *Thin Solid Films*, 377-378 (2000) 573.

21. F. Zhang, Z. Zheng, X. Zheng, X. Ding, *J. Vac. Sci. Technol. A.*, 15 (1997) 1824.

22. E.J. Mezey, *"Vapour deposition"*, C.F. Powell, J.H. Olxey, J.M. Blocher, (Eds), Wiley, New York (1966) p. 423.

23. M.R. Bankmann, R. Brand, B.H. Engler, J. Ohmer, *Catal. Today*, 14 (1992) 225.

24. J. Haber *"Perspectives in Catalysis"*, Blackwell scientific publications (1992) 371.

25. J.Y. Zheng, J.B. Pang, K.Y. Qiu, Y. Wei, *Micropor. Mesopor. Mater.*, 94 (2001) 189.

26. S.M. Jung, P. Grange, *Appl. Catal. A. Gen.*, 228 (2002) 65.

27. D. Vanhove, S. Rithi, A. Fernadez, M. Blanchard, *J. Catal.*, 57 (1975) 253.

28. K. Kohler, C.W. Schlapfer, A. Von Zelewsky, J. Nickl, J. Engweiler, A. Baiker, *J. Catal.*, 143 (1993) 201.

29. C.U.I. Odenbrand, J.G.M. Brandin, G. Busca, *J. Catal.*, 135 (1992) 505.

30. G. Busca, F. Cavani, F. Trifiro, *J. Catal.*, 106 (1987) 471.

31. T. Lopez, J.A. Moreno, R. Gomez, X. Bokhimi, J.A. Wang, H. Y. Madeira, G. Pecchi, P. Reyes, *J. Mater. Chem.*, 12 (2002) 714.

32. Masao Kaneko, Ichiro Okura (Eds.), *"Photocatalysis Science and Technology"*, Kodansha Ltd. Tokyo (2002) 1.

33. K.H. Wang, Y.H. Hsiech, M.Y. Chong, C.Y. Chong, *Appl.Catal. B. Environ.*, 21 (1999) 1.

34. Y. Takita, H. Yamada, M. Hashida, T. Ishihara, *Chem. Lett.*, (1990) 715.

35. D.W. Bahnemann, *Israel J. Chem.*, 33 (1993) 115.

36. B.E. Handy, M. Maciejewski, A. Baiker, *J. Catal.*, 134 (1992) 75.

37. K.Y.S. Ng, E. Gulari, *J. Catal.*, 95 (1985) 33.

38. A. Nobile jr, V. Van Brunt, M.W. Davis, *J. Catal.*, 127 (1991) 227.

39. O.V. Krylob, *"Catalysis by Nonmetals"*, Academic Press, New York (1970).

40. W. Zou, R. D. Gonzalez, *Catal. Lett.*, 12 (1992) 73.

41. A.L. Bonivardi, M.A. Baltanas, *J. Catal.*, 125 (1990) 243.

42. W. Zou, R.D. Gonzalez, *J. Catal.*, 152 (1995) 291.

43. F. Pinna, *Catal. Today*, 41 (1998) 129.

44. L.C. Klein, *Ann. Rev. Mat. Sci.,* 15 (1985) 227.

45. B.E. Yoldas, *J. Sol-Gel Sci. Tech.,* 1 (1993) 65.

46. S.J. Teichner, G.A. Nicolaon, M.A. Vicarini, G.E.E. Gardes, *Adv. Colloid Interface Sci.,* 5 (1976) 245.

47. T. Lopez, P. Bosch, M. Moran, R. Gomez, *J. Phys. Chem.,* 97 (1993) 1671.

48. Y. Han, S.H. Hong, K. Xu, *Mater. Lett.,* 56 (2002) 744.

49. Q. Zhang, L. Gao, J. Guo, *Appl. Catal. B. Environ.,* 26 (2000) 207.

50. D.M. Antonelli, *Micropor. Mesopor. Mater.,* 30 (1999) 315.

51. J.Y. Zheng, J.B. Pang, K. Y. Qiu, Y. Wei, *Micropor. Mesopor. Mater.,* 49 (2001) 189.

52. Y.Y. Huang, B.Y. Zhao, Y.C. Xie, *Appl. Catal. A. Gen.,* 171 (1998) 65.

53. L.L. Hench, L. Larry, J.K. West, K. Jon, "The Sol-Gel Process", *Chem. Rev.,* 90 (1990) 33.

54. J. Livage, M. Henry, C. Sanchez, *Prog. Solid State Chem.,* 18 (1988) 259.

55. S. Doeuff, M. Henry, C. Sanchez, J. Livage, *J. Non-Cryst. Solids,* 89 (1987) 206.

56. K.J. McNeil, J.A. Dicarpio, D.A. Walsh, R.F. Prat, *J. Amer. Chem. Soc.,* 102 (1980) 1859.

57. E.J.A. Pope, J.D. Mackenzie, *J. Non-Cryst. Solids,* 87 (1986) 185.

58. V. Baran, *Coord. Chem. Rev.,* 6 (1971) 65.

59. T. Lopez, M. Asomaza, P. Bosch, E. Garcia-Figueroa, R. Gomez, *J. Catal.,* 138 (1992) 463.

60. H.D. Gesser, P. C. Goswami, *Chem. Rev.,* 89 (1985) 765.

61. K. Tanabe, *Mater. Chem. Phys.,* 13 (1985) 347

62. R.D. Gonzalez, T. Lopez, R. Gomez, *Catal. Today,* 35 (1997) 293.

63. K. Tanabe, K. Kato, H. Miyazaki, S. Yamaguchi, A. Imai, Y. Iguchi, *J. Mater. Sci.,* 29 (1994) 1617.

64. J.P. Jolivet, in *De la solution a' l' oxyde,* Inter Edition, Paris (1994) p. 98.

65. E.F. Heald, C.W. Weiss, *Am. Mineral.*, 57 (1972) 10.

66. M. Ocana, J.V. Garcia-Romos, C.J. Serna, *J. Am. Ceram. Soc.*, 75 (1992) 201.

67. R.A. Eppler, *J. Am. Ceram. Soc.*, 70 (1987) c. 64.

68. X.Z. Ding, X.H. Lui, Y.Z. He, *J. Mater. Sci. Lett.*, 13 (1994) 462.

69. R.D. Shannon, J.A. Pask, *J. Am. Ceram. Soc.*, 48 (1965) 391.

70. J. Yang, J.M.F. Ferreira, *Mater. Lett.*, 36 (1998) 320.

71. K. Yanagisawa, J. Ovenstone, *J. Phys. Chem. B.*, 183 (1999) 7781.

72. C.J. Brincker, *J. Non-Cryst. Solids*, 100 (1988) 31.

73. H. Yin, Y. Wada, T. Kitamura, S. Kambe, S. Murasawa, H. Mori, T. Sakata, S. Yamagida, *J. Mater. Chem.*, 11 (2001) 1694.

74. Y. Suyama, A. Kata, *Yogyo Kyokaishi*, 86 (1978) 119.

75. T. Yamaguchi, *Appl. Catal.*, 61 (1990) 1.

76. K. Arata, *Adv. Catal.*, 37 (1990) 165.

77. B.H. Davis, R.A. Keogh, R. Srinivasan, *Catal. Today*, 20 (1994) 219.

78. A. Corma, *Chem. Rev.*, 95 (1995) 559.

79. X. Song, A. Sayari, *Catal. Rev. Sci. Eng.*, 38 (1996) 329.

80. G.D. Yadav, J.J. Nair, *Micropor. Mesopor. Mater.*, 33 (1999) 1.

81. Z. Gao, J.M. Chen, *Chem. J. Chin. Uni.*, 15 (1994) 873.

82. Z. Gao, J.M. Chen, W.M. Hua, Y. Tang, *Stud. Surf. Sci. Catal.*, 90 (1994) 507.

83. A.K. Dalai, R. Sethuraman, S.P.R. Kathikaneni, R.O. Idem, *Ind. Eng. Chem. Res.*, 37 (1998) 3869.

84. C. Guo, S. Yao, J. Cao, Z. Qian, *Appl. Catal. A.*, 107 (1994) 229.

85. A. Corma, A. Martinez, C. Martinez, *Appl. Catal. A.*, 144 (1996) 249.

86. A. Hess, E. Kemnitz, *Appl. Catal. A.*, 149 (1997) 373.

87. S.K. Samantaray T. Mishra, K.M. Parida, *J. Mol. Catal. A.*, 156 (2000) 267.

88. Y.D. Xia, W.M. Hua, Z. Gao, *Catal. Lett.*, 55 (1998) 101.

89. W.M. Hua, Y.D. Xia, Y.H. Yue, Z. Gao, *J. Catal.*, 196 (2000) 104.

90. G.Z. Lu, *Appl. Catal. A.,* 133 (1995) 11.

91. J. Lin, *Chin. J. Org. Chem.,* 20 (2000) 805.

92. J. Lin, H.T. Liu, R.Q. Zhal, *Chin. J. Inor. Chem.,* 16 (2000) 829.

93. X.Z. Fu, W.A. Zeltner, Q. Yang, M.A. Anderson, *J. Catal.,* 168 (1997) 487.

94. Z. Ma, W.M. Hua, Y. Tang, Z. Gao, *Chin. J. Chem.,* 18 (2000) 341.

95. S. M. Jung, P. Grange, *Catal. Today,* 59 (2000) 305.

96. J.P. Chen, R.T. Yang, *J. Catal.,* 139 (1993) 277.

97. C.H. Lin, S.D. Lin, Y.H. Yang, T. P. Lin, *Catal. Lett.,* 73 (2001) 121.

98. K. Tanabe, H. Hattori, T. Yamaguchi, *Crit. Rev. Surf. Chem.,* 1 (1990) 1.

99. F.R. Chen, G. Coudurier, J.F. Joly, J.C. Vedrine. *J. Catal.,* 143 (1993) 616.

100. C. Guo, S. Yao, J. Cao, Z. Qian, *Appl. Catal. A.,* 107 (1994) 229.

101. R.A. Comelli, C.R. Vera, J.M. Parera, *J. Catal.,* 151 (1995) 96.

102. C. Morterra, G. Cerrato, F. Pinna, M. Signoretto, *J. Catal.,* 157 (1995) 109.

103. K. Arata, *Appl. Catal. A. Gen.,* 146 (1996) 3.

104. M.R. Guisnet, *Acc. Chem. Res.,* 23 (11) (1990) 393.

105. J. Kijenski, A. Baiker, *Catal. Today,* 5 (1989) 1.

106. H. Matsuhashi, H. Motoi, K. Arata, *Catal. Lett.,* 26 (1994) 325.

107. H. Hattori, S. Miyashita, K. Tanabe, *Bull. Chem. Soc. Jpn.,* 44 (1971) 893.

108. J.L. Fores-Moreno, L. Baraket, F. Figueras, *Catal. Lett.,* 77 (2001) 1.

109. A. Corma, C. Rodellas, V. Fornes, *J. Catal.,* 88 (1984) 374.

110. H.A. Benesi, *J. Catal.,* 28 (1973) 176.

111. J.H. Lunsford, H. Sang, S.M. Campbell, C.H. Liang, R.G. Anthony, *Catal. Lett.,* 27 (1994) 305.

112. K. Nisriwaki, N. Kakuta, A. Ueno, H. Nakabayashi, *J. Catal.,* 118 (1989) 498.

113. O. Saur, M. Bensitel, A.B.M. Saad, J.C. Lavalleyl, C.P. Tripp, B.A. Morrow, *J. Catal.,* 99 (1986) 104.

114. Y. Tsutomu, *Appl. Catal.,* 61 (1990) 1.

115. R.T. Yang, W.B. Li, N. Chen, *Appl. Catal. A. Gen.*, 169 (1998) 215.

116. Z. Ma, Y. Yue, X. Deng, Z. Gao, *J. Mol. Catal. A. Chem.*, 178 (2002) 97.

117. G. Buska, H. Saussey, O. Saur, J.C. Lavalley, V. Lorenzelli, *J. Catal.*, 14 (1985) 245.

118. G.D. Parfitt, *Progr. Swrf. Membr. Sci.*, 11 (1976) 181.

119. H. Knozinger, *Advan. Catal.*, 25 (1976) 184.

120. J.T. Richardson, *J. Catal.*, 9 (1967) 182.

121. E.T. Shao, E. Mc. Innich. *J. Catal.*, 4 (1965) 586.

122. S. Zenon, *Appl. Catal. A.*, 159 (1997) 147.

123. A. Gedeon, A. Lassoued, J.L. Bonardet, J. Fraissard, *Micropor. Mesopor. Mater.*, 44-45 (2001) 801.

124. T. Mishra, K. Parida, *Appl. Catal. A. Gen.*, 166 (1998) 123.

125. K. Yamagishi, S. Namba, T. Yashima, *J. Catal.*, 121 (1990) 47.

126. P.M. Boorman, R.A. Kydd, Z. Sarbak, A. Somogyvari, *J. Catal.*, 96 (1985) 115.

127. P.M. Boorman, R.A. Kydd, Z. Sarbak, A. Somogyvari, *J. Catal.*, 100 (1986) 287.

128. Z. Sarbak, *Appl. Catal. A. Gen.*, 159 (1997) 147.

129. J.R. Sohn, H.J. Jang, *J. Mol. Catal.*, 64 (1991) 349.

130. K.M. Parida, S.K. Samantaray, H.K. Mishra, *J. Colloid Inter. Sci.*, 216 (1999) 127.

131. K. Tanabe, M. Misono, Y. Aso, H. Hattori, *" New solid acids and bases, Their catalytic properties"*, B. Belmon, J.T. Yates (Eds), 51 Elsevier, Amsterdam, (1989).

132. J. Cunningham, B.K. Hodnett, M. Ilyas, E.L. Leahy, J.L.G. Fierro, *Faraday Disc. USS. Chem. Soc.*, 72 (1981) 1283.

133. M. Ai, *Bull. Chem. Soc. Jpn.*, 50 (1977) 2579.

134. H. Nollery, G. Ritler, *J. Chem. Soc. Faraday. Trans.*, 80 (1984) 275.

135. C. Bezouhanava, M.A. al-Zihari, *Catal. Lett.*, 11 (1991) 245.

136. A. Gervasini, A. Auroux, *J. Catal.*, 131 (1991) 190.

137. A. Rachel, V. Durgakumari, P. Kanta Rao, *"Catalysis: Modern Trends"* (Eds., N.M. Guptha and D.K.. Chakrabarthy) 1995, Narosa publishing House, New Delhi, India.

138. M.A. Armendia, V. Borau, C. Jimenez, J.M. Marinas, F.J. Romero, *J. Catal.,* 151 (1995) 44.

139. H. Pines, C.N. Pillai, *J. Am. Chem. Soc.,* 82 (1960) 2401.

140. H.W. Kouwenhova, H. van Bekkum, *"Handbook of Heterogeneous Catalysis",* Eds. G. Ertl, H. Kozinger, J. Wietkamp, Vol. 5, p. 2358, Weinheim (1997).

141. J. March, *"Advanced Organic Chemistry"* 4th Edn., Wiley, New York, (1992).

142. J.H. Clark, A.P. Kybett, D.J. Macquarrie, S.J. Barlow, P. London, *J. Chem. Soc. Chem. Commun.,* (1998) 1353.

143. D. Das, S. Cheng, *Appl. Catal. A.,* 201 (2000) 159.

144. J.M. Miller, M. Goodchild, J.L. Lakshmi, D. Wails, J.S. Hartman, *Catal. Lett.,* 63 (1999) 199.

145. D. Baudry, A. Dormond, F. Montagne, *New J. Chem.,* 18 (1994) 871.

146. M.F. Gotta, H. Mayr, *J. Org. Chem.,* 63 (1998) 9769.

147. T.P. Smyth, B.W. Corby, *J. Org. Chem.,* 63 (1998) 8946.

148. K. Arata, H. Nakamura, M. Shouji, *Appl. Catal. A.,* 197 (2000) 213.

149. P. Laszio, A. Mathy, *Helv. Chim. Acta.,* 70 (1987) 577.

150. T. Cseri, S. Bekassy, F. Figueras, S. Rizner, *J. Mol. Catal. A. Chem.,* 98 (1995) 101.

151. J.H. Clark, G.L. Monks, D.J. Nightingale, P.M. Price, J.F. White, *J. Catal.,* 193 (2000) 348.

152. N. He, S. Bao, Q. Xu, *Appl. Catal. A. Gen.,* 169 (1998) 29.

153. K.R. Sabu, R. Sukumar, R. Rekha, M. Lallithambika, *Catal. Today,* 49 (1999) 321.

154. R. Sukumar, K.R. Sabu, L.V. Bindu, M. Lallithambika, *"Recent Advanced in Basic an Applied Aspects of Industrial Catalysis"*, T.S.R. Prasada Rao, G. Murali Dhar (Eds.) *Stud. Surf. Sci. Catal.*, 113 (1998) p. 557.

155. S.H. Patinuin, B.S. Friedman, *" Alkylation of Aromatics with Alkenes and Alkanes in Friedel Crafts and Related Reactions"*, Vol. 3, ed. G.A. Olah Interscience, New York (1964) p.75.

156. S. Subramanian, A. Mitra, C.V.V. Satyanarayana, D.K. Chakrabarty, *Appl. Catal. A.,* 159 (1997) 229.

157. K. Zhang, C. Huang, H. Zhang, S. Xiang, S. Liu, D. Xu, H. Li, *Appl. Catal. A.,* 166 (1988) 89.

158. A. Sakthivel, S.K. Badamali, P. Selvam, *Micropor. Mesopor. Mater.,* 39 (2000) 457.

159. S.K. Badamali, A. Sakthivel, P. Selvam, *Catal. Lett.,* 65 (2000) 153.

160. A. Sakthivel, N. Saritha, P. Selvam, *Catal. Lett.,* 72 (2001) 225.

161. S. Sato, S. Hasebe, H. Sakurai, K. Urabe, Y. Izumi, *Appl. Catal. A.,* 29 (1987) 107.

162. S. Sato, N. Ishii, K. Hirose, S. Nakamura, *Stud. Surf. Sci. Catal.,* 22 (1986) 187.

163. T. Komatsu, T. Maeda, T.Yashima, *Micropor. Mesopor. Mater.,* 35-3 (2000) 173.

164. A. Thangraj, S. Sivasanker, P Ratnaswamy, *J. Catal.,*137 (1992) 252.

165. P.S. Singh, R. Bandyopadhyay, S.G. Hegde, B.S. Rao, *Appl. Catal. A.,* 136 (1996) 249.

166. S. Sato, K. Urabe, Y. Izumi, *J. Catal.,* 102 (1986) 99.

167. J.D. Butler, T.C. Poles, *J. Chem. Soc. Perkin II,* (1973) 1262.

168. T. Yashima N. Oka, T. Komastu, *Catal. Today,* 38 (1997) 249.

169. H. Ichihashi, M. Kitamura, *Catal. Today,* 73 (2002) 23.

170. M. Ishida, T. Suzuki, H. Ichihashi, A. Shiga, *Catal. Today,* 87 (2003) 187.

171. A. Corma, H. Garcia, J. Primo, *Zeolites.,* 11 (1991) 593.

172. A. Aucejo, M.C. Burguet, A. Corma, V. Fomes, *Appl. Catal.,* 22 (1986) 187.

173. H. Sato, K. Hirose, Y. Nakamera, *Chem. Lett.*, (1993) 1987.

174. B.Q. Xu, S.B. Cheng, S. Jiang, Q.M. Zhu, *Appl. Catal. A.*, 188 (1999) 361.

175. D. Mao, G. Lu, Q. Chen, Z. Xie, Y. Zhang, *Catal. Lett.*, 77 (2001) 119.

176. D. Mao, Q. Chen, G. Lu, *Appl. Catal. A. Gen.*, 244 (2003) 273.

177. S.B. Cheng, B.O. Xu, S. Jiang, F.P. Tian, T.X. Cai, X.S. Wang, Chin, *J. Catal.*, 17 (1996) 512.

178. Y. Izumi, S. Sato, K. Urabe, *Chem. Lett.*, (1983) 1649.

179. G.A. Olah, R. Malhotra, S.C. Narang, *"Nitration, Methods and Mechanism"*, VCH, NewYork (1974).

180. L.V. Malysheva, E.A. Paukshtis, K.G.Ione, *Catal. Rev. Sci. Eng.*, 37 (1995) 179.

181. L.E. Bertea, H.E. Kouwenhoven, R. Prins, *Appl. Catal. A. Gen.*, 129 (1995) 229.

182. K. Smith, *Bull. Soc. Chim. Fr.*, (1989) 272.

183. O.L. Wright, J. Teipel, D. Thoennes, *J. Org. Chem.*, 30 (1965) 1301.

184. P. Laszlo, J.Vandormeal, *Chem. Lett.*, (1988) 1843.

185. B.M. Choudary, M. R. Sarma, K. Vijayakumar, *J. Mol. Catal.*, 87 (1994) 33.

186. J.M. Riego, Z. Sedin, J.M. Zaldivar, N.C. Marziano, C. Torato, *Tetrahedron Lett.*, 37 (1996) 513.

187. E. Suzuki, K. Tohmori, Y. Ono, *Chem. Lett.*, (1987) 2273.

188. H. Sato, K. Hirose, *Appl. Catal. A. Gen.*, 174 (1998) 77.

189. L.E. Bertea, H.E. Kouwenhoven, W. Harman, R. Prins, *Stud. Surf. Sci. Catal.*, 78 (1993) 607.

190. K. Halvarson, L. Melander, *Arkiv Kemi*, 11 (1957) 77.

191. F. Currie, K. Holmberg, G. Westman, *Colloids and Surfaces A.*, 182 (2001) 321.

192. H. Pervez, S.O. Onyisiuka, J.R. Rooney, J. Sukling, *Tetrahedron*, 44 (1988) 4555.

193. J.A.R. Rodrigues, A.P. de Oliveira Filho, P.J.S. Moran, R. Custodio, *Tetrahedron*, 55 (1999) 6733.

194. A. Germain, *J. Chem. Soc. Chem. Commun.*, (1990) 1697.

195. E. Santaniello, M. Ravasi, *J. Rog. Chem.*, 48 (1983) 739.

196. R.J. Maleski, M. Kunge, D. Sicker, *Synth. Commun.*, 25 (1995) 2327.

197. S.C. Bisarya, S.K. Joshi, A.G. Holkar, *Synth. Commun.*, 23 (1993) 1125.

198. A. Cornelis, P.P. Laszlo, *Synlett.*, (1994) 155.

199. S.M. Nagy, E.A. Zubkov, V.G. Shubin, E.A. Paukshitis, N.L. Razdobarova, *Acta Chim. Hung.*, 129 (1992) 576.

200. S.M. Nagy, K.A. Yarovoy, M.M. Shakirov, V.G. Shubin, L.A. Vostrikova, K.G. Ione, *J. Mol. Catal.*, 64 (1991) 31.

201. J.F. Waller, A.G.M. Barrett, D.C. Braddock, D. Ramprasad, *J. Chem. Soc. Chem. Commun.*, (1997) 613.

202. J.F. Waller, A.G.M. Barrett, D.C. Braddock, D. Ramprasad, *Tetrahedron Lett.*, 39 (1998) 1641.

203. H. Sato, K. Hirose, K. Nagai, H. Yoshioka, Y. Nagaoka, *Appl. Catal. A. Gen.*, 175 (1998) 201.

204. S. Lakshmi, R. Reganathan, S. Fujitha, *J. Photochem. Photobiol. A.*, 88 (1995) 163.

205. W.Z. Tang, *Chemosphere*, 9 (1995) 4171.

206. Z. Shourong, H. Qinggue, Z. Jun, W. Bingkun, *J. Photochem. Photobiol. A.*, 108 (1997) 235.

207. T. Wu, T. Lin, J. Zhao, H. Hidaka. N. Serpone, *Enviorn. Sci. Techmol.*, 33 (1999) 1379.

208. T. Wu, G. Liu, J. Zhao, H. Hidaka, N. Serpone, *J. Phys. Chem. B.*, 103 (1999) 4862.

209. M.A. Brown, S.C. De-Vito, *"Critical Reviews in Environmental Science and Technology"*, 23 (1993) 249.

210. M. Schiavello, (Eds.) *"Photocatalysis and Environment: Trends and Applications"*, Kluwer Academic Publishers, Dordrecht, (1988).

211. N. Serpone, T. Pelizzetti (Eds.), *"Photocatalysis: Fundamentals and Applications"*, Wiley Interscience, New York, (1989).

212. O. Legrini, E. Oliveros, A.M. Braun, *Chem. Rev.*, 93 (1993) 671.

213. W. Choi, A. Termin, M.R. Hoffman, *J. Phys. Chem.,* 98 (1994) 13669.

214. A.J. Maira, K. L. Yeung, J. Soria, J.M. Coronado, C. Belvee, C.Y. Lee, V. Augugliaro, *Appl. Catal. B.,* 29 (2001) 327.

215. A. Fujishima, K. Honda, *Nature,* 238 (1972) 5551.

216. M.R. Hoffman, S.T. Martin, W. Choi, D.W. Bahnemann, *Chem. Rev.,* 95 (1995) 69.

217. L. Cao, F. Spiess, A. Huang, S.L. Suib, T.N. Obee, S.O. Hay, J.D. Freihaut, *J. Phys. Chem.,* 103 (1999) 2912.

218. D.S. Muggli, J.L. Falconer, *J. Catal.,* 187 (1999) 230.

219. E.J. Wolfrum, J. Haung, D.M. Blake, P.C. Maness, Z. Haung, J. Fiest, W.A. Jacoby, *Environ. Sci. Technol.,* 36 (2002) 3412.

220. J. Theurich, D.W. Bahnemann, R. Vogel, F.E. Dhamed, G. Alhakimi, I. Rajab, *Res. Chem. Intermed.,* 23 (1997) 247.

221. S. Yanagida, Y. Ishimaru, Y. Miyake, T. Shiragmi, C. Pac, K. Hashimoto, T. Sakata, *J. Phys. Chem.,* 93 (1989) 2576.

222. B. Ohtani, J. Kawaguchi, M. Kozawa, S. Nishimoto, T. Inui, *J. Chem. Soc. Faraday. Trans.,* 91 (1995) 1103.

223. T. Ohno, T. Kigoshi, K. Nakabeta, M. Matsumura, *Chem. Lett.,* (1998) 877.

224. T. Ohno, K. Nakabeya, M. Matsumura, *J. Catal.,* 176 (1998) 76.

225. F. Soana, M. Sturini, L. Cermenati, A. Albini, *J. Chem. Soc. Perkin Trans.,* 2 (2000) 699.

226. R.W. Mattews, *J. Chem. Soc. Faraday Trans.,* 1, 80 (1984) 457.

227. M. Fujihira, Y. Satoh, T. Osa, *Nature,* 293 (1981) 206.

228. M. Dusi, C.A. Muller, T. Mallat, A. Bakier, *Chem. Commun.,* (1999) 197.

229. E. Baciocchi, C. Rol, G.V. Sevastiani, L. Taglieri, *J. Org. Chem.,* 59 (1994) 5272.

230. E. Baciocchi, T.D. Giacco, M.I. Ferrero, C. Rol, G.V. Sevastiani, *J. Org. Chem.,* 62 (1997) 4015.

231. T. Ohno, K. Tokieda, S. Higashida, M. Matsumura, *Appl. Catal.* A., 1 (2003) 6462.

232. L. Cao, F. Spiess, A. Huang, S.L. Suib, T.N. Obee, S.O. Hay, J.D. Freihaut, *J. Phys. Chem.*, 103 (1999) 2912.

233. T. Ohno, F. Tanigawa, K. Fujihara, S. Izumi, M. Matsumura, *J. Photochem. Photobiol. A.*, 127 (1999) 107.

234. M. Anpo, *Catal. Surv. Jpn.*, 1 (1997) 169.

235. T. Umebayashi, T. Yamaki, H. Ito, K. Asai, *Appl. Phys. Lett.*, 81 (2002) 454.

236. B. Ohtani, S.-w. Zhang, S.-I. Nishimoto, T. Kagiya, *J. Photochem. Photobiol. A.*, 64 (1992) 223.

237. A. Sclafani, I. Palmisano, M. Schiavello, *J. Phys. Chem.*, 94 (1990) 829.

238. J. Zhao, K. Wu, T. Wu, H. Hidaka, N. Serpone, *J. Chem. Soc. Faraday Trans.*, 94(5) (1998) 673.

239. T. Ohno, T. Mitsui, M. Matsumura, *Chem. Lett.*, 32(4) (2003) 364.

240. D. Chen, A.K. Ray, *Appl. Catal. B. Environ.*, 23 (1999) 143.

241. M.S. Dieckmann, K.Y.A. Gray, *Wat. Res.*, 30 (1996) 1169.

242. S.S. Hong, M.S. Lee, S.S. Park, G.D. Lee, *Catal. Today*, 87 (2003) 99.

243. S.K. Samantaray, P. Mohapatra, K. Parida, *J. Mol. Catal. A. Chem.*, 198 (2003) 277.

Chapter 2

Materials And Experimental Methods

The performance of a catalyst depends on the method of preparation and catalyst pretreatment conditions apart from the reaction parameters. It is possible to modify the properties of the catalyst by adopting various syntheses and post syntheses routes. Materials and a detailed description of the experimental procedures used for catalyst preparation and characterization are described in this chapter. In the present work sol-gel method is used for the preparation of catalysts. Surface acidity of the prepared systems is determined by ammonia TPD, perylene adsorption, 2,6-dimehtyl pyridine adsorption studies and test reactions like cumene cracking and cyclohexanol decomposition. Reactions of industrial importance such as Friedel-Crafts alkylation, *tert*-butylation of phenol, Beckmann rearrangement of cyclohexanone oxime and nitration of phenol are chosen for the catalytic activity studies. Photocatalytic activity of the catalysts is tested by methylene blue degradation reaction.

2.1 INTRODUCTION

Catalysis is a complex surface phenomenon occurring on the active sites on the surface of a catalyst. A proper understanding of the phenomenon of catalysis requires a thorough knowledge of the nature of the active sites and the type of interaction, which changes according to the preparation conditions and reaction variables. The recent technological advances have resulted in the development of several modern characterization techniques, a proper

utilization of which provides greater insight into the molecular aspects of the catalysts and the nature of the active sites involved.

2.2 CATALYST PREPARATION

The catalyst support was prepared through sol-gel technique. The modifications were done using different transition metals with different weight percentages by the same route. The sulfate modification of the samples is done by wet impregnation using 0.5 M sulfuric acid solution.

MATERIALS

The materials used for catalyst preparation are given below.

	Materials	Suppliers
1.	Titanium isopropoxide	Aldrich
2.	Conc. Nitric acid	Merck
3.	Conc. Sulfuric acid	Merck
4.	Chromium (III) nitrate	Merck
5.	Manganese (II) nitrate	Merck
6.	Iron (III) nitrate	Merck
7.	Cobalt (II) nitrate	Merck
8.	Nickel (II) nitrate	Merck
9.	Copper (II) nitrate	Merck
10.	Zinc (II) nitrate	Merck

METHODS

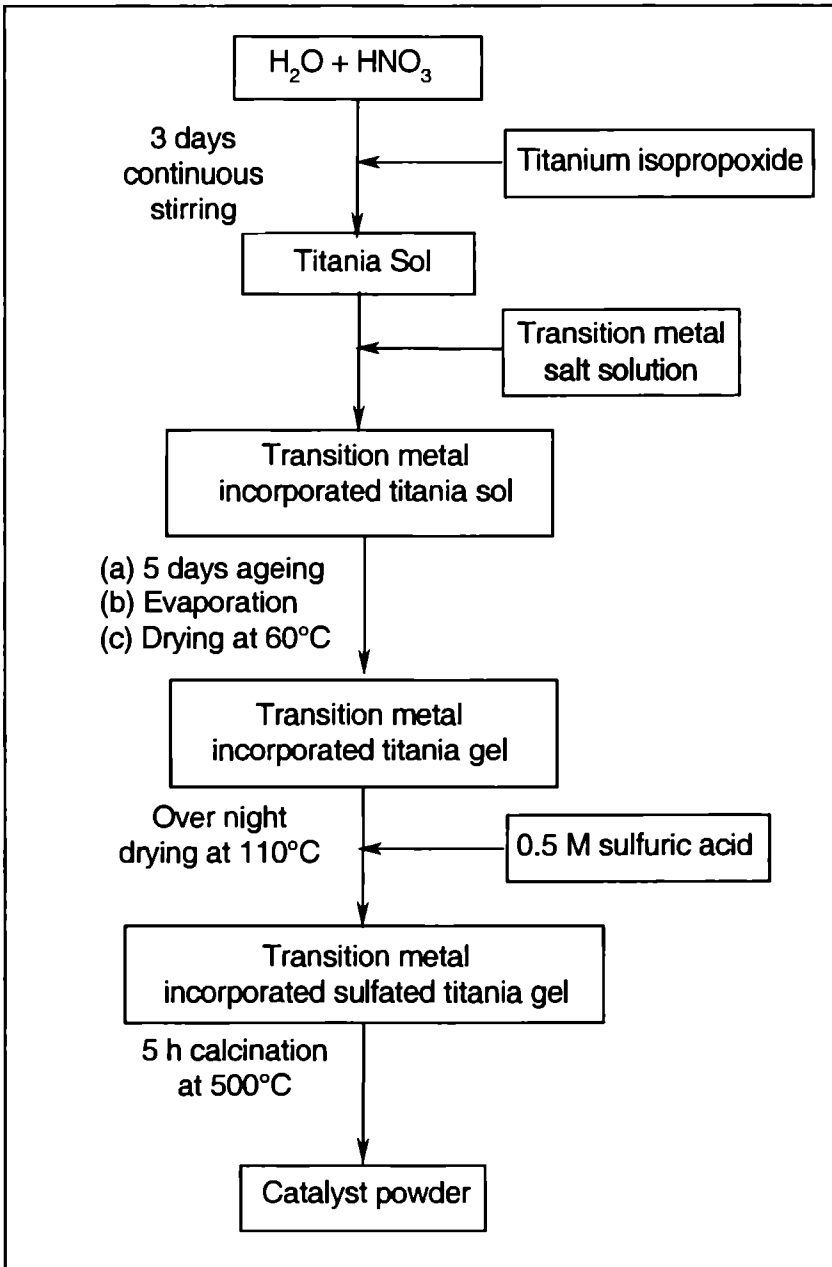A detailed experimental procedure is given as a flow chart in figure 2.1.

Figure 2.1 Preparation process of transition metal loaded sulfated titania

I. PREPARATION OF TITANIA

Titanium isopropoxide was added to water-nitric acid (Conc.) mixture in the volume ratio 5:60:05 with constant stirring. Precipitation occured immediately and the precipitate was stirred vigorously at room temperature to form a highly dispersed sol. After ageing the sol for 5 days, it was concentrated at 60°C to get the gel. The gel was dried at 110°C for 12 h in an air oven and powdered below 100 microns mesh size. The titanium hydroxide obtained was calcined at 500°C in air for 5 h in a muffle furnace.

II. PREPARATION OF SULFATED TITANIA

The sulfated titania is prepared from titanium hydroxide by a single step impregnation using 0.5 M sulfuric acid solution (2 mL g^{-1} of titanium hydroxide). The gel was dried at 110°C for 12 h, powdered and calcined for 5 h at 500°C in air.

III. PREPARATION OF TRANSITION METAL LOADED SULFATED TITANIA

25 mL of titanium isopropoxide was hydrolyzed in 300 mL water containing 2.5 mL Conc. nitric acid and the resulting precipitates were stirred continuously. To this highly dispersed sol, calculated amount of metal nitrate solution was added and stirred for 4 h. The metal loading was varied from 3, 6 and 9% and the metals incorporated include Cr, Mn, Fe, Co, Ni, Cu and Zn. After ageing it was concentrated and dried at 60°C to get the gel. Sulfation was done using 0.5 M sulfuric acid solution (2 mL g^{-1} of titanium hydroxide). The samples, after overnight drying at 110°C, were powdered and calcined at 500°C for 5 h.

2.3 CATALYST NOTATIONS

The catalyst systems developed for the present study and their designations are given below.

44

Notation	System
T	Pure titania
ST	Sulfated titania
STX (y)	Sulfated titania containing metals (X) such as Cr, Mn, Fe, Co, Ni, Cu and Zn having weight % (y) of 3,6 & 9.

2.4 CHARACTERIZATION TECHNIQUES

In heterogeneous catalysis, the reaction occurs on the surface of the catalyst. Catalysis and catalytic surface hence need to be characterized with reference to their physical properties and by their activity. The prepared catalytic samples were characterized using a variety of physico chemical methods like BET surface area and pore volume measurements, X-Ray Diffraction, Energy Dispersive X-Ray analysis, Scanning Electron Microscopy, Infrared Spectroscopy, UV-Vis-Diffuse reflectance spectroscopy, ^{1}H NMR and TG-DTG analysis. Before each characterization, except for thermogravimetric analysis, the samples were activated at 500°C for 2 h.

MATERIALS

The materials used for the characterization are

	Materials	Suppliers
1.	Liquid Nitrogen	Sterling gases Pvt. Ltd.
2.	Potassium bromide	Merck
3.	Magnesium oxide	Merck

METHODS

A brief discussion of each method of characterization and its experimental aspects is given in the following sections.

45

I. X-RAY DIFFRACTION (XRD) ANALYSIS

Characterization of a catalyst can be done by many techniques, among which the first and foremost is the technique of the X-ray diffraction. This gives information on the geometry of the crystal lattice, the unit cell structure and on the major and minor phases of the samples. It is a versatile method for the qualitative and quantitative analysis of solid samples and can provide useful information about the crystallite size of specific components and the purity of the substance[1].

The principle of XRD is based on the diffraction of monochromatic X-rays by the different planes in the crystal lattices. The diffraction principle developed by M.L. Bragg is the most general diffraction theory. X-rays are diffracted by each mineral differently, depending on the atoms constituting the crystal lattice and how these atoms are arranged. In X-ray powder diffractometer, X-rays are generated within a sealed tube under vacuum. When an X-ray beam hits a sample and is diffracted, we can measure the distance between the planes of the atoms that constitute the sample by applying Bragg's Law. $n\lambda = 2d \sin\theta$, where the integer n is the order of the diffracted beam, λ is the wavelength of the incident X-ray beam, d is the distance between adjacent planes of atoms (the d-spacing), and θ is the angle of incidence of the X-ray beam. The characteristic set of d spacing generated in a typical X-ray scan provides a unique "fingerprint" of the mineral or minerals present in the sample. When properly interpreted, by comparison with standard reference patterns and measurements, this "fingerprint" allows for identification of the material. Crystallite size L (Å) can be determined using Scherrer equation[2], $L = K\lambda / \beta \cos\theta$, where θ and λ are the Bragg angle and the wavelength of the X-ray respectively. L is the mean diameter of the crystallites composing the powder sample; K is a constant approximately equal to 0.9-1.0 and related to the crystallite shape. β is the full width half maximum (FWHM) of the strongest

peak on the 2θ scales in radians. XRD patterns were recorded in a *Rigaku D-max* X-ray diffractometer using Ni filtered Cu-K radiation ($\lambda = 1.5406$ Å). The crystalline phases were identified by comparison with the data from JCPDS (Joint Committee on Powder Diffraction Standards) data file[3].

II. SURFACE AREA AND PORE VOLUME MEASUREMENTS

In heterogeneous catalysis, the reaction occurs at the surfaces. To predict the catalyst properties, surface area determination is very important. Brunauer-Emmette-Teller (BET) method is the most widely used procedure for the determination of the surface area of solid materials and involves the use of BET equation. This method is based on the physical adsorption of gases on solid surfaces, which leads to multi layer adsorption[5]. A simple form of this equation can be written as

$$P / [V (P_o\text{-}P)] = [1 / V_m C] + [(C\text{-}1) / V_m C] [P / P_o]$$

where V is the volume of gas adsorbed at equilibrium pressure P and P_o is the standard vapour pressure of the adsorbate at liquid nitrogen temperature and C is isothermal constant. By plotting $P / [V (P_o\text{-}P)]$ vs P / P_o and determining V_m from the slope of the resultant straight line in the partial pressure range of 0.05 to 0.35, the specific surface area can be calculated using the relation

$$A = V_m N_o A_m / W \times 22414$$

where N_o is the Avagadro number, A_m the molecular cross sectional area of the adsorbate (0.162 nm^2 for nitrogen) and W the weight of the sample (g).

Micromeritics Gemini-2360 surface area analyzer was used to determine the surface area under liquid nitrogen temperature using nitrogen gas as the adsorbent. Previously activated samples at 500°C were degassed at 400°C under nitrogen atmosphere for 4 h prior to each measurement. The pore

volumes of the samples were also measured using the same instrument by the uptake of nitrogen at a relative pressure of 0.9.

III. ENERGY DISPERSIVE X-RAY (EDX) FLUORESCENCE ANALYSIS

Energy dispersive X-ray (EDX) fluorescence analysis is one of the most successful analytical methods for the quantitative and qualitative elemental analysis of solid samples. This method is used to determine the composition of individual particles in a catalyst sample. During EDX analysis, the specimen is bombarded with an electron beam. The bombarding electrons collide with the specimen atoms, knocking some of electrons off during the process. A position vacated by an ejected inner shell electron is eventually occupied by a higher energy electron from an outer shell, giving up some of its energy as a photon of X-ray. The atom of every element releases X-rays with unique amount of energy during the transferring process. Thus, by measuring the amount of energy present in the X-rays being released by a specimen during electron beam bombardment, the identity of the atom from which the X-ray was emitted can be established. The integrated peak areas, after application of appropriate correction factors, can give the percentage composition of each of the elements[4].

Powdered sample is put on a double sided carbon tape on a metal strip before analysis. EDX spectra of the samples were recorded in an *EDX-JEM-35* instrument (JEOL Co. link system AN-1000 Si-Li detector).

IV. SCANNING ELECTRON MICROSCOPY (SEM)

Scanning electron microscopy is used for inspecting topographies of specimens at very high magnifications. It is based on the interaction of electrons with matter and their appreciable scattering by quite small atomic clusters. During SEM inspection, a beam of electrons is focused on a spot volume of the specimen resulting in the transfer of energy to that. These bombarding electrons, also referred to as primary electrons, dislodge electrons

from the specimen itself. The dislodged electrons, also known as secondary electrons, are attracted and collected by a positively biased detector and then translated into a signal. To produce the SEM images, the electron beam is swept across the area being inspected, producing many such signals. These signals are then amplified, analyzed and translated into images of the topography being inspected. This enables very impressive, in-focus images to be obtained from highly irregular structures typical of catalyst specimens.

This technique is of great interest in catalysis, particularly because of its high spatial resolution[6]. The powdered sample is put on a double sided carbon tape on a metal strip. It is further sputter coated with gold to minimize the charging effect and to protect the material from thermal damage by the electron beam. A film of uniform thickness, about 0.1mm, was maintained for all the samples. Scanning electron micrographs of the samples were taken using *Cambridge Oxford 7060* scanning electron microscope with resolution of 1.38 eV.

V. THERMOGRAVIMETRIC ANALYSIS (TGA)

Thermogravimetric analysis (TGA) is a thermal analysis technique used to measure changes in the weight (mass) of a sample as a function of temperature and/or time. TGA is commonly used to determine the absorbed moisture content, decomposition temperature, drying range, calcination temperature and stability limit of a catalyst.

In TG analysis, the sample is placed into a tared TGA sample pan, which is attached to a sensitive microbalance assembly and is subsequently placed into a high temperature furnace. The balance measures the initial sample weight at room temperature and then continuously monitors changes in the sample weight (losses or gains) as heat is applied to the samples. From the thermogram, information about dehydration, decomposition and various forms

of products at various temperatures can be obtained. The derivative of the thermogram (DTG) gives a better understanding of the weight loss and can also be used to determine the thermal stability of the samples. *TGAQ V2.34* thermal analyzer (*TA instruments*) was used for carrying out thermogravimetric studies under nitrogen atmosphere at a heating rate of 20°C per minute.

VI. FOURIER TRANSFORM INFRARED (FTIR) SPECTROSCOPY

FTIR spectroscopy is one of the few techniques capable of exploring the catalyst, both in bulk and its surface, under the actual reaction conditions. FTIR spectroscopy is a technique that provides information about the chemical bonding or molecular structure of materials. It is used to identify unknown materials present in a specimen.

The technique works on the fact that bonds and groups of bonds vibrate at characteristic frequencies. A molecule that is exposed to infrared rays absorbs infrared energy at frequencies, which are characteristic to that molecule. The specimen's transmittance and reflectance of the infrared rays at different frequencies is translated into a plot consisting of peaks. In the case of sulfated metal oxide the frequencies and intensities of IR bands can give abundant evidence on the state of metal support interaction, structure, metal-metal interaction, etc. From the position and intensity of bands, the structure and co-ordination behavior of the sulfate groups present on the catalyst surface can be identified[7,8]. FTIR spectra of the powder samples were measured by the KBr disc method over the range 4000-400 cm^{-1} using *Magna 550 Nicolet* instrument.

VII. UV-VIS DIFFUSE REFLECTANCE SPECTROSCOPY (UV-VIS-DRS)

Diffuse reflectance spectroscopy (DRS) is a non-invasive technique that uses the interaction of light, absorption and scattering, to produce a characteristic reflectance spectrum, providing information about the structure and composition of the medium. It gives information regarding electronic

transition between orbitals or bands in the case of atoms, ions and molecules in gaseous, liquid or solid state. Electronic transition of transition elements are of two types, namely, metal centered transitions [d-d or (n-1)d–ns] and charge transfer (CT) transitions. d-d Transitions gives information about the oxidation state and co-ordination environment of transition metal ion. (n-1)d–ns Transitions are often too high in energy to be observed in the spectrum. The CT transitions are intense since they are Laporte-allowed and are sensitive to the nature of donor and acceptor atoms[9].

The surface of the sample is responsible for the reflection and absorption of the incident radiation and hence diffuse reflectance spectra is used in the study of chemistry and physics of surfaces. The most appropriate theory treating diffuse reflections and the transmission of light scattering layers is the general theory developed by Kubelka and Munk[10]. For an infinitely thick, opaque layer, the Kubelka- Munk equation can be written as,

$$F (R_\infty) = (1 - R_\infty)^2 / 2R_\infty = k / s$$

where 'R_∞' is the diffuse reflectance of the layer relative to a nonabsorbing standard such as MgO, 'k' is the molar absorption coefficient of the sample and 's' is the scattering coefficient. Provided 's' remains constant, a linear relationship should be observed between F (R_∞) and k. The spectra were computer processed and plotted as percentage absorbance vs wavelength using the principle of Kubelka-Munk analysis. Diffuse reflectance UV-Vis spectra of the samples were recorded at room temperature between 200 and 800 nm using MgO as standard in an *Ocean Optics AD 2000* instrument with a CCD detector.

VIII. SOLID STATE ^{1}H NUCLEAR MAGNETIC RESONANCE (NMR) SPECTROSCOPY

Solid-State Nuclear magnetic resonance (NMR) techniques represent a novel and promising tool in the repertoire of methods for examining the

molecular structure of amorphous, microcrystalline and crystalline powders. In heterogeneous catalysis, its principal use is to characterize the chemical and structural environment of atoms in the catalyst or in the species adsorbed on the catalyst surface[11]. The interaction of nuclear magnetic moment with an external magnetic field, leads to a nuclear energy level diagram with a certain eigen states. Transitions between the eigen states within the energy levels can occur and is recorded as a spectral line. In addition to the structural information provided, the direct proportionality of the signal intensity to the number of contributing nuclei makes NMR useful for quantitative studies[12].

Solid state NMR studies of heterogeneous catalysts are usually carried out by 'Magic Angle Spinning' (MAS) NMR i.e., rapid rotation of the sample about an axis subtended at an angle 54°44' with respect to the magnetic field. This technique removes line broadening from dipolar interactions, chemical shift anisotropy and quadrupolar interactions to the first order, since all of the interactions contain the angular term $3\cos^2? - 1$ which is zero for $? = 54.7°$. The number of signals in the solid state NMR spectrum gives the number of different structural environmental factors of the observed nucleus in the sample while the relative signal intensities correspond to the relative occupancies of the different environments[13]. ^1H MAS NMR spectroscopy has shown to be an exceedingly useful technique for characterizing the hydroxylated surfaces of metal oxides. All measurements were carried out using a *DSX 300 Avance* NMR instrument. The nucleus studied is ^1H resonating at 300 MHz at a field of 7.05 Tesla. The samples were loaded into 4 mm zirconia rotors. All experiments were carried out using MAS at a spinning speed in excess of 5 KHz.

2.5 SURFACE ACIDITY MEASUREMENTS

Surface acidity measurements of catalysts play decisive role in determining the catalytic activity and selectivity. Determination of the number, nature and strength of the acid sites are necessary to understand the

catalytic activity, selectivity and stability. A number of physico-chemical methods have been developed and accepted to evaluate the strength and amount of surface acid sties on catalysts. A large variety of probe molecules have been utilized to ascertain acidity quantitatively as well as to provide an insight on acid sight distribution[14].

MATERIALS

The materials used for the acidity determination of the prepared catalysts are given below.

	Materials	Suppliers
1.	Sulfuric acid	Merck
2.	Sodium carbonate	Merck
3.	Perylene	Aldrich
4.	Cumene	Aldrich
5.	Benzene	Merck
6.	Cyclohexanol	CDH
7.	2,6-dimethylpyridine	Merck

METHODS

In the present study, the surface acidity of the prepared catalytic systems were carried out by five independent techniques namely

I. Temperature Programmed Desorption (TPD) of Ammonia

II. Electron acceptor adsorption studies using perylene.

III. Thermodesorption studies using 2,6-dimethylpyridine

IV. Cumene conversion reaction

V. Cyclohexanol decomposition reaction

I. TEMPERATURE PROGRAMMED DESORPTION (TPD) OF AMMONIA

Temperature programmed desorption is the most promising and the simplest technique to find out the acidity and acid site distributions of a catalyst. It is generally recognized that ammonia is an excellent probe molecule for testing the acidic properties of solid catalysts as its strong basicity and small molecular size allow the detection of acidic sites located on the catalyst[15]. Ammonia can interact with the acidic protons, electron acceptor sites and hydrogen from neutral or weakly acidic hydroxyls and thus can detect most of the different types of acid sites[16].

Ammonia TPD measurements in the range 100-600°C were performed in a conventional flow type apparatus using a stainless steel reactor of 30 cm length and 1 cm diameter kept in a cylindrical furnace. Pelletized catalyst was degassed at 300°C inside the reactor under nitrogen flow for half an hour. After cooling to room temperature, ammonia was injected in the absence of the carrier gas flow and the system was allowed to attain equilibrium. The excess and physisorbed ammonia was flushed out using a current of nitrogen for half an hour. Under a controlled temperature program, the amount of chemisorbed ammonia leached out for each 100°C in the temperature range 100-600°C was absorbed in a known volume of dilute sulfuric acid and ammonia desorbed was estimated volumetrically by back titration with standard sodium carbonate solution. A plot of amount of ammonia desorbed against temperature will give the acid strength distribution. The amount of ammonia desorbed in the temperature ranges 100-200, 200-400 and 400-600°C was assigned as measures of weak, medium and strong acid sites respectively.

II. PERYLENE ADSORPTION STUDIES

Adsorption of electron acceptors has been investigated to study and characterize the acidity of the catalysts. Adsorption studies using perylene as

electron donor gives information regarding the Lewis acidity in presence of Brönsted acidity[16,17]. The principle is based on the ability of the catalyst surface sites to accept electrons from an electron donor, like perylene to form charge transfer complex. The amount of the adsorbed species can be measured by spectrophotometric method[18].

In this method, different concentrations of perylene in benzene were prepared and stirred with about 0.5 g of the activated catalyst in a 50 mL stoppered U-shaped tube for four hours. It is filtered and the absorbance of the filtrate was measured. Due to the adsorption of perylene on the catalyst surface from the solution, its concentration in the solution will be less after adsorption. The amount of perylene adsorbed was determined from the difference in the concentration of perylene solution before and after adsorption by means of a *Shimadzu UV-VIS spectrophotometer* (UV-160A) at a λ_{max} of 439 nm. The Langmuir type adsorption isotherms were obtained by plotting equilibrium concentration of perylene against amount of perylene adsorbed. From this, limiting amount of perylene adsorbed, which can be taken as a measure of Lewis acidity of the catalyst, was calculated.

III. THERMODESORPTION STUDIES OF 2,6-DIMETHYLPYRIDINE

The thermodesorption studies of 2,6-dimethylpyridine (2,6-DMP) were implemented to investigate the Brönsted acidic sites in the samples. Due to steric hindrance of the methyl groups, 2,6-DMP gets selectively adsorbed at the Brönsted acid sites and thus the percentage weight loss during thermal treatment will correspond to the Brönsted acidity of the sample. Previously activated catalysts were kept in a desicator saturated with vapours of 2,6-DMP for 48 hours for the effective and uniform adsorption. After this, the weight loss of the adsorbed samples was measured by thermogravimetric analysis in nitrogen atmosphere at a heating rate of 20°C min^{-1}. The fraction of

weight loss in the range of 300-600°C was found out and taken as a measure of the Brönsted acidity of the sample[19].

IV. CUMENE CRACKING REACTION

Cumene conversion reaction is widely studied to determine the functionality of an oxide catalyst. Cumene is cracked to benzene and propene over Brönsted acid sites and to α-methyl styrene over Lewis acid sites[20]. Thus cumene conversion reaction can be chosen as a test reaction to check the presence of Brönsted and Lewis acid sites. The relative amount of benzene and α-methyl styrene in the product mixture is a good indication of the acidity of the sample. The reaction was carried out in the vapour phase after optimizing the reaction parameters. The product analysis was achieved Gas Chromatographically by comparison with authentic samples.

V. CYCLOHEXANOL DECOMPOSITION REACTION

Cyclohexanol decomposition reaction was conducted as a test reaction for acidity. The selectivity of the products exhibited by a catalyst is related to its surface acid base properties. The amphoteric nature of the cyclohexanol permits their interaction with acidic and basic sites resulting in dehydration and dehydrogenations, which in turn are linked to the acid base properties of the catalyst[21]. The reaction was done in the vapour phase under optimized reaction conditions and the liquid products collected were analyzed by Gas Chromatography.

2.6 CATALYTIC ACTIVITY MEASUREMENTS

The catalytic activity of the prepared systems is tested for some well-known industrially important reactions. The reactions were carried out in solid, liquid and vapour phase. In the present case, nitration of phenol was carried out in solid state and Friedel-Crafts benzylation of aromatics, in the liquid

phase. *Tert*-butylation of phenol and Beckmann rearrangement of cyclohexanone oxime were done in the vapour phase whereas photochemical degradation of methylene blue was carried out in presence of sunlight.

MATERIALS

The materials used for catalytic activity studies are as follows.

	Materials	Suppliers
1.	Toluene	Merck
2.	*o*-xylene	Merck
3.	Benzyl chloride	Merck
4.	Benzene	Merck
5.	Cyclohexanone oxime	Prepared in the lab
6.	Phenol	Merck
7.	*tert*-butanol	Qualigens
8.	Nitric acid	Merck
9.	Methylene blue	s.d. fine Chemicals Ltd.

METHODS

A brief description of the experimental procedure for the different types of reactions studied is given below. The catalytic activity was expressed as the percentage conversion and the selectivity for a product is expressed as the amount of the particular product divided by total amount of products multiplied by 100.

I. SOLID STATE REACTIONS

Nitration of phenol is done in the solid phase. The reactants and the catalysts were mulled to form a paste at room temperature. After keeping in an ice bath, nitric acid is added slowly with stirring, maintaining the temperature in

the range of 0-5°C. The products were extracted after a definite interval of time and the analysis was done using a *Chemito 1000* Gas Chromatograph equipped with a flame ionization detector and capillary column.

II. LIQUID PHASE REACTIONS

Friedel-Crafts benzylation of toluene and *o*-xylene using benzyl chloride was performed in liquid phase. The reactants in the required molar ratio and a definite amount of the catalyst were taken in a 50 mL double-necked round bottom flask and refluxed in an oil bath using a spiral condenser. The temperature of the oil bath was adjusted according to the requirement of the reaction studied and kept constant by means of a dimmerstat. The reaction mixture was stirred magnetically, and the product analysis was done using gas chromatograph.

III. GAS PHASE REACTIONS

Tert-butylation of phenol and Beckmann rearrangement of cyclohexanone oxime were done in vapour phase. The catalytic reactions were carried out at atmospheric pressure in a tubular, down flow reactor using 0.5 g of the catalyst placed on a glass wool bed packed between silica beads. The temperature was regulated using a temperature controller. The feed mixture was injected from the top using a syringe pump at a controlled flow rate. The products were collected at regular intervals and analyzed Gas Chromatographically.

IV. PHOTOCHEMICAL REACTIONS

Methylene blue degradation was studied over the catalyst to test the photocatalytic activity of the prepared systems. A known concentration of methylene blue is mixed with the catalyst and placed under solar irradiation at room temperature. After a definite time the sample is taken out and filtered. The

amount of methylene blue degraded was determined from the difference in the concentration of methylene blue solution before and after reaction, by means of a *Shimadzu UV-VIS spectrophotometer* (UV-160A) at a λ_{max} of 660 nm.

The products of the various reactions were analyzed using Gas Chromatograph *(Chemito)* equipped with Flame Ionisation Detector and appropriate column. The details of the analysis are given in table 2.1.

Table 2.1 Analysis conditions for various catalytic reactions

Catalytic reaction	GC	Analysis conditions			
		Column	Temperature programme	Temperature (°C)	
				Injector	Detector
Cumene cracking	8610	OV-17	110°C-isothermal	230	230
Cyclohexanol decomposition	8610	Carbowax	90°C-isothermal	200	200
Toluene benzylation	8610	SE-30	80°C-2-3°C-230°C*	230	230
o-xylene benzylation	8610	SE-30	100°C-2-3°C-230°C	230	230
Tert-butylation of phenol	1000	BP-1 Capillary	60°C-1-10°C-150°C	150	150
Beckmann rearrangement	8610	OV-17	90°C-2-15°C-230°C	230	230
Nitration of phenol	1000	BP-1 Capillary	90°C-2-10°C-300°C	300	300

*Initial temperature - Duration in minutes – Rate of increase – Final temperature.

ॐ ७ॐ ७ॐ ७ॐ ॐ
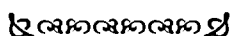
REFERENCES

1. D.K. Chakrabarthy, *"Solid-state Chemistry"*, New Age International Ltd, New Delhi (1996) p.14.

2. Clive Whiston, *"X-ray methods-Analytical Chemistry by Open Learning"*, John Wiley, New York (1987) Ch.3.

3. H. Lipson, H. Steeple, *"Interpretation of X-ray Powder Diffraction Patterns"*, Macmillan, London (1970) p. 261.

4. Clive Whiston, *"X-ray methods-Analytical Chemistry by Open Learning"*, John Wiley, New York (1991) p. 296.

5. S. Brunauer, P.H. Emmette, E. Teller, *J. Am. Chem. Soc.,* 60 (1938) 309.

6. A. Howie, *"In Characterization of Catalysts"*, J. Thomas and R.M. Lambert (Eds.), John Wiley, New York (1980) p. 89.

7. R.L. Parfitt, R.S.C. Smart, *J. Chem. Soc. Faraday trans.,* 1, 73 (1977) 796.

8. D.A. Ward, E.I Ko, *J. Catal.,* 150 (1994) 18.

9. G. Ertl, H. Koninger, J. Weitkamp, *"Handbook of Heterogeneous Catalysis"*, Vol.2, VCH, Weinheim (1997) p. 646.

10. H.G. Hecht, *"Modern aspects of Reflectance Spectroscopy"*, W.W Wendlandt (Eds.), Plenum Press, New York, (1968).

11. G. Ertl, H. Koninger, J. Weitkamp, *"Handbook of Heterogeneous Catalysis"*, Vol.2, VCH, Weinheim (1997) p. 256.

12. E.H. Park, M.H. Lee, J.R. Sohn, *Bull. Korean Chem. Soc.,* 21 (2000) 913.

13. C.N. Banwell, E.M McCash, *"Fundamentals of Molecular Spectroscopy"*, 4th edn., Tata McGraw Hill, New Delhi (1995).

14. P.A. Jacobs, *"Characterization of Heterogeneous Catalysts"*, F. Delanney (Eds.), Elsevier, Amsterdam, 311 (1985).

15. L. Yumin, L. Shetian, Z. Kaizheng, Y. Xingkai, W. Yue, *Appl. Catal. A. Gen.,* 169 (1998) 127.

16. J. Kijenski, A. Baiker, *Catal. Today,* 5 (1989) 1.

17. B.D. Flockart, J.A.N. Scott, R.C. Pink, *Trans. Faraday Soc.*, 62 (1966) 730.

18. J.J. Rooney, R.C. Pink, *Proc. Chem. Soc.,* (1961) 70.

19. A. Satsuma, Y. Kamiya, Y. Westi, T. Hattori, *Appl. Catal. A. Gen.*, 194-195 (2000) 253.

20. S.M. Bradley, R.A. Kydd, *J. Catal.,* 141 (1993) 239.

21. M. Ai, *Bull. Chem. Soc. Jpn.*, 50 (1997) 2579.

Chapter 3

Physico-Chemical Characterization

Physicochemical characterization of the prepared catalysts is usually done to ensure the purity of the systems and to get an insight to the nature of the active sites on the catalyst surface. Characterization of the prepared catalysts were done by different techniques such as X-ray diffraction analysis, energy dispersive X-ray analysis, surface area and pore volume measurements, scanning electron spectroscopy, infrared spectroscopy, thermogravimetry, UV-Vis diffuse reflectance spectroscopy and ^{1}H NMR spectroscopy. Strength and distribution of acid site were determined by three independent methods *viz.* ammonia TPD, perylene adsorption and thermodesorption of 2,6-dimethylpyridine. Cumene conversion reaction was employed to quantify the various types of acid sites on the surface of the catalysts. Acid base property of the catalysts was evaluated by cyclohexanol decomposition reaction.

3.1 INTRODUCTION

In heterogeneous catalysis, the reaction occurs at the surface. Catalysts and catalytic surfaces, hence, need to be characterized by reference to their physical properties and by their actual performance as a catalyst. The most important physical properties are those relating to the surface because catalyst performance is determined by surface parameters[1]. Atoms on surfaces are distinctly different from those in the bulk in terms of unsaturated coordination,

electronic properties and crystallographic arrangements. It is essential to know the exact structure of surface including defects as well as exact location of active sites. We present a brief discussion on characterization of surfaces of the catalysts since they are primarily responsible for catalytic activity of substances. Since solid supported catalysts and the sulfated metal oxides are well known for its surface acidity, a more detailed investigation of the acidity of the prepared systems are also discussed.

3.2 PHYSICAL CHARACTERIZATION

The catalyst systems synthesized were characterized by adopting various physical methods. The results are discussed in the following sections.

I. X-RAY DIFFRACTION ANALYSIS (XRD)

XRD profiles of titania and sulfated titania calcined at 500°C is given in figure 3.1. After calcination at 500°C, anatase appears as a crystalline phase manifested by its 101 peak (2θ = 25.5°). The anatase-rutile transformation takes place at this temperature and is confirmed by the occurrence of the 110 peak of rutile at 2θ = 27.5°). The sulfated titania possesses only diffraction lines, such as at 2θ = 25.5, 37.4, 48 and 53° simply indicating the anatase type of TiO_2. Diffraction lines for the rutile type of TiO_2 are observed at 2θ = 27, 36, 41 and 54° in the case of pure titania. The peaks corresponding to the rutile phase is completely eliminated in the case of sulfated samples. This indicates that sulfation retards the transformation from anatase to rutile in comparison with the sample without sulfation. The powder X-ray diffractograms of metal incorporated sulfated titania systems are shown in figures 3.2 and 3.3. The transition of amorphous TiO_2 to crystalline anatase TiO_2 takes place at 350 and 500°C for pure titania and sulfated titania respectively[2]. The intensity of XRD characteristic peaks of anatase TiO_2 for sulfated titania samples were lower and broader than those for the pure

titania. These observations are in support of the generally recognized viewpoint that sulfation inhibits the sintering of titania and stabilizes the surface area of sulfated titania catalyst[3].
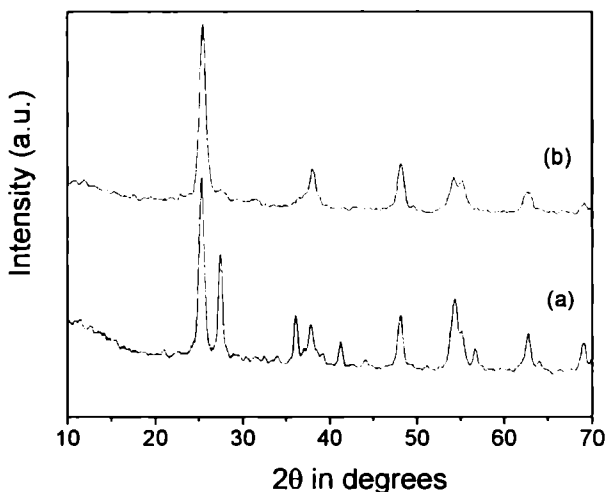

Figure 3.1 XRD profile of (a) T (b) ST

It is reported that ZrO_2 notably delay the anatase to rutile transformation, stabilizing the anatase phase[4]. In addition to stabilizing anatase TiO_2 crystallites, sulfate surface species inhibit sintering of TiO_2 crystallites leading to lower crystallites than in pure TiO_2. Low peak intensity, in the case of sulfate treated samples, indicates low crystallinity. It has been reported that the degree of crystallization of the sulfated oxides is much lower than that of the oxides without sulfation[5-7]. Dispersion of SO_4^{2-} species hinders agglomerization of the titania particles indicating delayed crystallization. The absence of any change in the peak intensity after sulfate treatment indicates that the amount of sulfate retained on the surface is insufficient to cause any change in the diffraction pattern and it is well dispersed on the surface.
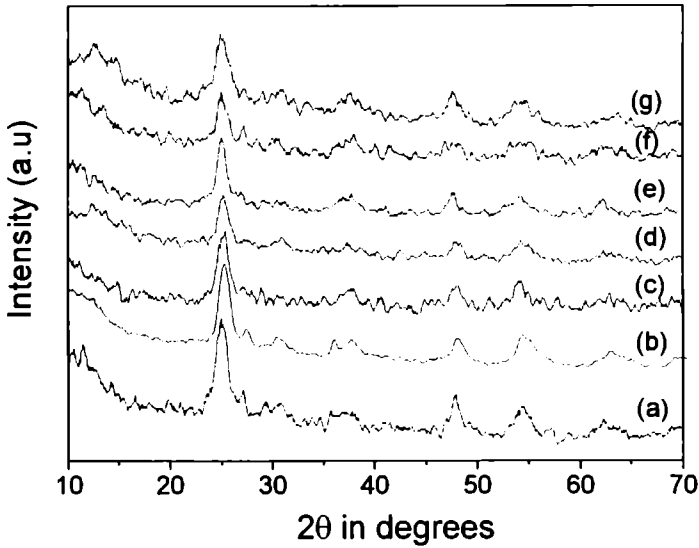
64

Figure 3.2:- XRD profiles of (a) STCr(3) (b) STMn(3) (c) STFe(3) (d) STCo(3) (e) STNi(3) (f) STCu(3) (f) STZn(3)

The average crystallite size is calculated using Scherrer equation[8] from the 101 reflection of anatase is given in table 3.1. The average crystallite size of titania decreases in presence of sulfate ion. The crystallite size decrease in presence of sulfate ions as SO_4^{2-} species could possibly interact with TiO_2 network and thus, hinder the growth of the particle. Even a very small amount of SO_4^{2-} species can be responsible for this effect. This type of effect is also observed in PO_4^{3-} [9,10] and WO_3[11,12]. From our earlier studies[13] it is noted that, crystallite size of titania decreases in the presence of sulfate ion, irrespective of the percentage of sulfate loading. This indicates that the crystallinity is more or less dependent on the presence of sulfate ion, but not on the percentage of sulfate loading. Among the different metal incorporated systems, chromia loaded systems show the lowest crystallite size. In the case of iron and nickel loaded samples there is an increase in the crystallite size than sulfated titania

65

due to the formation of bulk metal oxide rather than the dispersed form on the surface of titania. As the metal content increases the crystallite size increases.
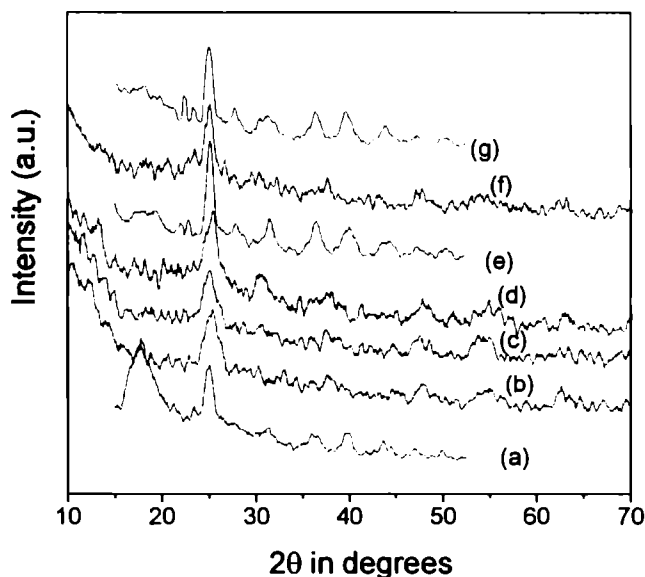
Figure 3.3 XRD profiles of (a) STCr(9) (b) STMn(9) (c) STFe(9) (d) STCo(9) (e) STNi(9) (f) STCu(9) (f) STZn(9)

Since no titanium sulfate is detected by XRD for the catalysts examined in the present study, the sulfur may exist in a form of sulfate on the surface of TiO_2. Choo *et al.*[14] reported that there was no formation of titanium sulfate for the ST calcined even at 900°C. In order to identify the state of sulfur species on the surface of TiO_2, they examined the sulfated supports by XPS and found that the sulfur compound exists in a form of sulfate (SO_4^{2-}) on the catalyst surface. The bulk structure of titania remains virtually unchanged by the incorporation of metal ions, except for a lowering in crystallinity. The absence of any characteristic peaks of the metal oxides, suggest that these oxides are present in the form of dispersed oxide species, since the total content of them is rather small and may be below the limits of detection with the XRD

technique. The bulk structure remains virtually unchanged by the incorporation of transition metals, except for a lowering in crystallinity.

II. SURFACE AREA AND PORE VOLUME MEASUREMENTS

The surface areas and pore volumes of the prepared catalysts are given in tables 3.1 and 3.2 measured using BET method by nitrogen adsorption at liquid nitrogen temperature. From the tables it is observed that pure titania has a BET surface area of 35 m^2 g^{-1} and Langmuir surface area of 45 m^2 g^{-1}. The surface area and pore volume of the sulfated samples are invariably higher than pure titania. Superacidity is created by adsorbing sulfate ions into amorphous metal oxides followed by calcination in air to convert to the crystalline forms. Specific surface areas of the sulfated catalysts are much larger than those of the oxides without the sulfate treatment. The main reason of surface area increment is due to the retardation of crystallization of the support oxides by the sulfate groups present on the surface[15]. The lowering of degree of crystallinity, as evident from the XRD patterns, supports the increase in the surface area by sulfate treatment.

It has been noted by Ma *et al.*[16] that the crystalline grain and specific surface area of the oxide precursor exert a significant influence on the properties of the catalyst. Since sulfation of the oxide is carried out by SO_4^{2-} adsorption onto the precursor, a small crystalline grain and higher surface area of the precursor enhance the adsorption and, hence, increase the sulfate content of the final catalyst, even if a part of sulfate is lost during thermal activation of the catalyst. Upon calcination, there is no phase transition and the presence of SO_4^{2-} species stabilizes the surface area, thus the final SO_4^{2-}/TiO_2 catalysts retain higher surface areas and higher catalytic activities.

Table 3.1 Surface area, pore volume and crystallite size of the prepared systems

Catalyst	Surface area $(m^2 g^{-1})$		Pore volume $(\times 10^{-6} m^3 g^{-1})$	Crystallite size (nm)	Pore diameter (nm)
	BET	Langmuir			
T	35	46	0.09	12.71	102.8
ST	91	138	0.21	9.62	92.3
STCr(3)	100	152	0.18	5.90	72.0
STMn(3)	87	134	0.15	7.09	69.0
STFe(3)	104	160	0.17	10.40	65.4
STCo(3)	90	137	0.14	11.99	62.2
STNi(3)	83	131	0.15	12.62	72.3
STCu(3)	70	106	0.15	16.06	85.7
STZn(3)	92	139	0.14	5.92	60.1
STCr(9)	128	226	0.17	6.38	53.1
STMn(9)	98	205	0.14	19.39	57.1
STFe(9)	138	250	0.17	13.56	49.3
STCo(9)	98	206	0.11	15.07	44.9
STNi(9)	95	201	0.11	18.14	46.3
STCu(9)	80	191	0.11	16.57	55.0
STZn(9)	98	216	0.11	14.86	44.9

Addition of transition metal species causes a further setback to the crystallization and sintering process, which is evident from the higher surface area of the samples in comparison with the simple sulfated system. The metal oxide species along with the sulfate ions prevent the agglomeration of titania particles resulting in a higher surface area. Only exception is STCu(3) and STNi(3) samples for which there was a slight lowering of surface area compared to ST. Among the different metal incorporated systems, there was

no significant variation in the surface area value. As the metal content increases, surface area is found to increase. The dispersed metal oxides along with the sulfate species prevent the agglomerization of titania particles leading to an enhanced surface area.

Table 3.2 Surface area, pore volume and crystallite size of the prepared systems

Catalyst	Surface area (m^2 g^{-1})		Pore volume ($\times 10^{-6}$ m^3 g^{-1})	Pore diameter (nm)
	BET	Langmuir		
STCr(6)	123	199	0.17	55.3
STMn(6)	89	180	0.12	53.9
STFe(6)	128	221	0.17	53.1
STCo(6)	91	186	0.11	48.4
STNi(6)	85	179	0.13	61.2
STCu(6)	72	170	0.12	66.7
STZn(6)	96	189	0.12	50.0

It has been shown[17,18] that in sulfated metal oxides, some of the hydroxyl bridges originally present in dried uncalcined and unsulfated titania are replaced by the sulfate ions. On calcination, the formation of oxy bonds takes place, and results in change in the Ti-O-Ti bond strength due to attachment of the sulfate bridges. Thus the changes in the Ti-O-Ti bond strength may be responsible for the formation of porous network. Consequently, the increase in surface area with an increase in sulfate content appears to be due to the stabilizing effect of the sulfate ions. In general, the pore volume of the samples is related to their crystallite size. The pore volume is increased as the anatase crystallite size in the samples becomes finer and more uniform. The pore volume of the different systems also remained in almost the same range. Comparatively low pore volume of metal loaded systems may be ascribed to

the blocking of the pores as the crystallites agglomerize by virtue of sintering. Assuming the pores are cylindrical, the average pore diameter is calculated using the formula: $d = 4V_P/S_p$, where d is the average pore diameter, V_p is the pore volume, and S_p is the surface area[5]. Decrease in the pore diameter is observed after sulfation. Metal incorporated samples also show a decrease in pore diameter. Colon *et al.*[4] reported that when ZrO_2 is incorporated into the titanium oxide, average pore diameter shifts slightly toward lower values, and the pore volume becomes significantly higher. It is known that the degree of agglomeration at constant pore diameter can be controlled by the concentration of the free hydroxide in the particle without the decrease of the number of bonds between particles[19]. Accordingly, this type of agglomeration occurring in TiO_2/SO_4^{2-} indicates that the free OH bind sites of $Ti(OH)_4$ in the particle, where the agglomeration/crystallization takes place during calcination, are consumed by the addition of SO_4^{2-} ion.

III. ENERGY DISPERSIVE X-RAY FLOURESCENCE ANALYSIS (EDX)

Elemental composition of the prepared catalytic systems is presented in table 3.3. Sulfated titania shows a sulfate content of 4.66%, while that of STCr(3) shows 9.16%. The sulfate content of the metal incorporated sample is considerably higher, when compared with sulfated titania, which indicate that metal doping brings about a considerable reduction in the extent of sulfate loss from the catalyst surface. Though the same concentration of sulfuric acid solution was used for sulfate modification of all the samples, their sulfate retaining capacity is different. The presence of these metal oxides stabilizes the sulfate over layers on the catalyst surface, which is apparent from the increase in the sulfate retaining capacity. The sulfate content for the various systems remained in the range 7.47 to 12.85%. Chromia loaded sample shows maximum sulfate retention capacity. The amount of sulfate retained in the samples shows a gradual increase as the metal content is increased. The

metal content of different systems clearly indicates that the expected catalyst profile can be successfully achieved by the present preparation method. From the results, it is evident that in all the cases, the amount of metal in the samples is very close to the expected value.

Table 3.3 Elemental composition from EDX (%)

Catalyst	TiO_2	SO_4	Metal	Catalyst	TiO_2	SO_4	Metal
T	100	-	-	ST	95.34	4.66	-
STCr(3)	88.05	9.16	2.78	STCr(6)	83.59	10.52	5.90
STMn(3)	90.49	7.28	2.23	STMn(6)	86.12	8.24	5.64
STFe(3)	89.44	7.83	2.98	STFe(6)	86.32	7.92	5.76
STCo(3)	89.81	7.83	2.36	STCo(6)	87.09	7.99	4.92
STNi(3)	89.43	8.34	2.23	STNi(6)	86.55	8.37	5.08
STCu(3)	89.89	7.47	2.67	STCu(6)	86.35	8.05	5.60
STZn(3)	89.11	8.14	2.75	STZn(6)	87.23	8.37	4.40
STCr(9)	81.60	10.58	7.82	STNi(9)	79.09	12.85	8.06
STMn(9)	83.52	9.64	6.84	STCu(9)	79.42	11.97	8.61
STFe(9)	82.92	10.21	6.81	STZn(9)	82.77	10.18	7.05
STCo(9)	80.18	11.30	8.52				

IV. SCANNING ELECTRON MICROSCOPY (SEM)

Regarding the morphology, figure 3.4 present the selected SEM images of the prepared catalysts. In SEM pictures spherical aggregates of small sub particles are observed. Particles present homogenous morphology and similar distribution in size and shape. The particle shape is spherical, but the particles are coagulated each other, and thus, the size of single particle could not be calculated accurately. The particles were clustered together due to the electrostatic effect of very fine particles. This is a very common phenomenon in

the case of nanoparticles[20]. However, it is confirmed that the particle size was distributed around 10 to 50 nm. Incorporation of transition metals does not alter the structure of titania. Particle size is observed to be larger in the case of pure titania. Crystallite size is decreased after sulfate incorporation. Addition of transition metals again changes the morphology greatly. Comparatively large particle size is observed in the case of nickel and copper loaded samples.
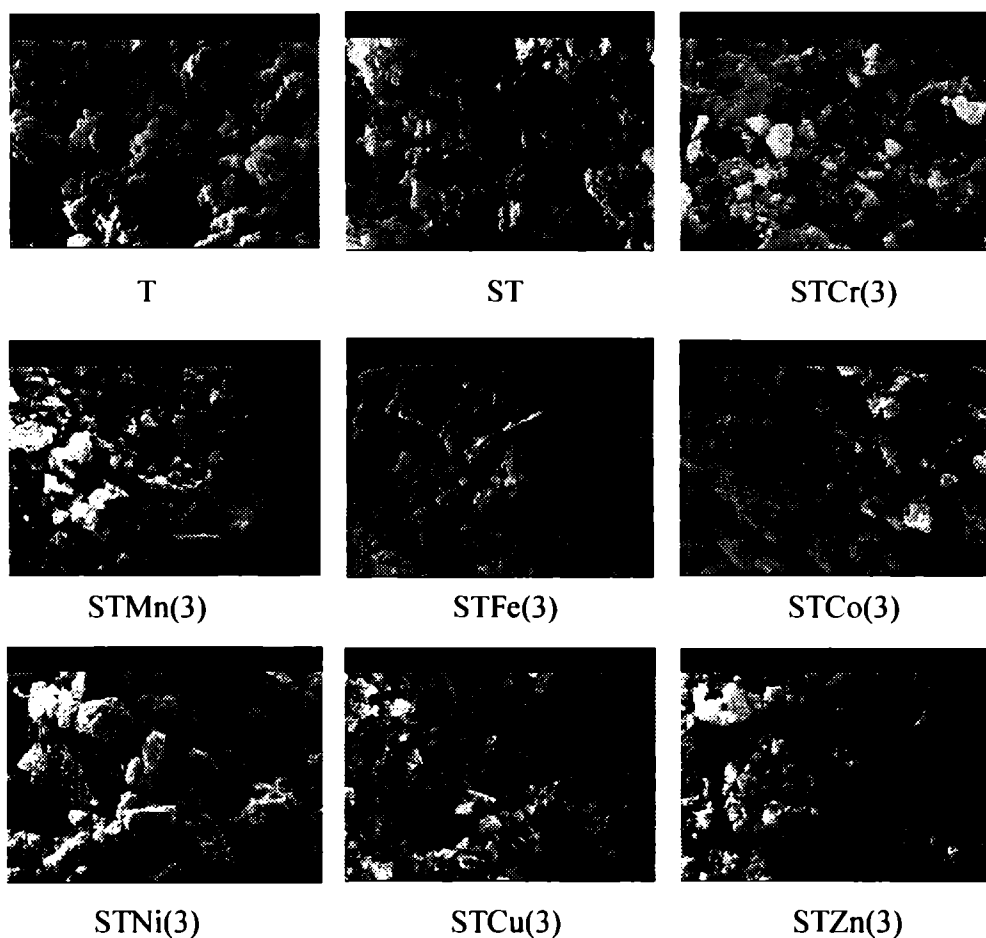

Figure 3.4 Scanning electron micrographs of representative systems

V. THERMOGRAVIMETRIC ANALYSIS (TGA)

Thermogravimetric analysis of representative samples heated under a flow of nitrogen can be seen in figures 3.5 and 3.6. The mathematically obtained differential curve is also plotted in order to clarify the weight loss processes. TG/DTG pattern of pure titania indicates a continuous dehydration over the entire temperature.
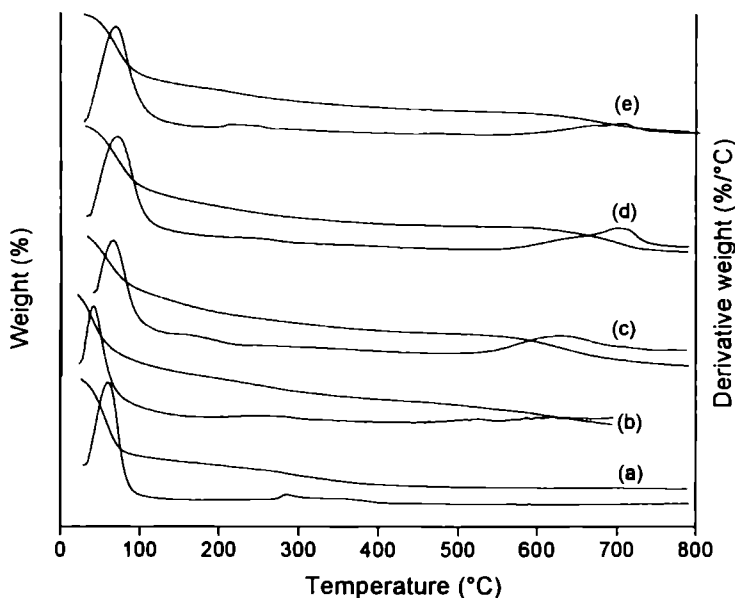
Figure 3.5 TG/DTG profiles of (a) T (b) ST (c) STCr(3) (d) STMn(3) (e) STFe(3)

The first loss of weight associated with hydration water, located between the particles, occurs in a wide temperature range, i.e., between room temperature and 100°C[21]. Another small dip in the region of 250 to 300°C may be due to the removal of structural water present in the sample. No additional weight loss is noticed in the higher temperature region in the case of pure titania. An additional decomposition in the case of sulfated samples is seen around 650-700°C and can be ascribed to the decomposition of the sulfate

73

species giving rise to evolution of oxides of sulfur[22]. The decomposition of surface sulfate groups above 700°C is reported in the case of sulfated metal oxide[23,24]. Here also the initial weight loss corresponds to the removal of surface adsorbed water of hydration. The metal incorporated samples exhibited a higher thermal stability. The commencement of decomposition in these cases occured only above 700°C. It is inferred that besides delaying the crystallization process, the addition of the metal species also serves to stabilize the surface sulfate species. In all these thermograms no apparent weight loss is observed up to 600°C after transformation of metal salts to corresponding metal oxide.
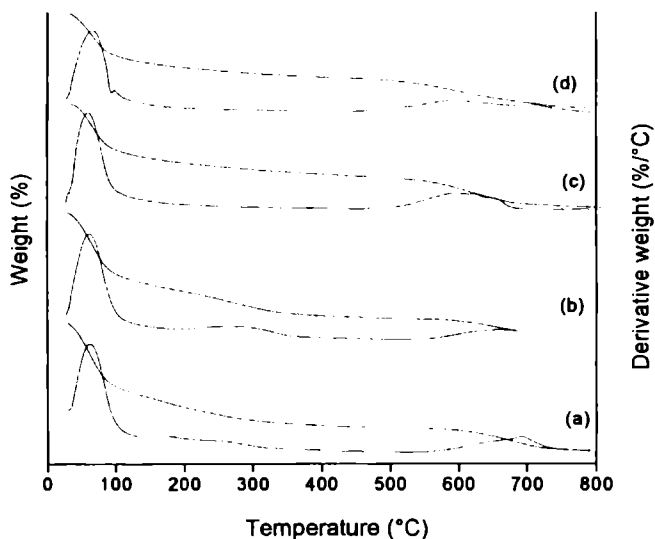
Figure 3.6 TG/DTG profiles of (a) STCo(3) (b) STNi(3) (c) STCu(3)(d) STZn(3)

VI. FOURIER TRANSFORM INFRARED (FTIR) SPECTROSCOPY

Figures 3.7 to 3.9 present the FTIR spectra of representative systems of sulfated titania catalysts calcined at 500°C. The IR spectrum of pure titania shows two strong absorption bands at 3436 and 1626 cm^{-1}. Additional bands at

around 400-500 cm^{-1} are also observed. The oxide supports generally terminate with surface OH groups, which are quite polar and give strong IR bands in the 3000-4000 cm^{-1} and 1600-1700 cm^{-1} regions[25]. The vibration modes of anatase skeletal O-Ti-O bonds are observed in the range of 400-900 cm^{-1} with a maximum at 474 cm^{-1} [26,27]. In the low energy region of the spectrum the bands at 595 and 467 cm^{-1} are assigned to bending vibrations of Ti-O bonds[28]. It was reported[29] that the bands at 1132, 979, 776and 669 cm^{-1} can be assigned as Ti-O asymmetric and symmetric stretching vibrations. The sulfate sample show IR spectra which are different from those of metal sulfates; the material show absorption bands at 980-990, 1040,1130-1150 and 1210-1230 cm^{-1}, which are assigned to the bidentate sulfate coordinated to the metal[30].
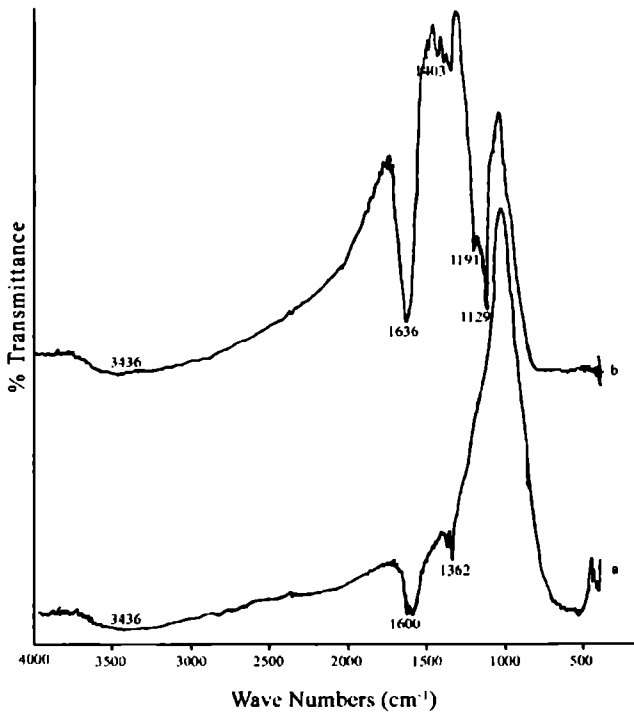

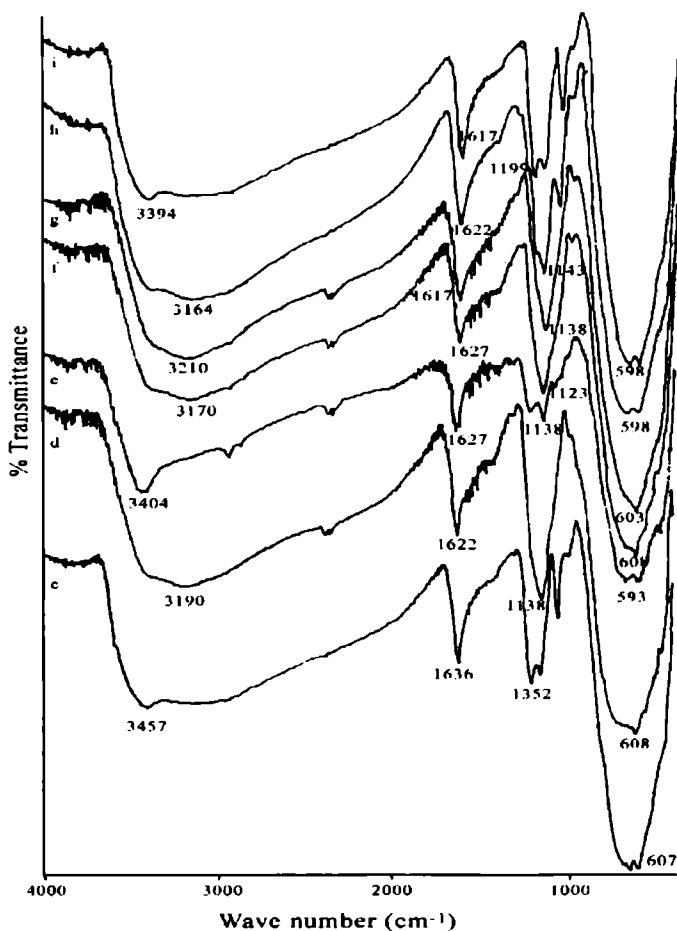Figure 3.7 FTIR spectra of (a) T (b) ST

Figure 3.8 FTIR spectra of (c) STCr(3) (d) STMn(3) (e) STFe(3) (f) STCo(3)
(g) STNi(3) (h) STCu(3)(i) STZn(3)

IR spectra of sulfated metal oxides gave a strong absorption band near 1380-1360 cm^{-1} and a broad band around 1000-1200 cm^{-1}. It has been reported that TiO_2/SO_4^{2-} give the bands of S=O at 1375 cm^{-1}. The drastic shift of the IR band indicates a strong interaction between the support and the surface sulfur complex[31]. The band around 1370 cm^{-1} arises from the highly covalent character of the S=O on a highly dehydrated oxide surface[24].

According to Morterra *et al.*[32] the peaks in this region correspond to isolated surface sulfates whereas generation of polynuclear sulfates at high sulfate loadings shifts the peak to around 1400 cm^{-1}. The absence of peaks around 1400 cm^{-1} suggests the absence of polynuclear species in the samples irrespective of high sulfate loading.
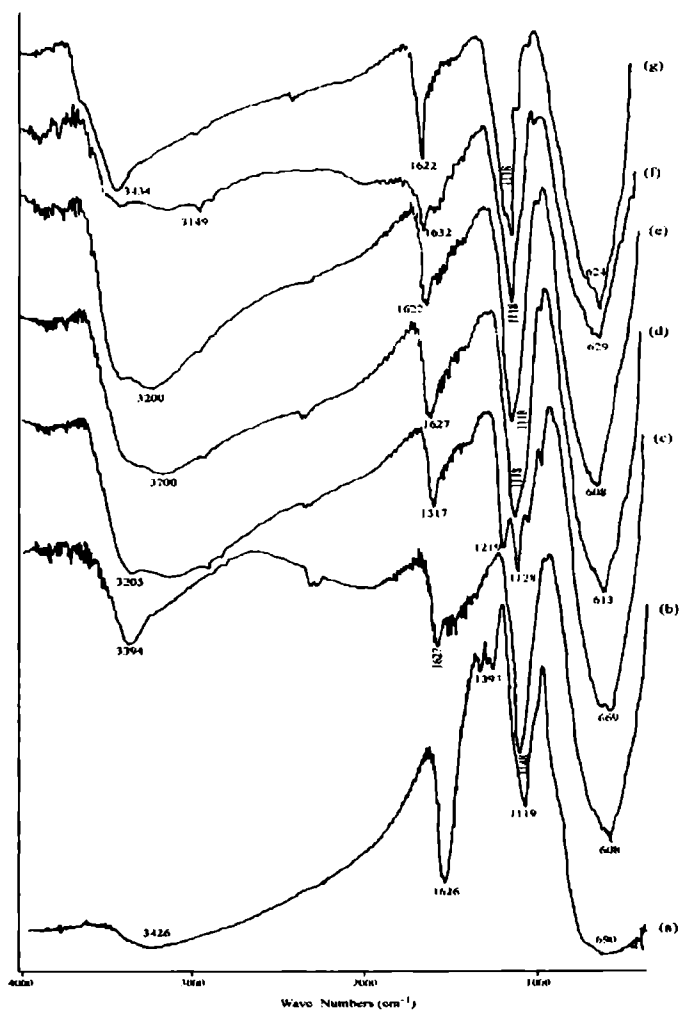

Figure 3.9 FTIR spectra of (a) STCr(9) (b) STMn(9) (c) STFe(9) (d) STCo(9)
(e) STNi(9) (f) STCu(9)(g) STZn(9)

A broad band due to the –OH species appear around 3436 cm^{-1} for pure titania, whereas for the modified samples, the peak maxima is shifted. This shift in the –OH peak to a lower stretching frequency is suggestive of an enhancement in acid strength for the sulfated samples. The increase in Brönsted acidity during sulfation may be ascribed to the generation of S-OH groups[33] or to the acidity enhancement of the surface –OH groups[34]. When SO_4^{2-} is bound to the titania surface, the symmetry can be lowered to either C_{3v} or C_{2v}. The bands obtained in the 1200-1100 cm^{-1} regions are typical of sulfato complexes in a bidentate configuration with C_{2v} symmetry[35]. Thus the IR spectral bands of the samples closely agree to the bidentate sulfate complex structure having bands around 1119 and 1129 cm^{-1}.

Sulfated titania exhibits a broad IR band at the region of 3470 cm^{-1}. The absence of IR peak at 3720 cm^{-1} reveals the absence of basic hydroxyl groups. This result indicates that the surface sulfates preferentially cover the hydroxyl sites at the 3720 cm^{-1} regions, reducing the number of sites for metal loadings[14]. Saur *et al.*[24] using isotope exchange and IR analysis proposed a $(Ti-O)_3S=O$ structure under dry conditions for SO_4^{2-}/TiO_2. The sulfate type changes from tridentate species to bidentate species with SO_4^{2-} content on the metal oxide surface. As the sulfate loading is increased, it is proposed that $S_2O_7^{2-}$ and $S_3O_{10}^{2-}$ species may also be present[32,36-38].

VII. UV-Vis DIFFUSE REFLECTANCE SPECTROSCOPY (UV-Vis DRS)

UV-Vis spectroscopy has been utilized to characterize the bulk structure of crystalline and amorphous titania. TiO_2 is a semiconductor oxide with easily measured optical band gap. UV-Vis DRS is used to probe the band structure, or molecular energy levels, in the materials since UV-Vis light excitation creates photogenerated electrons and holes. Information about the absorptive properties of metal oxides can be obtained from diffuse reflectance UV-Vis spectroscopy. This is very important for catalysts for photocatalytic applications

since it gives information about the bad gap of semiconductors. The UV-Vis absorption band edge is a strong function of tiania cluster size for diameter less than 10 nm, which can be attributed to the well-known quantum size effect for semiconductors[39].

Table 3.4 λ_{max} and band gap energy obtained from UV-Vis DRS analysis

Catalyst	λ_{max} (nm)	Band gap energy (eV)	Catalyst	λ_{max} (nm)	Band gap energy (eV)
T	372	3.25	ST	322	3.76
STCr(3)	316	3.83	STCr(6)	314	3.85
STMn(3)	319	3.79	STMn(6)	315	3.84
STFe(3)	324	3.74	STFe(6)	323	3.75
STCo(3)	327	3.70	STCo(6)	325	3.72
STNi(3)	330	3.67	STNi(6)	327	3.70
STCu(3)	335	3.61	STCu(6)	330	3.67
STZn(3)	317	3.82	STZn(6)	316	3.83
STCr(9)	310	3.90	STNi(9)	322	3.76
STMn(9)	314	3.85	STCu(9)	327	3.70
STFe(9)	320	3.78	STZn(9)	312	3.88
STCo(9)	321	3.77			

Zhang et al.[40] reported the UV-Vis spectra of titania samples calcined at different temperatures. Blue shift is observed for the absorption spectra as the calcination temperature is increased. In Table 3.4, we report the calculated values of band gap energy for all samples. Band gap energy observed for TiO_2 Degussa P25 and Hombikat UV-100 reported in the literature[41] is about 3.5 eV, depending on the anatase-rutile fraction present in the oxide. The band gap energy is found to increase after sulfate modification and metal incorporation. Figure 3.10 gives the diffuse reflectance spectra of representative samples.

Characteristic band for tetrahedrally coordinated titanium appear at about 300-400 nm. The absorption is associated to the $O^{2-} \rightarrow Ti^{4+}$ charge transfer corresponding to electronic excitation from the valence band to the conduction band. A progressive shift in the band gap absorption onset to the visible region and a decrease absorbance in UV region are noticed with increasing metal content.
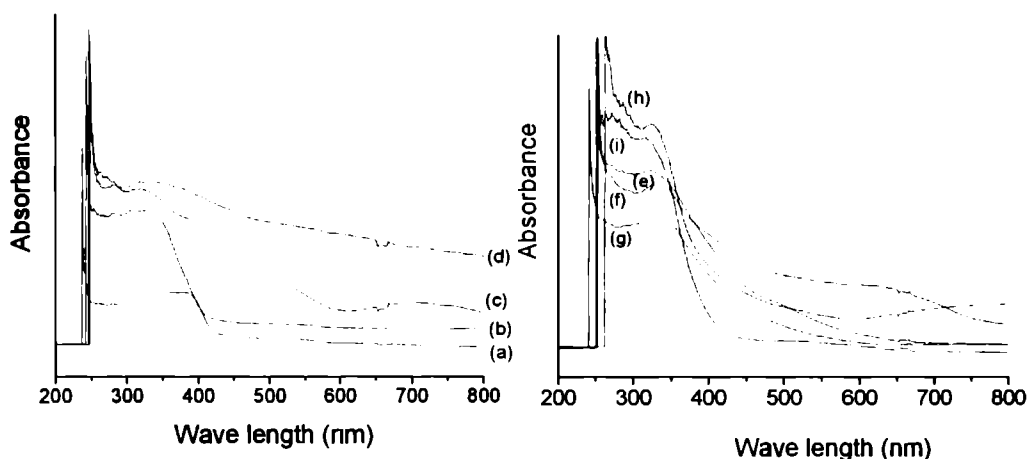

Figure 3.10 UV-Vis DR spectra of (a) T (b) ST (c) STCr(3) (d) STMn(3)
(e) STFe(3) (f) STCo(3) (g) STNi(3) (h) STCu(3) (i) STZn(3)

The presence of the doping ions caused significant absorption shifts into the lower wavelength region compared to pure titania. In the case of chromium loaded samples additional band near 600 nm is observed, which is attributed to $^4A_{2g} \rightarrow {}^4T_{1g}$ transitions for Cr(III) ions in an octahedral environment[42]. However, Cr(III) $\rightarrow$Ti(IV) charge transfer transitions, which may be alternatively described as excitation of an electron of Cr(III) into the conduction band of TiO_2, cannot be ruled out[43]. Manganese loaded samples revealed weak absorption bands in the 600-650 nm, and were assigned to the $^6A_{1g} \rightarrow {}^4T_{2g}$ crystal field transitions[44,45]. The absorption spectra of cobalt loaded samples show an increased absorption in the region of 600 nm, which may arise from charge transfer and d-d transitions[42].

VIII. SOLID STATE ^{1}H NUCLEAR MAGNETIC RESONANCE (NMR) SPECTROSCOPY

^{1}H MAS (magic angle spinning) NMR spectroscopy has proven to be an exceedingly useful technique for characterizing the hydroxylated surfaces of metal oxides. ^{1}H NMR measurements have been performed with the aim of measuring the characteristic proton chemical shifts of hydroxy groups bound to titania. Figures 3.11 and 3.12 gives the ^{1}H NMR spectra of representative samples. It is one of the best characterization techniques available for Brönsted acid amount determination as it directly probes the protons and their environments. In principle, ^{1}H MAS-NMR chemical shifts are correlated with the proton donor ability of Brönsted acid sites and hence can provide straight information about the Brönsted acidic strength[46-51].

Fraissard and coworkers[52] studied the distribution of protons between hydroxyl groups and adsorbed molecular water on different forms of tiania using a broad-line NMR technique. Recently, reports have appeared concerning the identification of hydroxy groups in mixed TiO_2-ZrO_2 supports[53]. Metal oxides have Brönsted acid sites involving oxygens at crystallographically different positions, i.e., bridging hydroxyls freely vibrating in small cages or channels[46]. Since the bridging hydroxyls interact with several other oxygens large broadening of peaks is observed. Perhaps, ^{1}H fast MAS-NMR spectroscopy at very high field is powerful technique for the atoms, their interactions may give rise to different downfield chemical shift in the ^{1}H NMR spectra, mostly reflecting an increase in Brönsted acidic strength[50,51]. Proton-proton interactions will also cause extreme line broadening and lowered resolution when the zeolite cages contain a high density of protons[47].
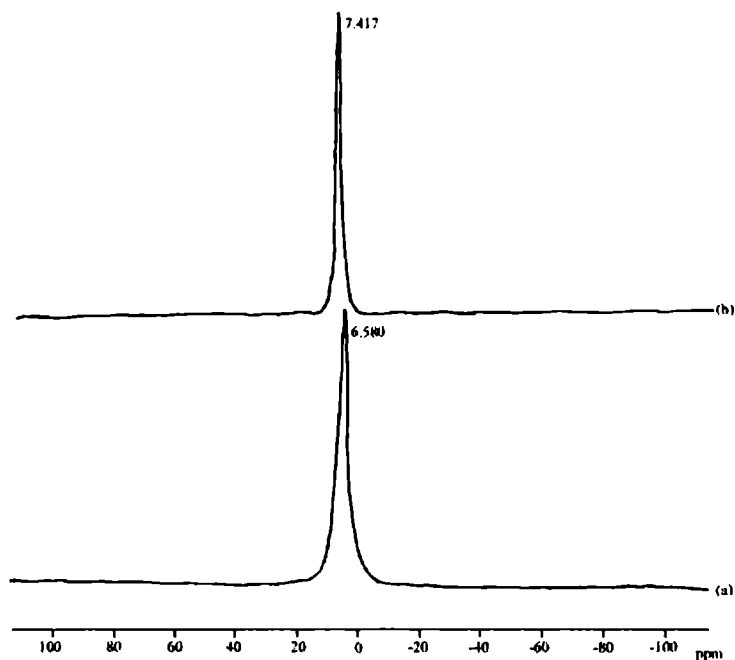
Figure 3.11 ^{1}H NMR spectra of (a) T (b) ST

Pure titania contains a major signal at δ=7.417 ppm, which is assigned to the bridging titanol group. These chemical shifts show good agreement with those of δ=6.4 ppm reported by Mastikhin, Nosov and co-workers[54-56] for anatase samples prepared by either precipitation from aqueous TiCl$_4$ or pyrolysis of TiCl$_4$. No signal corresponding to terminal titanol group is observed in any of the samples, which usually appears at δ=2.3 ppm[57]. After sulfation, the signal shift to δ=6.58 ppm, consistant with the greater acidity expected for sulfated titania and an increase of the OH bond strength. Chemical shifts of transition metal loaded samples were between -2.23 to 5.45 ppm. The relative large shift of the signal in the case of metal oxides could be taken as an indication of high Brönsted acidity[51,58]. Low chemical shift can be due to low acidity of the samples.
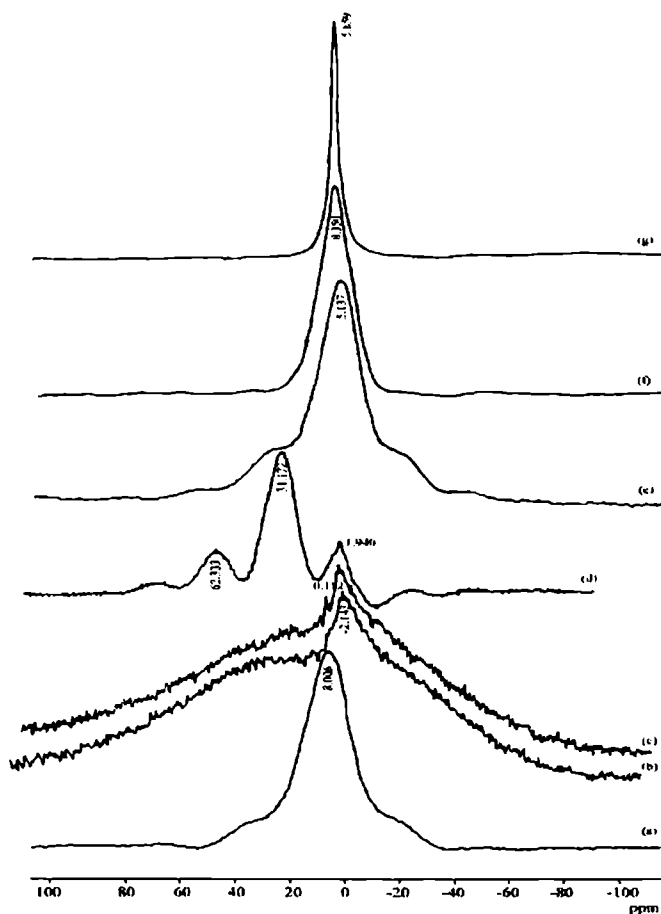
Figure 3.12 ^{1}H NMR spectra of (a) STCr(6)   (b) STMn(3)   (c) STFe(3)
(d) STCo(3) (e) STNi(3) (f) STCu(3) (g) STZn(3)

Manganese and iron loaded samples show relatively complex spectrum. The central Brönsted acid peak becomes completely featureless and we cannot say anything on the trend of Brönsted acid amount of these samples. We can interpret this in terms of the paramagnetic influence of the metal ions used while surface modification[59]. However, we cannot overemphasize on a one-to-one correlation between chemical shift values and strength of the Brönsted acid sites. In the case of cobalt loaded sample additional signals

arise at δ=31.177 and 63.33 ppm; these signals may correspond to hydroxy groups associated with Cu-OH groups. ^{1}H NMR of rutile samples contains signals at δ=6.9 (weak) and 5.3 ppm and are assigned to bridging hydroxyl groups. The peak at lower field corresponds to hydrogen bonded hydroxy groups, i.e., they correspond to bridging hydroxy groups located on different crystallographic planes[57].

3.3 SURFACE ACIDITY MEASUREMENTS

In reactions occurring by acid catalysis, the activity, stability and selectivity of solid acids are obviously determined to a large extent by their surface acidity. The acidic properties of the metal oxides are generally thought to play an important role in determining the adsorptive and catalytic properties of these materials. Acidity is found be the most important catalytic function of sulfated oxides. Hence determination of the acid sites exposed on the surface as well as their distribution is an essential requirement to evaluate the catalytic properties of acidic solids. The effect of incorporation of various transition metals on sulfated titania and their disparity in the surface acidity were investigated in detail by employing different methods.

It is known that the acidic properties of sulfate modified metal oxides are remarkably higher than that of the pure oxide. The generation of acid sites by sulfation has been explained by the inductive effect due to the difference in the electronegativity between metal oxides and sulfate ion. In the sulfate ion the S=O structure is essential for the generation of acidic sites on sulfate promoted oxide samples. The strong ability of S=O in sulfate complexes to accommodate electron from a basic molecule is a driving force in the generation of strong acid properties. Recent studies of supported sulfate catalyst suggest that the kind of sulfate species and acidic properties depend on the nature of the oxide[24,60,61]. In order to identify the state of the sulfur species on the surface of TiO_2, the sulfated supports were examined by Choo *et al.*[14] by XPS and found

that the sulfur is existing in a form of sulfate (SO_4^{2-}) on the catalyst surface. The bidentate sulfate on the surface of TiO_2, whether chelating or bridging, has been generally proposed as the structure of sulfur[62,63].

I. TEMPERATURE PROGRAMMED DESORPTION (TPD) OF AMMONIA

Temperature programmed desorption of simple bases is a widely used method to assess the total number and strength of acid sites[64,65] Basic molecules such as ammonia[66,67,68], pyridine[64] and n-butylamine are the generally used probe molecules. Among these molecules ammonia is most widely used; being a small molecule, it has greater accessibility to almost all acidic sites including the weak ones. Berteau *et al.*[69] have proposed that the desorption signals below 200°C correspond to weak acidity, those between 200 and 400°C to medium strength sites, and above 400°C the signal is associated to strong acidity in the case of NH_3-TPD. Tables 3.5 and 3.6 give the distribution of acid sites of pure titania and sulfated titania systems determined by ammonia TPD method.

Pure titania possesses comparatively very small amount of acidity. Upon sulfation, it is observed that, the amount of ammonia desorbed from all the temperature region is increased considerably. Samantaray *et al.*[5] also reported the same observation over sulfated titania.It is reported in literature[70] that the maxima in the TPD profile around 535°C is attributed to desorption of NH_3 from the strong acid sites and the peak at 202°C corresponds to the weakly adsorbed NH_3. The plateau area in the temperature region 270-450°C is attributed to the desorption of NH_3 from the medium-strong acid sties in the case of sulfated titania. Acid sites are the interaction product of TiO_2 with sulfate ions. The S=O structure is essential for the generation of acidic sites on sulfate promoted oxide samples. The strong ability of S=O in sulfate complexes to accommodate electrons from a basic molecule is a driving force in the generation of highly acidic properties[71,72].

85

Table 3.5 Influence of the type of metal loaded on the acid site
distribution of sulfated titania system

Catalyst	Amount of ammonia desorbed (mmol g^{-1})			
	Weak (100-200°C)	Medium (200-400°C)	Strong (400-600°C)	Total (100-600°C)
T	0.31	0.20	0.01	0.52
ST	0.50	0.32	0. 09	0.91
STCr(3)	0.56	0.59	0.29	1.44
STMn(3)	0.50	0.41	0.12	1.03
STFe(3)	0.48	0.32	0.15	0.95
STCo(3)	0.49	0.34	0.10	0.93
STNi(3)	0.49	0.39	0.04	0.92
STCu(3)	0.50	0.38	0.06	0.94
STZn(3)	0.50	0.34	0.15	0.99

The total acidity values obtained from ammonia TPD were comparable for the different metal incorporated systems. In fact, no correlation could be obtained between the sulfate content of the various samples and their total acidity values. STCr(6) is the one that has the maximum acidity value compared to other systems. Among the different metal loadings, 6% loaded systems show maximum acidity. This can be due to the uneven charge distribution of Ti-O-M bonds, which can donate electrons to stabilize the S=O stretching[73]. The acidic properties generated by the inductive effect of S=O bonds of the complex are strongly affected by the environment of the sulfate ion. Thus, it can be proposed that acid properties would be modified by both the type of S=O in the sulfate complex and the coverage of sulfate on the surface.

Table 3.6 Influence of the amount of metal loading on the acid site
distribution of sulfated titania system

Catalyst	Amount of ammonia desorbed (mmol g^{-1})			
	Weak (100-200°C)	Medium (200-400°C)	Strong (400-600°C)	Total (100-600°C)
STCr(6)	0.75	0.67	0.31	1.73
STMn(6)	0.50	0.66	0.28	1.44
STFe(6)	0.44	0.53	0.30	1.27
STCo(6)	0.51	0.52	0.12	1.15
STNi(6)	0.50	0.55	0.08	1.13
STCu(6)	0.54	0.54	0.09	1.17
STZn(6)	0.50	0.53	0.29	1.32
STCr(9)	0.42	0.47	0.02	0.91
STMn(9)	0.37	0.46	0.01	0.84
STFe(9)	0.36	0.34	0.03	0.73
STCo(9)	0.37	0.35	0.01	0.73
STNi(9)	0.37	0.35	0.00	0.72
STCu(9)	0.38	0.35	0.00	0.73
STZn(9)	0.36	0.35	0.03	0.74

Samantaray *et al.*[8] reported a decrease in surface acidity at high sulfate concentrations. In our studies, systems that contain high metal content (having high sulfate amount) decrease the acidity of the system. The increased loading of sulfate on TiO_2, as evident from EDAX, can form the polynuclear type of sulfate complex and increase the coverage of the Ti metal ion by the sulfate ion. The polynuclear sulfate cannot extract as many electrons as isolated sulfate, to generate a strong acidity. It is reported in literature[74] that the generation of total and strong acidity is not affected by the type of sulfate

species, such as isolated and polynuclear, but by the coverage of the surface of the Ti by sulfate ions. Accordingly, it is concluded that the free Ti ion surrounding the sulfate is responsible for the generation of strong acid sites. With respect to the kind of acid site, it has been reported that both Lewis and Brönsted acid sites can be generated when a sulfate ion is introduced into TiO_2[61,62]. The nature of the acid sites is greatly altered by the nature of the ions incorporated into the lattice. The change in distribution may be a coupled effect of the crystalline and structural changes. The change in the acid strength distribution for the different systems may be related to the interaction of the added metal cations with the titania. According to Clearfield[33], strong Brönsted acidity is a result of the interaction between bisulfate groups and adjacent Lewis acid sites.

II. PERYLENE ADSORPTION STUDIES

The interaction of acid sites and basic probe molecules is studied to distinguish between Brönsted and Lewis type of acid sites and to determine their amount and strength. Qualitative information regarding Lewis acidity in the presence of Brönsted sites is based on the investigation of the ability of the surface to accept a single electron. Polyaromatic hydrocarbons such as perylene, pyrene and chrysene have mainly been used as electron donors [75,76]. The adsorption of perylene from a solution in benzene was carried out at room temperature. Perylene being an electron donor can transfer its electron to the Lewis acid sites and get itself adsorbed as perylene radical cation[77]. As the concentration of perylene in the solution increases, amount adsorbed also increases up to a certain limiting value after which it remains constant. The limiting amount of perylene indicated the surface electron accepting capacity or the Lewis acidity of the sample. The results of the perylene adsorption studies on the different systems are presented in figures 3.13 and 3.14.
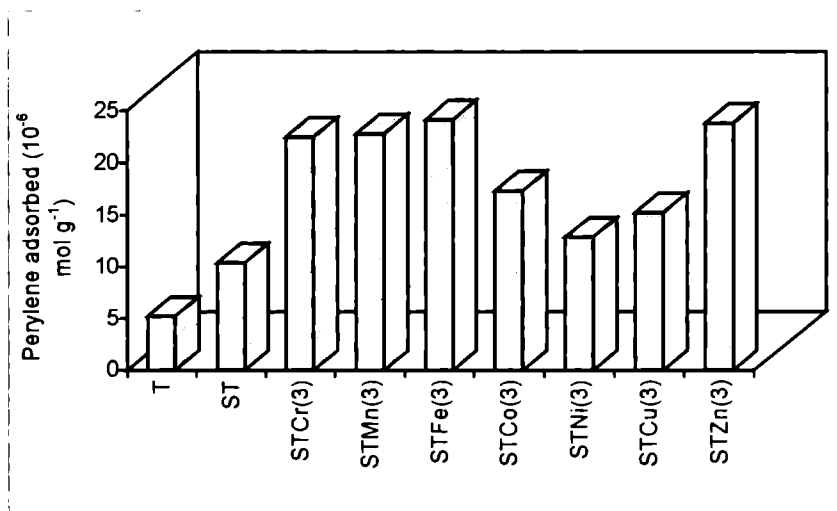
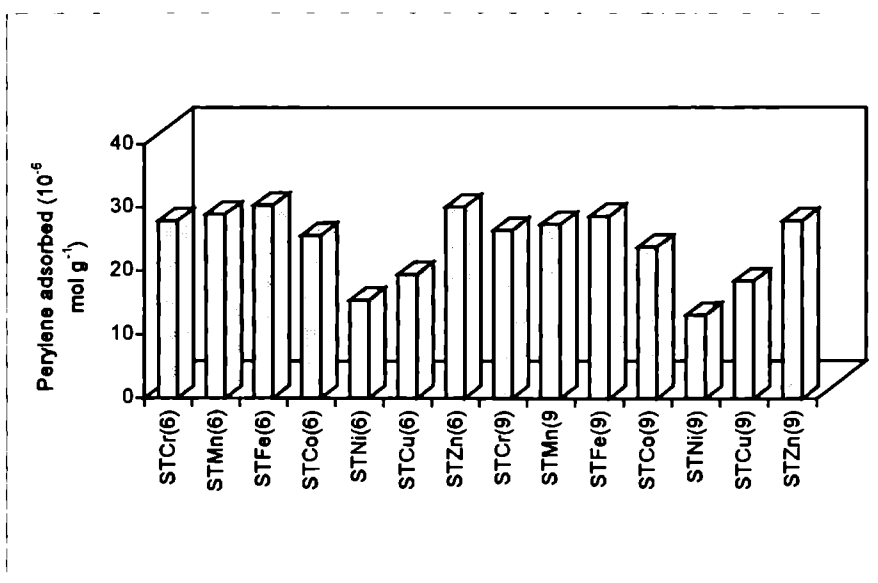Figure 3.13 Variation of Lewis acidity from perylene adsorption studies

Figure 3.14 Variation of Lewis acidity from perylene adsorption studies

The results of adsorption studies clearly show a considerable enhancement of Lewis acidity on sulfation. The limiting amount of perylene

89

adsorbed is very low in the case of pure titania. The amount of electron donor adsorbed increases gradually when we increase the metal content from 0 to 6% and for the samples containing higher metal content, it decreases. It is generally agreed that most sulfate groups which form on the exposed patches of regular crystalline planes can induce protonic acidity, especially if they are in the form of complex polynuclear sulfates whose formation is favoured at high loadings[78]. Lewis acidity enhancement upon sulfate doping can be ascribed to the increase in the electron acceptor properties of the three co-ordinated titania cations *via.* the inductive effect of the sulfate anions, which withdraw electron density from the titanium cations through the bridging oxygen atom[79,80]. According to the duel Brönsted-Lewis site model proposed by Clearfield[33] uncalcined catalyst contains protons as bisulfate and as hydroxyl groups bridging to metal ions. During calcination, either the bisulfate anion can react with an adjacent hydroxyl group resulting in a Lewis acid site or adjacent hydroxyl groups can keep bisulfate ion intact thereby generating Brönsted acidity. The combination of these Brönsted sites with the adjacent Lewis sites can also generate strong acidity.

Incorporation of metal ions into the crystal lattice may result in the formation of some complex structures in some local area on the surface, which results in an overall increase in the electronegativity of the surface complex[81]. Iron and zinc loaded samples show higher Lewis acidity among the metal loaded systems, where as copper and nickel loaded samples show lower Lewis acidity. The variation of metal content on Lewis acidity is shown in figure 3.15. Lewis acidity increases initially, reaches a maximum at 6% loading and decreases. The reduction in the case of high meal loaded samples may be due to the high sulfate loading where sulfate groups mostly exist in the form of polynuclear species[78].
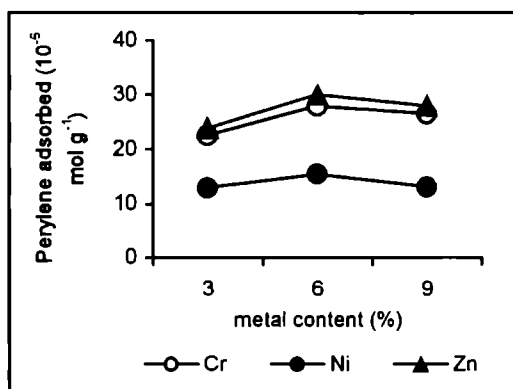
Figure 3.15 Variation of metal content on Lewis acidity

III. THERMODESORPTION STUDIES OF 2,6-DIMETHYLPYRIDINE

2,6-Dimethylpyridine (2,6-DMP) is a useful probe molecule for the selective determination of Brönsted acid sites. Corma *et al.*[82] reported that the IR bands corresponding to dimethyl pyridine associated with Lewis acid site disappeared with an increase in desorption temperature. The selective adsorption of 2,6-DMP on Brönsted acid sites is attributed to the steric hindrance of the methyl group. Satsuma *et al.*[83] reported a complete elimination of the co-ordinatively adsorbed 2,6-DMP on Lewis acid sites after purging at an appropriate temperature (above 300°C). Thus, we presume that the amount of 2,6-DMP desorbed at temperatures above 300°C originates exclusively due to desorption from Brönsted acid sites. The results of desorption studies are presented in tables 3.7 and 3.8.

The TG pattern of the samples were recorded after adsorption of 2,6-DMP to have a better understanding of the nature of surface acidity. Upon thermal treatment, 2,6-DMP gets desorbed at different temperature ranges depending on the strength of the acidic sites on which they are adsorbed. Those molecules adsorbed at strong acid sites desorbs only at high temperatures while those adsorbing on weak and medium acidic sites desorbs

91

at relatively low temperatures. Desorption below 300°C was omitted in the calculation since it contains contribution from Brönsted as well as weak Lewis acid sites. So as a crude approximation, it may be assumed that the desorption in the range 300 to 400°C arises from the weak sites and those in the range 400 to 500°C corresponds to medium acid strength while the strong acid sites give desorption between 500 to 600°C.

Table 3.7 Influence of the type of metal loaded on the Brönsted acid sites distribution from 2,6-DMP thermodesorption studies

Catalyst	Relative weight (%) loss of 2,6-DMP desorption			
	Weak (300-400°C)	Medium (400-500°C)	Strong (500-600°C)	Total (300-600°C)
T	0.13	0.45	0.19	0.77
ST	0.74	2.30	2.13	5.17
STCr(3)	1.03	2.61	1.96	5.60
STMn(3)	0.33	1.44	0.76	2.53
STFe(3)	0.51	1.49	0.31	2.31
STCo(3)	1.11	2.72	1.64	5.47
STNi(3)	0.84	2.51	1.78	5.13
STCu(3)	1.85	3.22	0.77	5.84
STZn(3)	0.44	1.29	1.70	3.43

From the table 3.7 it is clear that pure titania possesses only a very few Brönsted sites. Sulfated titania shows much higher Brönsted acidity compared to pure titania. Among the different metal loaded systems, copper loaded samples show the maximum Brönsted acidity. In the case of iron and zinc loaded systems the Brönsted acid sites are much less indicating that most of the acid sites are of Lewis type. Metal content also plays a beneficial role in determining the Brönsted acidity. 6% loading of the metal shows the maximum acidity and 3% loading, the minimum.

Table 3.8 Influence of the amount of metal loading on the Brönsted acid sites distribution from 2,6-DMP thermodesorption studies

Catalyst	Relative weight (%) loss of 2,6-DMP desorption			
	Weak (300-400°C)	Medium (400-500°C)	Strong (500-600°C)	Total (300-600°C)
STCr(6)	1.11	3.43	2.56	7.10
STMn(6)	0.38	0.98	2.46	3.82
STFe(6)	0.77	2.24	0.60	3.61
STCo(6)	0.97	2.38	3.23	6.58
STNi(6)	1.02	2.67	2.37	6.06
STCu(6)	1.58	2.71	3.22	7.51
STZn(6)	1.09	1.77	3.05	5.91
STCr(9)	0.75	3.25	2.04	6.04
STMn(9)	0.55	0.60	2.07	3.22
STFe(9)	0.48	1.85	0.51	2.84
STCo(9)	0.81	1.93	2.86	5.60
STNi(9)	1.00	2.33	2.15	5.48
STCu(9)	1.02	2.54	2.96	6.52
STZn(9)	0.72	1.84	2.29	4.85

IV. GAS-PHASE CUMENE CONVERSION REACTION

Cumene cracking reaction is generally used as a probe reaction to characterize the acidic properties of the catalyst. The cumene conversion and product selectivity could be correlated with the surface acidic properties. The major reaction occurring during the cumene cracking is dealkylation and dehydrogenation. Cumene is either dealkylated to benzene, dehydrogenated to α-methyl styrene, or the alkyl chain is cracked to produce ethyl benzene, toluene and styrene as shown in figure 3.15. Cracking of cumene mainly depends on Brönsted acid sties whereas dehydrogenation occurs on Lewis acid sites[84]. Thus it is possible to compare both Brönsted and Lewis acid sites in a catalyst through

cumene conversion reaction. Recently, Zenon *et al.*[85] published cumene decomposition over fluoride modified alumina. The cumene decomposition increases marginally and the selective products are benzene and propylene, while sodium modified alumina leads the cumene cracking into α-methyl styrene, which reveals that alumina surface is completely inactive in dealkylation.

Cumene

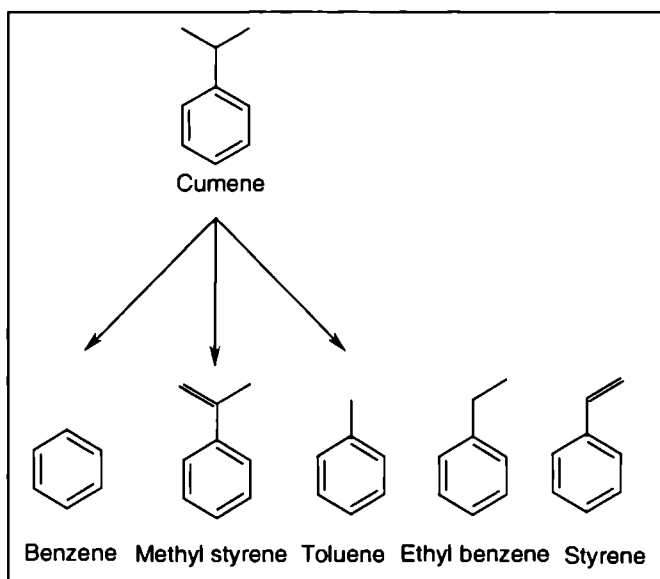Benzene Methyl styrene Toluene Ethyl benzene Styrene

Figure 3.15 General scheme of cumene conversion reaction

1. PROCESS OPTIMIZATION

A systematic study of cumene cracking reaction was carried out in a fixed bed down flow reactor of 1.2 cm ID and 25 cm length in the optimum temperature under atmospheric pressure. 0.5 g of the catalyst activated at 500°C for 2 h was secured between two plugs of glass wool inside the reactor. The temperature was controlled by a Cr-Al thermocouple placed inside the reactor. The reactant was supplied using a syringe pump and the liquid products were collected using a condenser at required time intervals. The products were analyzed by Gas Chromatography (*Chemito 8610* using SE-30

column having FID). The total conversion is defined as the sum of all aromatics except cumene divided by the sum of all aromatics including cumene. Among the products of cumene transformation, benzene and α-methyl styrene were detected as the major products. Small amounts of toluene, ethyl benzene and styrene are also detected as side products.

I. Effect of temperature

The reaction was done in a temperature range from 300 to 450°C at a flow rate of 3 mL h^{-1}. Figure 3.16 shows the influence of reaction temperature on the conversion and selectivity pattern. As the temperature increases cumene conversion also increases. The conversion is very low initially and it becomes 14.45% at 450°C.
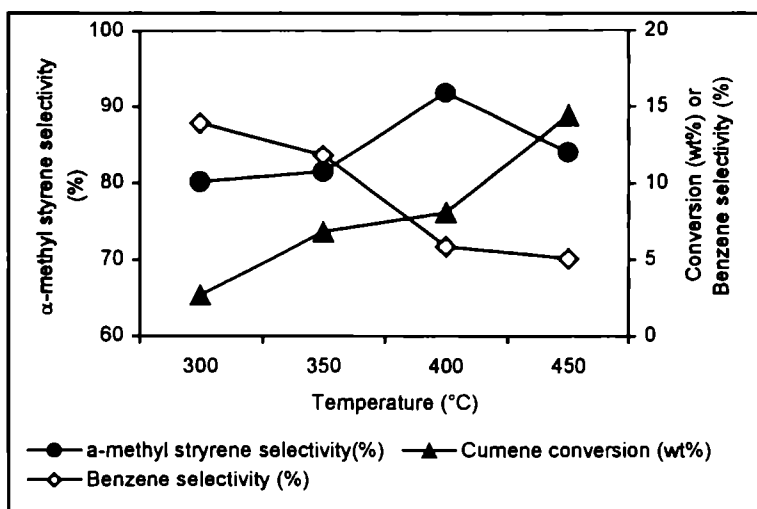

Figure 3.16 Influence of reaction temperature on cumene conversion.
Amount of catalyst: 0.5 g STMn(6), Flow rate: 3 mL h^{-1} Reaction time: 2 h.

From the figure, it is clear that α-methyl styrene is produced to a much higher extent when compared to the formation of benzene. At 400°C, the selectivity towards α-methyl styrene increases upto 91.87% and that of

95

benzene decreases to 5.88%. The catalyst is possessing large number of Lewis acid sites and hence dehydrogenation was favored more. The selectivity to α-methyl styrene increases and reaches a maximum at 400°C and then decreases. As the temperature increased from 350 to 400°C some of the Brönsted acid sites are converted into Lewis acid sites resulting in the increased selectivity of α-methyl styrene at 400°C.There is an optimum temperature at which the selectivity towards α-methyl styrene is maximum. At higher temperatures the amounts of both benzene and α-methyl styrene are low, while the amount of side products are higher.

II. Effect of Flow Rate

A typical activity profile of cumene conversion as a function of flow rate over STMn(6) is shown in figure 3.17. The conversion decreases as we increase the flow rate. At higher flow rates, the contact time between the reactant and the catalyst is less, which results in less conversion. As the feed rate is increased from 3 to 6 mL h^{-1}, the conversion decreased from 8.11 to 5.82 %. The contact time between the reactant and the catalyst surface is a decisive factor in determining the activity of the catalyst. At higher flow rates the contact time will be less leading to decrease in conversion. At all flow rates major product was α-methyl styrene with small amounts of benzene, toluene, ethyl benzene and styrene. The catalyst showed above 80% selectivity to α-methyl styrene at all flow rates and this indicates that surface acidity of the system is mainly due to the Lewis acid sites. With increase in flow rate, decrease in the dehydrogenation activity is observed. Maximum selectivity for α-methyl styrene is observed at a flow rate of 3 mL h^{-1}.
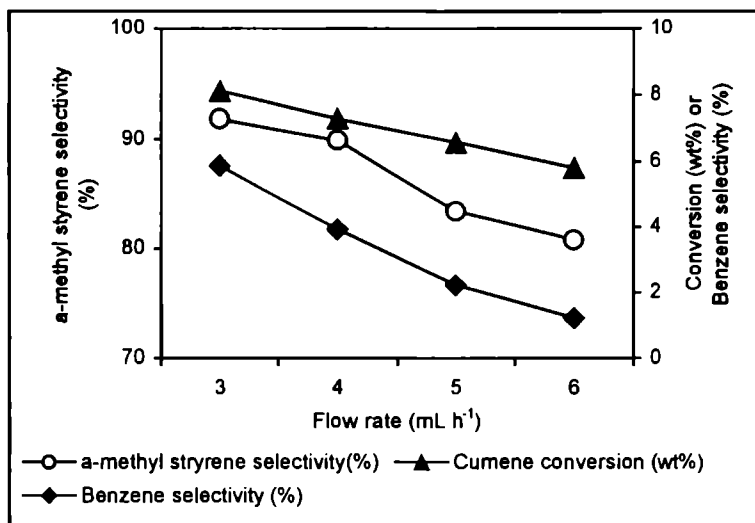
Figure 3.17 Influence of flow rate on cumene conversion and product selectivity

Amount of catalyst: 0.5 g STMn(6), Reaction temperature: 400°C, Reaction time: 2 h.

III. Effect of Time on Stream-Deactivation Study

Performance of the reaction for a continuous 7 hours run was studied to test the deactivation of the catalyst. The products were collected and analyzed after every one hour. Figure 3.18 shows that even after 7 h of reaction time, the selectivities do not vary much. In the case of metal incorporated systems, there is an increase in the selectivity initially, after that it remains almost constant. This may be due to the fact that the coke formed during the reaction may not be bulky to block all the pores of the catalyst[86].

2. COMPARISON OF DIFFERENT SYSTEMS

The cumene conversion reactions for the different catalytic systems were performed under the optimized condition. Reaction temperature-400°C, flow rate-3 mL h^{-1} and time on stream-2 h. The conversion and selectivity for various products are given in tables 3.9 and 3.10.
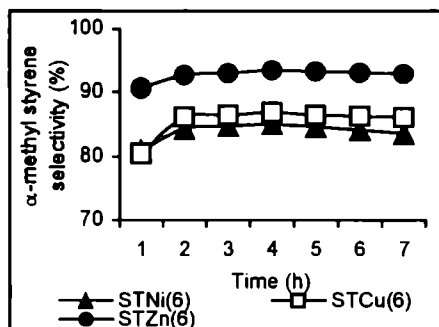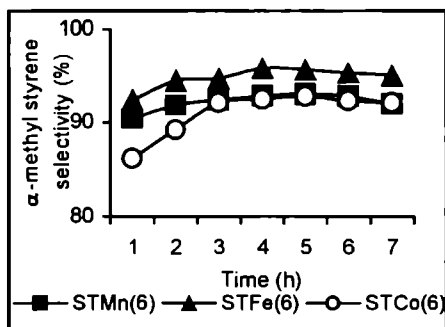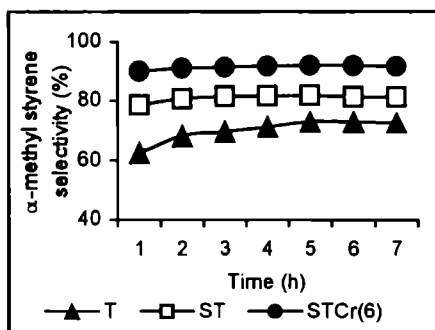
97

Figure 3.18 Deactivation studies on cumene conversion over different systems

Amount of catalyst: 0.5 g, Reaction temperature: 400°C, Flow rate: 3 mL h^{-1}.

In all the systems, α-methyl styrene is the predominant product, which confirms that dehydrogenation of cumene is the main reaction occurring under the reaction conditions. Compared to pure titania, metal incorporated systems are showing increased activity and selectivity. Titania possesses as very few Lewis acid sites and hence exhibits low α-methyl styrene selectivity. Maximum conversion is shown by STCr(3) while the α-methyl styrene selectivity is high for STFe(3). From tables 3.9 and 3.10 it is clear that all the systems except T are showing more than 80% selectivity for α-methyl styrene. Incorporation of transition metals, increases the Lewis acidity as revealed from perylene adsorption studies, and hence the α-methyl styrene selectivity. As the metal loading is increased, the conversion and selectivity increases up to 6% and then decreases in the case of 9% loading.

Table 3.9 Influence of the type of metal loaded in the cumene conversion

Systems	Conversion of cumene (wt%)	Selectivity (%)	
		α-methyl styrene	Benzene
T	1.31	67.93	3.60
ST	2.49	80.85	6.25
STCr(3)	5.22	86.34	7.23
STMn(3)	5.08	87.91	4.57
STFe(3)	4.80	92.44	4.20
STCo(3)	4.20	84.23	6.78
STNi(3)	2.54	81.33	5.38
STCu(3)	4.31	82.54	7.89
STZn(3)	4.36	89.48	4.93

Amount of catalyst: 0.5 g, Flow rate: 3 mL h^{-1}, Reaction time: 2 h, Reaction temperature: 400°C.

Rana *et al.*[87] studied the cumene cracking reaction over sulfided Co(Ni)Mo/TiO$_2$-SiO$_2$ catalyst and found that 8 wt% loading is optimum for maximum activity. Supporting evidence for these conclusions is provided by the ammonia TPD and adsorption studies. Cumene cracking was carried out over γ-alumina impregnated with fluoride, cobalt, molybdena and combination of these additives by Boorman *et al.*[88,89], and catalytic activities of these systems were correlated with the acidity. In the present case also we can correlate the cumene conversion with total acidity obtained from ammonia TPD measurements (figures 3.19 and 3.20).

Table 3.10 Influence of amount of metal loading in the cumene conversion

Systems	Conversion of cumene (wt%)	Selectivity (%)	
		α-methyl styrene	Benzene
STCr(6)	8.57	91.00	9.88
STMn(6)	8.11	91.87	5.88
STFe(6)	7.92	94.41	5.14
STCo(6)	6.47	89.22	8.85
STNi(6)	5.90	84.26	7.47
STCu(6)	6.92	86.12	12.11
STZn(6)	7.63	92.64	6.93
STCr(9)	2.46	87.84	7.36
STMn(9)	2.38	88.16	4.96
STFe(9)	2.35	93.53	4.50
STCo(9)	2.30	84.14	7.05
STNi(9)	2.28	82.13	6.78
STCu(9)	2.30	83.21	8.09
STZn(9)	2.35	89.08	5.27

Amount of catalyst: 0.5 g, Flow rate: 3 mL h^{-1} Reaction time: 2 h, Reaction temperature: 400°C.

Brönsted acidity obtained from the thermodesorption of 2,6-DMP and benzene selectivity from cumene conversion shows very good correlation (figures 3.21 and 3.22). Brönsted acidity changes with respect to the metal ions and the maximum is possessed by STCu(3), and minimum by STFe(3) for 3 % loading. Benzene selectivity also follows the same trend.
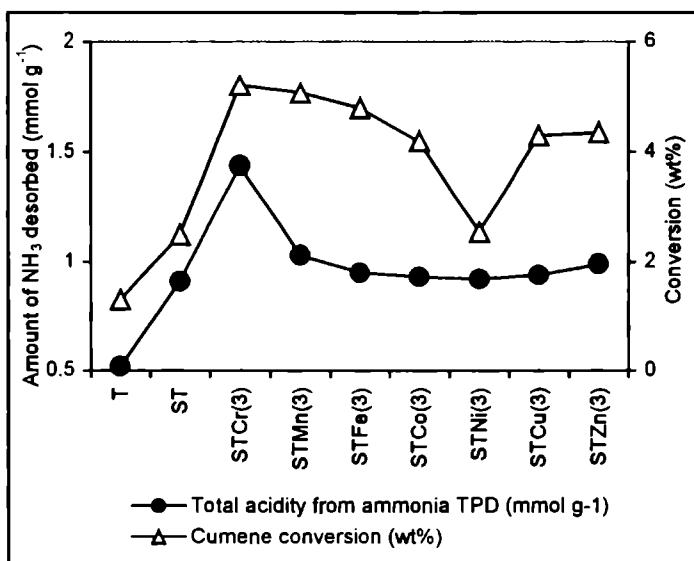
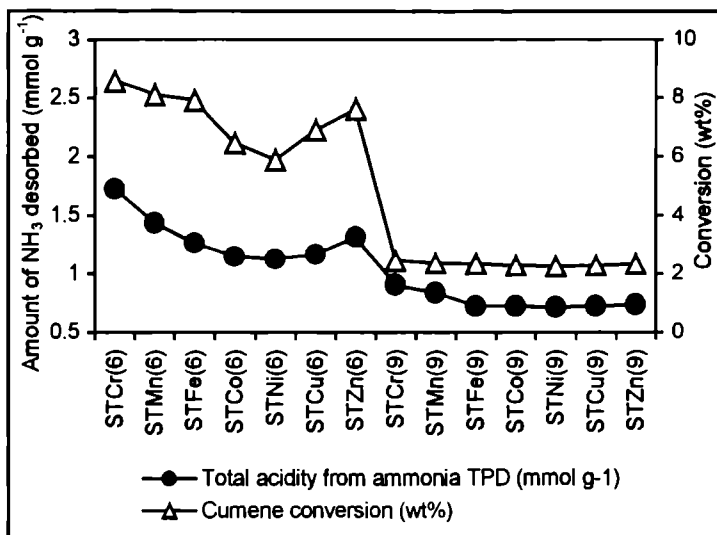Figure 3.19 Correlation between cumene conversion and total acidity

Figure 3.20 Correlation between cumene conversion and total acidity

Chromia is reported to be a strong Lewis acid[90]. The presence of chromium in the samples may lead to high Lewis acidity and hence the dehydrogenation selectivity. The comparatively high value of limiting amount for perylene adsorption also supports the high Lewis acidity of chromia containing systems. Change in the metal content also changes the selectivity. High loading of metals resulted in the decrease of percentage conversion. This can be attributed to the decrease in the acidity for the high loaded samples due to the formation of polysulfate species[17]. The inhibition of Lewis acidity due to the high loading led to the reduction of percentage selectivity of α-methyl styrene. In all the cases the selectivity to α-methyl styrene is more than 80%. All the systems show very low selectivity for benzene showing less number of Brönsted acid sites in the samples.
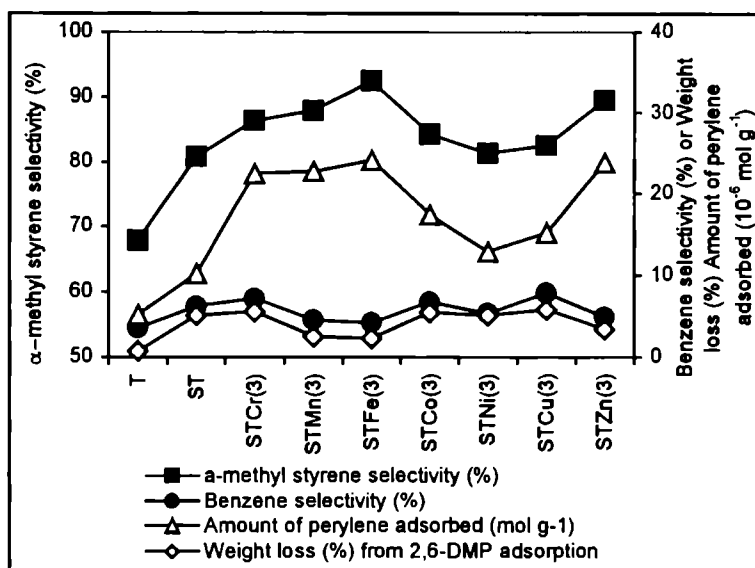

Figure 3.21 Correlation of α-methyl styrene selectivity with Lewis acidity and benzene selectivity with Brönsted acidity
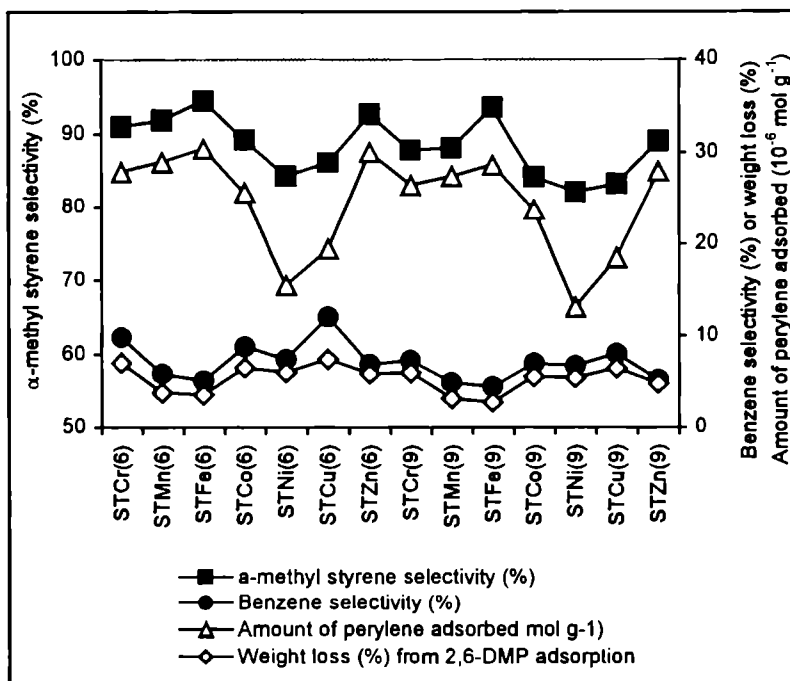
Figure 3.22 Correlation of α-methyl styrene selectivity with Lewis acidity and benzene selectivity with Brönsted acidity

3. MECHANISAM OF CUMENE CONVERSION REACTION

The major reactions occurring during cumene conversion may be grouped into dealkylation (cracking) and dehydrogenation. Cracking of cumene to benzene is generally attributed to the action of Brönsted sites by a carbonium ion mechanism[17,90-94], while dehydrogenation of cumene yields α-methyl styrene as the major product, the formation of which has been ascribed to the Lewis acid sites[17]. Corma *et al.*[95] reported that dealkylation of cumene requires the presence of a small number of Brönsted acid sites which are capable of formation of a σ-complex with cumene molecule. Bautista *et al.*[96,97] assumed the mechanism for cumene decomposition on the basis of Brönsted acid sites which is taking place by the protonation of cumene

molecule to form π-complex and subsequently this complex is transformed into σ-complex. A plausible mechanism of cumene conversion reaction is represented in figure 3.23.
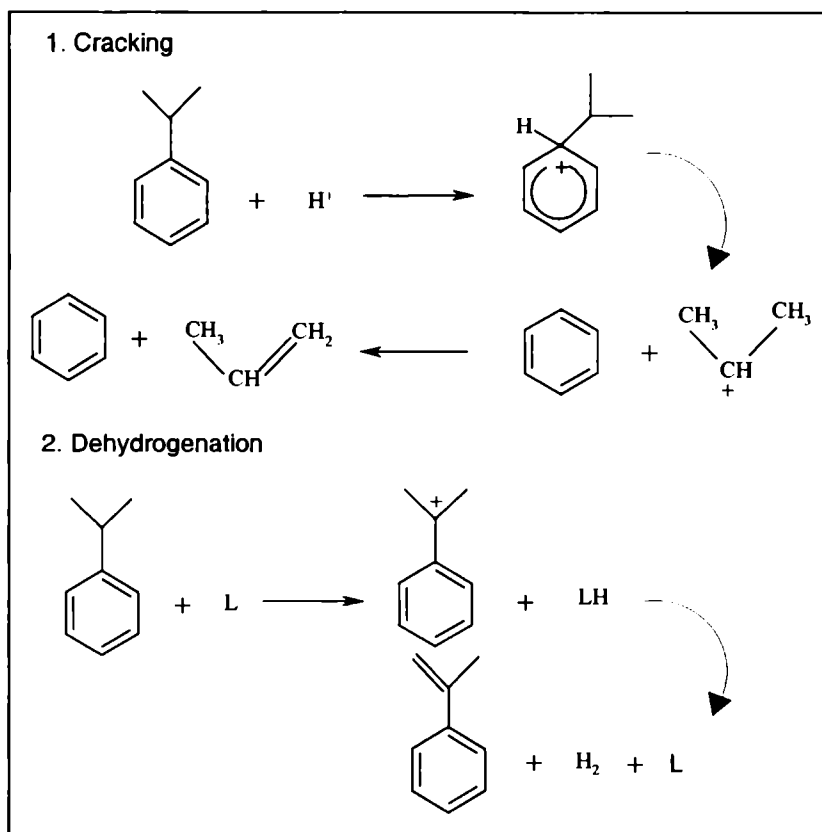
Figure 3.23 Mechanism of cumene conversion reaction

V. CYCLOHEXANOL DECOMPOSITION REACTION

Alcohol decomposition reaction is widely studied to check the acid-base property of the catalyst system[98]. The amphoteric character of the alcohol permits its interaction with both acidic and basic centers. Decomposition of isopropanol[99,100] and of cyclohexanol[101,102] are the most widely studied reactions in this category. Dehydrogenation and dehydration can take place

resulting in the formation of cyclohexanone and cyclohexene[103] (figure 3.24) in the case of cyclohexanol decomposition reaction. Dehydration activity is linked to acidic property and dehydrogenation activity to the combined effect of both acidic and basic properties.
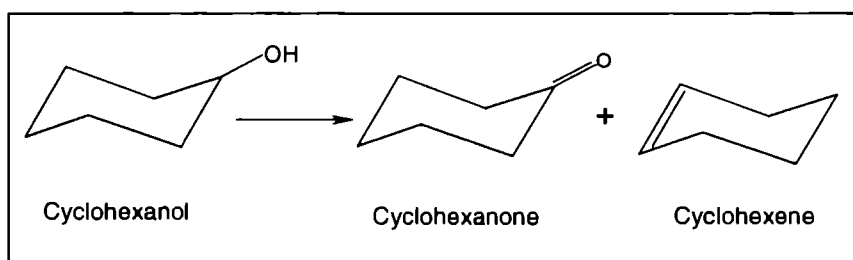

Figure 3.24 Scheme of cyclohexanol decomposition reaction

1. PROCESS OPTIMIZATION

Cyclohexanol decomposition was carried out in a continuous flow fixed bed reactor. 0.5 g of the preactivated catalyst was placed in the middle of the reactor and cyclohexanol was fed by a syringe pump at different flow rates. The temperature is monitored using a Cr/Al thermocouple placed in the middle of the reactor. The liquid products were analyzed by a *Chemito 8610* Gas Chromatograph analyzer fitted with FID using Carbowax column (2 m). The products were identified as cyclohexene, cyclohexanone, benzene, methyl cyclopentene and cyclohexane. Among these cyclohexene and cyclohexanone were the major products and the selectivities were calculated accordingly. For any catalyst system, the activity and selectivity towards a particular reaction depend on reaction parameters in addition to the physical and chemical properties of the catalysts. The optimum parameters for cyclohexanol decomposition were determined by carrying out the reaction at different temperatures and flow rates.

I. Effect of temperature

The reaction is carried out at various reaction temperatures in the range of 200-350°C. Table 3.11 shows the influence of reaction temperature on the conversion and the product distribution. As the temperature increases the percentage conversion also increases.

Table 3.11 Effect of reaction temperature on the conversion of cyclohexanol

Temperature (°C)	Conversion of Cyclohexanol (wt%)	Selectivity (%)	
		Cyclohexene	Cyclohexanone
200	72.95	90.85	8.89
250	89.46	92.24	7.02
300	97.40	93.53	6.34
350	98.58	92.83	6.54

Amount of catalyst: 0.5 g STCr(6), Flow rate: 4 mL h^{-1} Reaction time: 2 h.

The conversion reached a maximum of 98.5% at a temperature of 350°C. Cyclohexene is found to be the major product with selectivity more than 90% at all temperatures. Increase in the temperature will decompose surface hydroxyl ions and subsequently will create more Lewis acid centers. Cyclohexanone selectivity is less, which was formed by the participation of both acidic and basic sites[104,105]. Even though there is enough number of acidic sites, absence of basic sites on the titania surface restricts the formation of cyclohexene. Cyclohexene selectivity is maximum at 300°C, and then decreases.

II. Effect of Flow Rate

A series of experiments were conducted at a reaction temperature of 300°C at different flow rates viz. 3, 4, 5 and 6 mL h^{-1} to understand the

influence of flow rate on the reaction. Figure 3.25 shows the effect of flow rate on cyclohexanol conversion and selectivity.
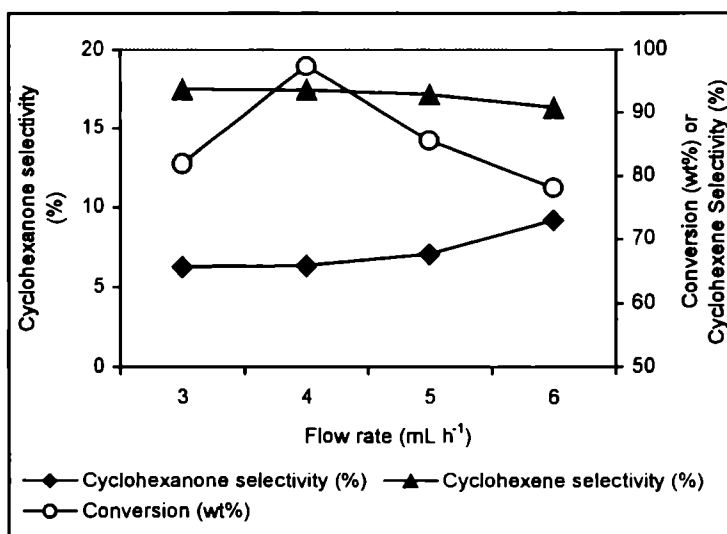

Figure 3.25 Influence of flow rate on cyclohexanol conversion and selectivity
Amount of catalyst: 0.5 g STCr(3), Reaction temperature: 300°C. Reaction time: 2 h.

Conversion increases initially as the flow rate changes from 3 to 4 mL h⁻1, however further increase in flow rate decreases the conversion. The conversion decreases from 97.40 to 78.14%, as the flow rate increases from 4 to 6 mL h^{-1}. Decrease in contact time leads to reduction in conversion. Increase in flow rate did not alter the selectivity of catalyst to a considerable extent. At all flow rates about 90% selectivity for cyclohexene is observed. Maximum conversion and maximum selectivity is shown at 4 mL h^{-1} and is selected for further studies.

III. Effect of Time on Stream-Deactivation Study

Stability studies of different catalysts were performed by observing the conversion over a period of 7 hours. Reactions were carried at 400°C at a flow rate of 4 mL h^{-1} and the product analysis was done at regular intervals of 1 hour and is given in figures 3.26 . All systems are showing excellent activity

over a period of 3 hours after that it decreases slowly. The decrease in the activity indicates that there is some decrease in the acidity of catalyst with time. Rate of deactivation is more or less same in all the cases. Even after 7 h reaction time metal incorporated systems show more than 60% conversion.
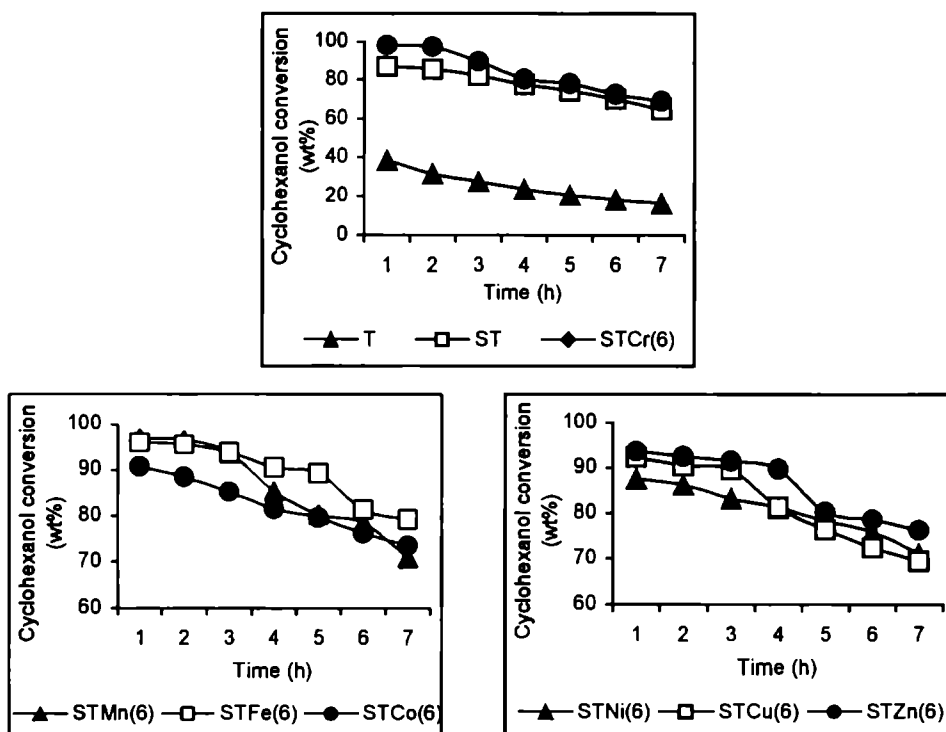
Figure 3.26 Deactivation studies on cyclohexanol decomposition
over different systems

Amount of catalyst: 0.5 g, Reaction temperature: 300°C, Flow rate: 4 mL h^{-1}.

2. COMPARISON OF DIFFERENT SYSTEMS

In order to compare catalytic performance of different systems for the cyclohexanol decomposition reaction, we carried out the reaction under optimized conditions (reaction temperature-300°C, flow rate-4 mL h^{-1} and reaction time-2 h) over all the prepared systems. The results obtained are

presented in tables 3.12 and 3.13. From the tables it is obvious that the activity of the systems is greatly influenced by the presence of metal incorporated as well as the sulfate ions on the surface. Chromia loaded systems show the maximum activity. This may be due to the high acidity of these samples as evident from results of ammonia TPD.

Table 3.12 Influence of the type of metal loaded in the cyclohexanol decomposition reaction

Systems	Conversion of Cyclohexanol (wt%)	Selectivity (%)	
		Cyclohexene	Cyclohexanone
T	31.54	62.45	16.24
ST	85.36	82.36	10.10
STCr(3)	92.20	89.81	7.96
STMn(3)	91.48	87.95	8.40
STFe(3)	84.25	80.40	9.02
STCo(3)	85.54	84.32	9.28
STNi(3)	86.92	84.34	7.68
STCu(3)	87.00	86.08	9.87
STZn(3)	86.32	84.88	7.27

Amount of catalyst: 0.5 g, Flow rate: 4 mL h^{-1}. Reaction time: 2 h, Reaction temperature: 300°C.

Since pure titania possess very low acidity, its activity is also less. Depending upon the percentage of metal, selectivity also changes. The metal content also plays an important role in cyclohexanol decomposition reaction. All the sulfated systems show more than 70% conversion and high selectivity towards cyclohexene. Sulfating agents, being acidic species, preferentially attack the basic sites converting these to acidic sites[108]. The high activity in the formation of cyclohexene may be due to the weak and medium acid centers on the catalyst surface, which is apparent from ammonia TPD measurements[106].

The considerably small amount of other products like benzene, methyl cyclohpentene and cylohexane points to the absence of strong acid sites on the catalyst surface.

Table 3.13 Influence of the amount of metal loading in the cyclohexanol decomposition reaction

Systems	Conversion of Cyclohexanol (wt%)	Selectivity (%)	
		Cyclohexene	Cyclohexanone
STCr(6)	97.40	93.53	6.34
STMn(6)	96.53	90.26	7.78
STFe(6)	85.49	88.00	7.59
STCo(6)	88.48	80.34	9.74
STNi(6)	90.24	81.83	7.68
STCu(6)	95.49	88.46	6.45
STZn(6)	89.24	89.25	9.22
STCr(9)	83.56	85.39	11.61
STMn(9)	80.32	83.14	9.71
STFe(9)	72.54	70.49	9.76
STCo(9)	76.21	72.54	7.68
STNi(9)	76.75	78.26	9.69
STCu(9)	78.00	80.75	10.68
STZn(9)	73.62	74.07	6.76

Amount of catalyst: 0.5 g, Flow rate: 4 mL h^{-1}, Reaction time: 2 h, Reaction temperature: 300°C.

Gervasini and Auroax[99,107] attempted to correlate the dehydration and dehydrogenation activity of isopropanol decomposition with the acid base character obtained by the calorimetric investigation of a large series of metal oxides. Ramankutty *et al.*[105] had studied the cyclohexanol decomposition

reaction over the ferrospinels and reported that the sulfation had increased the dehydration activities of all the ferrites. Bezouhanova *et al.*[108] recommend dehydration activity of cyclohexanol decomposition as a simple method of determining Brönsted acid sites on a catalyst surface. The same opinion was also expressed by Martin and Duprez[102] and Armendia *et al.*[100]
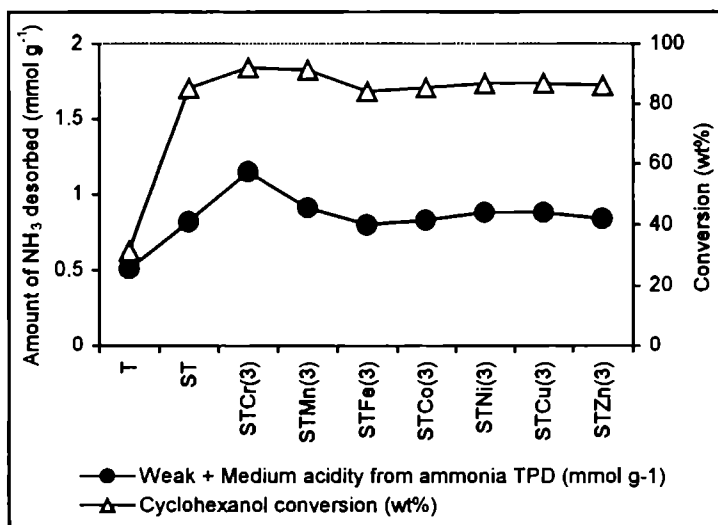

Figure 3.27 Correlation between cyclohexanol conversion and 'weak + medium' acidity from NH₃-TPD

The formation of cyclohexanone over any catalyst indicates the presence of strong and medium basic centers. The formation of cyclohexanone is low at the optimized reaction temperature indicating the absence of strong basic centers though medium and weak basic centers exist in the catalyst. But for high loadings, selectivity to cyclohexanone is found to be slightly higher. With high loadings, the basic centers might have increased which accounts for the higher selectivity to cyclohexanol. It is also confirmed by the decrease in acidity values from ammonia TPD. The selectivity in alcohol decomposition is mainly controlled by the acid-base properties[109]. Variation in the dehydrogenation and dehydration selectivity for the

catalyst systems suggests that acidic and basic properties of sulfated titania vary with incorporation of different transition metal oxides.
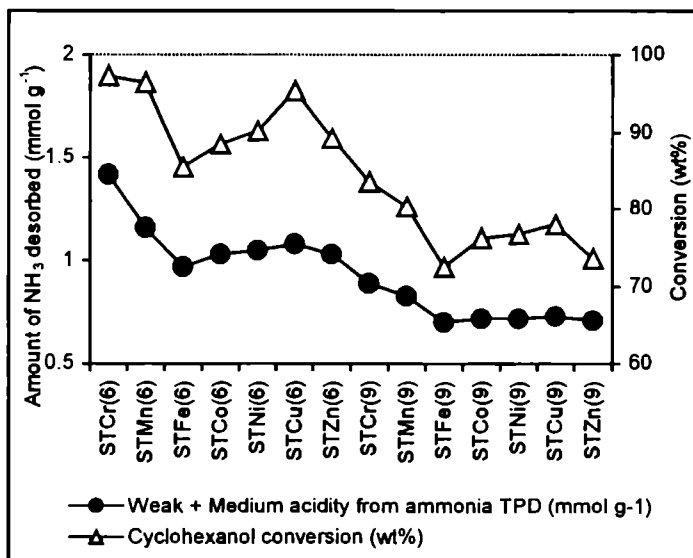

Figure 3.28 Correlation between cyclohexanol conversion and 'weak + medium' acidity from NH_3-TPD

Comparing the reaction data with various acidity data, we could find a direct relationship between the percentage conversion and the sum of weak and medium acidity obtained from ammonia TPD. Figures 3.27 and 3.28 show the correlation between the acidity and the conversion of cyclohexanol. As the percentage loading of metal increases the conversion and cyclohexene selectivity increase, but for higher loadings both decrease. On modification with sulfate ions some of the basic sites are converted to acidic sites. The mechanism of sulfation is an anion exchange between SO_4^{2-} and OH^-, which is already reported[110]. During their study of cyclohexanol conversion at 300°C, Martin and Duprez[102] noted that the presence of sulfate on zirconia increased its protonic acidity as proved by an increase in the cyclohexene selectivity. So in the case of sulfated titania systems there are enough acidic sites to catalyze the dehydrogenation giving better cyclohexene selectivity.

3. MECHANISAM OF CYCLOHEXANOL DECOMPOSITION REACTION

Cyclohexanol dehydration leads to cyclohexene whereas dehydrogenation gives cyclohexanone. It has been well established that Brönsted acid sties of the catalyst are directly involved in the alcohol dehydration mechanism. It is similar to E-1 elimination in which the reaction proceeds through initial formation of carbocation.
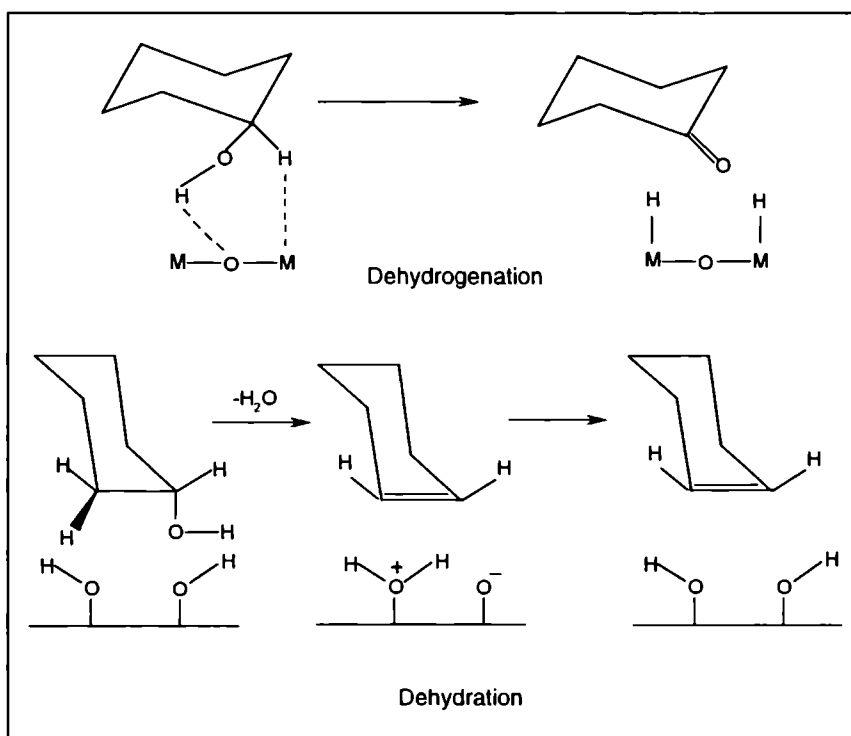
Figure 3.29 Mechanism of dehydrogenation and dehydration
of cyclohexanol on oxide surface

In the case of dehydrogenation, the fission of the O-H and C_α-H bond is involved. The metal cation is acting as a Lewis acid site accepting a hydride ion whereas the oxygen anion of the catalyst is acting as a Brönsted base accepting the proton of the OH group of the alcohol[111,112]. The mechanism of dehydration and dehydrogenation of cyclohexanol is given in figure 3.29. In

113

addition to cyclohexene and cyclohexanone, trace amount of phenol, benzene and cyclohexane were also detected. Benzene and cyclohexane were formed via the disproportionation of cyclohexene formed as a result of dehydration of cyclohexanol[113]. It was reported[114] that cyclohexanone undergoes further transformation to phenol at high contact times. Costa *et al.*[115], by means of deuterium labeling experiments, have shown that the gas phase dehydration of cyclohexanol over a solid zirconium phosphate catalyst, involves a long lived carbocation intermediate and that the reaction proceeds via the E1 mechanistic route.

3.4. CONCLUSIONS

The following conclusions can be drawn from the different physico chemical characterization techniques as well as acidity determination of the sulfated titania systems.

  Nanocrystalline materials of crystallite size upto 5 nm can be easily prepared by this sol-gel method. Anatase is found to be the major phase in all the samples as apparent from XRD data. Sulfate ions hinder the crystallization of titania particles by preventing the agglomerization of surface particles. Sulfation retards the transformation of anatase to rutile.

  Surface area and pore volume of sulfated samples are higher than that of pure titania. The metal oxide species along with the sulfate ions prevent the agglomeration of titania particles resulting in a higher surface area.

  EDX results prove that sol-gel method is an efficient method to prepare supported systems with desired loading of transition metals. The presence of transition metal oxides stabilizes the sulfate over layers on the catalyst surface is apparent from the increase in the sulfate retaining capacity, which is evident from EDX results. SEM pictures clearly give the surface morphology of these catalysts.

❧ TG/DTG analysis of the catalysts reveals the higher thermal stability of metal incorporated sulfated titania systems even after 700°C. Sulfate incorporation is confirmed by FTIR analysis. λ_{max} and hence band gap energy is calculated from UV-Vis DR spectra, which again confirms the anatase phase of these catalysts. ^1H NMR studies give an idea about the titanol groups present in the catalysis.

❧ Acidities of the systems are measured by different techniques like NH_3-TPD, perylene adsorption and thermodesorption of 2,6-DMP. Among the different systems 6% metal loaded samples shows the maximum acidity. Cumene conversion reaction proved to be a satisfactory test reaction for surface acidity. The percentage conversion could be correlated with the total acidity of the systems, while the dehydrogenation and cracking selectivity followed trends in the Lewis and Brönsted acidity of the samples respectively. Cyclohexanol decomposition reveals the acid base properties of the prepared catalysts.

ॐ ঙ্কাক্কাক্কা ॐ
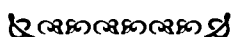
REFERENCES

1. A.V. Ramaswamy, "*Catalysis Principles and applications*", Narora, New Delhi.

2. Z. Gao, J.M. Chen, *Chem. J. Chin. Uni.*, 15 (1994) 873.

3. X. Song, A. Sayari, *Catal. Rev. Sci. Eng.*, 38 (1996) 329.

4. G. Colon, M.C. Hidalgo, J.A. Navio, *Appl. Catal.*, 231 (2002) 185.

5. S.K. Samantaray, T. Mishra, K.M. Parida, *J. Mol. Catal. A. Chem.*, 156 (2000) 267.

6. M.M. Dubinin, *Chem. Rev.*, 60 (1960) 235.

7. M.P. Rosynek, P.T. Magnuson, *J. Catal.*, 46 (1977) 402.

8. H. Lipson, H. Steeple, *"Interpretation of X-ray powder Diffraction Patterns"*, Macmillan, London, (1970) 261.

9. K. Kandori, S. Uchida, S. Kataoka, T. Ishikawa, *J. Mater. Sci.,* 27 (1992) 719.

10. K.M. Parida, M. Acharya, S.K. Samantaray, T. Mishra, *J. Colloid Interface Sci.,* 217 (1999) 388.

11. D.G. Barton, S.L. Soled, G.D. Meitzner, G.A. Fuentes, E. Iglesia, *J. Catal.,* 181 (1999) 57.

12. L.J. Alemany, M.A. Larrubia, M.C. Jimenez, F. Delgado, J.M. Blasco, *React. Kinet. Catal. Lett.,* 60 (1997) 41.

13. K.R. Sunajadevi, S. Sugunan, *React. Kinet. Catal. Lett.,* 82 (2004) 11.

14. S.T. Choo, Y.G. Lee, I.S. Nam, S.W. Ham, J.B. Lee, *Appl. Catal. A. Gen.,* 200 (2000) 177.

15. A. Corma, *Chem. Rev.,* 95 (1995) 559.

16. Z. Ma, Y. Yue, X. Deng, Z. Gao., *J. Mol. Catal. A. Chem.,* 178 (2002) 97.

17. A.K. Dalai, R. Sethuraman, S.P.R. Katikeneni, R.O. Idem, *Ind. Eng. Chem. Res.,* 37 (1998) 3869.

18. B.I.I. Davis, R.A. Kcogh, R. Sreenivasan, *Catal. Toady,* 20 (1994) 219.

19. J.F. Le Page, J. Cosyns, P. Courty, E. Freund, J.P. Franck, Y. Jacquin, B. Juguin, C. Marcilly, G. Martino, J. Miquel, R. Montarnal, A. Sugier, H. Van Landeghem, *"Applied Heterogeneous Catalysis"*, Editions Technip, Paris, (1987) p. 92.

20. C.G. Granqvist, R.A. Buhraman, *J. Appl. Phys.,* 47 (1996) 2200.

21. J. Livage, K. Doi, C. Maziieres, *J. Phys. Chem.,* 93 (1989) 6769.

22. R. Srinivasan, R.A. Keogh, D.R. Milburn, B.H. Davis, *J. Catal.,* 153 (1995) 23.

23. R.A. Keogh, R. Srinivasan, B.H. Davis, *J. Catal.,* 153 (1995) 23.

24. O. Saur, M. Bensitel, A.B.M. Saad, J.C. Lavalley, C.P. Tripp, B.A. Morrow, *J. Catal.,* 99 (1986) 104.

25. H.P. Bochnm, H. Knozinger, *"Catalysis"*, J.R. Anderson and M. Boudart, Eds. Vol. 4, Springer, Berlin (1983) Chp. 2.

26. G. Cristallo, E. Roncari, A. Rinaldo, F. Trifiro, *Appl. Catal. A. Gen.*, 209 (2001) 249.

27. J.M. Gallardo-Amores, T. Armaroli, G. Ramis, E. Finocchino, G. Busca, *Appl. Catal. B. Environ.*, 22 (1999) 249.

28. T. Lopez, J.A. Moreno, R. Gomez,X. Bokhimi, J.A. Wang, H. Y. Madeira, G. Pecchi, P. Reyes, *J. Mater. Chem.*, 12 (2002) 714.

29. Y. Su, M.L. Balmer, B.C. Bunker, *J. Phys. Chem. B.*, 104 (2000) 8160.

30. G.D. Yadav, J.J. Nair, *Micropor. Mesopor. Mater.*, 33 (1999) 1.

31. S.M. Jung, O. Dupont, P. Grange, *Appl. Catal. A. Gen.*, 208 (2001) 393.

32. C. Morterra, V. Bolis, G. Cerrato, *Catal. Today*, 17 (1993) 505.

33. A. Clearfield, G.P.D. Serrette, A.H. Khazi-Syed, *Catal. Today*, 20 (1994) 295.

34. L.M. Kustov, V.B. Kazansky, F. Figueras, D. Tichit, *J. Catal.*, 150 (1994) 143.

35. K. Nakamoto, *"Infrared and Raman Spectra of Inorganic and Coordination Compounds"*, 4th edition, Wiley, New York (1986).

36. M. Bensitel. O. Saur, J.C. Lavalley, B.A. Morrow, *Mater. Chem. Phys.*, 19 (1988) 147.

37. C. Morterra, G. Cerrato, C. Emanuel, V. Bolis, *J. Catal.*, 142 (1993) 349.

38. M.T. Tran, N.S. Gnep, G. Szabo, M. Guisner, *Appl. Catal.*, 171 (1998) 207.

39. M. Anpo, T. Shima, S. Kodama, Y. Kubokawa, *J. Phys. Chem.*, 91 (1987) 4305.

40. Q. Zhang, L. Gao, J. Guo, *Appl. Catal. B. Environ.*, 26 (2000) 207.

41. Degussa Canada Ltd., Bull. 56, Burlington, Ont., Canada.

42. M.A. Malathi, W.K. Wong, *Surf. Technol.*, 22 (1984) 305.

43. W.K. Wong, M.A. Malathi, *Solar Energy*, 36 (1986) 163.

44. S. Velu, N. Shah, T.M. Jyothi, S. Sivasanker, *Micropor. Mesopor. Mater.*, 33 (1998) 61.

45. F. Milella, j.M. Gallardo-Amores, M. Baldi, G. Busca, *J. Mater. Chem.*, 8 (1998) 2525.

46. G. Ertl, H. Knozinger, J. Weitkamp, *"Handbook of Heterogeneous Catalysis"*, (Ed. G. Ertl, H. Knozinger, J. Weitkamp), Vol. I (Wiley VCH), (1997), p. 324.

47. M. Stoker, *Stud. Surf. Sci. Catal.*, 85 (1994) 429.

48. H. Pfeifer, D. Freude, M. Hunger, *Zeolites*, 5 (1985) 274.

49. P.A. Jacobs, W.J. Mortier, *Zeolites*, 2 (1982) 226.

50. M. Weihe, M. Hunger, M. Breuninger, H.G. Karge, J. Weitkamp, *J. Catal.*, 198 (2001) 299.

51. M. Hunger, Catal. *Rev. Sci. Eng.*, 39 (1997) 345.

52. M.A. Enriquez, C. Doremieux-Morin, J. Fraissard, NATO, *Adv. Study Inst. Ser., Ser. C.*, 61 (1980) 409.

53. B.M. Reddy, E.P. Reddy, S.T. Srinivas, V.M. Mastikhin, A.V. Nosov, O.B. Lapina, *J. Phys. Chem.*, 96 (1992) 7076.

54. K.V.R. Chary, V. Vijayakumar, P. Kanta Rao, A.V. Nosov, V.M. Mastikhin, *J. Mol. Catal.*, 96 (1994) L5.

55. L.G. Pinaeva, O.B. Lapina, V.M. Mastikhin, A.V. Nosov B.S. Balzhinimaev, *J. Mol. Catal.*, 88 (1994) 311.

56. V.M. Mastikhin, A.V. Nosov, *React. Kinet. Catal. Lett.*, 46 (1992) 123.

57. M. Crocker, R.H.M. Herold, A.E. Wilson, M. Mackay, C.A. Emeis, A.M. Hoogendoorn, *J. Chem. Soc. Faraday Trans.*, 92(15) (1996) 2791.

58. S. Khabtov, T. Chevreau, J. C. Lavelley, *Micropor. Mater.*, 3 (1994) 133.

59. James E. Huheey, Ellen A. Keiter, ichard L. Keiter, *"Inorganic Chemistry Principles of Structure and Reactivity"* 4th Edn. Published by Pearson Education (Singapore) (2004).

60. B.A. Morrow, R.A. McFarlane, M. Lion, J.C. Lavalley, *J.Catal.*, 107 (1987) 232.

61. J.R. Sohn, H.T. Jang, *J. Catal.*, 136 (1992) 267.

62. J.P. Chen, R.T. Yang, *J. Catal.*, 139 (1993) 277.

63. D. Fraenkel, *Ind. Eng. Chem. Res.*, 36 (1997) 52.

64. S.B. Sharma, B.L. Meyers, D.T. Chen, J. Miller, J. Dumesic, *Appl. Catal. A. Gen.*, 102 (1993) 253.

65. H. Karge, V. Dondur, *J. Phys. Chem.*, 94 (1990) 765.

66. A. Auroux, A. Gervasini, *J. Phys. Chem.*, 94 (1990) 6371.

67. J. LeBars, A. Auroux, *J. Therm. Anal.*, 40 (1993) 1277.

68. D.J. Parrillo, R.J. Gorte, W.E. Farneth, *J. Am. Chem. Soc.*, 115 (1993) 12441.

69. P. Berteau, B. Delmon, *Catal. Today*, 5 (1989) 121.

70. C.H. Lin, S.D. Lin, Y.H. Yang, T. P. Lin, *Catal. Lett.*, 73 (2001) 121.

71. R.J. Gillespie, E.A. Ribinson, *Can. J. Chem.*, 41 (1963) 2074.

72. T. Yamauchi, T. Jin, K. Tanabe, *J. Phys. Chem.*, 90 (1986) 3148.

73. S.M. Jung, P. Grange, *Appl. Catal. A. Gen.*, 228 (2002) 65.

74. S.M. Jung, P. Grange, *Catal. Today*, 59 (2000) 305.

75. J.J. Rooney, R.C. Pink, *Proc. Chem. Soc.*, (1961) 70.

76. B.D. Flockart, J.A.N. Scott, R.C. Pink, *Trans.Farad. Soc.*, 62 (1966) 730.

77. J. Kijenski, A. Baiker, *Catal. Today*, 5 (1989) 1.

78. F. Arena, R. Dario, A. Parmaliana, *Appl. Catal. A. Gen.*, 170 (1998) 127.

79. T. Yamaguchi, *Appl. Catal.*, 61 (1990) 1.

80. A. Corma, V. Fornes, M.I. Juan Rajadell, J.M. Lopez Nieto, *Appl. Catal. A. Gen.*, 116 (1994) 151.

81. R.T. Sanderson, *"Chemical Bonds and Bond Energy"*, Academic Press, NewYork (1976) p.75.

82. A. Corma, C. Rodellas, V. Fornes, *J. Catal.*, 88 (1984) 374.

83. A. Satsuma, Y. Kamiya, Y. Westi, T. Hattori, *Appl. Catal. A. Gen.*, 194-195 (2000) 253.

84. J.T. Richardson, *J. Catal.*, 9 (1967) 182.

85. S. Zenon, *Appl. Catal. A.*, 159 (1997) 147.

86. P. Wu, T. Komatsu, T. Yashima, *Micropor. Mesopor. Mater.,* 22 (1998) 343.

87. M.S. Rana, S.K. Maity, J. Ancheyta, G. Murali Dhar, T.S.R. Prasada Rao, *Appl. Catal. A. Gen.,* (2003) in press.

88. P.M. Boorman, R.A. Kydd, Z. Sarbak, A. Somogyvari, *J. Catal.,* 100 (1986) 287.

89. P.M. Boorman, R.A. Kydd, Z. Sarbak, A. Somogyvari, *J. Catal.,* 96 (1985) 115.

90. Narayanan, K. Deshpande, *Appl. Catal. A. Gen.,* 199 (2000) 1.

91. A. Corma, B.W. Wojciechowski, *Catal. Rev. Sci. Eng.,* 24 (1982) 1.

92. J.W. Ward, *J. Catal.,* 9 (1967) 225.

93. W. Przystajko, R. Fieddorow, I.G. Dalla Lana, *Appl. Catal.,* 15 (1985) 265.

94. H.Pines, *"The chemistry of catalytic hydrocarbon conversions",* Academic Press, New York (1981) p.85.

95. A. Corma, J.L.G. Fiero, R. Montanana, F. Tomas, *J. Mol. Catal.,* 30 (1985) 361.

96. F.M. Bautista, J.M. Campelo, A. Garcia, D. Leina, J.M. Marinas, A.A. Romero, *Appl. Catal.,* 104 (1993) 109.

97. F.M. Bautista, J.M. Campelo, A. Garcia, D. Luna, J.M. Marinas, A.A. Romero, J.A. Navio, M. Macias, *J. Catal.,* 145 (1994) 107.

98. S.J. Kulkarni, R. Ramachandra Rao, M. Subrahmanyam, A.V. Rama Rao, *J. Chem. Soc. Chem. Commun.,* (1994) 273.

99. A. Gervasini, A. Auroux, *J. Catal.,* 131 (1991) 190.

100. M.A. Armindia, V. Borau, I.M. Garcia, C. Jimenez, A. Marinas, J.M. Marinas, A. Porras, F.J. Urbano, *Appl. Catal.,* 184 (1999) 115.

101. M.C.C.C. Costa, L.F. Hodson, R.A.W. Johnstone, J.Y. Liu, D. Whitaker, *J. Mol. Catal.,* 142 (1999) 349.

102. D. Martin, Duprez, *J. Mol. Catal.,* 118 (1997) 113.

103. M. Ai, *J. Catal.,* 40 (1975) 318.

104. M. Ai, *Bull. Chem. Soc. Jpn.,* 50 (1977) 2587.

105. C.G. Ramankutty, S. Sugunan, Bejoy Thomas, *J. Mol. Catal. A. Chem.*, 187 (2002) 105.

106. K.V.V.S.B.S.R. Murthy, B. Srinivas, S.J. Kulkarni, M. Subramanyan, P. Kanta Rao, *"Catalysis:Modern Trends"*, N.M.Gupta, D.K.Chakrabarthy (Eds), Narosa Publishing House, New Delhi, (1995) 189.

107. A. Auroux, A. Gervasini, *J. Phys. Chem.*, 94 (1990) 6371.

108. C.P. Bezouhanova, M.A. Al-Zihari, *Catal. Lett.*, 11 (1991) 245.

109. O.V. Krylov, *"Catalysis by Non- metals"*, Academic press, New York (1970).

110. J. Navarette, T. Lopez, R. Gomez, *Langmuir.*, 12 (1996) 4385.

111. L. Nodek, J. Sedlacek, *J. Catal.*, 40 (1975) 34.

112. M. Bowker, R.W. Petits, K.C. Waugh, *J. Catal.*, 99 (1986) 53.

113. M. Dobrovosky, P. Tenyi, Z. Paal, *J. Catal.*, 74 (1982) 31.

114. N.J. Jebaratjoma, V. Krishnaswamy, *"Catalysis: Present and Futures"* (P. Kanta Rao and B.S. Benwal (Edn.)) Publication and information Directorate, New Delhi, p. 288.

115. M.C.C. Costa, L.F. Hudson, R.A.W. Johnstone, J.Y. Liu, D. Whittaker, *J. Mol. Catal.*, 142 (1999) 349.

Chapter 4

Alkylation Of Arenes

One important consequence for chemistry due to new environmental legislation and drive towards "Clean Technology" will be the use of "Environmentally Friendly Catalysis", typically involving the use of solid catalysts. The present chapter and the results therein show the great versatility of sulfated titania based catalysts in Friedel-Crafts reactions of aromatic compounds. The chapter is divided into two sections. The first section depicts the liquid phase benzylation of toluene and o-xylene using benzyl chloride over different sulfated titania systems and the effects of various operational parameters on the catalytic activity. The reaction is found to be very clean and produces the desired monoalkylated product with very high yield. The catalytic efficiency of the prepared systems in tert-butylation of phenol in the vapour phase is presented in the second section. Variation of catalytic activity over the systems is compared and discussed in terms of the strength of the acid sites.

SECTION 1
FRIEDEL - CRAFTS BENZYLATION OF ARENES

4.1 INTRODUCTION

The Friedel-Crafts reactions are of great interest due to their importance and common use in synthetic and industrial chemistry. Strongly acidic reagents are normally employed as catalysts in Friedel-Crafts reactions. Traditional mineral acids such as HF and H_2SO_4 or Lewis acids such as $AlCl_3$ and BF_3 are not environmentally benign[1]. The use of these substances involves technological

economic and environmental problems due to their corrosive nature, the difficulty of recycling and the formation of large amounts of harmful wastes. The high Lewis acidity of these homogeneous catalysts also results in several undesirable side reactions leading to secondary reaction products. Several solid acid catalysts relevant to Friedel-Crafts reactions have recently been developed to replace conventional homogeneous catalysts. A wide range of solid acid catalysts from clays[2] and zeolites[3-5] to heteropolyacids[6] have been tested for their applicability towards this reaction. These solid acid catalysts are more selective, safe, environmentally friendly, regenerable and reusable.

Benzylation of toluene using benzyl chloride over sol-gel derived titania and sulfated titania was reported[7]. Inversion of relative reactivities and selectivities of benzyl chloride and benzyl alcohol in Friedel-Crafts alkylation with toluene using different solid acid catalyst was also investigated[8,9]. $CuCr_{2-x}Fe_xO_4$ spinel catalysts were used for benzylation of benzene with benzyl chloride[10]. Sebti *et al.*[11] compared the activities of $ZnCl_2$, $NiCl_2$ and $CuCl_2$ supported on hydroxyapatite for Friedel-Crafts alkylation of benzene, toluene and *p*-xylene by benzyl chloride. Sulfated zirconia[12], sol-gel derived silica[13] and rare earth oxides[14] were also used for Friedel-Crafts alkylation reactions. Benzylation of toluene over iron incorporated sulfated rutile was studied by Sugunan *et al.*[15]. The general scheme of benzylation reaction of a typical arene is represented as in figure 4.1.

It is well documented that sulfated metal oxides can be used as solid acid catalysts due to its high acid strength. More recently, these sulfated metal oxide catalysts have been found to have increasing applications and utility in Friedel-Crafts reactions. Catalytic activity of titania, sulfated by different agents for the gas phase alkylation of benzene and substituted benzenes using isopropanol was investigated by Samantaray *et al.*[16] By contrast, the utility of modified sulfated titania catalysts in the Friedel-Crafts alkylation of aromatic

compounds has not been explored in sufficient detail. Hence we report the benzylation of toluene and o-xylene by benzyl chloride over the sulfated titania systems. In the present investigation, structural stability, catalytic activity and reusability of transition metal-loaded sulfated titania systems have been investigated.
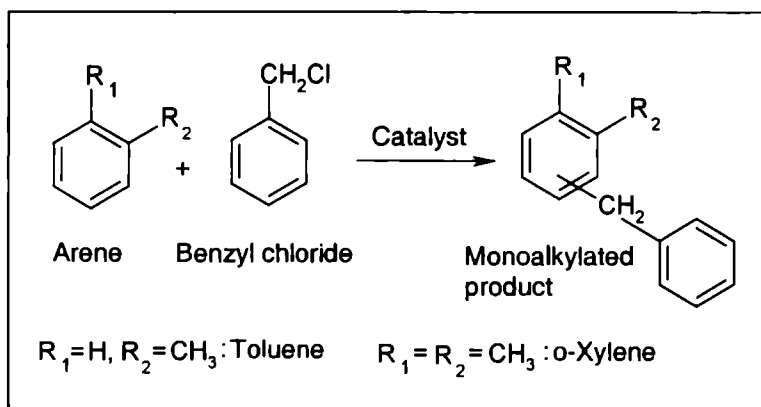

Figure 4.1 General scheme for Friedel-Crafts benzylation of arenas

4.2 PROCESS OPTIMIZATION

All the reactions were carried out in a round bottomed flask (50 mL) equipped with a reflux condenser, calcium chloride guard tube and magnetic stirrer. In a typical reaction procedure, the preactivated catalyst, the substrate (toluene or o-xylene) and benzyl chloride in a required molar ratio at a particular temperature were refluxed using an oil bath. The reaction mixture was withdrawn at specific time intervals and was filtered and analyzed using Gas Chromatograph equipped with SE-30 column and FID detector. The reaction always yielded a single major product, which is identified as the monoalkylated product (MAP). Due to the difficulty of identifying the product as *ortho* or *para*, we name as MAP.

I. Effect of the Catalyst

We made the reaction run using benzyl chloride and toluene in the absence of a catalyst (blank run) and in the presence of the catalyst [0.1 g STCr(6)] at the refluxing temperature of the mixture. We observed a percentage conversion of 2.1 and 98.5 after 60 minutes of reaction in the absence and presence of the catalyst respectively. Low yield for the reaction in the absence of the catalyst is due to the higher activation energy of the uncatalyzed reaction. Addition of the catalyst significantly reduced the activation energy and the reaction proceeded through a different path with a lower activation energy, resulting in a higher percentage conversion.

II. Effect of Reaction Temperature

The reaction temperature seems to play a major role in deciding the catalytic activity and selectivity. The influence of conversion of benzyl chloride (wt%) and product selectivity (%) on the reaction temperature is studied in the range of 70-110°C using STCr(6) catalyst over the two substrates (Table 4.1). At low temperatures, the percentage conversion is very low. An increase in the temperature results in enhanced activity. This is due to the speedy desorption of the alkylated product from the catalyst surface as the temperature increases, which facilitates the further adsorption of reactant molecules, resulting in the increased conversion of benzyl chloride. Maximum conversion is found to be at the refluxing temperature in the case of toluene with 100% selectivity to monoalkylated product (MAP). For o-xylene, at low temperatures, 100% selectivity to MAP is observed. At higher temperatures conversion of benzyl chloride increases, while selectivity to the MAP decreases. This may be due to the formation of consecutive products at higher temperatures. The results are in agreement with the literature report[17] that the higher reaction temperature favours the consecutive alkylation, disproportionation and decarboxylation.

Table 4.1 Influence of reaction temperature on benzylation of arenes

Temperature (°C)	Substrate			
	Toluene		*o*-xylene	
	Conversion of BC (wt%)	Selectivity (%) to MAP	Conversion of BC (wt%)	Selectivity (%) to MAP
70	19.50	100	49.54	100
80	39.25	100	76.85	100
90	62.20	100	93.82	100
100	90.50	100	98.59	98.74
110	98.54	100	100	94.23

Amount of catalyst: 0.1 g STCr (6), Substrate: benzyl chloride molar ratio: 10:1,
Reaction time: 1 h.

III. Effect of Substrate to Benzyl chloride molar ratio

The stoichiometric ratio between substrate and benzyl chloride influences the conversion and selectivity. To investigate the influence of molar ratio, we studied the benzylation of toluene and *o*-xylene at various molar ratios over STCr(6) keeping the amount of aromatic substrate constant. As shown in table 4.2, a continuous increase in the percentage conversion of benzyl chloride is registered with increase in substrate to benzyl chloride molar ratio. The product selectivity also depends on the molar ratio. At lower substrate to benzyl chloride ratios, the amount of polyalkylation is negligible while it considerably increases at higher molar ratios. The results show that the benzylation is favoured with a lower concentration of benzylating agent. Rohan *et al.*[18] reported that when the concentration of benzylating agent is high, there may be enhanced poisoning effect by the alkylated products, which is strongly adsorbed on the catalyst surface. This restricts further adsorption of the reactant molecules and thus reduces the conversion of benzyl chloride. At high arene to benzyl chloride molar ratio, this inhibition would be less

significant, which helps to desorb the products formed from the catalyst surface easily. Similar observation is also reported for benzylation of toluene over H-Y[19] and o-xylene over H-β zeolites[5].

Table 4.2 Effect of substrate to benzyl chloride molar ratio in benzylation of arenes

Substrate: benzyl chloride	Substrate			
	Toluene[a]		o-Xylene[b]	
	Conversion of BC (wt%)	Selectivity (%) to MAP	Conversion of BC (wt%)	Selectivity (%) to MAP
5:1	50.42	100	68.67	100
10:1	90.50	100	93.82	100
15:1	96.24	96.84	100	95.30
20:1	100	89.53	100	90.78

Amount of catalyst: 0.1 g STCr(6), Reaction time: 1 h, Temperature: [a]100°C, [b]90°C

IV. Effect of Catalyst Concentration

The catalyst concentration is varied by taking different amount of STCr(6) catalyst and keeping the amount of benzylating agent constant. Table 4.3 shows the influence of amount of catalyst on catalytic activity and selectivity. In the absence of catalyst the conversion is too low. Addition of 0.05 g catalyst changes the percentage conversion from 1.8 to 75.4% in the case of toluene. An initial steep increase in the conversion is observed when 0.1 g catalyst is used, and reaches 100% when the amount is 0.2 g. These results indicate that only a small amount of catalyst is needed for the reaction to take place. At high catalyst concentration, decrease in selectivity to MAP is observed. As the amount of catalyst is increased, there was a steady increase in conversion, because of the increase in the total number of acid sites available for the reaction[4]. The product yield is found to be proportional to the amount of the

catalyst taken establishing that the reaction proceeds through a pure heterogeneous mechanism. Singh *et al.*[5] studied the influence of catalyst concentration in the benzylation of *o*-xylene using zeolite catalysts and found similar results.

Table 4.3 Influence of the amount of catalyst in benzylation of arenes

| Amount of the catalyst | Substrate | | | |
| | Toluene[a] | | *o*-Xylene[b] | |
	Conversion of BC (wt%)	Selectivity (%) to MAP	Conversion of BC (wt%)	Selectivity (%) to MAP
-	1.80	100	8.85	100
0.05	75.42	100	80.64	100
0.10	90.50	100	93.82	100
0.15	95.84	96.67	98.73	97.40
0.20	100	93.40	100	95.23

Catalyst: STCr(6), Substrate: benzyl chloride molar ratio: 10:1, Reaction time: 1 h,
Temperature: [a]100°C, [b]90°C

V. Effect of Substrate

Catalytic activity depends largely on the substrate used. Variation of reactivity with substrate was studied by carrying out the reaction using benzene, toluene and *o*-xylene over the same catalyst under the same reaction conditions. Table 4.4 gives the details of results for reactions conducted with different substrates. The reactivity is in the order *o*-xylene > toluene > benzene, which is in perfect agreement with the electron releasing nature of the alkyl groups. -CH$_3$ being an electron-donating group will increase the electron density on the benzene ring and makes it more favorable to the attack by an electrophile. Thus it is worth mentioning that the reactivity of aromatic nucleus increases with the number of electron donating groups attached to the aromatic ring. Hence *o*-xylene, which has two methyl groups, reacts more easily than

toluene with only one methyl group. Benzene, since it does not possess any substituent methyl groups, is much less reactive than *o*-xylene and toluene. Sebti *et al.*[11] reported similar results over different Lewis acid supported on hydroxyapatite for benzylation reaction.

Table 4.4 Influence of substrate on catalytic activity in benzylation of arenes

Substrate	Time (min)	Conversion of BC (wt%)	Selectivity (%) to MAP
Benzene	60	4.86	100
Toluene	60	39.25	100
o-xylene	60	76.85	100

Amount of Catalyst: 0.1 g STCr(6), Substrate: benzyl chloride molar ratio: 10:1, Reaction Temperature: 80°C

VI. Effect of moisture

Normally used homogeneous Friedel-Crafts catalysts suffer an inherent drawback of high moisture sensitivity. This makes the handling of these systems very difficult[20]. Conventional catalysts also demand moisture free solvent and reactants, anhydrous catalyst and dry atmosphere for their handling. In order to test the effect of moisture on catalyst performance two parallel runs were carried out, one using the fresh activated catalyst and another with the catalyst adsorbed with moisture. To prepare the catalyst adsorbed with moisture, the catalyst was first activated and then kept in a dessicator containing water vapour for 48 h. The results are presented in figure 4.2.

In the case of fresh samples the reaction commenced quickly, but for the moisture adsorbed sample, conversion remained very low even after 45 minutes. After that, catalytic activity of moisture adsorbed samples showed an increase and as the time progressed the catalytic conversion of benzyl chloride over moisture adsorbed system increased and became the same as that given by the fresh catalyst. Thus it is evident that presence of moisture

developed an induction period for the reaction, but in no way influenced the catalytic activity of the system. There is a time period for which the catalyst is inactive towards the reaction, when it is adsorbed with moisture. The moisture gets adsorbed on the active sites on the catalyst surface and prevents the interaction of benzyl chloride molecule with these sites. Once these water molecules are removed, reaction proceeds at the same rate as that of the fresh catalyst. Thus, though moisture initially blocks the active sites, after the induction period, the reaction rate is same in the case of fresh catalyst itself.
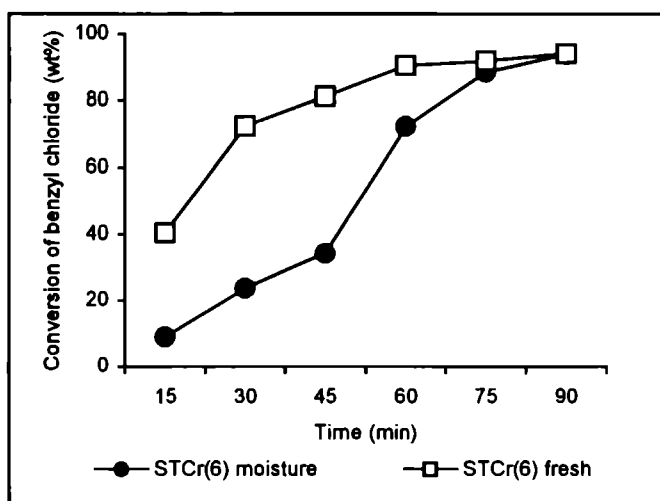
Figure 4.2 Influence of moisture on benzylation of toluene

Amount of catalyst: 0.1 g STCr(6), Toluene: benzyl chloride molar ratio: 10:1,
Reaction Temperature: 100°C.

VII. Effect of Metal Leaching

For any catalyst, chemical stability is an essential requirement, in addition to thermal stability. Leaching can occur during a catalyzed reaction without an induction period and the nature of reaction may gradually change from heterogeneous to homogeneous without any indications in the reaction profile[21].

130

Table 4.5 Effect of metal leaching in benzylation of arenes

Systems	Toluene[a]		o-Xylene[b]	
	Conversion of benzyl chloride (wt%)			
	After 60 minutes	*After 90 minutes	After 60 minutes	*After 90 minutes
STCr(6)	90.50	91.00	93.82	94.15
STMn(6)	93.63	93.94	100.00	100.00
STFe(6)	100.00	100.00	100.00	100.00
STCo(6)	85.39	86.47	90.06	90.89
STNi(6)	75.50	76.14	80.62	81.47
STCu(6)	80.78	81.55	85.98	86.02
STZn(6)	90.00	90.57	100.00	100.00

Amount of catalyst: 0.1 g, Substrate: Benzyl chloride: 10:1, Reaction temperature: [a]100°C, [b]90°C (*Reaction done after filtering the catalyst)

To prove the heterogeneous character of the reactions, the catalyst was removed from the reaction mixture after one hour and the filtrate was allowed to react under the same conditions for 30 minutes. The filtrate was further subjected to qualitative analysis for testing the presence of leached metal ions. No noticeable change in the conversion is obtained in any case after the removal of the catalyst (table 4.5). Qualitative analysis of the filtrate also confirmed the absence of any metal ion in the filtrate. Thus it is clear from the results that metal ions are not leaching form the metal oxide surface during benzylation reaction. These observations imply that the reaction is 100% heterogeneously catalyzed.

VIII. Catalyst Regeneration

One of the major objectives guiding the development of solid acid catalysts includes the easy separation of final products from the reaction mixture and efficient catalyst recovery.

131

Table 4.6 Regeneration of catalyst

No. of cycles	1	2	3	4
Conversion of benzyl chloride (wt%)	78.10	75.54	72.28	61.48

Amount of Catalyst: 0.1 g STCr(3), Toluene: benzyl chloride molar ratio: 10:1,
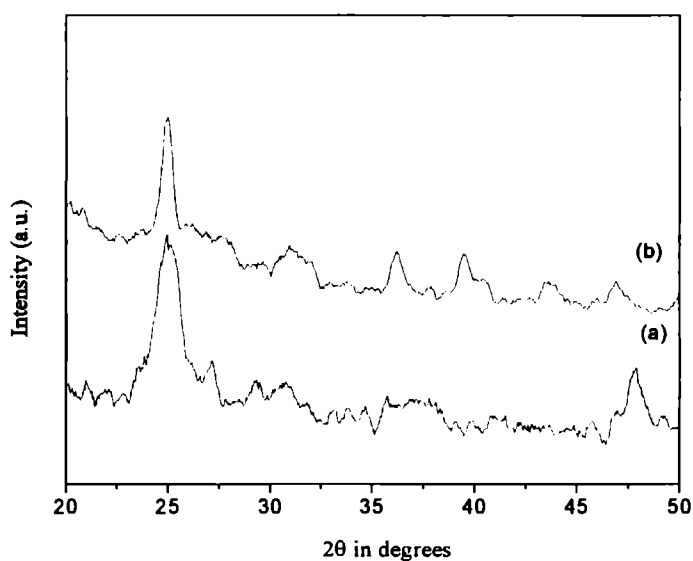Reaction Temperature: 100°C

Figure 4.3 XRD patterns of STCr(3) catalyst (a) Before reaction
(b) After reaction

Regeneration studies were done by removing the catalyst by filtration from the reaction solution, washed thoroughly with acetone and then dried and activated at 500°C for 5 h. The same catalyst was again used for carrying out subsequent runs under similar reaction conditions. To check the structural change during the reaction, the XRD spectrum of the used catalyst was taken. No pronounced change could be observed in the XRD pattern, except a slight lowering of intensity, symptomatic of the retention of the crystalline nature

(figure. 4.3). It was tested for catalytic activity and only a slight decrease was observed. This suggests the resistance to rapid deactivation in benzylation reactions. However, the decrease becomes more pronounced as the cycles are repeated. Table 4.6 displays the conversion of benzyl chloride obtained for toluene benzylation using regenerated STCr(3) catalyst during a four times recycling process. The hydrogen chloride produced in the electrophilic benzylation of toluene is responsible for the deactivation of the catalyst. These results are consistent with the earlier reports[22,23].

IX. Effect of Reaction Time

The reaction mixture is analyzed at various time intervals in order to study the effect of reaction time on conversion of benzyl chloride. The variation of product selectivity with time is also subjected to screening (table 4.7). These results show that the reaction time is also having a deciding effect on the catalytic activity and product selectivity.

Table 4.7 Effect of reaction time on benzylation of arenes

Time (minutes)	Substrate			
	Toluene[a]		o-Xylene[b]	
	Conversion of BC (wt%)	Selectivity (%) to MAP	Conversion of BC (wt%)	Selectivity (%) to MAP
30	72.48	100	83.40	100
60	90.50	100	93.82	100
90	94.12	100	97.43	100
120	98.66	100	100	98.64
150	100	100	100	95.74

Amount of catalyst: 0.1 g STCr(6), Reaction Temperature: [a]100°C, [b]90°C, Reaction time: 1 h

There is an increase in the conversion as time proceeds, but the selectivity remained constant throughout the course of the reaction, when the substrate as toluene. Conversion becomes 100% at 2.5 h of reaction time.

Only monoalkylated product is detected in the case of *o*-xylene upto 1.5 h. Prolonged reaction time is found to generate undesirable products in the case of *o*-xylene. After 1.5 h, secondary alkylation is observed, resulting in low selectivity towards MAP. Conversion reaches 100% at 2 h reaction time at the expense of selectivity to the monoalkylated product for *o*-xylene. The increase in conversion of benzyl chloride with time confirms the heterogeneity of the catalytic reaction.

4.3 COMPARISON OF DIFFERENT SYSTEMS

After optimization studies, catalytic activity of all the systems were evaluated at a molar ratio of 10:1, using 0.1 g catalyst and at a reaction temperature of 100°C and 90°C for toluene and *o*-xylene respectively. Tables 4.8 and 4.9 present the results of benzylation of toluene and *o*-xylene using benzyl chloride over different metal loaded sulfated titania systems.

Table 4. 8 Influence of the type of metal loaded in the benzylation of arenes

Systems	Toluene[a]		*o*-Xylene[b]	
	Conversion (wt%)	Selectivity (%) to MAP	Conversion (wt%)	Selectivity (%) to MAP
T	20.20	100	38.60	100
ST	60.65	100	70.78	100
STCr(3)	78.10	100	80.82	100
STMn(3)	83.60	100	85.41	100
STFe(3)	100.00	100	100.00	100
STCo(3)	72.80	100	76.62	98.54
STNi(3)	65.29	100	71.51	98.20
STCu(3)	70.18	100	73.75	97.58
STZn(3)	96.98	100	100.00	100

Amount of catalyst: 0.1 g, Substrate: Benzyl chloride: 10:1, Reaction time: 1 h,

Reaction temperature: [a]100°C, [b]90°C

Pure TiO_2 gave very low conversions under the specified reaction conditions. An interesting observation was that only monoalkylated product was obtained in all the cases when toluene is used as the substrate. An enhanced conversion at the expense of monoalkylated product is observed in the case of *o*-xylene. The sulfated system gives comparatively high conversion than the pure titania. Among the various metal loaded systems, a notable deviation was observed in the case of iron incorporated systems. Abnormally high conversions, which do not commensurate with the Lewis acidity values, may be attributed to the reducible character of the iron. The conversion becomes 100% within 15 minutes in the case of iron loaded systems. This may be an indication of the fact that the iron content or the Lewis acidity is not the only factor favouring the reaction.

Table 4. 9 Influence of amount of metal loading in benzylation of arenes

Systems	Toluene[a]		*o*-Xylene[b]	
	Conversion (wt%)	Selectivity (%) to MAP	Conversion (wt%)	Selectivity (%) to MAP
STCr(6)	90.50	100	93.82	100
STMn(6)	93.63	100	100.00	100
STFe(6)	100.00	100	100.00	100
STCo(6)	85.39	100	90.06	100
STNi(6)	75.50	100	80.62	98.20
STCu(6)	80.78	100	85.98	99.00
STZn(6)	90.00	100	100.00	100
STCr(9)	85.63	100	89.43	100
STMn(9)	90.39	100	96.78	97.34
STFe(9)	100.00	100	100.00	100
STCo(9)	80.02	100	87.05	97.04
STNi(9)	70.15	100	77.63	95.54
STCu(9)	73.79	100	80.78	96.80
STZn(9)	99.30	100	100.00	100

Amount of catalyst: 0.1 g, Molar ratio: 10:1, Reaction time: 1 h, temperature: [a]100°C, [b]90°C

It is reported that catalysts containing reducible cations like Fe^{3+}, Sn^{4+}, Cu^{2+}, Sb^{3+}, etc. exhibit high alkylation activity regardless of their low Lewis acidities[24-26]. When the redox mechanism is operating there will be a homolytic rupture of the carbon-chlorine bond of the alkylating agent (benzyl chloride). The radicals so formed are powerful reductants, which would be readily oxidized to carbocations in the presence of reducible metallic ions such as Fe^{3+}. When o-xylene was used as the substrate, catalytic activity followed the same trend as in the case of toluene. Monoalkylated products were obtained in major proportion, with a small amount of polyalkylated product. The maximum conversion was shown by the systems with 6% metal loading and minimum by those with 3% metal loading i.e., as the percentage loading increases conversion increases and then decreases at high loadings.
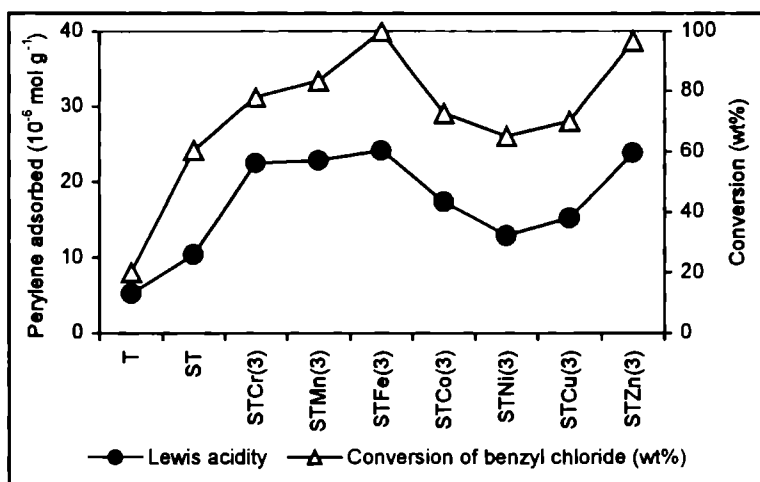

Figure 4.4 Catalytic activity correlated with Lewis acidity
determined from perylene adsorption studies

The acid base properties of metal oxide carriers can significantly affect the final selectivity of heterogeneous catalysts[19]. So an attempt is made to correlate the catalytic activity with the acidic characteristics determined by different methods. Figures 4.4 and 4.5 show the correlation of benzylation

activity of the systems with the acidity in benzylation of toluene. From the figures it is clear that the percentage conversion for different systems are in agreement with the amount of Lewis acid sites measured from perylene adsorption studies.
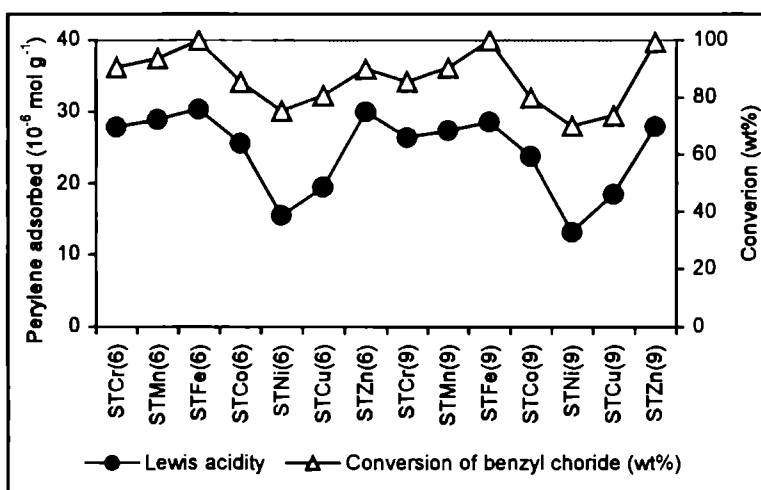

Figure 4.5 Catalytic activity correlated with Lewis acidity determined from perylene adsorption studies
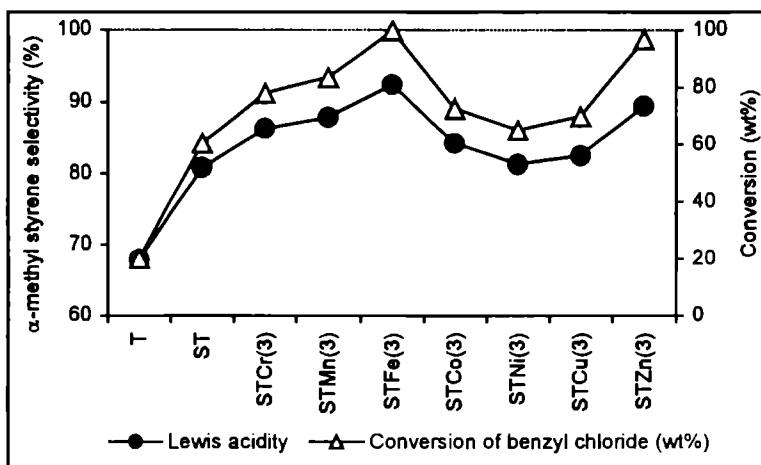

Figure 4.6 Catalytic activity correlated with α-methyl styrene selectivity from cumene conversion reaction

The Lewis acidity trend predicted by α-methyl styrene selectivity from cumene conversion reaction also parallels the reactivity observed with the increase in the percentage conversion (figures 4.6 and 4.7). Metal loading and sulfate modification provoke considerable synergistic effect leading to an enhanced activity. The metal oxide surface contains both Brönsted and Lewis acid sites and the above observations clearly indicate the dominating impact of Lewis acid sites for the benzylation reaction over the sulfated titania systems. Introduction of sulfate ions increases the surface acidity due to electron withdrawing nature of sulfate groups, which increases the number of Lewis sites.
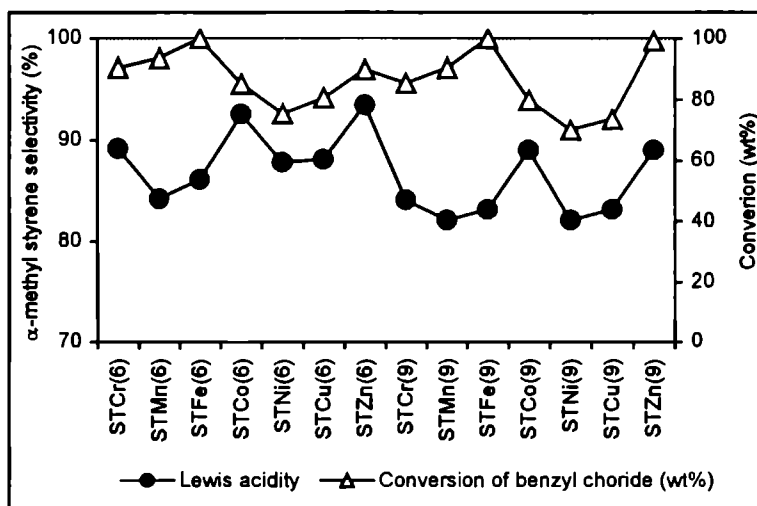

Figure 4.7 Catalytic activity correlated with α-methyl styrene selectivity from cumene conversion reaction

4.4 MECHANISM OF BENZYLATION REACTION

The catalytic activity studies on different transition metal loaded sulfated titania systems suggest the involvement of Lewis acid sites in the reaction. Barlow *et al.*[27] reported the benzylation of anisole over Clazic is catalyzed by

Brönsted sites, below 40°C. Rhodes *et al.*[28] found that the enhanced catalytic activity of adsorbed $ZnCl_2$ (Clazic) was not due to increased Lewis acidity but may be due to the increased accessibility of Lewis sites to reactant molecules.

The reaction appears to proceed by an electrophile, which involves the reaction of benzyl chloride with the acidic titania catalyst. The acidic catalyst polarizes the benzylating agent and, in turn, produces an electrophile ($C_6H_5CH_2^+$). Thus, the generated electrophilic species attack the benzene ring, resulting in the formation of the corresponding dimethyl diphenyl derivative[29,30]. Nonpolar nature of the substrate molecules also supports the formation of the electrophilic species by adsorption of benzyl chloride molecule on the catalyst surface. A plausible mechanism for the reaction can be represented schematically as shown in figure 4.8.
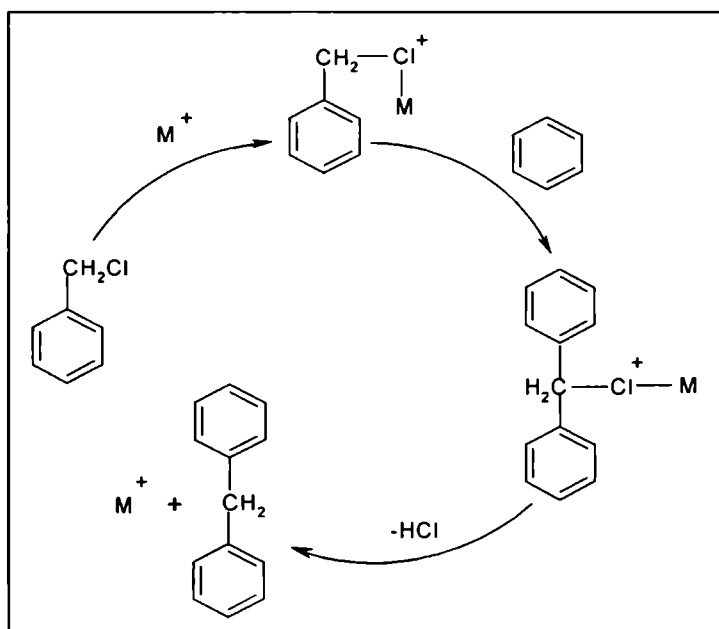

Figure 4.8 Mechanism of Friedel-Crafts benzylation using benzyl chloride showing the active involvement of Lewis acid sites.

The percentage conversions obtained in the case of iron loaded systems were much higher than that expected from its Lewis acidity. The high activity of iron systems, which does not commensurate with the acidity values, can be attributed to the redox or free radical mechanism (figure 4.9). Recently Choudary *et al.*[18] suggested the possibility of a redox mechanism for reducible cations when benzyl chloride was the alkylating agent. Considering all the aspects, we propose the existence of a redox or a free radical mechanism in the case of Fe loaded samples side by side with the involvement of Lewis acid sites. Radicals are powerful reductants, which can readily be oxidized to cations in presence of reducible metal cations. Thus the high activity associated with these reducible cations involves the initiation of the reaction by the homolytic cleavage of the carbon-chlorine bond followed by the oxidation of the radical to the corresponding ion.
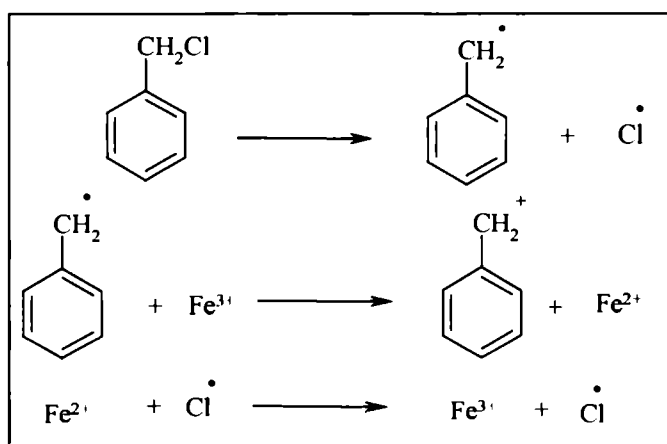

Figure 4.9 Free radical mechanism for benzylation of arenes

4.5 CONCLUSIONS

The following conclusions can be drawn from the present study.

✦ Sulfated titania catalysts can be used for the benzylation of toluene and *o*-xylene, leading to the formation of monoalkylated products. The

conventional catalyst, AlCl$_3$ does not possess shape selectivity and favours the formation of large amount of polyalkylated products.

✍ The conversion of benzyl chloride and product distribution largely depends on the experimental condition. The conversion of benzyl chloride increases with increasing reaction time, catalyst concentration, reaction temperature and substrate to benzyl chloride molar ratio.

✍ The reaction is found to be clean with negligible formation of polyalkylated products. The activity of the systems is found to be increasing with the number of electron donor methyl groups present in the aromatic substrates. Catalysts are reusable and resistant to rapid deactivation in benzylation reaction even in the presence of moisture.

✍ The Lewis acid sites in the catalysts appears to be very important for the polarization of benzyl chloride into an electrophile (C$_6$H$_5$CH$_2^+$) which then attacks the benzene ring resulting in the formation of products.

✍ Free-radical mechanism explains the exceptionally high activity of iron loaded samples for the benzylation reaction.

SECTION 2

TERT-BUTYLATION OF PHENOL

Phenol alkylation with *tert*-butyl alcohol (TBA) has been studied extensively owing to industrial interest in the production as antioxidants, ultraviolet adsorbers and heart stabilizers of polymeric materials. The catalytic efficiency of the prepared titania systems in the *tert*-butylation of phenol in vapour phase has been studied and is presented in this section. Influence of various reaction parameters such as temperature, flow rate and molar ratio of the reactants on phenol conversion and selectivity of the product is discussed in detail. Variation of catalytic activity among the systems are compared and discussed in terms of the strength of the acid sites. Medium acid sites on the catalysts are advantageous in producing 4-*tert*-butylphenol, whereas strong acid sites are helpful for the formation of 2,4-di-*tert*-butylphenol.

4.6 INTRODUCTION

Short chain alkyl phenols are important intermediates for the production of resins, antioxidants, drugs, dyes, polymer additives, agrochemicals and antiseptic substances[1]. The direct alkylation of phenol with short-chain alcohols and olefins is widely used for the preparation of these intermediates. The catalytic reactions of phenol with *tert*-butyl alcohol or isobutene as well as with methyl-*tert*-butyl ether are important, because C-alkylation products such as 4-*tert*-butylphenol (4-TBP), 2-*tert*-butylphenol (2-TBP) and 2,4-*di-tert*-butylphenol (2,4-DTBP) have great commercial significance. Some commonly used catalysts for alkylation of phenol are H_2SO_4, BF_3, aluminum phenoxide, etc[2]. Catalytic alkylation of phenol using solid acid catalysts is a very promising way for their synthesis considering the increasing demand for eco-friendly routes in the chemical industry. Reports and patents concerning this catalytic reaction, which has been carried out both in the liquid and gas phase, are available[3-14].

Generally, in the alkylation of aromatics over zeolites, catalytic activity is controlled by acidity where as selectivity is controlled by pore structure and acid strength of the catalyst[15-19]. The catalyst reacts with the alkylating agent to form a carbocation or a carbanion, which further rearranges to one which is as branched as possible. The carbanion attacks the phenol ring preferentially in the *ortho* and/or *para* position to the –OH group according to the rules of electrophilic substitution[20]. In addition to alkylation, etherification of the –OH group can also occur under mild reaction conditions. Since the monoalkylated products are more reactive than phenol, they get further alkylated provided there is no steric hindrance. The ratio of mono to di and tri alkyl phenol is proportional to the ratio of phenol to alkylating agent.

SYNTHESIS OF BUTYL PHENOLS

Depending on the nature of the catalyst, alkylation of phenol can take place at the oxygen (O-alkylation) and/or at ring carbon atoms (C-alkylation). Reports[21-23] indicate that the selectivity largely depends on the acid strength of the catalyst. In general, C-alkylation requires stronger acid sites than those responsible for O-alkylation[11,24,25]. C-alkylation of phenol can give rise to 2-,3- and 4-alkylphenols as well as multi substituted products. *Tert*-butyl phenols (TBP's) are formed by the reaction of phenol with isobutene or *tert*-butanol. 2-*tert*-butyl phenol is produced as the main product if phenol is reacted with isobutene in presence of an acidic ion-exchange resin catalyst. *Tert*-butyl phenyl ether (TBPE), which is the O-alkylated product, can also be formed as a byproduct but its amount decreases with increasing the temperature. Zhang *et al.*[26] have shown that 2-TBP selectivity can be enhanced by the use of beta zeolites under specific conditions. Padmasri *et al.*[27] have shown that the production of 2-TBP can be performed with good selectivity over aluminum hydrotalcites. In the US patent by Chang and Hellring[12], they have demonstrated that *tert*-butanol can be used as the butylating agent. On catalysts namely MCM-22 and beta zeolite, they obtained high selectivity for 4-TBP.

4.7 PROCESS OPTIMIZATION

The vapour phase *tert*-butylation of phenol was carried out in a conventional fixed bed reactor under atmospheric pressure. The reaction is found to be extremely sensitive to reaction conditions. The most important concern with respect to catalytic alkylation of phenol is the catalytic activity and catalytic selectivity towards the desired C-alkylated product, with regard to the structural and acid properties of the catalysts.

In the present study, the major products obtained were 2-TBP, 4-TBP and 2,4-DTBP. The last one mentioned is the product of further alkylation of

2- or 4-*tert* butyl phenol. 2-*tert* butyl phenol easily isomerises to 4-*tert* butyl phenol whereas the reverse reaction is not significant. 3-TBP and 2,6-DTBP are not formed on any of the catalysts, while a trace amount of *tert*- butyl phenyl ether (TBPE) is detected. A detailed investigation on the optimization of the process is discussed below.

I. Effect of Phenol to TBA Molar ratio

In order to understand the optimum feed mix ratio, a series of experiments were performed at 180°C with various molar ratios of phenol to TBA over STFe(6). The formation of 2-TBP, 4-TBP and 2,4-DTBP is observed at different reactant ratios. From Table 4.10, we can find that at high phenol content, the production of 4-TBP is dominant and at lower content the selectivity of 2,4-DTBP is enhanced.

Table 4.10 Influence of molar ratio on the conversion and product
selectivity in *tert*-butylation of phenol

Phenol: TBA	Conversion of Phenol (wt%)	Selectivity (%)			p/o ratio
		2-TBP	4- TBP	2,4-DTBP	
1:1	21.02	18.49	70.48	5.93	3.81
1:2	29.25	21.93	68.75	7.47	3.13
1:4	31.04	23.51	66.22	9.49	2.82
1:6	35.60	26.15	58.53	14.24	2.24

Amount of catalyst: 0.5 g STFe(6), Flow rate: 4 mL h^{-1}, Reaction temperature: 180°C, Reaction time: 2 h.

Phenol conversion increases on increasing TBA concentration in the feed. Higher amount of TBA in the feed helps in promoting the alkylation, provided the alkylating agent is not consumed in non-selective parallel reactions. The *p/o* ratio is decreasing as the amount of TBA in the feed increases. Higher amount of TBA on the catalyst surface, result in the

formation of 2,4-DTBP. An optimum feed mixture of phenol to TBA in 1:2 molar ratio is chosen for further investigations, considering the phenol conversion and selectivity to 4-TBP.

II. Effect of Reaction Temperature

The reaction temperature has a profound influence on the catalytic activity as well as the product selectivity. The reaction is carried out at various reaction temperatures in the range of 160-220°C, close to the boiling point of phenol (180°C). Table 4.11 clearly shows the product distribution and selectivity of desired products at various temperatures. The general trend for the alkylation reaction is that the conversion increases with increase in temperature and reaches a steady state at high temperature. The selectivity of 4-TBP was enhanced, while that of 2-TBP and 2,4-DTBP decreased with increase in reaction temperature. There is a clear cut relation between the concentration of 2-TBP and 2,4-DTBP in the products as the latter falls along with 2-TBP.

Table 4.11 Influence of reaction temperature on the conversion and product selectivity in *tert*-butylation of phenol

Temperature (°C)	Conversion of Phenol (wt%)	Selectivity (%)			*p/o* ratio
		2-TBP	4- TBP	2,4-DTBP	
160	29.05	23.04	65.43	7.58	2.84
180	29.25	21.93	68.75	7.47	3.13
200	32.20	20.91	70.48	7.25	3.37
220	25.30	20.05	73.42	5.34	3.66

Amount of catalyst: 0.5 g STFe(6), Flow rate: 4 mL h^{-1}, Phenol:TBA: 1:2 Reaction time: 2 h.

It is reported in literature[28] that the formation of 2,4-DTBP takes place in a consecutive step by alkylation of mono alkylated product. It was also observed[28] that when a mixture of 4-TBP and 2-TBP were reacted, the latter

preferably react to form 2,4-DTBP. Our results also demonstrate a similar trend. The fall in 2-TBP selectivity also lead to a fall in 2,4-DTBP selectivity. A moderate reaction temperature is helpful in enhancing the selectivity of 2,4-DTBP. At higher reaction temperatures the formation of undesired products are enhanced and they consume reactants (TBA) without producing the desired products, which may lead to lower phenol conversion and 2,4-DTBP selectivity. The conversion of phenol increases up to 200°C, and after that it decreases. Considering the phenol conversion and product distribution, the proper reaction temperature chosen is 200°C. At this temperature the conversion of phenol is higher compared to the other investigated temperatures.

III. Effect of Flow Rate

The contact time between the catalyst and the reactants greatly influence the reaction rate. Very low contact time (high flow rate) may lead to poor reaction on account of the fact that little time is available for the adsorption of the reactants on the catalyst surface. At the same time, very high contact time (low flow rate) mostly results in undesired side reactions. Thus each reaction requires an optimum contact time with which maximum conversion and desired product yield is achieved.

The reaction is carried out at various flow rates at a reaction temperature of 200°C and with phenol to TBA molar ratio of 1:2 and the trend is presented in figure 4.10. There is an increase in phenol conversion when we change the flow rate from 3 mL h^{-1} to 4 mL h^{-1}. After that phenol conversion decreases with increasing flow rate, due to the shorter contact time values at higher flow rate. 2,4-DTBP selectivity is low for higher contact time values whereas it improves and remains almost steady at lower contact time values. There is an optimum contact time for the reaction to take place and 4 mL h^{-1} is chosen as the flow rate for further studies.
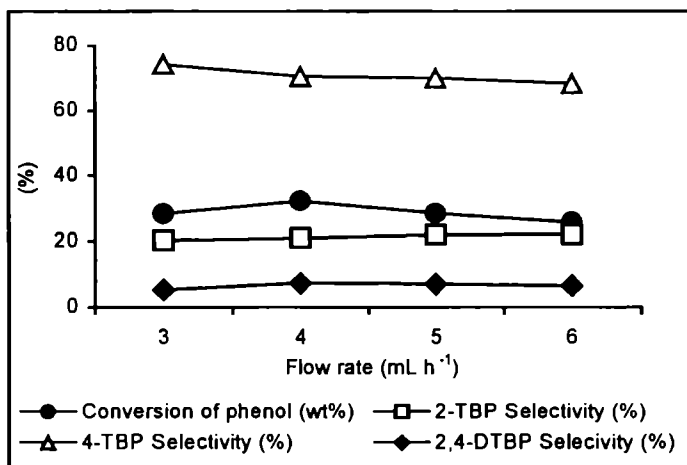
Figure 4.10 Influence of flow rate on phenol conversion and product selectivity

Amount of catalyst: 0.5 g STFe(6), Phenol:TBA: 1:2, Reaction time: 2 h,

Reaction temperature: 200°C.

IV. Effect of Time on Stream-Deactivation study

The effect of time on stream is expected to throw light on deactivation of a particular catalyst and its influence on product selectivities. The performance of the reaction for a continuous 7 h run tests the susceptibility of deactivation of the catalyst. The products were collected and analyzed after every one hour. Figure 4.11 represent the phenol conversion of representative systems towards time on stream. In the initial hours the catalyst may adsorb phenol strongly and after 2 h, the catalyst activity established an equilibrium level. The conversion of phenol gradually increased with time on stream in the initial reaction period for 2 h, and then the conversion level attained a steady value at 5 h and after that it decreases for T and ST. In the case of metal incorporated systems, the deactivation starts slowly from 3 h onwards. At 7 h, conversion decreases to a greater extent. This can be explained by the fact that the catalytic activity progressively decreases with time having a reduction in conversion.
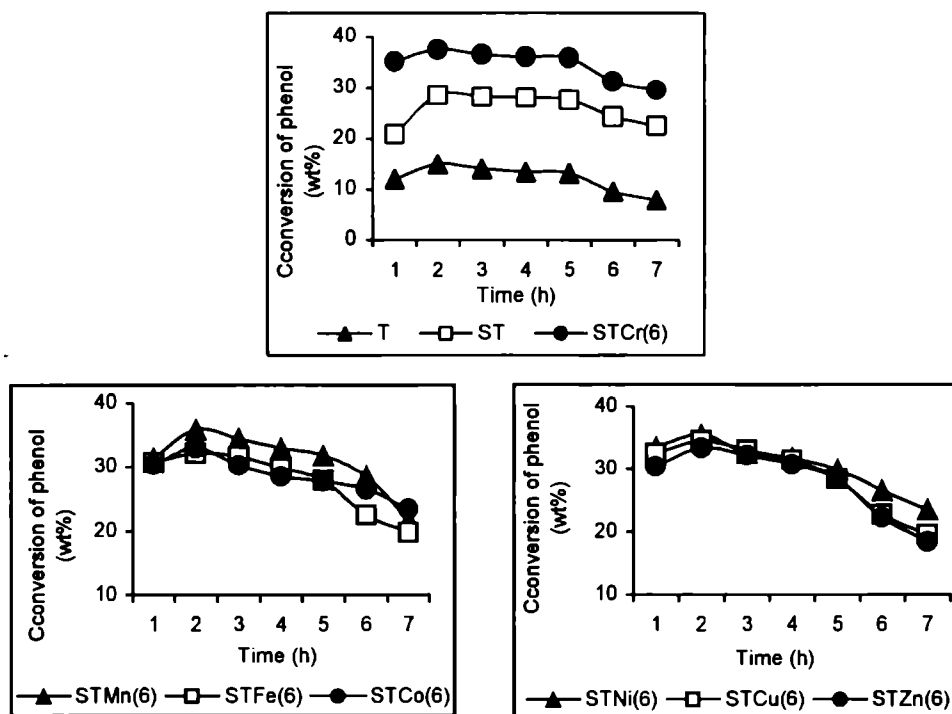
Figure 4.11 Deactivation studies on the conversion of phenol over different systems

Amount of catalyst: 0.5 g, Phenol: TBA: 1:2, Flow rate: 4 mL h^{-1}, temperature: 200°C

4.8 COMPARISON OF DIFFERENT SYSTEMS

A comparative account of the catalytic activity of various sulfated titania systems in the butylation reaction is given in this section. All the prepared systems were tested for activity over a reaction time of 2 h under the optimized reaction conditions, temperature of 200°C, flow rate of 4 mL h^{-1} and a reactant ratio of 1:2. An attempt to correlate the surface acidity with the product selectivity is carried out. Pure titania exhibited poor activity towards *tert*-butylation of phenol under the specified reaction conditions. The reaction proceeds very efficiently over different sulfated titania systems. In comparison with simple sulfated system, metal incorporated samples are more efficient for

the butylation reaction (Tables 4.12 and 4.13). Chromium loaded samples show the highest activity when compared with the other systems. In all cases *ortho* and *para* isomers were obtained with a high selectivity for the *para* isomer. The *p/o* ratio was maximum for chromium and minimum for iron.

Table 4.12 Influence of the type of metal loaded in the *tert*-butylation of phenol

Systems	Conversion of Phenol (wt%)	Selectivity (%)			p/o ratio
		2-TBP	4- TBP	2,4-DTBP	
T	14.90	23.53	50.64	2.54	2.15
ST	28.45	19.81	65.64	5.44	3.31
STCr(3)	35.54	14.71	73.82	6.97	5.02
STMn(3)	33.55	16.18	69.88	6.04	4.32
STFe(3)	28.95	19.95	66.63	6.82	3.34
STCo(3)	29.10	19.99	67.05	5.94	3.35
STNi(3)	33.01	16.27	69.14	3.47	4.25
STCu(3)	32.54	17.20	68.97	4.14	4.01
STZn(3)	30.08	17.60	67.22	6.52	3.82

Amount of catalyst: 0.5 g, Flow rate: 4 mL h^{-1}, Phenol: TBA: 1:2, Reaction time: 2 h, Reaction temperature: 200°C

An attempt to investigate the influence of the metal loading on catalytic activity is quite reasonable. As expected, variation in metal loading had a significant impact on the catalytic activity. An increase in metal content resulted in enhanced catalytic activity. As the metal loading was increased from 0 to 6% the conversion gradually increased, thereafter the conversion declined. In all the cases *para* isomer is the major product. Selectivity to 4-TBP and 2,4-DTBP also changed with respect to the metal loading. Selectivity to 4-TBP is maximum for 6% loading and minimum for 3% loading.

Table 4.13 Influence of the amount of metal loading in the *tert*-butylation of phenol

Systems	Conversion of Phenol (wt%)	Selectivity (%)			p/o ratio
		2-TBP	4- TBP	2,4-DTBP	
STCr(6)	37.48	14.54	76.87	7.89	5.29
STMn(6)	35.89	15.07	75.05	6.51	4.98
STFe(6)	32.20	20.91	70.48	7.25	3.37
STCo(6)	33.06	20.06	70.74	6.09	3.53
STNi(6)	35.47	17.00	73.07	3.85	4.30
STCu(6)	34.46	17.33	72.11	4.51	4.16
STZn(6)	33.42	18.13	71.61	6.85	3.95
STCr(9)	34.12	14.47	70.95	4.98	4.83
STMn(9)	33.85	14.94	70.02	3.47	4.68
STFe(9)	29.47	20.04	67.32	4.62	3.36
STCo(9)	32.94	19.79	69.05	4.25	3.49
STNi(9)	32.54	16.72	68.89	2.45	4.12
STCu(9)	31.25	17.17	68.01	2.92	3.96
STZn(9)	31.09	17.63	67.98	4.09	3.85

Amount of catalyst: 0.5 g, Flow rate: 4 mL h^{-1}, Phenol: TBA: 1:2, Reaction time: 2 h,
Reaction temperature: 200°C

The acid base properties of the catalysts affect the final selectivity of heterogeneous catalysts[29]. Figures 4.12 to 4.15 gives the correlation between the product selectivity and the acidity assessed by ammonia TPD. It was observed that the *p/o* ratio was very low in the case of pure titania and sulfated titania. Metal incorporation increased the selectivity to *para* isomer. Considering the acid site distribution from the TPD measurements, the increase in the medium acid sites with increase in the metal content is in agreement with the enhanced activity of the systems.
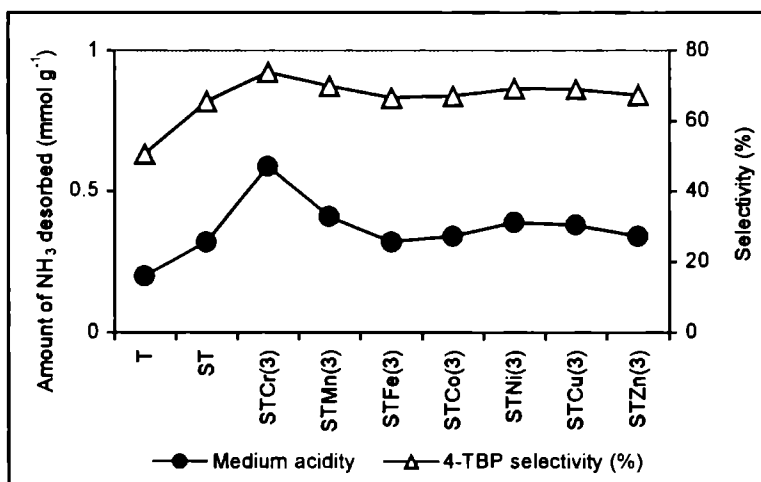
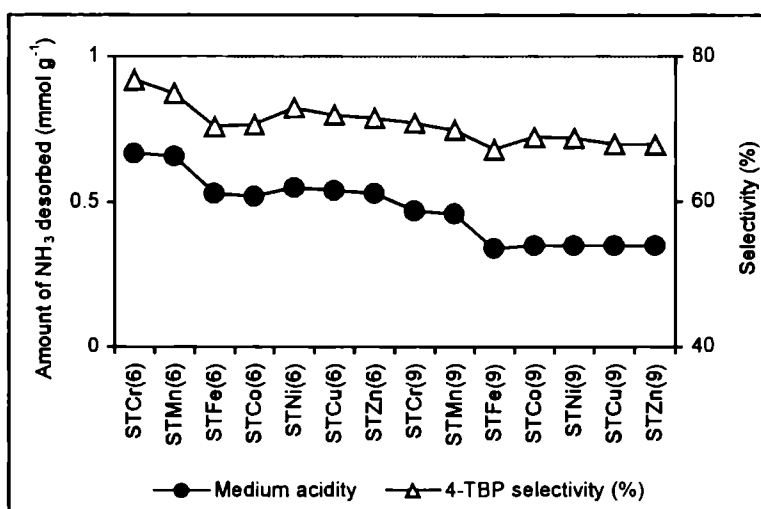Figure 4.12 4-TBP selectivity correlated with the medium acidity from NH₃ TPD

Figure 4.13 4-TBP selectivity correlated with the medium acidity from NH₃ TPD

In the present study the reaction was promoted by medium and strong acid sites. Strong acid sites are necessary to get higher selectivity of 2,4-DTBP while medium acid sites are helpful in enhancing the selectivity of 4-TBP. Corma *et al.*[11] reported the same observation in zeolites Y. Medium

acid sites may promote the isomerization or transalkylation reaction of o-TBP to p-TBP, while strong acid sites are helpful in forming 2,4-DTBP.
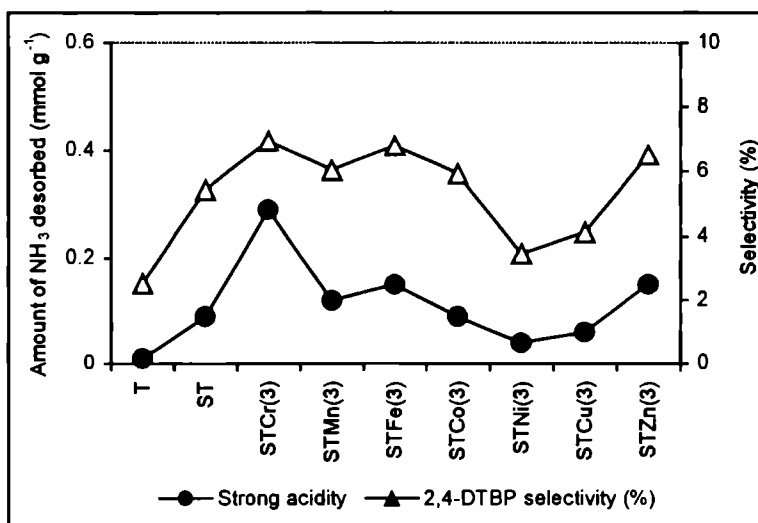

Figure 4.14 2,4-DTBP selectivity correlated with strong acidity from NH_3 TPD

The catalytic alkylation of phenol with alcohols gives rise to two distinct classes of products depending on the site where the alkyl group alkylates phenol. The formation of O-alkylated products depends both on the intrinsic properties of the alcohol and on the structural and acid-base properties of the catalysts. Corma *et al.*[11] found that the alkylation of phenol by TBA over the solid acid HNa-Y zeolites at 303 K occurs both at O- atoms and C-atoms, but the O-alkylation had a higher selectivity, whereas ring alkylation alone occured at higher temperatures. Zhang *et al.*[26] already reported that the strong acidity was required for the formation 2,4-DTBP and acid sites of medium strength were responsible for the formation of 4-TBP. But it differs from our result as they speculate that weak acid sites are effective in producing 2-TBP. We do not get any correlation between weak acid sites and 2-TBP selectivity. Figures 4.16 to 4.17 indicate that the selectivity to 4-TBP and 2,4-DTBP lies nicely with the

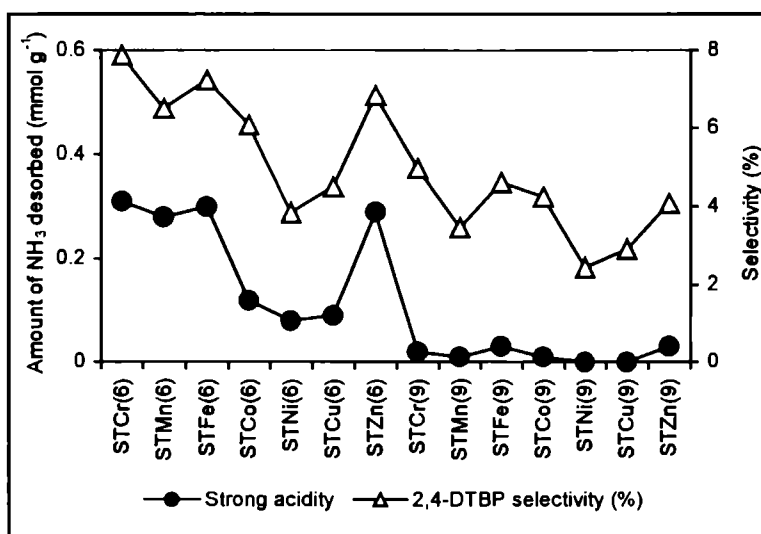medium and strong acid sites from the TPD of ammonia of the prepared systems.

Figure 4.15 2,4-DTBP selectivity correlated with strong acidity from NH_3 TPD

4.9 MECHANISM OF *TERT-* BUTYLATION OF PHENOL

The interesting aspect of this reaction is the high selectivity of alkylation at the *para* position. The generally accepted mechanism for aromatic alkylation is that the tertiary carbenium ion interacts with adsorbed phenol forming a π-complex, which then rearranges to σ-complex by the electrophile attacking a ring carbon atom. The complex on proton elimination gives *tert*-butyl phenol. General scheme for the reaction can be represented schematically as shown in figure 4.16. Alkylation reactions carried out in the gas-phase system at high reaction temperature in the presence of catalysts with weak[30], medium[12,28,31] or strong acid sites[32] are suitable for the formation of *para*-C-alkylated isomer. Generally, the electrophilic substitution takes place in the *ortho* and *para* positions of the phenyl ring. The presence of phenolic group kinetically favors *ortho* alkylation[33]. It is accepted that when the product is not thermodynamically

153

controlled, both the electronic and the steric factors are very important for the alkylation reactions in heterogeneous catalysis[20].
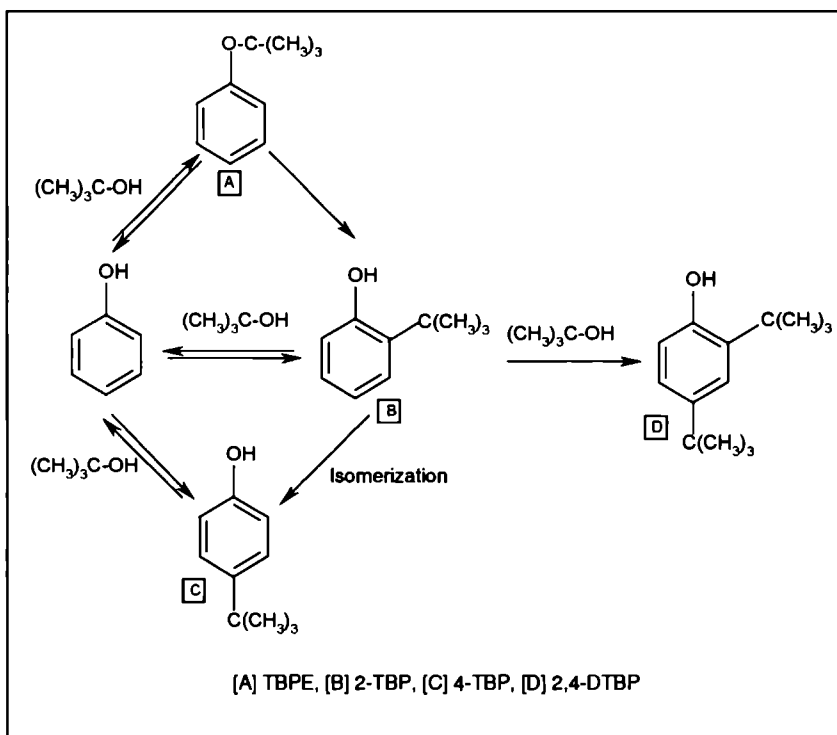

[A] TBPE, [B] 2-TBP, [C] 4-TBP, [D] 2,4-DTBP

Figure 4.16 General scheme for *tert*-butylation of phenol

It is noticed that the presence of strong acid sites and higher reaction temperatures promoted the formation of 4-TBP. Another observation is that as the amount of 2-TBP increases, the amount of 2,4-DTBP also increases. This proves that 2-TBP is a precursor to the formation of 2,4-DTBP. 4-TBP can be formed either directly from phenol or from 2-TBP *via* rearrangement. The 3-TBP is formed only at higher temperatures (so also 3,5-DTBP) due to thermodynamic constraints. The formation of 2,6-DTBP can also take place from 2-TBP. These are competing reactions for 2,4-DTBP. The 2,6 product has, however, not been detected as its formation is promoted on basic sites

154

It has been suggested[25,34,35] that Brönsted acid sites interact with the π-cloud of aromatic ring bringing the molecule parallel to the surface. This will allow alkylation at the *para* position easier as compared to the *ortho* positions. The para selectivity of the catalysts can be attributed to the nature of adsorption of phenol over the catalyst surface. According to Tanabe[36], the phenolate ion is adsorbed such that the *ortho* position is very near to the catalyst surface in the case of basic catalysts such as MgO, hence the *ortho* position can be alkylated. However the interaction of acidic catalysts are different which influence the electron current around the benzene ring such that the aromatic ring lie parallel to the catalyst surface (figure 4.17) favouring *para* alkylation. Also it has been reported that the steric hindrance in the transition state due to the substitution of bulkier *tert*-butyl group at the *ortho* positions, enhances the *para* selectivity[37].
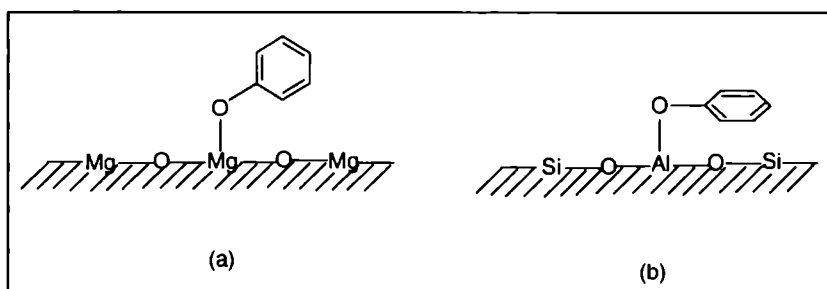

Figure 4.17 Adsorption of phenol on (a) MgO and (b) Al_2O_3

4.10 CONCLUSIONS

The conclusions from the present results can be summarized as given below:

- Alkylation of phenol with *tert*-butyl alcohol over sulfated titania based catalysts shows good catalytic activity. The interesting aspect of this reaction is the high selectivity of alkylation at the *para* position.

- Reaction variables such as temperature, flow rate, molar ratio and reaction time have strong influence on the conversion and product selectivity.

ॐ Higher flow rate is helpful in producing 4-TBP.The suitable reaction temperature range is from 180 to 200°C. Lower molar ratios are beneficial to 4-TBP. All the systems showed good resistance to catalytic deactivation.

ॐ The acidity plays an important role in the butylation reaction. Medium acid sites are helpful to produce 4-TBP and strong acid sites govern the formation of 2,4-DTBP.

ॐ In order to promote the formation of 4-TBP at higher conversions of phenol, a proper reaction temperature, lower reactant ratio and medium acidity on the sulfated titania based catalysts are recommended.

ॐ ୧୫୭୧୫୭୧୫୭ ॐ
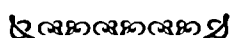
REFERENCES

SECTION 1

1. G.A. Olah, *"Friedel-Crafts Chemistry"*, Wiley-Interscience, New York, London, Sydney, Toronto (1973).

2. A. Cornelis, C. Dony, P. Laszlo, K.M. Nsunda, *Tetrahedron Lett.*, 34 (1993) 529.

3. V.R. Choudhary, S.K. Jana, B.P. Kiran, *Catal. Lett.*, 59 (1999) 217.

4. B. Jacob, S. Sugunan, A.P. Singh, *J. Mol. Catal. A. Chem.*, 139 (1999) 43.

5. A.P. Singh, B. Jacob, S. Sugunan, *Appl. Catal. A. Gen.*, 174 (1998) 51.

6. I. Yusuke, O. Mayumi, U. Kazuo, *Appl. Catal. A. Gen.*, 132 (1995) 127.

7. K.R. Sunajadevi, S. Sugunan, *React. Kinet. Catal. Lett.*, 82 (2004) 11.

8. G.D. Yadav, T.S. Thorat, P.S. Kumbhar, *Tetrahedron Lett.*, 34 (3) (1993) 529.

9. G.D. Yadav, T.S. Thorat, *Tetrahedron Lett.*, 37 (30) (1996) 5405.

10. S.P. Ghorpade, V.S. Dharsane, S.G. Dixit, *Appl. Catal. A. Gen.*, 166 (1998) 135.

11. S. Sebti, R. Tahir, R. Nazih, S. Boulaajaj, *Appl. Catal. A. Gen.*, 218 (2001) 25.

12. S.N. Koyande, R.G. Jaiswal, R.V. Jayaram, *Ind. Eng. Chem. Res.*, 37 (1998) 98.

13. J. Miller, M. Goodchild, J.L. Lakshmi, D. Wails, J.S. Hartman, *Catal. Lett.*, 63 (1999) 199.

14. K.B. Sherly, V.T. Bhatt, *React. Kinet. Catal. Lett.*, 75 (2002) 239.

15. S. Sugunan, T. Radhika, H. Suja, *React. Kinet. Catal. Lett.*, 79 (2003) 27.

16. S.K. Samantaray, T. Mishra, K.M. Parida, *J. Mol. Catal. A. Chem.*, 156 (2000) 267.

17. P. Botella, A. Corma, J. M. Lopez Nieto, S. Valencia, R. Jacquot, *J. Catal.*, 195 (2000) 161.

18. D. Rohan, C. Canaf, E. Romeafin, M. Guismet, *J. Catal.*, 177 (1998) 2743.

19. S. Jun, R. Ryoo, *J. Catal.*,195 (2000) 237.

20. V.R. Choudhary, S.K. Jana, V.S. Narkhede, *Catal. Commun.*, 2 (2001) 331.

21. Y. Deng, C. Lettmann, W.F. Maier, *Appl. Catal. A. Gen.*, 214 (2001) 31.

22. A.P. Singh, D. Bhattacharya, S. Sharma, *J. Mol. Catal.*, 49 (1995) 139.

23. A. Corma, M.J. Climent, H. Garcia, P. Prima, *Appl. Catal.*, 49 (1989) 109.

24. A.B. Despande, A.R. Bajpai, S.D. Samant, *Appl. Catal A. Gen.*, 209 (2001) 229.

25. T. Cseri, S. Bekassy, F. Figueras, S. Rizner, *J. Mol. Catal. A. Chem.*, 98 (1995) 101.

26. B.M. Choudary, M.L. Kantam, M. Sateesh, K.K. Rao, P.L. Santhi, *Appl. Catal A. Gen.*, 149 (1997) 257.

27. S.J. Barlow, T.W. Bastock, J. H. Clark, S.R. Cullen, *Tetrahedron Lett.*, 34 (1993) 3339.

28. C.N. Rhodes, D.R. Brown, *J. Chem. Soc. Faraday Trans.*, 89 (1993) 1387.

29. B. Coq, V. Gourves, F. Figueras, *Appl. Catal. A.*, 100 (1993) 69.

30. K. Arata, K. Sato, I. Toyoshima, *J. Catal.*, 42 (1976) 221.

SECTION 2

1. J.S. Beck, W.O. Haag, in: G. Ertl, H. Knozinger, J. Weitkamp (Eds.), *"Handbook of Heterogeneous Catalysis"*, Vol. 5, Wilely-VCH, Weinheim (1997) p. 2131.

2. J.F. Lorenc, G. Lambeth, W. Scheffer, in: M. Howe-Grnt, J.L. Kroschwitz (Eds.), Kirk-Othmrer, *"Encyclopedia of chemical technology"*, 4th ed., Vol.2, Wiley, New York (1992) p. 113.

3. M. Schulz, K. Seiffarth, M. Nuechter, C. Bayer, Ger. (East) D.D. 267 (1989) 250.

4. O.N. Tsevktov, K.D. Kovenev, *Int. J. Chem. Eng.*, 6 (1966) 328.

5. S. van den Bosch, E. van't Land, J. Stoffelsma, *US patent.*, 4,414,233 (1983).

6. B.E. Firth, *US patent.*, 4,275,249 (1981).

7. G.K. Chandra, M.M. Sharma, *Catal. Lett.*, 19 (1993) 309.

8. S. Wieland, P. Panster, *Stud. Surf. Sci. Catal.*, 108 (1997) 67.

9. S. Inoki, M. Yasuhara, F. Matsunaga, K. Omura, *JP.*, 63165336 (1984).

10. M. Imamuri, H. Iwane, S. Otaka, *JP.*, 61251633.

11. A. Corma, H. Garcia, J. Primo, *J. Chem. Res.*, (1988) 40.

12. C.D. Chang, S.D. Hellring, *US Patent.*, 5 288 927 (1994).

13. M. Yamamoto, A. Akyama, *Japanese Patent.*, 6 122 639 (1994).

14. A.U.B. Queiroz, L.T. Aikawa *French Patent.*, 2 694 000 (1994).

15. G. Bellussi, G. Pazzuconi, C. Perego, G. Girotti, G. Terzoni, *J. Catal.*, 157 (1995) 227.

16. S. Namba, T. Yashima, Y. Itaba, N. Hara, *Stud. Surf. Sci. Catal.*, 5 (1980) 105.

17. J. Cejka, N. Zilkova, B. Wichterlova, G. Eder-Mirth, J. A. Lercher, *Zeolites.*, 17 (1996) 265.

18. S.J. Chu, Y.W. Chen, *Appl. Catal. A. Gen.*, 123 (1995) 51.

19. J.L.G. Almeida, N. Dufauz, Y. B. Taarit, C. Naccache, *Appl. Catal. A. Gen.*, 114 (1994) 141.

20. E. Dumitriu, V. Hulea, *J. Catal.*, 218 (2003) 249.

21. S. Balasama, P. Beltrame, P. L. Beltrame, L. Fermi, G. Zuretti, *Appl. Catal.*, 13 (1984) 161.

22. M. Marezewski, J.P. Bodibo, G. Perot, M. Guisnet, *J. Mol. Catal.*, 50 (1989) 211.

23. Z.H. Fu, Y. Ono, *Catal. Lett.*, 21 (1993) 43.

24. R. Pierantozzi, A.F. Nordquist, *Appl. Catal.*, 21 (1986) 263.

25. R.F. Parton, J.M. Jacobs, H. Van Ootehem, P.A. Jacobs, *Stud. Surf. Sci. Catal.*, 46 (1989) 211.

26. K. Zhang, H. Zhang, C. Hung, S. Xiang, S. Liu, D. Xu, H. Li., *Appl. Catal. A.*, 166 (1988) 89,.

27. A. H. Padmasri, V. Durga Kumari, P. Kanta Rao, *Stud. Surf. Sci. Catal.*, 113, (1988) 563.

28. S. Subramanian, A. Mitra, C.V.V. Satyanarayana, D.K. Chakrabarty, *Appl. Catal. A.*, 159, (1997) 229.K.

29. Tanabe, *"Solid acids and bases and their catalytic properties"*, Academic Press, New York (1970) 103.

30. C.V. Satyanarayana, U. Sridevi, B.S. Rao, *Stud. Surf. Sci. Catal.*, 135 (2001) 457.

31. P. Xu, B. Feng, S. Chen, *Huadong Huagong Xueyuan Xuebao* 14 (1988) 476.

32. K. Zhang, Ch. Hung, H. Zhang, S. Xiang, S. Li, *Appl. Catal. A.* 166 (1998) 163.

33. A.J. Kolka, J.P. Napolitano, G.G. Elike, *J. Org. Chem.*, 21 (1956) 712.

34. K. Tanabe, *Stud. Surf. Sci. Catal.*, 20 (1985).

35. H. Hattori, K. Shimazu, N. Yoshii, K. Tanabe, *Bull. Chem. Soc. Jpn.*, 49 (1976) 969.

36. K. Tanabe, *"Catalysis by acids and bases"*, Elsevier, (1985) p. 4.

37. R.F. Parton, J.M. Jacobs, D.R. Huybrechts, P.A. Jacobs, *Stud. Surf. Sci Catal.*, 46 (1989)163.

Chapter 5

Beckmann Rearrangement Of Cyclohexanone Oxime

Most popular industrial route for the synthesis of ε-caprolactam, the starting material for the manufacture of nylon fibers, is through Beckmann rearrangement of cyclohexanone oxime. The environmental regulations and process safety continue to drive the industry to develop solid acids to replace liquid acid processes. The vapour phase Beckmann rearrangement of cyclohexanone oxime over the prepared nano sulfated titania catalysts is described in this chapter. The influence of the main process variables like reaction temperature, oxime feed rate, oxime to solvent molar ratio, reaction time, etc on the conversion and selectivity is investigated in detail. The catalytic performance of various systems for the reaction is correlated with acidity of the prepared systems. The acid sites of medium strength on the catalyst surface play an important role in the selective formation of lactam.

5.1 INTRODUCTION

Beckmann rearrangement of cyclohexanone oxime to ε-caprolactam (Figure 5.1), which is the precursor to nylon-6, is now being carried out using fuming sulfuric acid as the catalyst[1]. However, this process yields the undesirable ammonium sulfate to a greater extent than the desired lactam. Moreover, the use of corrosive sulfuric acid should be avoided for environmental and economical reasons.
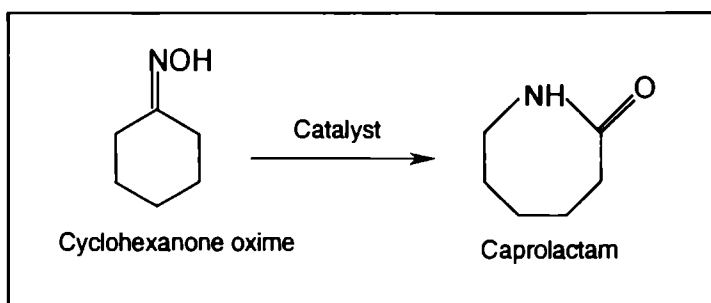
Figure 5.1 General scheme for preparation of caprolactam

There are numerous studies on the rearrangement of cyclohexanone oxime to ε-caprolactam over solid acid catalysts[1-11]. Since vapour-phase Beckmann rearrangement on solid catalyst would eliminate environmental problems, a wide variety of solid acid catalysts have been studied in search for an alternative clean process. Compared with the conventional method of preparation of ε-caprolactam, this is an energetically and economically favorable as well as environmentally friendly alternative route, since there is no inevitable salt formation of ammonium sulfate. The oxide supports used as catalysts are single metal oxides, such as alumina[2], silica[3,4], thoria[5], titania[6], zirconia[7,8] etc.

Corma and co workers[9,10] reported that on H-Na-Y Zeolite cyclohexanone oxime is converted to 5 cyanopent-1-ene. Sato *et al.*[11] found that the use of high siliceous ZSM-5, a catalyst with low acidity, leads to high selectivity of ε-caprolactam due to the smooth desorption of the same. Among the various solid acid catalysts, boron oxide supported on alumina was one of the successful catalysts, showing high lactam selectivity[4,12]. Various factors including catalyst preparation, reaction temperature and surface acidity were shown to have strong influence on oxime conversion, lactam selectivity and the decay rate of the catalysts[12,13]. In table 5.1, we cite some examples from the patents regarding vapour phase Beckmann rearrangement[14]. Till date, no report has been found in literature regarding the Beckmann rearrangement

catalyzed by sulfated titania systems. Nano sulfated titania and its modified forms are shown to be a new catalyst advantageous for the vapour phase Beckmann rearrangement of cyclohexanone oxime, as revealed by this study, which is explained in detail in the following sections.

Table 5.1 Some catalysts for the vapour phase Beckmann rearrangement

Patent assignee	Patent number	Year	Catalyst	Solvent	Conversion (%)
UPO	US4873325	1986	SAPO-11	Acetonitrile	98
Sumitomo	US4709024	1986	High silica MFI	Benzene	74
Sumitomo	US4968793	1989	High silica MFI	Methanol	99
Mobil	US4927924	1989	ZSM-5	Benzene	99
Mitsubishi	EP509493	1991	Ta_2O_5/SiO_2	Benzene	98
Degussa	DE19608660	1995	B-MFI	Methanol	99
Sumitomo	JP-291074	1996	ALPO-5	Ethanol	27
Enichem	EP819675	1996	Amorphous SiO_2/Al_2O_3	Methanol	99
Ube	JP10-87612	1996	Zeolite L	n-Hexanol	99

5.2 PROCESS OPTIMIZATION

The vapour-phase Beckmann rearrangement of cyclohexanone oxime was conducted under atmospheric pressure in a conventional continuous flow fixed bed type reactor. Exactly 0.5 g of the catalyst was placed using quartz wool in a pyrex glass reactor (inner diameter = 14 mm, length = 32 cm). It was heated by an electrical tubular furnace, and the temperature was controlled with a temperature controller with a sensor placed in the center of the catalyst bed. A mixture of oxime and benzene in the liquid phase supplied from a syringe pump at a constant flow rate was fed into the reactor. The effluents were collected in a trap and the liquid products were identified by gas chromatography using SE-30 column and FID detector. Among the various

products formed, only ε-caprolactam and cyclohexanone were estimated separately while all the remaining minor products such as 5-cyanopentane, 5-cyano-pent-1-ene and 2-cyclohexene-1-one were set aside under the banner 'others' during the calculation of selectivity.

I. Effect of Reaction Temperature

The influence of reaction temperature on the catalytic reaction was investigated in the range of 300 to 500°C. Figure 5.2 shows the dependence of oxime conversion and yield of ε-caprolactam and cyclohexanone with respect to temperature. The conversion is found to increase drastically as the temperature increases from 350 to 400°C. It was assumed that the deactivating compounds desorb more easily at elevated temperatures. At 400°C, the conversion of oxime is 97% with a ε-caprolactam selectivity of 48.54% at 3 h reaction time. On increasing the temperature to 500°C, the conversion reaches 100%, however the ε-caprolactam selectivity declines.

Anand *et al.*[15] has also reported similar results on the same reaction done over different ferrierite zeolites catalysts. The low selectivity of ε-caprolactam may be due to its decomposition at high temperature on the catalyst surface. Another reason suggested is an increased rate of side reaction at higher temperatures. Similar results were obtained over B_2O_3 catalysts supported on Al_2O_3[12,16], SiO_2[4] and ZrO_2[7]. At higher temperatures, the colour of the product solution changes to yellow due to the formation of side products. Murthy *et al.*[17] varied the temperature from 200 to 390°C for the rearrangement reaction over Ti-SAPO-11 catalyst and found that the oxime conversion and lactam selectivity increased with temperature. Above 390°C, selectivity to ε-caprolactam decreased, which was accounted for the decomposition of caprolactam on the catalyst surface.
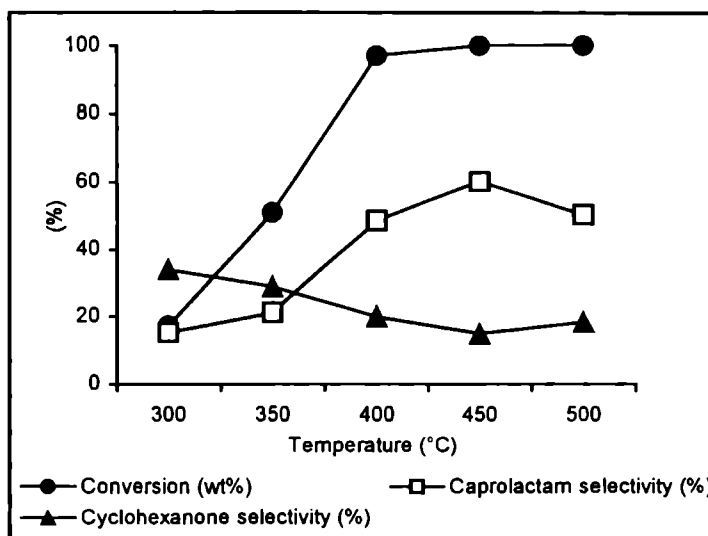
Figure 5.2 Influence of reaction temperature on oxime

conversion and product selectivity.

Amount of catalyst: 0.5 g STMn(3), Flow rate: 4 mL h^{-1} Reaction time: 3 h,

oxime concentration in feed: 6 % in benzene

Mao *et al.*[18] reported that the conversion of oxime increased with increase in temperature and the selectivity to lactam is high at 300°C over B_2O_3/TiO_2-ZrO_2 catalyst. By comparing these results with the observations of the present work, we can conclude that the temperature has a positive effect on Beckmann rearrangement over transition metal loaded sulfated titania in the range of 300-450°C and above 450°C, the selectivity is affected adversely. The increase in cyclohexanone selectivity above 450°C suggests an increased rate of side reactions at higher temperature. The change in the product yield at higher temperature also supplements the formation of side products. The conversion of oxime and selectivity towards ε-caprolactam has a drastic increase at 400°C. Further increase in temperature, though increase the catalytic activity, does not improve the ε-caprolactam selectivity. 400°C is selected as the optimum reaction temperature for further investigations.

II. Effect of Flow Rate

Table 5.2 shows the influence of contact time on the catalytic activity and product selectivity. The flow rate alters the contact time and at high flow rate, the encounter of the reactants and the products with the catalyst surface will be less compared to that at lower feed rates. Progressive decrease in conversion of oxime is noticed with increase in the flow rate. The oxime conversion changes from 100 to 74.17% when we change the flow rate from 3 mL h^{-1} to 6 mL h^{-1}.

Table 5.2 Influence of flow rate on oxime conversion and product selectivity

Flow rate (mL h^{-1})	Conversion of Oxime (wt%)	Selectivity (%)		
		ε-caprolactam	cyclohexanone	others
3	100	40.67	19.58	39.75
4	97.06	48.54	20.08	31.38
5	90.57	51.39	22.62	25.99
6	74.17	49.77	25.74	24.49

Amount of catalyst: 0.5 g STMn(3), Reaction temperature: 400°C, Reaction time: 3 h, oxime concentration in feed: 6 % in benzene

As the contact time is decreased, selectivity increases initially, reaches a maximum and then decreases. The lactam selectivity shows an initial increase and at the flow rate of 5 mL h^{-1} and finally reaches a maximum of 51.39%. Decrease in the lactam selectivity was observed when feed rate is increased from 5 to 6 mL h^{-1}. Thus, the selectivity to caprolactam is maximum at a flow rate of 5 mL h^{-1} suggesting an optimum velocity of the feed for lactam formation. The formation of other products is less at higher feed rate because the reactants are in contact for less time and hence side reaction is suppressed. Thankaraj et al.[19] made similar observations on the effect of feed rate in vapour phase Beckmann rearrangement of cyclohexanone oxime over titanium silicates. For further studies 4 mL h^{-1} is taken as the flow rate, which showed a maximum yield of caprolactam under the experimental conditions.

III. Effect of Concentration of Cyclohexanone Oxime

In order to understand the effect of the concentration of oxime in the feed, a series of experiments were conducted at reaction temperature of 400°C and at a flow rate of 4 mL h^{-1} by varying the oxime concentration from 2 to 8% (w/v). It can be seen from table 5.3 that the dilution of cyclohexanone oxime in benzene improves the conversion of oxime. At low oxime concentration (2%) the yield of caprolactam is high (63.77%). As the concentration increases the yield of ε-caprolactam decreases. At high oxime concentration the formation of by-products is high.

Table 5.3 Influence of oxime concentration on oxime conversion

and product selectivity

Oxime concentration in benzene (%)	Conversion of Oxime (wt%)	ε-caprolactam		cyclohexanone	
		Selectivity (%)	Yield (%)	Selectivity (%)	Yield (%)
2	100	63.77	63.77	15.99	15.99
4	99.05	51.97	51.47	18.43	18.25
6	97.06	48.54	47.11	20.08	19.49
8	91.36	41.16	37.60	21.44	19.59

Amount of catalyst: 0.5 g STMn(3), Flow rate: 4 mL h^{-1}, Reaction time: 3 h,

Reaction temperature: 400°C

IV. Effect of Solvent

Solvents with varying polarities (like benzene ethanol and acetonitrile) are utilized to investigate their influences on the catalytic activity and the product selectivity. Both the oxime conversion and ε-caprolactam selectivity are affected by the nature of the solvent. Roseler *et al.*[20] have reported the deactivation of MFI borosilicate in the Beckmann rearrangement of

cyclohexanone oxime using different organic solvents and found that the degree of deactivation depends on the kind of solvent used. This is due to the difference in the polarity of solvents.

Table 5.4 shows the influence of solvent for the reaction of cyclohexanone oxime on STMn(3) catalyst. There is not any appreciable change in the conversion, but the selectivity of ε-caprolactam is influenced by the type of solvent used. The selectivity increases as the dipole moment of the solvent increases. The selectivity in presence of benzene (dipole moment = 0) was low (48.54%), selectivity in presence of ethanol (dipole moment = 1.44) was 54.79% while selectivity in presence of acetonitrile (dipole moment = 3.92) was high (59.21%). The most likely reason for this is that the polar solvents increase the desorption rate of lactam, decreasing its contact time on the catalyst surface, thus lowering the likelihood for acid catalyzed opening of lactam to form polymers and the coke precursors on the catalyst surface. Chung et al.[21] studied the solvent effects in the liquid phase Beckmann rearrangement of oxime over H-Beta catalyst. The nature of the solvent determines the performance of the reaction. The stronger the solvent-adsorption site interaction, the more difficult will be the access of the reactant to the active sites. This may lead to a decrease in the catalytic activity.

According to Ko et al.[22] ethanol dehydrates to ethylene, diethyl ether and water over the Al-MCM-41 catalyst under the reaction conditions and, during the reaction, the water produced suppresses the formation of coke on the catalyst surface. Our studies also show the formation of water during the reaction, when we use ethanol as the solvent. The positive effect of water on preventing deactivation was verified in the oxime conversion using B-MFI zeolites[20]. Komatsu et al.[23] have reported that the solvent with medium polarity was preferable for this reaction on silicalite-1. In our studies solvent effect is not much pronounced, as the selectivity does not vary much among the different solvents.

Table 5.4 Influence of various solvents for oxime conversion
and product selectivity

Solvent	Conversion of Oxime (wt%)	Selectivity (%)		
		ε-caprolactam	cyclohexanone	others
Acetonitrile	98.56	59.21	22.95	17.84
Ethanol	97.95	54.79	21.40	23.81
Benzene	97.06	48.54	20.08	31.38

Amount of catalyst: 0.5 g STMn(3), Flow rate: 4 mL h^{-1}, Reaction time: 3 h, Reaction temperature: 400°C, oxime concentration in feed: 6 % in the solvent

V. Effect of Time on Stream-Deactivation study

To establish the stability of the systems towards deactivation, a continuous 7 h run was carried out over various catalysts and the products were analyzed after every one hour. From figure 5.3, it is clear that the oxime conversion remains almost constant until 5 h of reaction time in the case of T and ST.

Deactivation rate is different for different systems. The conversion of oxime already began to decrease at a time on stream of 5 h in the case of T and ST. On the other hand, the complete oxime conversion was maintained until 5 h over the metal loaded sulfated titania. Fe, Co, Ni, Cu and Zn loaded systems show an initial increase in conversion for the first 3 h and after 5 h of reaction time they deactivates slowly. Two main mechanisms have been suggested for the deactivation of solid acid catalysts in the rearrangement of oxime, namely the formation of coke[2,24,25] over the catalyst surface and/or the irreversible adsorption of basic reaction by-products[10]. Corma and co-workers[9,10] reported that organic bases such as pyridine suppress the conversion of cyclohexanone oxime on H-Na-Y zeolites. Ushikubo[26] reported that the total pore volume and pore volume of fine pores decreased considerably due to coke formation. Ko *et al.*[22] characterized the used catalysts (Al-MCM-41) and found a small variation in their

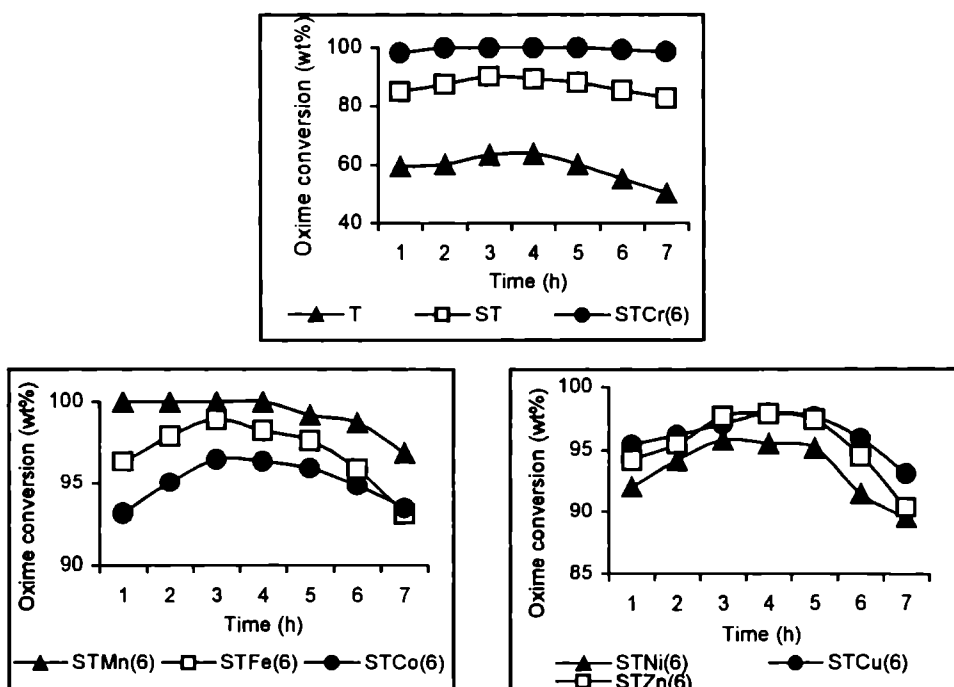acidities and a decrease in he surface area and pore volume, which may be due to pore blockage by coke formation.

Figure 5.3 Deactivation studies on oxime conversion over different systems

Amount of catalyst: 0.5 g, Reaction temperature: 400°C, Flow rate: 4 mL h^{-1}, oxime concentration in feed: 6 % in benzene

The present investigation is consistant with the possibility of coke formation over the catalyst surface, which can be correlated with the significant decrease of oxime conversion over 7 h. The coke deposition may be due to the eventual formation of carbonaceous deposits resulting from the reaction between the side products or arise from the polymerization of caprolactam[27]. The colour of the catalysts changed to dark grey or black due to coke deposition on the surface of the catalysts. The catalytic activity reached an equilibrium level after 3 to 4 h and hence all the experimental data were obtained after the stabilization of the activity.

5.3 COMPARISON OF DIFFERENT SYSTEMS

A comparative evaluation of the catalytic activity of various sulfated titania systems in the vapour phase Beckmann rearrangement is given in this section. After analyzing the optimization results, catalytic activity of the systems were studied under the following conditions, temperature - 400°C, flow rate - 4 mL h^{-1}, oxime concentration - 6% in benzene and time on stream - 3 h. Sulfation and metal loading improved the activity of tiania to a considerable extent. An attempt to correlate the surface acidity with oxime conversion and ε-caprolactam selectivity is also done. Tables 5.5 and 5.6 present the results of the vapour phase Beckmann rearrangement of cyclohexanone oxime over different transition metal loaded sulfated titania systems.

Table 5.5 Influence of the type of metal loaded in the vapour phase
Beckmann rearrangement of cyclohexanone oxime

Systems	Conversion of Oxime (wt%)	ε-caprolactam		cyclohexanone		Selectivity to others (%)
		Selectivity (%)	Yield (%)	Selectivity (%)	Yield (%)	
T	63.45	20.43	12.96	16.97	10.77	62.60
ST	90.36	41.13	37.17	24.65	22.27	34.22
STCr(3)	98.41	54.41	53.54	19.43	19.12	26.16
STMn(3)	97.06	48.54	47.11	20.08	19.48	31.38
STFe(3)	96.23	42.08	40.49	20.85	20.06	37.07
STCo(3)	94.14	43.84	41.27	19.18	18.06	36.98
STNi(3)	92.00	47.92	44.09	22.77	20.95	29.31
STCu(3)	95.08	46.53	44.24	17.64	16.77	35.83
STZn(3)	95.69	45.00	43.06	18.24	17.45	36.76

Amount of catalyst: 0.5 g, Flow rate: 4 mL h^{-1}, Reaction time: 3 h, Reaction temperature: 400°C, oxime concentration in feed: 6 % in benzene

From the results of NH_3-TPD as well as cyclohexanol decomposition reaction, it is understood that the catalysts possess acidic character. These acid sites are strong enough to catalyze Beckmann rearrangement of cyclohexanone oxime to ε-caprolactam. From table 5.5, it is clear that titania in the pure form is much less active in this rearrangement. Also it results in the formation of unwanted products to a greater extent. Sulfated titania and transition metal loaded sulfated titania systems are very active towards the reaction along with increased selectivity for ε-caprolactam.

Table 5.6 Influence of the amount of metal loading in the vapour phase Beckmann rearrangement of cyclohexanone oxime

Systems	Conversion of Oxime (wt%)	ε-caprolactam		cyclohexanone		Selectivity to others (%)
		Selectivity (%)	Yield (%)	Selectivity (%)	Yield (%)	
STCr(6)	100.00	57.88	57.88	22.25	22.25	19.87
STMn(6)	100.00	56.10	56.10	26.16	26.16	17.74
STFe(6)	98.93	46.84	46.34	24.23	23.97	28.93
STCo(6)	96.55	50.32	48.58	23.54	22.73	26.14
STNi(6)	95.84	52.21	50.04	25.14	24.09	22.65
STCu(6)	97.10	51.89	50.39	25.59	24.85	22.52
STZn(6)	97.68	51.10	49.91	25.3	24.78	23.53
STCr(9)	89.56	50.84	45.53	23.58	21.12	25.58
STMn(9)	89.03	49.08	43.70	21.93	19.52	28.99
STFe(9)	88.36	44.03	38.90	18.18	16.06	37.79
STCo(9)	86.81	44.92	39.00	25.11	21.80	29.97
STNi(9)	86.59	46.83	40.55	19.47	16.86	33.70
STCu(9)	87.14	46.00	40.08	21.59	18.81	32.41
STZn(9)	87.95	45.73	40.22	19.42	17.08	34.85

Amount of catalyst: 0.5 g, Flow rate: 4 mL h^{-1}, Reaction time: 3 h, Reaction temperature: 400°C, oxime concentration in feed: 6 % in benzene

As the metal loading increases from 3 to 6% the oxime conversion is found to increase (Tables 5.5 and 5.6). However it is found that high metal content of 9%, decreases the oxime conversion. Among all the catalysts, the maximum selectivity to ϵ-caprolactam formation is 57.8% for system with 6% chromia loading. All the sulfated systems show more than 85% conversion. In the case of STCr(6) and STMn(6) the conversion reaches 100%.
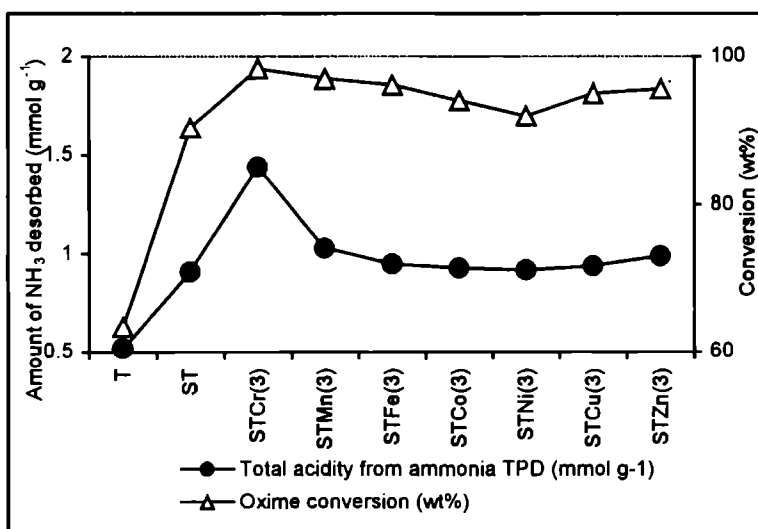

Figure 5.4 Correlation between oxime conversion and total acidity

As Beckmann rearrangement is considered as an acid catalysed reaction, an attempt has been made to obtain a correlation between the acidity and the oxime conversion. As seen from NH_3-TPD studies, the metal loading affects their acidity remarkably. The concentration of acid sites (per m^2 of catalyst) on the surface and the extent of metal loading show a direct relationship. As the metal content increases, the total concentration of acid sites increases initially, but at high loadings acidity decreases. Activity results revealed that a maximum oxime conversion was obtained at a loading of 6 wt% and lactam selectivity got saturated when the metal loading was more than 6 wt%. These results suggested that the activity and selectivity of the catalysts

depend on their acid strength distribution. Figures 5.4 and 5.5 show the correlation between oxime conversion and total acidity obtained from NH_3-TPD.

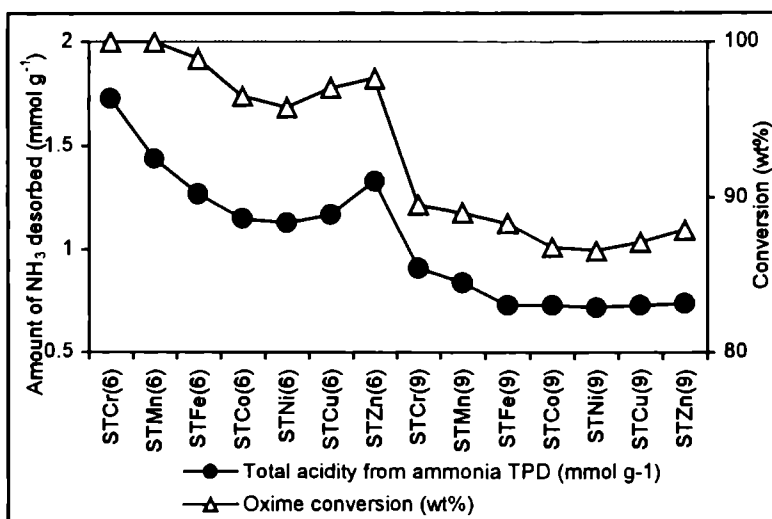Figure 5.5 Correlation between oxime conversion and total acidity

Xu et al.[29] reported that the active sites for Beckmann rearrangement are the medium and strong acid sites on the surface of B_2O_3/ZrO_2 catalysts. Dai et al.[30] studied the catalysis of H-USY zeolites and showed that an appropriate amount of relatively weak acid sites of H-USY was effective for a high selectivity of lactam. The results of our investigation also show that the oxime conversion depends on the total acidity of the systems, while the lactam selectivity depends on medium acid sites as obtained from NH_3-TPD method. Figures 5.6 and 5.7 show the correlation between ε-caprolactam selectivity and medium acidity obtained from NH_3-TPD. Medium acid sites govern the formation of ε-caprolactam. The good agreement between NH_3-TPD results and conversion suggests that all the surface acid sites irrespective of their strength, take part in the rearrangement reaction. The higher conversion of the sulfated titania and metal loaded sulfated titania catalysts may be due to the substantial amount of strong acid sites on the surface.

173
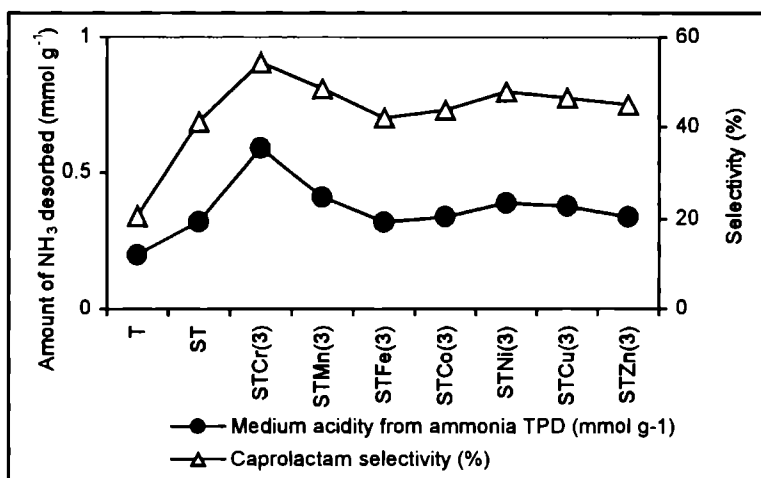
Figure 5.6 Correlation between ε-caprolactam selectivity and medium acidity
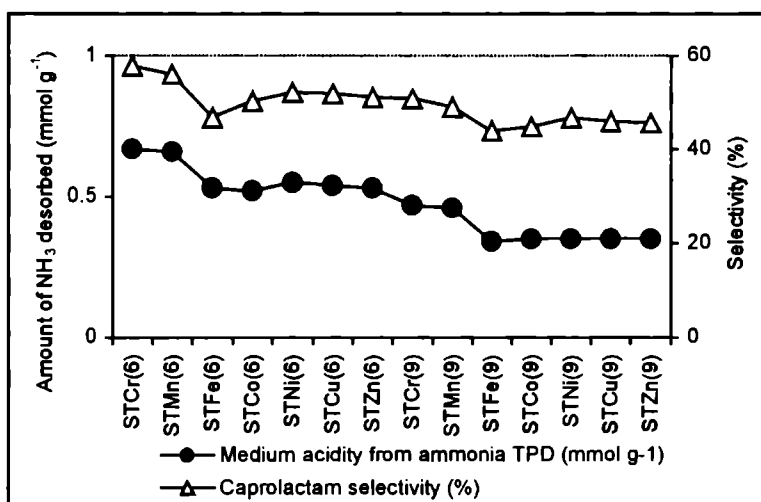
Figure 5.7 Correlation between ε-caprolactam selectivity and medium acidity

5.4 MECHANISM OF BECKMANN REARRANGEMENT REACTION

The mechanism of the liquid phase Beckmann rearrangement promoted by sulfuric acid is well known as a typical concerted intermolecular S_N2 reaction

where the alkyl group in *anti* position migrates against the OH of the oxime group[31]. The mechanism of Beckmann rearrangement is shown in figure 5.8.
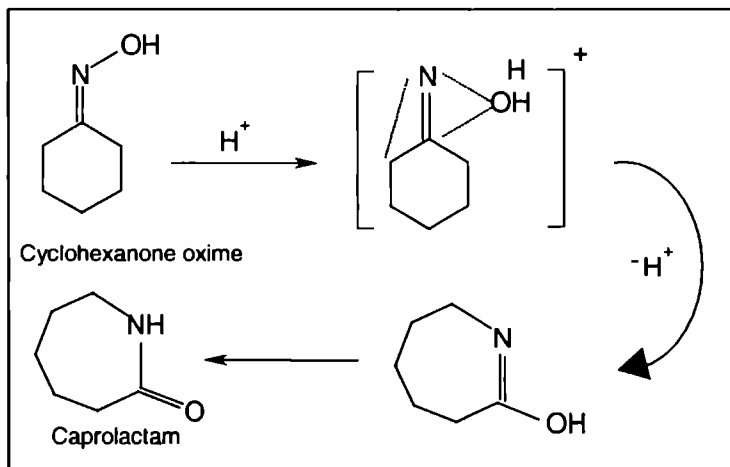

Figure 5.8 Suggested mechanism for Beckmann rearrangement of cyclohexanone oxime
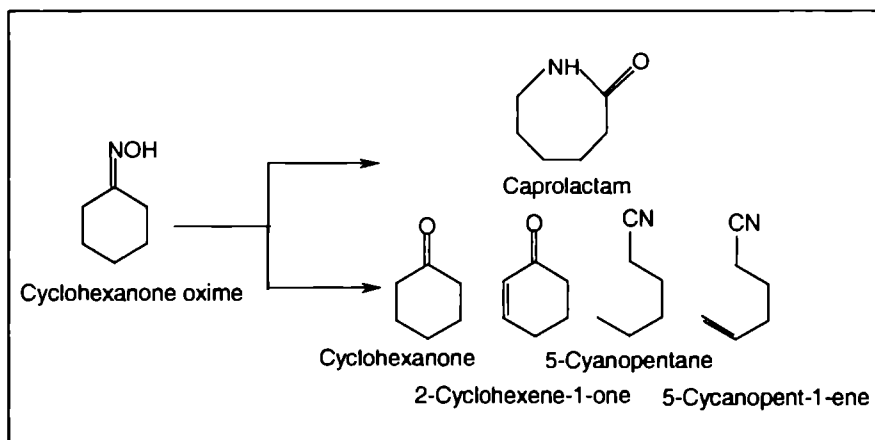

Figure 5.9 Reaction scheme for Beckmann rearrangement of cyclohexanone oxime

The reaction conditions are quite different for liquid and vapour phase. Kajikuri *et al.*[32] concluded that the mechanism of the vapour phase Beckmann rearrangement reaction is the same as in liquid phase. The major product of

175

the reaction is ε-caprolactam, while minor quantities of 5-cyanopentane, 5-cyanopent-1-ene, cyclohexanone and 2-cyclohexene-1-one are also formed as side products[33] in the rearrangement of cyclohexanone oxime. The reaction scheme is presented in figure 5.9.

5.5 CONCLUSIONS

The following conclusions can be drawn from the present study.

- Transition metal loaded sulfated titania systems are found to be active for the Beckmann rearrangement reaction.

- Chromia loaded systems are found to be better catalysts than others among the investigated catalyst systems.

- Acid sites of intermediate strength play important role in the selective formation of lactam.

- Reaction variables such as reaction temperature, flow rate, solvent, reaction time and oxime concentration have strong influence on the oxime conversion and ε-caprolactam selectivity.

- Conversion of oxime increased with increase in temperature, and the highest selectivity to lactam was obtained at an optimum reaction temperature of 400°C.

- Polar solvents give higher selectivity to lactam than other solvents. Catalysts get deactivated after 5 h due to coke formation, which may block the active sites.

- The acidic and catalytic property of the catalyst was found to be affected by the percentage of metal loading. Catalysts with optimum metal loading of 6 wt%, which contained the maximum number of medium strength acid sites, shows good selectivity towards ε-caprolactam.
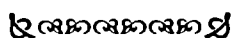
REFERENCES

1. J.E. Kent, S. Riegel, *"Handbook of Industrial Chemicals"*, 8th edn, Van Nostrand, New York., (1983) p402.

2. S. Sato, S. Hasebe, H. Sakurai, K. Urabe, Y. Izumi, *Appl. Catal. A.*, 29 (1987) 107.

3. S. Sato, H. Sakurai, K. Urabe, Y. Izumi, *Chem. Lett.*, (1985) 277.

4. S. Sato, K. Urabe, Y. Izumi, *J. Catal.*, 102 (1986) 99.

5. W.F. lates, Ro. Downs, J.C. Burleson. *US Patent.*, 3639391 (1972).

6. K. Yoshida, K. Fujiki, T. Harada, Y. Moroi, T. Yamaguchi, *Jpn, Patent.*, 7310478 (1973).

7. S.B. Cheng, B.O. Xu, S. Jiang, F.P. Tian, T.X. Cai, X.S. Wang, Chin, *J. Catal.*, 17 (1996) 512.

8. B.Q. Xu, S.B. Cheng, X. Zhang, Q.M. Zhu, *Catal. Today.*, 63 (2000) 275.

9. A. Corma, H. Garcia, J. Primo, *Zeolites.*, 11 (1991) 593.

10. A. Aucejo, M.C. Burguet, A. Corma, V. Fomes, *Appl. Catal.*, 22 (1986) 187.

11. H. Sato, K. Hirose, Y. Nakamera, *Chem. Lett.*, (1993) 1987.

12. T. Curtin, J.B. McMonagle, B.K. Hondnett, *Appl. Catal. A. Gen.*, 93 (1992) 75.

13. A. Thangra, S. Sivasanker, P. Ratnasamy, *J. Catal.*, 137 (1992) 252.

14. H. Ichihashi, H. Sato, *Appl. Catal. A. Gen.*, 221 (2001) 359.

15. R. Anand, R.B. Khomane, B.S. Rao, B.D. Kulkarni, *Catal. Lett.*, 78 (2002) 189.

16. T. Curtin, J.B. McMonagle, B.K. Hodnett, *Stud. Surf. Sci. Catal.*, 59 (1991) 531.

17. K.V.V.S.B.S.R. Murthy, M. Chandrakala, S.J. Kulkarni, K. V. Raghavan, *Ind. J. Chem. Tech.*, 8 (2001) 368.

18. D. Mao, Q. Chen, G. Lu, *Appl. Catal. A. Gen.*, 244 (2003) 273.

19. A. Thankaraj, S. Sivakumar, P. Ratnasamy, *J. Catal.*, 137 (1992) 252.

20. J. Roseler, G. Heitmann, W.F. Holderich, *Appl. Catal. A.*, 144 (1996) 319.

21. Y.M. Chung, H.K. Rhee, *J. Mol. Catal. A. Chem.*, 175 (2001) 249.

22. A.N. Ko, C.C. Hung, C.W. Chen, K.H. Ouyang, *Catal. Lett.*, 71 (2001) 219.

23. T. Komatsu, T. Maeda, T. Yashima, *Micropor. Mesopor. Mater.*, 35-36 (2000) 173.

24. T. Curtin, J.B. McMonagle, B.K. Hondnett, *Appl. Catal. A. Gen.*, 93 (1992) 91.

25. J.C. Wu, C.S. Chung, C.L. Ay, I. Wang, *J. Catal.*, 87 (1984) 98.

26. T. Ushikubo, K. Wada, *J. Catal.*, 148 (1994) 138.

27. A. Ravue, *"Organic chemistry of Macro molecules"* Decker, New York, (1969).

28. T. Takahashi, K. Ueno, T. Kai, *Canad. J. Chem. Eng.*, 69 (1991) 1096.

29. B.Q. Xu, S.B. Cheng, S. Jiang, Q.M. Zhu., *Appl. Catal. A.*, 188 (1999) 316.

30. L. Dai, K. Koyama, M. Miyamoto, T. Tatsumi, *Appl. Catal. A.*, 189 (1999) 237.

31. A.H. Blatt, *Chem. Rev.*, (1933) 215.

32. H. Kajikuri, M. Kitamura, H. Ichihashi, in: Proceedings of the KISPOC-VII, Fukuoka, Japan, (1997) p 507.

33. D. Shouro, Y. Ohya, S. Mishima and T.Nakajima, *Appl. Catal. A. Gen.*, 214 (2001) 59.

Chapter 6

Nitration Of Phenol

Electrophilic aromatic substitution reactions are of considerable importance in the production of fine chemicals. However, the traditional processes suffer a number of disadvantages, such as low selectivity towards the desired product and the requirement for large quantities of mineral or Lewis acids as activators. In addition, these acids are responsible for corrosion problems within the plant and the generation of large volumes of spent reagents, which, given the current environmentally conscious climate, are increasingly unacceptable. Inorganic solid acids offer significant benefits for these processes by providing both effective catalysis and, in some cases, enhanced selectivity, and are easily removable from reaction mixtures. Herein, we report a green nitration process using transition metal loaded sulfated titania catalysts and try to correlate the activity with the acidity of these systems.

6.1 INTRODUCTION

Aromatic nitro compounds represent particularly versatile chemical feedstocks for a wide range of industrial products, such as pharmaceuticals, agrochemicals, dye stuffs and explosives. Nitration of organic compounds has long been a very active and rewarding area of research and is the subject of a large body of literature. Nitrophenols are important intermediates for the manufacture of drugs and pharmaceuticals[1]. Traditionally, nitration has been performed by a mixture of nitric and sulfuric acids (mixed acid method)[2].

However, the method is notoriously unselective for nitration of substituted aromatic compounds and the disposal of the spent acid reagents presents a serious environmental issue. The obvious disadvantage of the commercial manufacturing process currently used has led to a substantial effort to develop viable alternatives, using solid acid catalysts, other sources of NO_2^+, organic nitrating agents, other acids replacing H_2SO_4, etc. Compared to the conventional process, phenol nitration over solid acid catalyst is a clean and environment friendly process with a simpler workup procedure for quantitative isolation of the products. Solid acids effectively play the role of sulfuric acid in the reaction, assisting the formation of nitronium species. The general scheme of the reaction can be written as in figure 6.1.
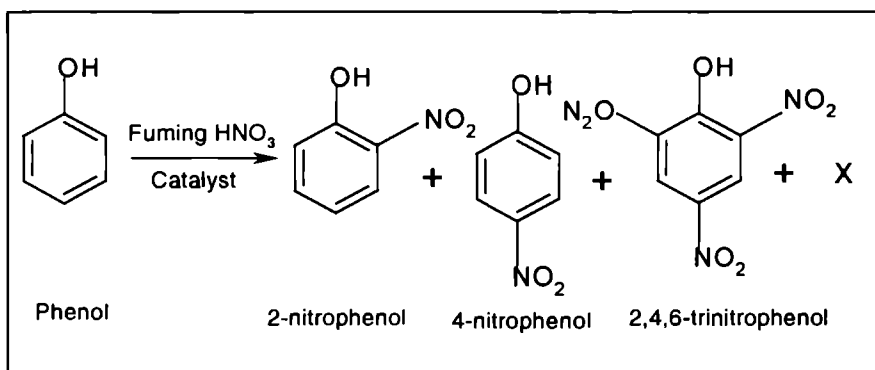

Figure 6.1 General scheme for nitration of phenol

Recently, novel nitration systems composing of nitric acid, trifluoroacetic anhydride and H-β are reported for the nitration of deactivated aromatic compounds[3]. The *para*-selective nitration of halogenobenzenes using a nitrogen dioxide-oxygen-zeolite H-β/HY systems is also reported[4]. Yadav *et al.*[5] proposed the selective synthesis of *para*-nitro derivative from chlorobenzene by using nitric acid over an electrically engineered sulfated zirconia carbon molecular sieve catalyst. Tomasz[6] has recently achieved a high yield and selectivity for the nitration of phenol to *p*-nitrophenol over metal oxide catalysts.

o-nitrophenol is an important starting material used in multiple step synthesis of valuable compounds[7]. Mixed metal oxides treated with sulfuric acid were found to be efficient for the nitration reaction[8]. The increase in the activity was attributed to the increase in the Brönsted acidity created by the high temperature treatment with sulfuric acid. The life of the catalyst depends on the support's capability of holding sulfuric acid to prevent its diffusion. Sato *et al.*[9] succeeded in maintaining high nitration activity of the supported sulfuric acid catalyst for more than two months by co-feeding trace amounts of sulfuric acid.

To our knowledge, very little study has been done on the regioselective nitration of phenol using nitric acid as a nitrating agent over solid acid catalyst. Phenol is selectively nitrated in solid phase to *o*-nitrophenol in high yield using concentrated nitric acid over solid acid catalysts. Regioselective nitration of phenol to *o*-nitrophenol as a special case has been studied under different reaction conditions.

6.2 PROCESS OPTIMIZATION

Nitration of phenol was carried out in the solid state. To a solution of phenol, activated catalyst was added and the mixture was mulled to get a homogeneous paste. This is kept at 0-5°C and nitric acid is added drop wise with continuous shaking. The reaction mixture is kept aside for 30 minutes at room temperature and then extracted with dichloromethane, after 2 h. Products are identified by G.C. analysis using BP-1 capillary column (12 m x 0.32 mm) and FID detector. Prior to injection in G.C. unreacted nitric acid in the reaction mixture was neutralized using sodium carbonate solution to a pH of 6-7. Reaction was done under varying conditions to optimize the reaction parameters.

I. Effect of Nitric acid Concentration

The catalytic activity of titania system was tested by varying the percentage of nitric acid. Concentrated, 1:1, 1:5 and 1:10 nitric acid in water were used for the reaction. As we expected, increase in the concentration of

181

nitric acid increases the conversion of phenol. The results are shown in figure 6.2. Selectivity towards *o*-nitrophenol increases when concentration of nitric acid increases.
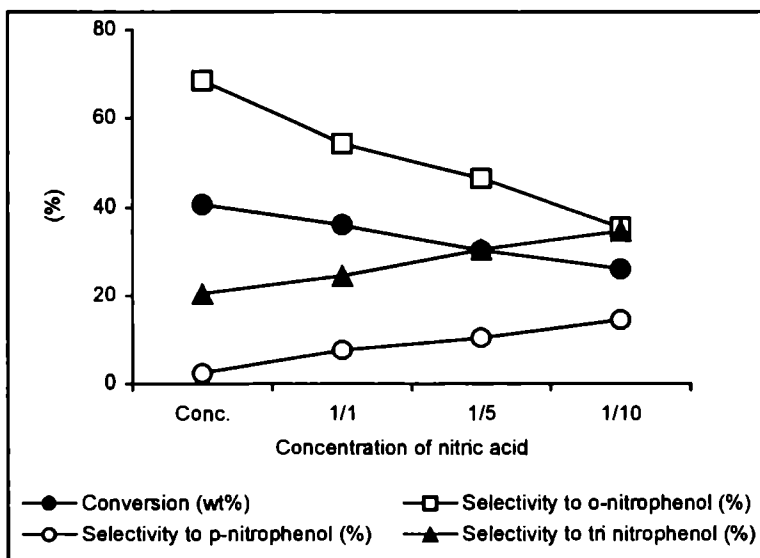

Figure 6.2 Influence of concentration of nitric acid on

conversion and product selectivity

Amount of catalyst: 0.1 g T, temperature: 0°C Reaction time: 2 h, phenol: nitric acid: 1:1.

Previous reports suggest the absence of any significant alteration of the product selectivity with change in the concentration of nitrating agent[10]. However, a slight alteration of product selectivities was observed in this case when the nitric acid concentration was varied. The selectivity for *o*-nitrophenol decreased from 68.58 to 54.32% when the nitric acid concentration changes from concentrated to 1:1.

The approximate charge distribution of phenonium ion arising from the protonation of benzene as calculated by Olah and co-workers[11] is shown in figure 6.3. If used as a model for the arenium ion in the electrophilic aromatic substitution, the *para* substituent has a greater effect on the adjacent carbon than an *ortho*

substituent. In the absence of other effects, this would predict a product ratio higher than 33 for the *para* isomer and less than 67 for the *ortho* isomer.
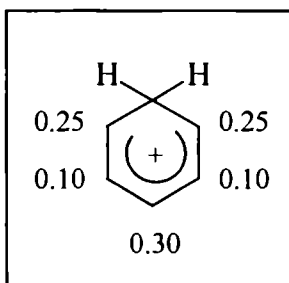

Figure 6.3 Approximate charge distribution in the phenonium ion

ii. Effect of Volume Ratio

Phenol to nitric acid ratio influences the percentage conversion and selectivity of the products. We varied the amount of nitric acid (concentrated) from 0.5 to 5 mL keeping the volume of phenol as 1 mL. The results are summarized in table 6.1. As the amount of nitric acid increases, conversion also increases. When 5 mL of nitric acid is used, the conversion is 60.62%, but the selectivity towards *ortho* isomer showed a constant decline, as the volume of nitric acid changes from 0.5 to 5 mL (from 78.94 to 23.77%). An increase in the amount of nitric acid, though increases the percentage conversion, decreases the regioselectivity.

Volume of phenol was changed in order to know its effect on the percentage conversion and selectivity. On increasing the volume of phenol from 0.5 to 5 mL, keeping the volume of nitric acid constant, the percentage conversion decreases. On the other hand the selectivity towards *o*-nitrophenol increases. For further studies we used an optimum volume ratio of phenol: nitric acid as 1:1 in which the selectivity towards *o*-nitrophenol is maximum with respect to percentage conversion.

183

Table 6.1 Influence of volume ratio on the catalytic activity and product selectivity

Phenol : HNO$_3$	Conversion of phenol (wt%)	Selectivity (%)		
		o-nitrophenol	p-nitrophenol	trinitrophenol
1:5	60.62	23.77	18.57	38.64
1:2	51.38	39.49	10.54	27.93
1:1	40.74	68.58	2.31	20.54
1:0.5	33.78	78.94	-	17.32
5:1	21.41	75.98	-	12.63
2:1	34.58	70.62	-	15.48
1:1	40.74	68.58	2.31	20.54
0.5:1	54.10	48.63	9.64	28.75

Amount of catalyst: 0.1 g T, Reaction temperature: 0°C, Reaction time: 2 h,
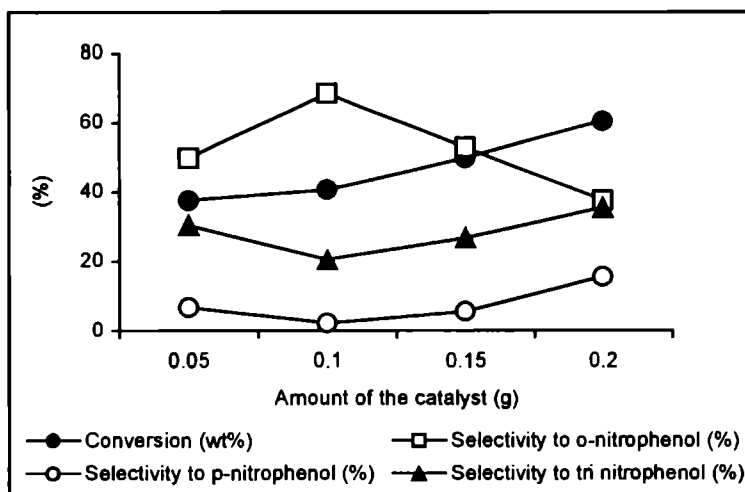
iii. Effect of Amount of the Catalyst.

Figure 6.4 Influence of amount of the catalyst on conversion
and product selectivity

Amount of the catalyst plays an important role in any catalytic reaction. An increase in the amount of the catalyst proved beneficial for the reaction as evident from figure 6.4. The conversion increases with increase in the amount of catalyst. But the selectivity towards *o*-nitrophenol initially increases and after an optimum amount of the catalyst, it declines. Thus an optimum amount of 0.1g is sufficient for the reaction to take place.
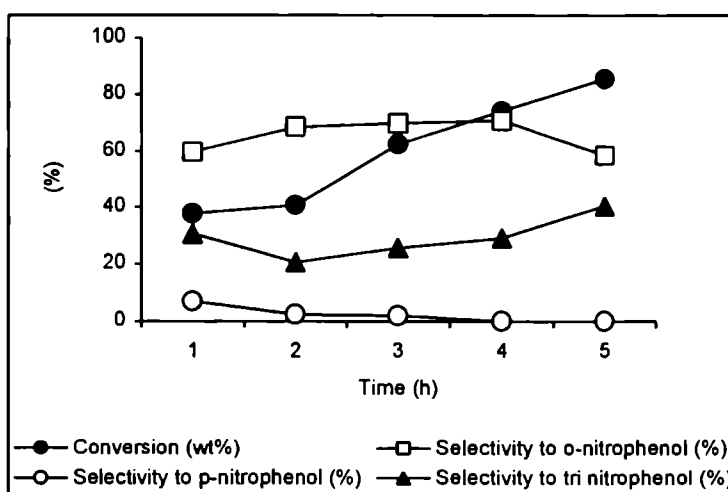
IV. Effect of Time on Stream-Deactivation study

Figure 6.5 Deactivation study on conversion of phenol and product selectivity

After the reaction, the products were extracted with dichloromethane at different time intervals. The results are furnished in figure 6.5. As the reaction time increases from 2 to 5 h there is an increase in the conversion. The selectivity to *o*-nitrophenol remains as such in the initial period. As time increases the *o*-nitrophenol selectivity decreases. Meanwhile 2,4,6-trinitrophenol selectivity increases and after 24 h, the major product is 2,4,6-trinitrophenol.

6.3 COMPARISON OF DIFFERENT SYSTEMS

Tables 6.2 and 6.3 present the results of nitration of phenol over the prepared systems under the optimized reaction conditions. From the results it is clear that the sulfated titania systems comprising transition metal oxides show good activity towards nitration of phenol. Pure titania shows the least activity.

Table 6.2 Influence of the type of metal loaded in the nitration of phenol

Systems	Conversion of phenol (wt%)	Selectivity (%)		
		o-nitrophenol	*p*-nitrophenol	2,4,6-trinitrophenol
T	40.74	68.58	2.31	20.54
ST	85.60	92.35	3.85	1.35
STCr(3)	87.79	90.78	2.38	1.16
STMn(3)	80.21	89.51	5.88	2.56
STFe(3)	70.77	84.06	6.08	1.54
STCo(3)	86.53	94.02	2.07	2.85
STNi(3)	85.00	92.65	1.69	3.28
STCu(3)	88.61	97.67	-	1.11
STZn(3)	83.82	91.75	1.39	4.48

Amount of catalyst: 0.1 g T, Reaction temperature: 0°C, Reaction time: 2 h,
Phenol: Concentrated nitric acid: 1:1.

Maximum conversion is observed for the system with 6 wt% metal content. The highest conversion is found to be 90% for STCu(6) and STCr(6). The conversion then reduces slightly for 9 wt% loading. Preferential formation of *ortho* isomer is observed in all cases. When the reaction was carried out without catalyst, the conversion was low (34%) with nearly equal amounts of

ortho- and *para-* isomers. This suggests the influence of solid acid catalysts on the conversion and selectivity.

Table 6.3 Influence of amount of metal loading in the nitration of phenol

Systems	Conversion of phenol (wt%)	Selectivity (%)		
		o-nitrophenol	*p*-nitrophenol	2,4,6-trinitrophenol
STCr(6)	90.00	97.51	-	1.37
STMn(6)	84.64	96.94	1.02	1.12
STFe(6)	80.82	80.47	4.57	3.27
STCo(6)	89.22	94.19	4.08	1.04
STNi(6)	88.76	94.31	3.18	2.08
STCu(6)	90.00	98.26	-	1.38
STZn(6)	87.80	84.17	5.24	2.07
STCr(9)	89.00	95.57	2.04	1.69
STMn(9)	82.46	86.74	6.49	1.89
STFe(9)	77.61	70.98	10.08	4.16
STCo(9)	88.56	90.98	5.43	1.54
STNi(9)	86.26	94.57	2.47	2.16
STCu(9)	89.00	95.36	-	3.50
STZn(9)	85.43	80.65	6.28	3.64

Amount of catalyst: 0.1 g T, Reaction temperature: 0°C, Reaction time: 2 h,
Phenol: Concentrated nitric acid: 1:1.

Esakkidurai *et al.*[12] reported regioselective nitration of phenol in solid state over modified zeolites. Sato *et al.*[13] examined various metal oxides and found that TiO_2 or ZrO_2 as an essential component for the vapour phase nitration of benzene using aqueous nitric acid. Dagade *et al.*[14] reported the nitration of phenol over different solid acids using 30% nitric acid. Sato *et al.*[8]

proved that Brönsted acid sites are the active sites for the vapour phase nitration. The same authors reported that metal oxides treated by sulfuric acid at 500°C such as $SO_4^{2-}/[TiO_2\text{-}MoO_3]$, $SO_4^{2-}/[TiO_2\text{-}WO_3]$ and SO_4^{2-}/TiO_2 show increase of nitration activity. The increase of the nitration activity is attributed to the increase in acidity of the catalysts by SO_4^{2-} treatment. Brei and coworkers[15] observed that the catalytic activity correlate with the acidic strength for the nitration of benzene over WO_3/ZrO_2 catalysts.

A closer scrutiny clearly establishes a crude association between the catalytic activity and the amount of Brönsted acid sites as obtained from the thermodesorption studies of 2,6-DMP. The reason for the low activity for the titania is the low acidity of the system. The active site for the nitration by nitric acid is the Brönsted acid sites. However, the high activity cannot be explained simply by the solid acidity (acid strength and acid amount) of the catalyst.
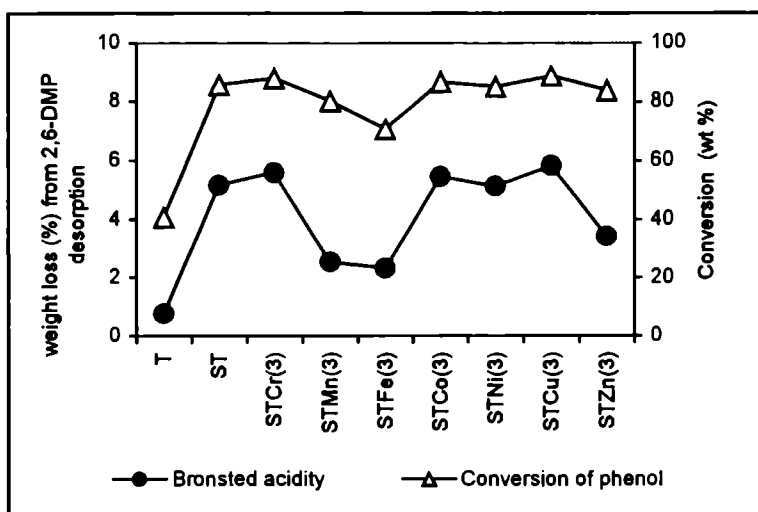

Figure 6.6 Correlation between conversion of phenol and Brönsted acidity

The product selectivity remained almost constant irrespective of the nature of the metal incorporated. With increase of the metal oxide content, the acidity of the catalyst increases up to 6 wt%, and then gradually decreases.

This difference in the nitration activity can be explained by the difference in the acidity strength. The correlation between the nitration activity and the Brönsted acidity is given in figures 6.6 and 6.7. The typical Brönsted acid catalyst namely 80% tungstioic acid on SiO_2, was examined by Sato *et al.*[13] as a reference catalyst, and it was found to have low activity due to low dispersion of heteropolyacids on SiO_2.
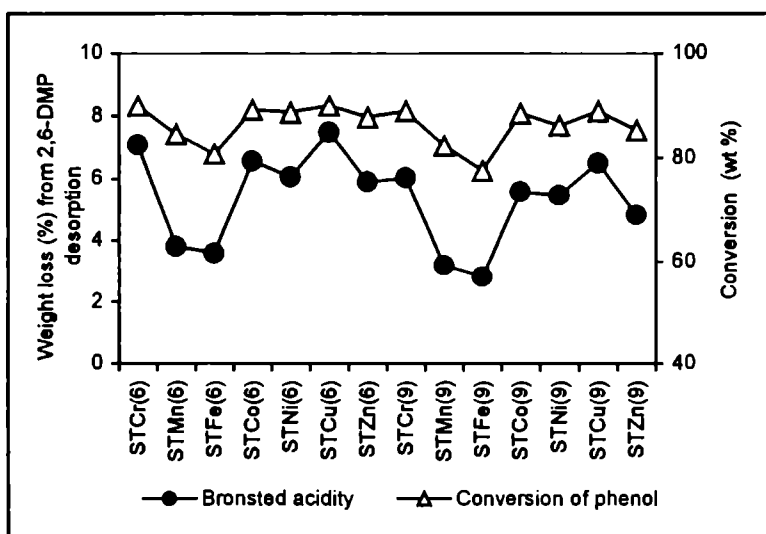

Figure 6.7 Correlation between conversion of phenol and Brönsted acidity

Among the various catalysts examined for the nitration of phenol, copper and chromium loaded catalysts are found to be most active. The life of various catalysts depends on the support's capability of holding sulfuric acid to prevent its effusion. Even on very good supports like silica gel, silica sand, etc., the sulfuric acid effuses slightly and gradually, and the activity of the sulfuric acid catalyst supported on these carriers is suddenly lost after a certain time on stream[9].

6.4 MECHANISM OF NITRATION REACTION

The nitration proceeds *via.* nitronium ion mechanism, in which the nitronium ion is generated by the interaction of nitric acid with the Brönsted acid sites and thus catalytic activity depends on Brönsted acidity. A close examination of the experimental results suggests a simple correlation between the Brönsted acidity of the systems and the catalytic activity towards nitration (figures 6.6 and 6.7). The Brönsted acid sites were found to have an influential hand on the reaction. Fairly strong acidity is necessary for formation of nitronium ion from nitric acid in the reaction conditions and the nitration activity is proportional to the acid amount.
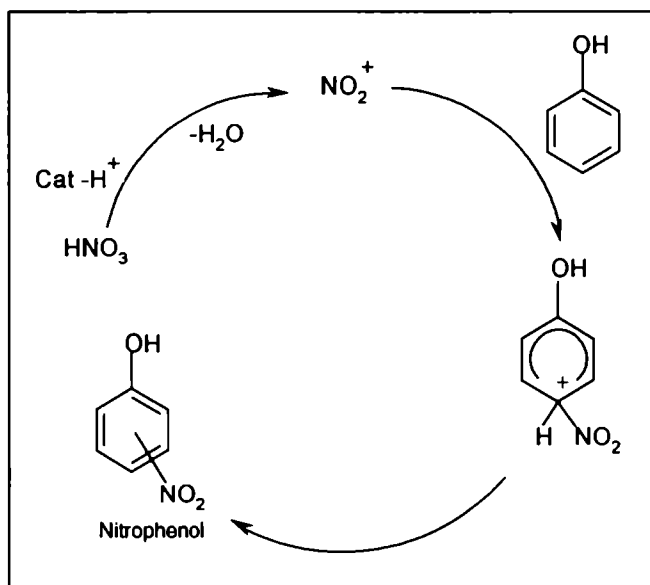

Figure 6.8 Plausible mechanism for the nitration of phenol using nitric acid

Brei *et al.*[15] explained that strong Brönsted sites are necessary for an effective formation of intermediate NO_2^+ ions from nitric acid. Attraction between cationic species and aromatic compounds are well known and originate from the fact that the 'edge' of the aromatic ring is positively charged, and the 'face' is negatively charged[16]. Because of the electronegative hydroxyl

group of phenol, the electron cloud of the aromatic ring is pulled towards this group. This will make the approach by the positively charged attacking species, the nitronium ion, more favorable. A plausible mechanism for the reaction is suggested in figure 6.8.

6.5 CONCLUSION

In conclusion, we have discovered a very efficient nitration process in the presence of sulfated titania catalysts under mild reaction conditions. Thus, it is much eco-safer protocol of nitration. The key points of the investigation can be summarized as:

⧆ Regioselective nitration of phenol using HNO_3 over solid acid catalyst without any use of acetic anhydride/acylnitrate, metal nitrates or H_2SO_4 is a comparatively clean and environmental friendly process.

⧆ Phenol is selectively nitrated to *o*-nitrophenol in high yields with nitric acid over sulfated titania catalysts.

⧆ The catalytic activity is influenced significantly by the reaction parameters like concentration of nitric acid, amount of the catalyst, molar ratio and time on stream.

⧆ A predominant formation of the *ortho* isomer was observed in all the cases suggesting involvement of the statistical factors in determining the relative product selectivity.

⧆ The nitration proceeds *via* nitronium ion mechanism, and the increase of nitration activity can be attributed to the increase of Brönsted acidity by the sulfation of metal oxides.

ఓ ‌లజలజలజ ‌
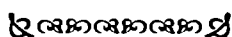
REFERENCES

1. D.A. Conlon, J.E. Lynch, F.W. Hartner, R.A. Reamer, R.P. Volante, *J. Org. Chem.*, 61 (1996) 6425.

2. E.R. Ward, *Chem. Br.*, 15 (1979) 297.

3. K. Smith, T. Gabbins, R.W. Miller, R.P. Claridge, *J. Chem. Soc. Perkin. Trans.*, 1 (2000) 2753.

4. K. Smith, S. Almeer, C. Peters, *Chem. Commun.*, (2001) 2748.

5. G.D. Yadav, J.J. Nair, *Catal. Lett.*, 62 (1999) 49.

6. M. Thomasz, J. Jaroslaw, Z. Janusz, S. Wincenty, *Synth. Commun.*, 31 (2) (2001) 173.

7. D.A. Conlon, J.E. Lynch, F.W. Hartner, Jr, R.A. Reamer, R.P. Volante, *J. Org. Chem.*, 61 (1996) 6425.

8. H. Sato, K. Nagai, H. Yoshioka, Y. Nagaoka, *Appl. Catal. A. Gen.*, 175 (1998) 209.

9. H. Sato, K. Nagai, H. Yoshioka, Y. Nagaoka, *Appl. Catal. A. Gen.*, 180 (1999) 359.

10. K.L. Nelson, H.C. Brown, *J. Am. Chem. Soc.*, 73 (1951) 5605.

11. G.A. Olah, *Acc. Chem. Res.*, 4 (1970) 240.

12. T. Esakkidurai, K. Pitchumani, *J. Mol. Catal. A. Chem.*, 185 (2002) 305.

13. H. Sato, K. Hirose, K. Nagai, H. Yoshioka, Y. Nagaoka, *Appl. Catal. A. Gen.*, 175 (1998) 201.

14. S.P. Degade, V.S. Kadam, M.K. Dongare, *Catal. Comm.*, 3 (2002) 67.

15. V.V. Brei, S.V. Prudius, O.V. Melezhyk, *Appl. Catal. A. Gen.*, 239 (2003) 11.

16. F. Currie, K. Holmberg, G. Wesman, *Colloids and Surfaces A. Physicochem. and Eng. Asp.*, 182 (2001) 321.

Chapter 7

Photochemical Degradation
of Methylene Blue

Heterogeneous photocatalysis is one of the advanced oxidation processes that has proven to be a promising method for the elimination of toxic and bio-resistant organic and inorganic compounds from waste water by transforming them into innocuous species. Abundant solar energy can be utilized efficiently in the photocatalytic processes for the degradation of organic pollutants. Photochemical degradation of methylene blue, which is an organic pollutant, is described in this chapter under solar illumination that is free and inexhaustible. The percentage degradation of various systems for this reaction is correlated with the band gap energy of the prepared systems.

7.1 INTRODUCTION

Heterogeneous photocatalysis is a promising technology for the removal of toxic organic and inorganic contaminants from water. However, the development of a practical photocatalytic system focuses on the cost effectiveness of the process by the use of renewable solar energy source. Photocatalytic degradation of organic contaminants using solar radiation can be highly economical compared with the processes using artificial UV radiation, which require substantial electrical power input. Voluminous literature is available on photocatalytic destruction of various organic and inorganic pollutants using artificial UV radiation[1-5]. Photocatalytic oxidation of these

pollutants using sunlight has also been reported[6-11]. In recent years, photocatalytic degradation mediated by titania has received considerable attention. Titania is a wide band gap semiconductor with many interesting properties, such as transparency to visible light, high refractive index and low absorption coefficient. Other than these properties, eminent capability of photocatalytic decomposition of organic materials has come to utilization in the environmental business. Development of TiO_2 photocatalytic systems with high efficiency by controlling the nature of TiO_2 is one of the most attractive targets of fundamental studies in this field. The TiO_2 films grown on various substrates promise to have a high commercial potential in the environment applications such as self-cleaning, anti bacterial and waste water purification containment[12].

Heterogeneous photocatalysis is capable of degrading many classes of pollutants, but requires ultraviolet light and thus may be energy intensive. The basic principle of dye sensitization has been demonstrated showing the dependence of sensitization on the intrinsic properties of the support material and the adsorbed dye. The incident photons possessing energies greater than the band gap of the catalyst are absorbed. The absorbed photon then excites valence electrons into the conduction band, creating a positive hole. The resulting electron-hole pair can migrate toward the catalyst surface and initiate redox reactions that oxidize the adsorbed organic molecules[13]. A photocatalyst must posses a large catalytic surface and should also exhibit high proton utilization efficiency. The size of the primary catalyst particles defines the surface area available for adsorption and decomposition of the organic pollutants. When the size of a semiconductor particle is decreased to the extent that the relative proportions of the surface and bulk regions of the particle are comparable, its energy band structure becomes discrete and will exhibit chemical and optical properties different from those of the bulk material[14]. This is known as the quantum size effect and has been observed for nanosized TiO_2 particles[15].

Anatase type TiO_2 have attracted attention of scientists because of its photocatalytic activity for the decomposition of various environmental pollutants, such as NO_x in air and fertilizers in water[5,16-24]. Some problems related to their practical applications, however, have been pointed out; fine particles are desired for high photoactivity without the formation of rutile phase, which has lower photo activity than anatase. A few reports are available on SO_4^{2-}/TiO_2 for photocatalytic degradation of CH_3Br, NO_2^- and textile wastewater[25]. Toyoda and coworkers[26] studied the effect of crystallinity of anatase on photoactivity for methylene blue decomposition in water. Kwon *et al.*[27] reported the photocatalysis of titania prepared via sol-gel process using different alkoxide precursors for the degradation of methylene blue. Degradation rates of various organic dyes such as methylene blue, remazol blue R and orange G under solar irradiation using combustion synthesized nano titania were reported[28]. The photocatalyzed degradation of pyridine in the gas phase was investigated using titanium dioxide semiconductor supported on mordenite[29]. Photocatalytic oxidation of methylene blue and victoria blue in aqueous medium was studied using hydrothermally treated titania pillared clay[30]. In the present case the prepared systems are studied for the decomposition of methylene blue (figure 7.1) in its aqueous solution. Titanium dioxide represents one of the most efficient photocatalyst, however, the effective photo excitation of TiO_2 semiconductor particles requires the application of light with energy higher than the titania band gap energy (E_{bg}). For anatase E_{bg} (anatase) = 3.2 eV and for rutile E_{bg} (rutile) = 3.02 eV, therefore the absorption thresholds corresponding to 380 and 410 nm for the two titania forms respectively[5,31-33]. Consequently, only the ultraviolet fraction of the solar irradiation (about 5%) is active in the photoexcitaiton processes using pure TiO_2 solids. The present interest is to use solar light, which is free and inexhaustible.
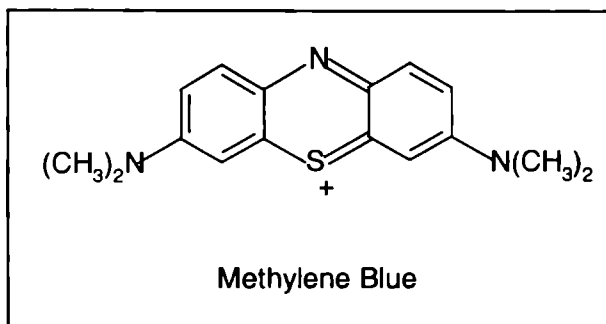
Figure 7.1 The structure of the methylene blue (MB)

7.2 PROCESS OPTIMIZATION

Photocatalytic degradation of methylene blue was performed taking 50 mL of (0.06 mmol L^{-1}) aqueous solution of methylene blue ($C_{16}H_{18}N_3S$, MB) and 0.1 g of catalyst. The solutions were exposed to sunlight in closed Pyrex flasks at room temperature with stirring. Direct sunlight was used in the present study and all the irradiation was performed during the second half of February 2004 (sunny days), from 11.00 to 14.00 h when solar intensity fluctuations were minimum. The samples were immediately centrifuged and the quantitative determination of methylene blue was performed using *Shimadzu UV-VIS spectrophotometer* (UV-160A) before and after reaction at 660 nm. Experiments were repeated three times to get better results. Control runs were carried out in darkness to monitor the changes in dye concentration due to adsorption. Experiments were also conducted under solar irradiation without catalyst to measure any possible direct photolysis of these organics. The pH variation during the course of reaction was not significant, so all the runs were conducted at natural conditions.

I. Effect of Time

An approximate reaction time is the main assurance for a perfect reaction. MB degradation is conducted and the absorbance measurements are

done at various times and the percentage degradation is calculated. Figure 7.2 illustrates the influence of time on the degradation experiments under solar irradiation. Degradation becomes 78.6% after one hour and increases to 91.6% after four hours of reaction time. As we expected, increase in time favours the percentage degradation. As time increases amount of radiation falling increases and this facilitates the degradation.
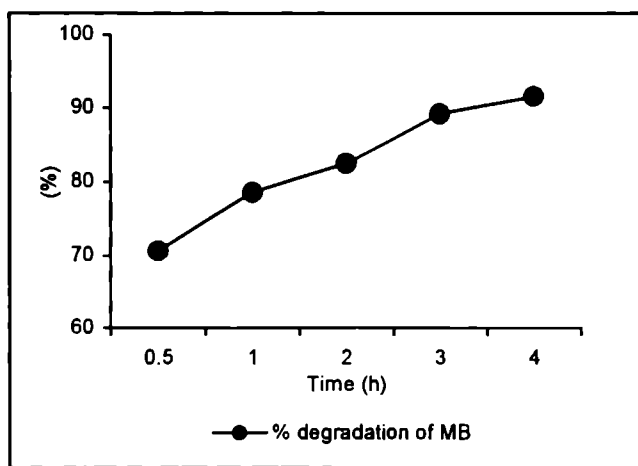

Figure 7.2 Influence of time on degradation of MB

Concentration of MB: 0.06 mmol L^{-1}

II. Effect of catalyst concentration

The effect of catalyst loading on the photocatalytic degradation of MB is studied by varying the amount of titania from 1 to 5 g L^{-1} of methylene blue solution. The percentage degradation of MB for a time period of 60 minutes is calculated and is given in table 7.1. Adsorption of MB by the sample powders is confirmed to be very small in the dark (without solar irradiation). Therefore, the observed decrease in absorbance of the solution is concluded to be due to the decomposition of MB by photocatalytic reaction on anatase samples.

197

Table 7.1 Influence of catalyst concentration on MB degradation

Amount of catalyst (g L^{-1})	-	1	2	3	4	5
% degradation of MB	2.9	65.3	78.6	70.1	55.8	32.6

Catalyst: T, Reaction time: 1 h, Concentration of MB: 0.06 mmol L^{-1}

From the preliminary study a little change in the degradation of MB is observed when the reaction is conducted in the absence of catalyst. Percentage degradation increases as we increase the catalyst concentration upto 2 g L^{-1} and then decreases with increasing catalyst loading. Percentage degradation changes from 78.6 to 32.6 when the catalyst amount increases from 2 to 5 g L^{-1}. This could be attributed to a shadowing effect, wherein the high turbidity due to high TiO_2 concentration decreases the penetration depth of radiation[28]. Hence an optimal catalyst loading of 2 g L^{-1} is enough for the degradation to occur effectively. Similar results were obtained for Nagaveni *et al.*[28] over Degussa P-25 TiO_2 catalyst under solar irradiation.

III. Effect of Concentration of Methylene blue

The effect of initial concentration of MB on the degradation rate is investigated over the concentration range of 0.04 to 0.07 mmol L^{-1}. It can be seen from the figure 7.3 that the concentration has a significant effect on the degradation rates. Madras and coworkers[4] proposed a model for photocatalytic degradation of dyes by taking into account of various controlling steps and Langmuir-Hinshelwood (L-H) parameters were determined for various dyes under UV irradiation. The degradation decreases from 100% to 64.2% as concentration of MB increases from 0.04 to 0.07 mmol L^{-1}. As the concentration of MB increases the percentage degradation decreases. At high concentration, the irreversible adsorption of the dye may occur on the catalyst surface leading to saturation during degradation[28].
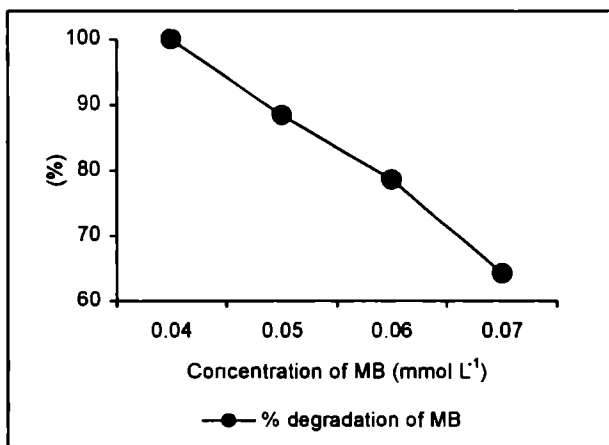
Figure 7.2 Influence of MB concentration on degradation

Reaction time: 1 h, Amount of catalyst: 2 g L^{-1} of T

IV. Catalyst Reusability

In order to understand the catalyst stability the experiments were conducted for one hour and the catalyst is taken at the end of the first cycle and used for the second cycle after activation. The percentage degradation of MB changes from 78.6 to 45.2 as the number of cycle changes from 1 to 4. Degradation rates are comparable in the first two cycles, but from the third cycle onwards a decrease in the percentage degradation is seen (table 7.2). This clearly indicates that the catalyst undergoes deactivation due to blocking of active sites by dye molecules, as the number of cycle increases.

Table 7.2 Catalyst reusability

No. of cycles	1	2	3	4
% degradation of MB	78.6	75.4	65.5	45.2

Amount of catalyst: 2 g L^{-1} of T, Reaction time: 1 h, Concentration of MB: 0.06 mmol L^{-1}

7.3 COMPARISON OF DIFFERENT SYSTEMS

The results obtained for the photo degradation of methylene blue over different systems under the optimized conditions is given in tables 7.3 and 7.4. Pure titania shows good activity. Among the various metal incorporated systems, copper loaded system shows high activity. The high activity may be due to low band gap energy of this catalyst compared to other systems.

Table 7.3 Influence of type of metal loaded in the photo degradation of MB

Catalyst	Percentage degradation of MB	Catalyst	Percentage degradation of MB
T	78.6	STCo(3)	65.2
ST	60.9	STNi(3)	68.4
STCr(3)	50.8	STCu(3)	70.5
STMn(3)	54.7	STZn(3)	52.1
STFe(3)	63.0		

Reaction time: 1 h, Concentration of MB: 0.06 mmol L^{-1}, Amount of catalyst: 2 g L^{-1}

The increase in band gap energy, evident from UV-Vis DRS studies, due to red shift in the λ_{max} leads to decrease in the photoactivity for the modified systems. Polyvalent heterocations negatively affect the photoactivity of TiO_2. It is postulated that the electrons in the d orbitals of these cations act as donors to quench the photogenerated holes by indirect recombination before they can diffuse to the surface. It can create acceptor and donor centers that behave as recombination centers for the photo generated charge carriers[34]. Amount of metal content does not give much difference in the results, because the absorbance maxima vary slightly among these systems and thus their band gap energy. Correlation between the percentage degradation of MB and λ_{max} obtained from UV-Vis DRS is given in figures 7.3 and 7.4.

Table 7.4 Influence of the amount of metal loading in the photo degradation of MB

Catalyst	Percentage degradation of MB	Catalyst	Percentage degradation of MB
STCr(6)	50.3	STCr(9)	49.8
STMn(6)	54.0	STMn(9)	53.5
STFe(6)	62.8	STFe(9)	62.0
STCo(6)	65.0	STCo(9)	64.4
STNi(6)	68.3	STNi(9)	67.8
STCu(6)	69.9	STCu(9)	69.3
STZn(6)	51.6	STZn(9)	51.2

Reaction time: 1 h, Concentration of MB: 0.06 mmol L^{-1}, Amount of catalyst: 2 g L^{-1}

Toyoda *et al.*[26] studied the effects of crystallinity of anatase on the photoactivity for MB decomposition over TiO_2 calcined at different temperature. According to them, both larger full width half maximum (FWHM) of anatase phase and also smaller FWHM obtained by annealing at high temperatures are not desirable for high photoactivity. Decomposition of MB suddenly increases at certain FWHM and then decreases gradually with decreasing FWHM. The degradation is rather low for anatase with small crystallite size and increases suddenly at about 12 nm, but then decreases with further growth of crystallites. In figure 7.5, percentage decomposition of MB against FWHM of 101 plane of anatase is plotted for the sulfated titania systems. Zhang and coworkers[35] reported that improved crystallinity has a beneficial effect on the increasing of photocatalytic degradation of phenol by titania powders. They also reported that mixtures of anatase and rutile are found to be more active than anatase crystallites or rutile crystallites at the same calcination temperatures.
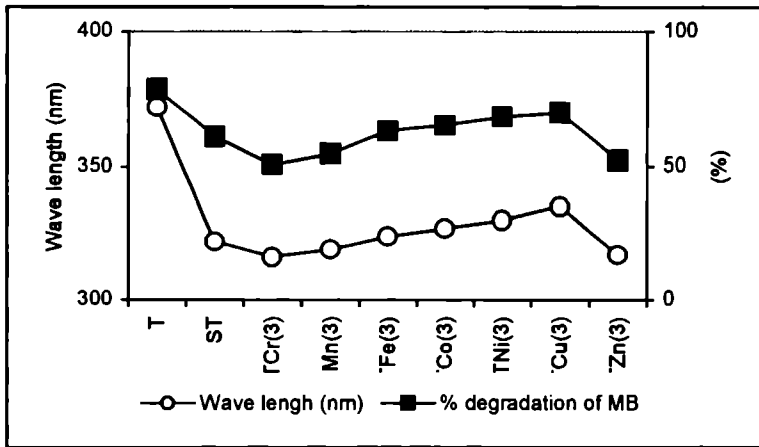
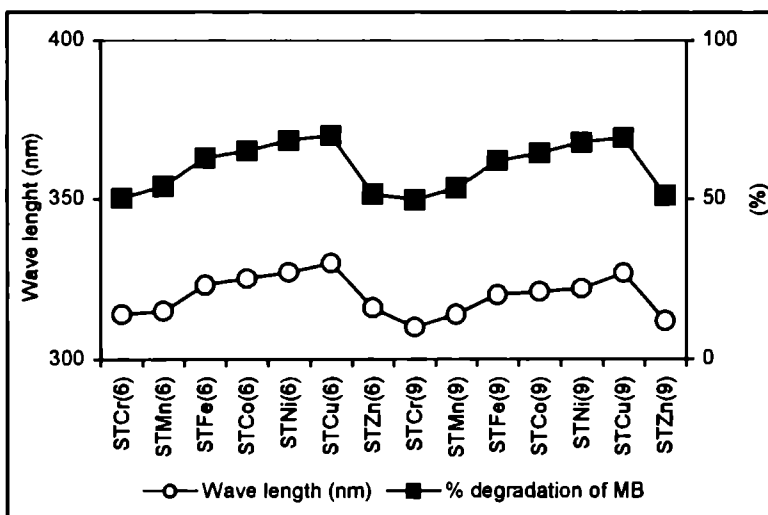Figure 7.3 Correlation between % degradation of MB and λ_{max}

Figure 7.4 Correlation between % degradation of MB and λ_{max}

It was reported[36,37] that the pore structure, pore size, particle size and activation temperature of TiO_2 affect the photocatalytic activity of organic pollutants in wastewater. The effects of sizes of primary particles (crystal) and secondary particles (aggregates) of anatase were examined in detail on the decomposition of trichloroethylene gas[13,38]. Chromia loaded samples having

low crystallite size show low photoactivity. In practice narrow range of FWHM, is found to be effective for high photoactivity. Reaction depends strongly on primary particle size, a maximum degradation rate at around 12 nm size and then there is a gradual decrease with increasing size. The decrease in photoactivity due to increase in crystallite size may be due to the cooperative effects of partial transformation of rutile.
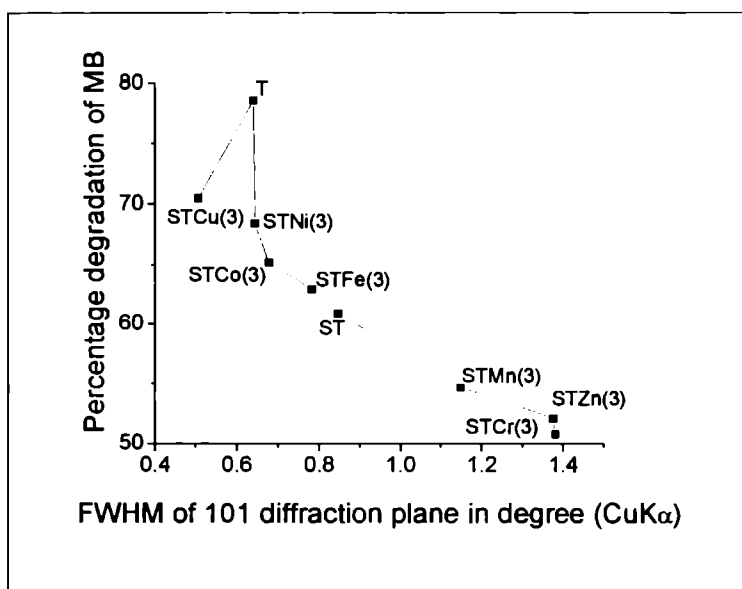

Figure 7.5 Relation between % degradation of MB and FWHM of 101 diffraction line of anatase phase on the sulfated titania samples

The influence of the particle size of TiO_2 nanostructured catalyst on its reactivity for trichloroethylene (TCE) photo-oxidation has been studied[13]. The TCE degradation over TiO_2 exhibits a maximum at a primary particle size of 7 nm. For the TiO_2 catalysts with a crystal size larger than 7 nm, the smaller crystals afford a larger surface area and exhibit higher TCE degradation. When TiO_2 is smaller than 7 nm, the catalyst activity decreases with smaller particle size. A blue shift in the band gap was observed for these smaller catalysts

resulting in a lower photon utilization and a different reactivity for the generated e^-/h^+ depending on the redox potential of the adsorbed molecules. However, it is difficult to attribute the decrease in TiO_2 catalyst activity solely to the structural or electronic effects. Anpo[39] observed an increase in the TiO_2 photocatalytic activity for the hydrogenation of CH_3COH with decreasing particle size. They associated the pronounced activity enhancement for particles smaller than 10 nm with the combined effects of larger surface area and size quantization. A similar observation was also made for the photocatalytic degradation of methylene blue in aqueous suspension for a series of TiO_2 particles larger than 30 nm[36]. However, other reports[40-42] showed that the photocatalytic efficiency does not monotonically increase with decreasing particle size. An optimal particle size of about 10 nm was observed for nanocrystalline TiO_2 photocatalysts in the liquid-phase decomposition of chloroform[40,41].

Reports show that the interface between anatase and rutile enhances the photoactivity of titania, in which anatase phase is directly exposed to UV rays[43]. In the case of pure titania, the interface between rutile and anatase might be formed, so that both phases can be exposed to sunlight and give high activity. The photocatalytic reaction on the TiO_2 surface is very sensitive to its surface structure because the photocatalytic reaction is a surface reaction. Samples that show low crystallite size have various structural defects. These defects were reasonably supposed to act as scattering centers for electrons and holes formed as a result of UV irradiation and consequently, promote the recombination of these couples. This seems to be the reason for low photoactivity for methylene blue in the case of metal incorporated systems.

Nagaveni *et al.*[28] showed that surface hydroxyl groups play an important role in determining photocatalytic activity. Since OH^- and H_2O groups are the most abundant adsorbates, these groups accept holes generated by solar or

UV illumination to form hydroxyl radicals thus preventing electron-hole recombination. Thus the high photocatalytic activity of pure titania can be attributed to high crystallinity as seen from XRD, nano size distribution (10-12 nm) as seen from the line width in XRD as well as SEM, large amount of surface hydroxyl groups evident from FTIR spectra and lower band gap energy of 3.2 eV as seen from the UV-Vis DR spectra.

7.4 MECHANISM OF PHOTOCHEMICAL REACTION

Photo irradiation of TiO_2 with photon energy greater than the band gap energy creates electrons and holes. Consequently following the irradiation, TiO_2 acts as either electron or hole donor to reduce or oxidize the materials present in the surrounding media.

$$TiO_2 \xrightarrow{\ h\nu\ } e^-_{C.B.}(TiO_2) + h^+_{V.B.}(TiO_2)$$
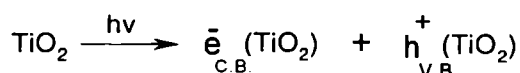
These electrons and holes are responsible for the photochemical reactions taking place on the surface of TiO_2. It is well known that photocatalytic activity strongly depends on bulk and surface physicochemical properties of the titania powder, such as the kind of crystal structure[44,45], surface area and particle size[46,47] and surface hydroxyls[48,49]. The mechanism of photocatalysis is discussed in recent reviews by Hoffmann *et al.*[5], Fox and Dulay[23]. Fewer recombination sites on the surface lead to slower recombination of electrons and holes, thus a higher photocatalytic activity[50]. The small crystal size also gave rise to quantum size effects[51]. This results in a net shift in the semiconductors band-gap energies. A blue shift in the TiO_2 band gap occurred for the modified samples. This means that for the same light source, there are fewer photons with the required energy to generate the e^-/h^+ pairs needed for the reaction. This results in a lower utilization of photons.

Titanium dioxide in the form of anatase is widely used mainly because of its high photocatalytic activity. Anatase is a wide bandgap semiconductor with bandgap energy of 3.2 eV, so only solar radiation with wavelengths below 387 nm is absorbed to form the e^-/h^+ pairs. At the ground level, however, solar irradiation starts at about 300 nm; thus approximately 4% of the total spectrum can activate TiO_2. During photocatalytic process, light activates a photocatalyst and establishes a redox environment in the aqueous solution. The semiconductor photocatalyst absorbs impinging photons with energies higher than the bandgap or threshold energy and generates oxidation sites on its surface. These oxidation sites react with adsorbed water molecules or hydroxyl to produce hydroxyl radicals, very strong oxidants capable of oxidizing virtually any organic compounds. When the TiO_2 surface is exposed to UV light, negatively charged particles-electrons-are released, just as the same way as the electron released when sunlight hits the surface of the solar power cells. Simultaneously, positively charged holes are formed on the surface of the catalyst and an electron is released. These electrons and holes create very strong oxidizers, called the hydroxide radical, even stronger than hypochlorous acid and ozone. When harmful substance sticks to the positive holes, they are completely broken down to harmless compounds. The hydroxide radical also can inhibit the growth of bacteria and mold.

7.5 CONCLUSIONS

The following conclusions can be drawn from the present study

- Photo degradation of methylene blue occurs effectively confirming that the prepared systems are photochemically active.

- Crystallite size of anatase was shown to be an important factor in order to get high photocatalytic activity for the decomposition of MB in water.

ℒ Among the different systems pure titania shows the highest activity. The activity could be well correlated to their band gap energy.

ℒ Activity difference among different metal incorporated systems is due to the combined effect of surface area, pore volume, crystallite size, pore structure and band gap energy.

ℒ Abundant solar energy can be utilized efficiently in the photocatalytic processes for the degradation of organic pollutants. This is highly economical compared with the processes using artificial UV radiation which require substantial electrical power input.

ଛ ଔଶୋ ଔଶୋ ଔଶୋ ℒ
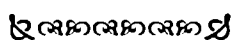
REFERENCES

1. H. Lachheb, F. Puzenat, A. Houas, M. Ksibi, F. Elaloui, C. Guillard, J.M. Hermann, *Appl. Catal. B. Environ.*, 39 (2002) 75.

2. A.L. Linsebrigler, G. Lu, J.T. Yates, *Chem. Rev.*, 95 (1995) 735.

3. J.F. Tanguay, S.L. Suib, R.W. Coughlin, *J. Catal.*, 117 (1989) 335.

4. G. Sivalingam, K. Nagaveni, M.S. Hegde, G. Madras, *Appl. Catal. B. Environ.*, 45 (2003) 23.

5. M.R. Hoffmann, S.T. Martin, W. Choi, D.W. Bahnemann, *Chem. Rev.*, 95 (1995) 69.

6. M. Stylidi, D.I. Kondaries, X.E. Vertkios, *Appl. Catal. B. Environ.*, 40 (2003) 271.

7. J.M. Herrmann, C. Guillard, J. Disdier, C. Lehaut, S. Malato, J. Blanco, *Appl. Catal. B. Environ.*, 35 (2002) 281.

8. A.A. Yawalkar, D.S. Bhatkhande, V.G. Pangarkar, A.A.C.M. Beenackers, *J. Chem. Technol. Biotechnol.*, 76 (2001) 363.

9. W.S. Kuo, P.H. Ho, *Chemosphere*, 45 (2001) 77.

10. D. Robert, S. Malato, *Sci. Total Environ.*, 291 (2002) 85.

11. D.S. Bhatkhande, V.G. Pangarkar, A.A.C.M. Beenackers, *Water Res.*, 37 (2003) 1223.

12. T. Wang, H. Wang, P. Xu, X.C. Zhang, S. Chao, *Thin Solid Films.*, 334 (1998) 103.

13. A.J. Maria, K.L. Leung, C.Y. Lee, P.L. Yue, C.K. Chan, *J. Catal.*, 192 (2000) 185.

14. L. Brus, *J. Phys. Chem.*, 90 (1986) 2555.

15. T. Kariyone, M. Anpo, K. Chiba, M. Tomonari, *Hyomen (surface)* 29 (1991) 156.

16. D.F. Ollis, H. Al-Ekabi (Eds), *"Photocatalytic Purification and Treatment of Water and Air"*, Elsevier, Amsterdam, (1993).

17. K. Kato, Y. Torii, H. Tada, T. Kato, Y. Butsugan, K. Nihara, *J. Mater. Sci. Lett.*, 15 (1996) 913.

18. J.M. Hermann, H. Tahiri, Y. Ait-Icho, G. Lassaletta, A.R. Gonzalez-Elipe, A. Fernandez, *Appl. Catal. B. Environ.*, 13 (1997) 219.

19. R.R. Basco, J. Kiwi, *Appl. Catal. B. Environ.*, 16 (1998) 19.

20. J. Grechulska, M. Hamerski, A.W. Morawski, *Water Res.*, 34 (2002) 1638.

21. N. Serpone, *Res. Chem. Intremed.*, 20 (1994) 953.

22. D.F. Ollis, C. Turchi, *Environ. Prog.*, 9 (1990) 229.

23. M.A. Fox, M.T. Dulay, *Chem. Rev.*, 93 (1993) 341.

24. P. Pichat, *Catal. Today*, 19 (1994) 313.

25. S.K. Samantaray, P. Mohapatra, *J. Mol. Catal. A. Chem.*, 198 (2003) 277.

26. M. Toyoda, Y. Nanbu, Y. Nakazawa, M. Hirano, M. Inagaki, *Appl. Catal. B. Environ.*, 49 (2004) 227.

27. C.H. Kwon, H. Shin, J.H. Kim, W.S. Choi, K.H. Yoon, *Mater. Chem. Phys.*, (2004) in press.

28. K. Nagaveni, G. Sivalingam, M.S. Hegde, G. Madras, *Appl. Catal. B. Environ.*, 48 (2004) 83.

29. S. Sampath, H. Uchida, *J. Catal.*, 149 (1994) 189.

30. S.V. Awate, K. Suzuki, *Adsorption*, 7 (2001) 319.

31. G.H. Li, L. Yamg, Y.X. Jin, L.D. Zhang, *Thin Solid Films*, 368 (2000) 163.

32. V. Mikhelashvili, G. Eisenstein, *Microelectr. Reliab.*, 41 (2001) 1057.

33. V.-H. Hsien, C.-F. Chang, Y.H. Chen, S. Cheng, *Appl. Catal. B. Environ.*, 31 (2001) 241.

34. W. Mu, J.M. Herrmann, P. Pichat, *Catal. Lett.*, 3 (1989) 73.

35. Q. Zhang, L. Gao, J. Guo, *Appl. Catal. B. Environ.*, 26 (2000) 207.

36. N. Xu, Z. Shi, Y. Fan, J. Dang, J. Shi, M.Z.C. Hu, *Eng. Chem. Res.*, 33 (2) (1999) 373.

37. A. Soni, R. Amcta, B. Sharma, S.C. Amcta, *J. Ind. Pollut. Control.*, 15 (1) (1999) 117.

38. S.D. Mo, W.Y. Ching, *Phys. Rev.*, B 51 (1995) 13023.

39. M. Anpo, T. Shima, S. Kodama, Y. Kubokama, *J. Phys. Chem.*, 91 (1987) 4305.

40. C.-C. Wang, Z. Zhang, Y.J. Ying, *Nanostr. Mater.*, 9 (1997) 583.

41. Z. Zhang, C.-C. Wang, R. Zakaria, Y. Ying, *J. Phys. Chem.*, 102 (1998) 10871.

42. P. Rivera, K. Tanaka, T. Hisanaga, *Appl. Catal. B. Environ.*, 37 (1993).

43. T. Kawahara, Y. Konishi, H. Tada, N. Tohge, J. Nishi, S. Ito, *Angew. Chem. Int. Ed.*, 114 (2002) 2935.

44. A. Mills, R.H. Davies, D. Worsley, *Chem. Soc. Rev.*, (1993) 417.

45. R.I. Bickley, T. Gonzallez-Carreno, J.S. Lee, L. Palmisano, R.J.D. Tilley, *J. Solid State Chem.*, 92 (1991) 178.

46. B. Ohtani, S.-w. Zhang, S.-I. Nishimoto, T. Kagiya, *J. Photochem. Photobiol. A.*, 64 (1992) 223.

47. A. Sclafani, I. Palmisano, M. Schiavello, *J. Phys. Chem.*, 94 (1990) 829.

48. Y. Oosawa, M. Gratzel, *J. Chem. Soc. Faraday Trans.*, 1, 84, (1988) 197.

49. B. Ohtani, Y. Okugawa, S.-I Nishimotot, t. Kagiya, *J. Phys. Chem.*, 91 (1987) 3550.

50. H. Inoue, H. Moriwaki, K. Maeda, H. Yoneyama, *J. Photochem. Photobiol. A. Chem.*, 86 (1995) 191.

51. L. Brus, *J. Phys. Chem.*, 90 (1986) 2555.

Chapter 8

Summary And Conclusions

To meet the challenges related to the industry, development of new generation of catalysts is necessary. In this connection, sulfated titania catalysts play an important role. The fundamental aspects, with focus on the preparation of heterogeneous catalysts by sol-gel method, its characterization, acidity determination and some industrially important reactions are briefly reviewed in this thesis. Systematic investigation of the physico-chemical properties and catalytic activity of some transition metal loaded sulfated titania catalysts are given in the previous chapters. A number of trends were found in the catalytic activity from the present study. This chapter deals with the summary and conclusions of the results described in the preceding chapters of the thesis.

8.1 SUMMARY

The present work is devoted to the synthesis of titania, sulfated titania and transition metal loaded sulfated titania catalysts. Its characterization and acidity determination using various methods are also discussed in detail. Titania has gained much attention in catalyst industry due to its application as a catalyst or catalyst support for metal or metal oxide catalysts used in heterogeneous catalysis including photocatalysis of industrially important and environment friendly reactions. Sulfated titania catalysts are prepared by sol-gel method, which is a homogeneous process resulting in a continuous transformation of a solution into a hydrated solid precursor. The nanochemistry

involved in the sol-gel method is a direct way to prepare highly divided materials. Sulfate modification is done using sulfuric acid to enhance the surface acidity so that they can replace the environmentally unfriendly catalyst in acid catalyzed reactions. Various characterization techniques have been used to evaluate the structural and textural properties of these solids. Finally, the catalytic activities of these materials in various industrially important reactions are investigated. Sulfation and incorporation of transition metals have positive influence on the acidity and catalytic activity. The characterization and catalytic activity results are compared with that of pure titania and sulfated titania. The present thesis comprises of eight chapters expounding the introduction, experimental and results and discussion parts. The chapter-wise depiction of the thesis is as follows.

Chapter 1 covers a brief literature review on titania and sulfated titania systems. The effect of sulfate doping on the physico-chemical characteristics and catalytic properties are included in this chapter. This chapter also includes literature survey on heterogeneous Friedel-Crafts alkylation, *tert*-butylation of phenol, nitration of phenol, photo degradation of methylene blue and Beckmann rearrangement reaction.

Chapter 2 deals with the various materials and experimental methods adopted for the synthesis and characterization of the catalyst systems. It also gives a brief account of the relevant theory of each method of characterization employed. Surface acidity determination by different techniques, including the test reactions like cumene conversion and cyclohexanol decomposition are the additional features of the chapter. The experimental procedures used to evaluate the catalytic activity are also incorporated in this chapter.

Chapter 3 discusses the physico-chemical characteristics of the catalyst systems. The catalyst systems are characterized by XRD analysis, surface area and pore volume measurements, EDX analysis, Scanning Electron

Microscopy, thermal studies, UV-Vis DRS, ^{1}H NMR and FTIR spectroscopy. Surface acidic properties are examined by three independent techniques namely ammonia TPD, perylene adsorption and thermodesorption studies using 2,6-dimethylpyridine as probe molecule. Cumene conversion reaction served as a test reaction for acidity. Cyclohexanol decomposition is performed to know the acid base properties of the catalysts.

Chapter 4 focuses on the application of the catalytic systems for Friedel-Crafts reactions. Benzylation of aromatics is achieved using benzyl chloride in liquid phase and *tert*-butylation of phenol in vapour phase. The influence of different reaction parameters on the catalytic activity and selectivity is subjected to investigation. The reusability of the catalytic systems is also checked. Attempt has been made to correlate the catalytic activity with the surface acidic properties of the catalyst systems and plausible mechanisms have been drawn out in each case based on the experimental observations.

Chapter 5 illuminates the application of sulfated titania systems towards the Beckmann rearrangement of cyclohexanone oxime. Influence of various reaction parameters like temperature, flow rate, concentration of oxime, influence of solvent etc. are discussed.

Chapter 6 narrates the nitration reaction of phenol over sulfated titania systems under different reaction conditions. It is found that certain optimum parameters are required for the better performance of the catalysts in the reaction.

Chapter 7 explains the photocatalytic activity of the prepared systems towards methylene blue degradation under solar irradiation.

Chapter 8 presents the summary and important conclusions of the present work.

8.2 CONCLUSIONS

The following conclusions are drawn from the present investigation.

- Titania, sulfated titania and transition metal loaded sulfated titania systems can be successfully prepared by sol-gel method. In all the catalysts, predominant phase is anatase. Sulfate modification retards the transformation from anatase to rutile.

- Incorporation of transition metals and sulfate modification improve the physico-chemical characteristics and surface properties of pure titania. Increase in surface area and decrease in crystallite size have been observed after sulfate modification, which is clear from XRD and SEM pictures.

- An optimum metal loading of 6% is found to be active in all the cases. High loading leads to the blockage of the active sites. Different characterization techniques like FTIR, ^{1}H NMR, and UV-Vis DRS show the presence of tetrahedrally coordinated Ti^{4+} ions.

- The surface acidity increases upon modification. Good correlation is obtained among the surface acidities measured by three independent methods. Vapour phase cumene conversion reaction works out as a test reaction for acidity. Good correlation is obtained between cumene conversion and the amount of total acid sites. Cracking and dehydrogenation product selectivity could be correlated with the Brönsted acidity and Lewis acidity of the systems respectively. Cyclohexanol decomposition reaction confirms the acidic character of the prepared systems.

- The systems are very active towards the Friedel-Crafts benzylation of toluene and o-xylene using benzyl chloride. High selectivity towards monoalkylated product is obtained in all the cases. Activities could be well

213

correlated with the Lewis acidity of the samples. *Tert*-butylation of phenol gives 4-TBP as the major product, which is catalyzed by medium acid sites.

✍ Beckmann rearrangement of cyclohexanone oxime proceeds effectively on the prepared systems. The conversion and selectivity depends greatly on the reaction conditions. ε-caprolactam selectivity could be correlated to the medium acid sites of the samples obtained from NH_3-TPD.

✍ Nitration of phenol is achieved over the different systems and the conversion could be correlated with the Brönsted acidity of the samples. The product selectivity remained the same for different catalytic systems while a slight alteration is observed with variation in the reaction conditions.

✍ Photochemical degradation of methylene blue occurs effectively, confirming that the prepared systems are photochemically active. The activity could be correlated with their band gap energy. Abundant solar energy can be utilized efficiently in the photocatalytic processes for the degradation of organic pollutants, which is highly economical compared with the processes using artificial UV radiation which require substantial electrical power input.

Future Outlook

Goal of both academic and industrial researchers is to obtain new catalytic systems having an enhanced activity and high selectivity towards the required product. Titania has created strong foundations in today's industrial and manufacturing world. A great deal of effort has been devoted in recent years to develop oxide catalysts by sol-gel process using metal alkoxides as precursors at room temperature. The results of present investigations reveal that sulfated titania systems are excellent catalysts for various industrially

important reactions such as Friedel Crafts benzylation of aromatic compounds, *tert*-butylation of phenol, Beckmann rearrangement of cyclohexanone oxime and nitration of phenol. The reason for selecting these reactions is that, metal oxides have long been known as favorable catalyst for these reactions but there is still plenty of room for improvement, particularly in the selectivity to a particular product as well as in catalyst life in view of practical application. The work can be extended to the development of environmentally friendly sulfated titania catalysts for the alkylation of various aromatic compounds using different alkylating agents. Since the prepared systems are acidic in nature, studies can be extended for various industrially important acid catalyzed reactions and rearrangements.

Huge improvements towards the development of environmentally friendly processes have been achieved in the nitration reactions. Nitration of other aromatics can be done over these catalysts to give better results under mild reaction conditions. Degradation of methylene blue occurs effectively over the prepared catalytic systems under solar irradiation. A great deal of attention has been directed towards various applications of photocatalyst for achieving a better environment. These catalysts can be used as photocatalysts to reduce toxic pollutants in the atmosphere and water, especially CO_2 and other volatile organic compounds in the atmosphere. Currently, the photocatalytic processes for the reduction of global air pollution have been focused due to the lower energy consumption, lower operating cost, lower operation temperature and utilization of solar energy for environmental protection.
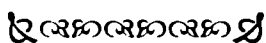
Publications:

Journal Papers

1. Surface characterization and catalytic activity of sulfated titania prepared via sol-gel route, K.R. Sunajadevi and S. Sugunan, React. Kinet. Catal. Lett., Vol. 82, No. 1, 11-17 (2004).

2. Surface properties and catalytic activity for cyclohexanol decomposition of ceria loaded rutile and their sulfated analogues, J. Babu, K.R. Sunajadevi and S. Sugunan, Ind. J. Chem., 43 A, 473-480 (2004).

3. Synthesis, characterization and benzylation activity of nanocrystalline chromia loaded sulfated titania, K.R. Sunajadevi and S. Sugunan, Catal. Commun., Vol. 5 (10) 575-581 (2004).

4. Preparation and characterization of nanocrystalline transition metal loaded sulfated titania through sol-gel method, K.R. Sunajadevi and S. Sugunan, Mater. Lett., Vol. 58 (26) 3290-3296 (2004).

5. Para-selective tert-butylation of phenol over nano sulfated titania catalysts via sol-gel route, K.R. Sunajadevi and S. Sugunan, Catal. Lett., (in press).

6. Surface acidity and cumene conversion over nanocrystalline chromia loaded sulfated titania prepared via sol-gel route, K.R. Sunajadevi and S. Sugunan, React. Kinet. Catal. Lett., (in review).

7. Vapour-phase Beckmann rearrangement of Cyclohexanone Oxime Over Nanocrystalline Transition metal loaded SO_4^{2-}/TiO_2 Catalyst via Sol-Gel Route, Sunaja Devi K.R. and Sugunan S. J. Mol. Catal., (in review).

8. Characterization of nano titania, sulfated titania and iron loaded sulfated titania, K.R. Sunajadevi and S. Sugunan, J. Mater. Sci., (in review).

National and International Conferences:

9. Surface properties and catalytic activity for cyclohexanol decomposition of ceria loaded rutile and their sulfated analogues, J. Babu, K.R. Sunajadevi and S. Sugunan, National seminar on Frontiers of Clay Research, March 2003, Regional Research Laboratory, Trivandrum.

10. Benzylation of toluene over nano titania and its modified forms via sol-gel route, K.R. Sunajadevi and S. Sugunan, National Symposium on Light and Smart Materials, Material Research Society of India, (MRSI) February 2004, Banaras Hindu University, Varanasi.

11. Phase transformation of sol gel derived nanocrystalline titania and sulfated titania-An XRD investigation, K.R. Sunajadevi and S. Sugunan, Current Trends in Inorganic Chemistry, (CTIC) March 2004, Cochin University of Science and Technology, Kochi.

12. Catalysis by sol gel titania and sulfated titania, K.R. Sunajadevi and S. Sugunan, A National Seminar on Recent Developments in Catalysis, (CATSEM) March 2004, Maharaja's college, Ernakulam.

13. Characterization of nano titania, sulfated titania and iron loaded sulfated titania, K.R. Sunajadevi and S. Sugunan, International Conference on Solvo Thermal Reactions (ICSTR-6) August 2004, Mysore University, Mysore.

ॐ ঙঙঙঙঙ ॐ
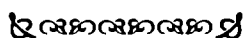
Resume

I born in Aluva, a small town in Kerala, the southern state of India on 3^{ed} March 1977. I received my Master of Science degree in Chemistry from the Mahatma Gandhi University, Kerala in 1999. I was awarded the Joint CSIR-UGC Junior Research Fellowship (JRF) and National Eligibility Test (NET), Junior Research Fellowship in Chemical Sciences under the CSIR Fellowship Scheme in December 2000 and Graduate Aptitude Test in Engineering (GATE) conducted by Indian Institute of Technology (IIT) Mumbai, in February 2001. From August 2001 onwards, I pursued my education by research on catalysis at Cochin University of Science and Technology, Kochi, under the guidance of Dr. S. Sugunan.

Sunaja Devi.K.R.

8/273 (A) – Keraleswaram parambu

South Cherlai, Kochi-2, Kerala

Phone: 91 484 2575804 (Dept), 91 484 2212829 (Res)

Email: sunaja@cusat.ac.in, sunajapai@yahoo.co.in